

Pharmacological Targeting of Sphingosine Kinase:
Conventional, Bisubstrate, and Irreversible Inhibitors

Thomas Keith Dawson
Lander, Wyoming

B.S. Chemistry
University of Wyoming, 2011

A Dissertation presented to the Graduate Faculty of the University of Virginia in
Candidacy for the Degree of Doctor of Philosophy

Department of Chemistry

University of Virginia
April 2016

Abstract

Cancer is rapidly becoming the world's greatest health problem, and current treatments are often harsh and ineffective. The demand for improved modes of therapy has fueled research in recent decades and led to a deeper, more fundamental understanding of cancer biology. Today, drug discoverers exploit knowledge of tumor growth and stress-support pathways to develop therapeutics with novel mechanisms of action, greater selectivity for cancer cells, lower toxicity, and, theoretically, greater efficacy.

A particularly attractive target for new cancer drugs is the sphingolipid signaling pathway. Cellular levels of the lipids ceramide, sphingosine, and sphingosine 1-phosphate (S1P) are strictly regulated by various enzymes, and play a large role in determining cellular growth and fate. Specifically, S1P has emerged as a driver of processes such as cell growth, proliferation, inflammation, resistance to apoptosis, and angiogenesis, and has been implicated in nearly every type of cancer. Thus, biomolecular agents that affect levels of S1P may be viable as targeted cancer therapies or for the treatment of hyperproliferative and inflammatory diseases.

As the sole producers of physiological S1P, the two sphingosine kinases (SphK1 and SphK2) have been the subject of intense investigation during the last decade. Many inhibitors of the SphKs have been discovered, and have proven to be effective pharmacological probes of these kinases. However, significant improvements in the potency, SphK-subtype selectivity, and pharmacokinetic properties of SphK inhibitors

remain necessary to fully elucidate the roles of SphK1 and SphK2 in the context of cancer and other diseases, and to maximize the therapeutic potential of these molecules. To this end, our efforts of the last several years have centered on the development of SphK inhibitors.

The work described herein represents the culmination of one phase of our SphK inhibition project, and the early stages of another. In Chapter 3, the design, evaluation, and *in silico* analysis of a unique class of amidine-containing SphK1 inhibitors is detailed. This study revealed key structural requirements for inhibition of SphK1 and resulted in the identification of the most selective SphK1 inhibitor reported to date. Next, in Chapter 4, efforts to target SphK2 are described that employed a conventional, substrate-based approach. In this work, one of the most active substrates of SphK2 was identified, and a small library of related inhibitors was generated. Finally, Chapter 5 describes two novel methods of targeting SphK2: bisubstrate and irreversible inhibition. The pharmacological justification, design, synthesis, and evaluation of these molecules are presented in detail.

To my parents,

sisters,

friends,

and

Robin

Contents

Abstract	i
Dedication	iii
Contents	iv
Figures	vi
Schemes.....	vi
Tables	vii
Abbreviations	vii
VPC Number Index.....	ix
 Chapter 1: Cancer, Cancer Treatments, and Sphingolipid Signaling	1
1.1 Cancer statistics	1
1.2 Oncogenesis and traditional cancer therapy	3
1.3 The hallmarks of cancer	5
1.4 Targeted cancer therapy.....	7
1.5 Cellular signaling and important glycerolipid messengers	10
1.6 The sphingolipid rheostat and the fate of cells	12
1.7 Sphingosine 1-phosphate signaling in homeostasis	15
1.8 Sphingosine 1-phosphate and cancer	17
1.9 Conclusion	19
 Chapter 2: Targeting Sphingolipid Signaling	20
2.1 Therapeutic validation of sphingolipid signaling: FTY720.....	20
2.2 Sphingosine kinase 1: properties and roles in physiology and disease	23
2.3 Sphingosine kinase 2: different by sub-cellular localization	25
2.4 Sphingosine kinase inhibitors	29
2.5 Early amidine-based inhibitors of SphK1	33
2.6 Conclusion	35
 Chapter 3: Amide Bioisosteres in Amidine-Based SphK1 Inhibitors.....	37
3.1 Structural requirements and docking analysis of amidine-based sphingosine kinase 1 inhibitors containing oxadiazoles	37
3.2 Low blood concentration and poor cellular uptake.....	52
3.3 Synthesis, and evaluation of additional bioisoteres	55
3.4 Conclusion	58

Chapter 4: Targeting SphK2 with Substrate-Based Inhibitors	60
4.1 A lack of inhibitors and a plethora of substrates for SphK2	61
4.2 Optimizing substrates of SphK2	62
4.3 Substrate-based inhibitors of SphK2	66
4.4 Conclusion	70
Chapter 5: Bisubstrate and Irreversible Inhibitors of SphK2	71
5.1 Bifunctional inhibitors of SphK2: born of necessity	71
5.2 Design, synthesis, and evaluation of bisubstrate inhibitors of SphK2	72
5.3 Irreversible inhibitors of SphK2: preliminary efforts	79
5.4 Conclusion	86
Chapter 6: Supplementary Information	88
6.1 Biological methods	88
6.2 General synthetic materials and methods	90
6.3 Syntheses and NMR data	98
6.4 References	196

Figures

1.1 Rates of cancer incidence and mortality	2
1.2 The hallmarks of cancer.....	5
1.3 Principles of targeted therapy	8
1.4 The Philadelphia chromosome	9
1.5 Lysophosphatidic acid and VPC12249.	12
1.6 The sphingolipid rheostat.....	13
1.7 Sphingolipid metabolism and S1P signaling	15
1.8 S1P receptors.....	16
1.9 S1P production in response to growth factors	18
2.1 Structures of myriocin and FTY720.....	21
2.2 FTY720 mechanism of action.....	22
2.3 SphK2 functional domains	26
2.4 Nuclear S1P and inhibition of HDAC1/2	27
2.5 Shared and differing traits of SphK1 and SphK2.....	28
2.6 Early SphK inhibitors.....	29
2.7 New and improved SphK inhibitors	30
2.8 Design and SAR strategy of early SphK inhibitors.....	34
2.9 Metabolism of 5	35
3.1 Docking studies with SphK1.....	47
3.2 Docking of 11g , 21b , and 26b	51
3.3 Metabolism of 11c	53
4.1 Examples of SphK2 inhibitors	61
4.2 SphK2 substrate lead series.....	63
4.3 SphK2 activity as measured for various substrates	66
4.4 Phosphorylation of 34g	67
4.5 Substrate-based inhibitors	67
4.6 Inhibition of SphK2 by derivatives of 34g	68
4.7 FTY720-OMe and potential substrate-based inhibitors	69
5.1 Structural components of SphK2 bisubstrate inhibitors.....	73
5.2 Bisubstrate inhibitor lead series	75
5.3 Selectivity for SphK1 by bisubstrate inhibitors.....	77
5.4 Building in SphK2 selectivity in bisubstrate inhibitors.....	78
5.5 SLR080811 and potential irreversible inhibitors of SphK2	82
5.6 Possible mechanism of T-817ma bioactivation	86

Schemes

3.1 Synthesis of oxadiazole 11c	42
3.2 Synthesis of 14	44
3.3 Synthesis of 15	44

3.4 Synthesis of 1,2,4-oxadiazole 21a	49
3.5 Synthesis of 1,3,4-oxadiazole 26a	49
3.6 Synthesis of thiadiazole 27c	56
3.7 Synthesis of pyrazole 28d	56
3.8 Synthesis of triazole 29f	57
3.9 Synthesis of sulfonamide 30c	57
4.1 Synthesis of 31i	64
4.2 Synthesis of 34g	65
5.1 Synthesis of 43e	76
5.2 Synthesis of 50	84
5.3 Synthesis of T-817ma (51d)	85

Tables

3.1 Previously described amidine-based SphK inhibitors	41
3.2 K_i values of oxadiazole 11c compared to amides 2 and 3	43
3.3 K_i of compound 15 compared to 11c	45
3.4 K_i values of <i>para</i> - and <i>meta</i> -substituted oxadiazoles 11a-h compared to amide analogs 2 and 13	46
3.5 K_i values of oxadiazole isomers with <i>meta</i> - and <i>para</i> -substituted tails	50
3.6 K_i and IC_{50} values of oxadiazoles and amide 3	54
3.7 K_i values of other amide isosteres at SphK1	58

Abbreviations

ABL	Abelson murine leukemia
ATP	adenosine triphosphate
9-BBN	9-Borabicyclo(3.3.1)nonane
Bcl-2	B-cell lymphoma 2
BCR	breakpoint cluster region
Boc	tert-butyloxycarbonyl
cAMP	cyclic adenosine monophosphate
Cbz	carboxybenzyl
Cer	ceramide
CML	chronic myelogenous leukemia
COX2	cyclooxygenase 2
DAG	1,2-diacylglycerol
DCM	dichloromethane
DHS	DL-threo-dihydrosphingosine
DMAP	4-dimethylaminopyridine

DIEA	N,N-diisopropylethylamine
DMF	dimethylformamide
DMS	N,N-dimethylsphingosine
DMSO.....	dimethylsulfoxide
EOC	epithelial ovarian cancer
GPCR	G protein-coupled receptor
HDAC1	Histone deacetylase 1
HDAC2	Histone deacetylase 2
iBCF.....	isobutyl chloroformate
IP ₃	inositol 1,4,5-triphosphate
JNK.....	Jun amino-terminal kinases
KRAS	Kirsten rat sarcoma
LPA.....	lysophosphatidic acid
LPA ₁₋₆	LPA receptors 1-6
NF-κB	transcription factor nuclear-factor κB
NLS.....	nuclear-localization sequence
NMM	N-methyl morpholine
NOA	non-oncogene addiction
OA.....	oncogene addiction
PC.....	phosphatidylcholine
PIK3CA	phosphatidylinositol-4,5-bisphosphate 3-kinase, catalytic subunit alpha
PKA	protein kinase A
PKC.....	protein kinase C
PLC	phospholipase C
PLD.....	phospholipase D
PIP ₂	phosphatidylinositol 4,5-bisphosphate
PTEN	Phosphatase and tensin homolog
PyBOP	benzotriazol-1-yl-oxytripyrrolidinophosphonium hexafluorophosphate
Sph.....	sphingosine
RRMS	relapsing-remitting multiple sclerosis
SAPK.....	stress-activated protein kinase
SphK1	sphingosine kinase 1
SphK2	sphingosine kinase 2
S1P	sphingosine 1-phosphate
TBAF.....	tetra-n-butylammonium fluoride
TBDPS	tert-butyldiphenylsilyl
TEA.....	triethylamine
TFA.....	trifluoroacetic acid
THF.....	tetrahydrofuran
TLC	thin layer chromatography
TMS.....	trimethylsilyl
TNFα.....	tumor necrosis factor alpha

TRAF2..... TNF receptor-associated factor 2

VPC Number Index

11a.....	VPC184143
11b.....	VPC184141
11c.....	VPC184091
11d.....	VPC185047
11e.....	VPC185027
11f.....	VPC185029
11g.....	VPC18a1143
11h.....	VPC185049
13.....	VPC14a10123
15.....	VPC184093
21a.....	VPC185083
21b.....	VPC201091
26a.....	VPC185081
26b.....	VPC201075
27c.....	VPC202181
28d.....	VPC174171
29f.....	VPC174065
30c.....	VPC202163
31i.....	VPC202099
32g.....	VPC202119
33g.....	VPC202141
34g.....	VPC202147
35c.....	VPC203101
36d.....	VPC20a2073
37d.....	VPC202171
38d.....	VPC204015
39e.....	VPC20a2169
41e.....	VPC204003
42e.....	VPC203301
43e.....	VPC203257
44e.....	VPC203279
45e.....	VPC203223
46e.....	VPC203221
47e.....	VPC203203
49.....	VPC204081
50.....	VPC204083
51d.....	VPC204131

Chapter 1

Cancer, Cancer Treatments, and Sphingolipid Signaling

Today, cancer is one of the deadliest diseases in the United States and other affluent countries, and is fast becoming a bigger problem in the underdeveloped world. Conventional cancer treatments are extremely harsh, and are limited in efficacy over time; improved therapies will be of paramount importance in the near future. To address this need, a new generation of drugs is being developed to target cancer-specific liabilities, and thereby selectively destroy cancer cells. One such liability is the dependence of cancer cells on the action of sphingosine 1-phosphate (S1P), a pleiotropic signaling lipid. Biomolecular agents that modulate levels of S1P may be valuable components of future cancer chemotherapy regimens.

1.1 Cancer statistics

Among all present-day human diseases, cancer is by far one of the deadliest. In the United States, cancer remains the second leading cause of death, behind only heart disease.¹ Worldwide, various types of cancer are the leading cause of death in developed countries,² but the problem is not limited to the affluent; rates of incidence and mortality are rapidly increasing in poorer parts of the world.³

However, this is not to say that cancer is a problem without a solution. Remarkable advancements have been made in recent years, which have resulted in

significant increases in survival rates. In the United States, deaths from cancer went down by 20% from 1991 to 2010 (Figure 1.1).⁴

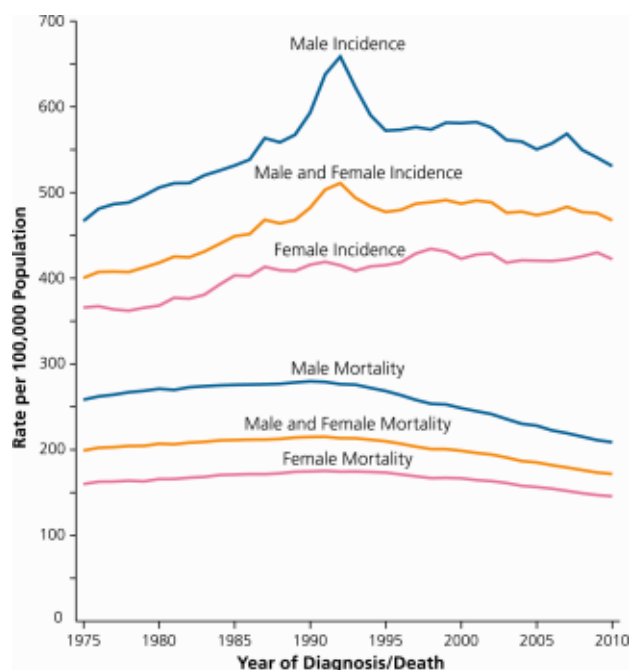


Figure 1.1. Rates of cancer incidence and mortality. For men and women, from 1975-2010. Used with permission.⁴

These lower mortality rates are promising, and are the combined result of greater detection, prevention, and treatment; however, they are nowhere near an acceptable value. To continue to drive these rates down, it will be essential to develop improved chemotherapies. Driven by this goal, decades of pan-disciplinary research have resulted in great advancements in the understanding of cancer at a systems level. What, then, do we know about cancer today? Cancer is—in a word—complex, and this makes its treatment exceedingly difficult.

1.2 Oncogenesis and traditional cancer therapy

When considering problems in drug discovery, researchers can usually follow the mantra, “one disease, one target, one drug.” This means that for most pathological cases, there is a specific, consistent underlying cause, oftentimes a malfunctioning or hyperactive protein. Once validated as a target, drugs are designed to diminish or eliminate the activity of the aberrant protein, and thus treat the disease.⁵

Cancer, however, can seldom be treated this way. The term cancer refers to a myriad of distinct diseases, each of which arises from a series of genetic mutations that collectively grant cells survival advantages. Moreover, specific oncogenic mutations leading to tumors can vary significantly, *even within specific cancer types*. Epithelial ovarian cancer (EOC) is a particularly complex and illustrative example.⁶ At least ten different mutated, overexpressed, or amplified genes have been identified in EOC tumors, including *BRAF*, *Kras*, *PTEN*, *beta-catenin*, *PIK3CA*, *c-erbB-2*, *bcl-2*, *c-myc*, and others.⁷ Compounding this convolution, the specific roles that each gene plays in the transformation of healthy ovarian cells is unknown. The unfortunate reality of this complexity is that EOC is very difficult to treat; the specific cellular systems responsible for the onset and progression of the disease have not been clarified, so designing drugs to treat EOC is extremely difficult. Sadly, this is not the exception, but is the rule for most cancers.

Because particular cellular targets cannot always be identified, most cancers must be treated with a combination of surgery, radiation, and chemotherapy. If tumors

are identified before metastasizing, surgery is highly effective, even curative, provided that all of the malignancies can be removed.⁸ If surgery cannot be used, or is insufficient, radiation or chemotherapies are employed. Radiotherapy delivers localized, high-energy gamma rays or X-rays to the tumor. While radiotherapy is becoming more advanced and precise, it is not without side-effects, and considerable damage is often done to surrounding healthy tissues.⁹ Chemotherapy is the final approach, and despite severe side effects, is the mainstay treatment today. Cytotoxic agents may fall into the following categories: alkylating agents, platinum compounds, antimetabolites, anthracyclines, topoisomerase inhibitors, tubulin-binders, and anitmitotics.^{10,11}

Radiation and each type of chemotherapy may vary extensively in their mechanisms of action, but the overall effect is the same—they interfere with DNA synthesis and replication in dividing cells. This is why they are effective against cancer cells, which are constantly proliferating and replicating.¹² However, other systems in the body may be affected as well, as any dividing cell is at risk. Because of the indiscriminate nature of traditional radiotherapy and chemotherapy, these approaches cause drastic side effects such as nausea, vomiting, diarrhea, tiredness, hair-loss, low white blood cell counts, and even cognitive dysfunction. Besides the morbidity of a cancer diagnosis, patients must cope with treatments that severely decrease their quality of life.¹³ The reality of this has not been ignored in the scientific community. During the last two decades, a much deeper understanding of the systems that control and sustain cancer cells has begun to emerge, and with it, the hope and promise of a new class of drugs.¹⁴

Chemotherapies developed now and in the near future will not indiscriminately attack rapidly dividing cells. Rather, they will be designed to target and exploit tumor-specific liabilities in order to destroy cancer cells *selectively*.

1.3 The Hallmarks of Cancer

The unpredictable nature of the genetic mutations driving tumorigenesis and tumor progression is a considerable difficulty—but while the genotype of cancer is not constant, the phenotype is. In 1999, Hanahan and Weinberg first characterized this phenotype by outlining six traits, common across cancer types, that they termed the Hallmarks of Cancer (summarized in Figure 1.2).¹⁵

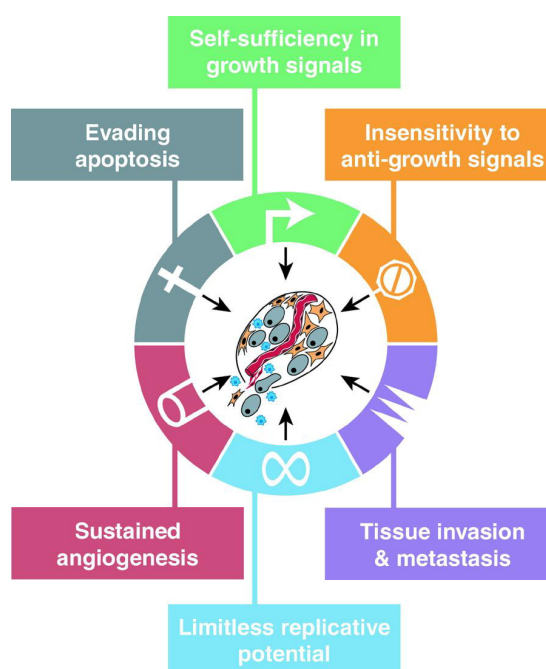


Figure 1.2. The Hallmarks of cancer. Also described as "acquired capabilities." Used with permission.¹⁵

The consequences of this classification and simplification were foundational, and announced the beginning of a paradigm-shift in the field of oncology. The authors

themselves foresaw this shift, predicting, “With holistic clarity of mechanism, cancer prognosis and treatment will become a rational science, unrecognizable by current practitioners... We envision anticancer drugs targeted to each of the hallmark capabilities of cancer.”¹⁵ Essentially, rather than attempting to catalogue each and every example of mutations leading to gain-of-function oncoproteins or loss-of-function tumor suppressors, researchers can instead focus on understanding the finite cellular systems accompanying and supporting cancer hallmarks;¹⁶ each hallmark represents a specific trait that differentiates cancer cells from healthy cells. Again, these traits are common *across cancer types*, and are the ultimate, phenotypic result of complex and varying genetic mutations. Viewing the distinct diseases of cancer through the lens of these hallmarks greatly simplifies and focuses oncological research.

Finally, it is important to emphasize that the hallmarks are traits that collectively grant cancer cells near-immortality. However, while the cellular systems driving each hallmark may be present in all cells, *healthy* cells do not rely on them to such a great extent; for this reason, they represent an Achilles’ heel, and their exploitation is goal of targeted therapy.¹⁷

1.4 Targeted cancer therapy

As outlined in the previous sections, the greatest difficulties in treating cancer are twofold. The first is the unpredictable nature of oncogenic mutations, which makes traditional drug design extraordinarily difficult, and the second is the widespread cytotoxicity of traditional chemotherapy that results in well-known and devastating side effects. In response to these challenges, the elegant solution of targeted cancer therapy has emerged. The hallmarks of cancer provide the simplifying framework within which to view the diseases of cancer. Then, the objective of targeted therapy is simply to disrupt the altered or pre-existing cellular processes upholding particular hallmarks. By doing so, these types of drugs can potentially sidestep the common problems in treating cancer: the biological targets they disrupt are often predictable across cancer types, and they may have significantly improved therapeutic windows over blanket cytotoxic agents.

Since their first description in 2000, the hallmarks of cancer have grown and evolved. In addition to the original six, at least two others have been added, namely alterations to cellular metabolism and immune cell evasion.¹⁸ Moreover, several accompanying traits of cancer cells were suggested by Luo, Solimini, and Elledge in 2009 that are particularly relevant to targeted therapy. These are the so-called “stress phenotypes” of cancer, and include metabolic stress, proteotoxic stress, oxidative stress, DNA damage stress, and mitotic stress.¹⁹ The authors suggest that tumors must survive these normally deadly conditions through the recruitment of cellular stress-

support pathways. These support pathways are termed oncogene addictions (OA) when associated with mutated cellular machinery and non-oncogene addictions (NOA) in any other case. Targeted therapies disrupt these support pathways, usually with small-molecule inhibitors of proteins, possibly killing cancer cells selectively through what the authors call “stress sensitization” or “stress overload” (Figure 1.3).

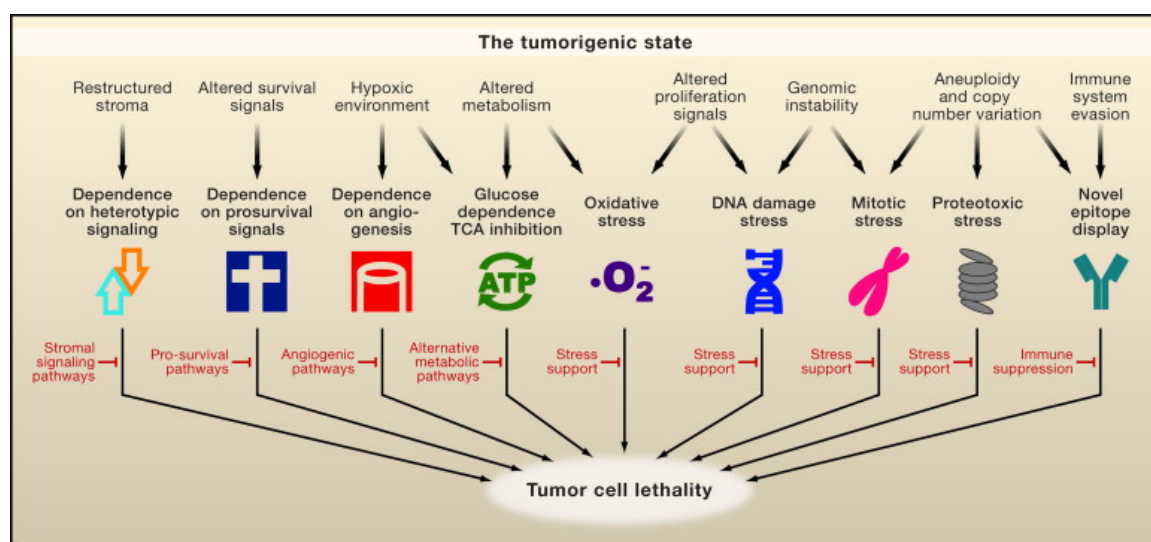


Figure 1.3. Principles of targeted therapy. The hallmarks of cancer are associated with additional stress phenotypes. Targeted therapies work by disrupting the cellular OA or NOA pathways that allow tumors to survive in these environments. Used with permission.¹⁹

One of the first and most successful examples of a targeted cancer therapy is that of Gleevec (Imatinib, marketed by Novartis). Developed to treat chronic myeloid leukemia (CML), the increase in survival rates of recipients of the drug can only be called astonishing. Before Gleevec, only 30% of CML patients survived past five years; after Gleevec, this number rose to 89%.²⁰ Equally impressive was the relative lack of side effects compared to traditional treatments.²¹ Gleevec is the definitive case of exploiting an oncogene addiction through the use of small molecules. The drug works through

inhibition of Bcr-Abl kinase, the product of a reciprocal translocation mutation between chromosomes 9 and 22 (Figure 1.4).^{22,23} Remarkably, Bcr-Abl is solely responsible for the onset of this type of leukemia.²⁴ The Abl protein is a tyrosine kinase, and when fused to Bcr becomes hyperactive. The mechanism of action of Gleevec is simply ATP-competitive inhibition of Bcr-Abl,²⁵ and this results, in the majority of cases, in complete remission for CML patients.

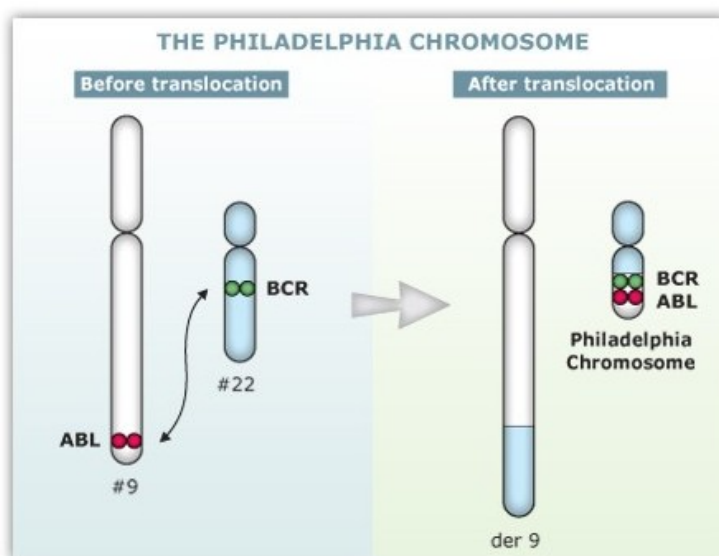


Figure 1.4. The chromosomal translocation responsible for the generation of the Bcr-Abl gene. The resultant mutated chromosome is also termed the "Philadelphia Chromosome."²³

While the supreme success of Gleevec in treating CML is unique and may not be replicated completely for other cancers, it is a testament to the great potential of this type of drug. With knowledge of the biomolecular systems driving cancer, drugs can be designed to specifically target tumors; this can result in greater efficacy and therapeutic indexes. Most cancers, however, are unlike Bcr-Abl-positive CML, in that they arise under more complex circumstances. For this reason, and to combat the sobering

problem of acquired drug resistance, future targeted therapies are likely to be used in conjunction with today's conventional treatments.²⁶

In the years following the release of Gleevec, a multitude of biological systems have been identified as candidates for targeted therapy. Since 2000, the FDA has approved at least fifteen such compounds for clinical use, and twenty additional kinase inhibitors are currently in clinical trials.²⁷ Again, these molecules are targeted to the hallmarks of cancer and their associated OA and NOA tumor liabilities. An interesting example of such a liability is the dependence of tumors on the action of S1P, a pleiotropic lipid-signaling molecule. In the following sections, the physiology and pathophysiology of lipid signaling in general and S1P signaling in particular are described.

1.5 Cellular signaling and important glycerolipid messengers

The influence of second-messengers on nearly all aspects of cellular physiology cannot be overstated. This is evidenced by the sheer number of proteins that deal in some way with signaling; genome sequencing has revealed that at least half of the large protein families play a role. The coordinated reception of molecular signals and their subsequent transduction can affect gene expression, enzymatic activity, and even the life or death of a cell.^{28,29} Biochemically speaking, the responses to external stimuli take the form of changes in concentration of intracellular pools of molecular messengers, which in turn mediate further responses or cascades. Common second messengers

include calcium ions, cyclic adenosine monophosphate (cAMP), inositol 1,4,5-trisphosphate (IP₃), and 1,2-diacylglycerol (DAG).³⁰ During the last few decades, the importance of lipid messengers in particular has become apparent in human molecular physiology.

While originally thought to serve only two main purposes, namely as energy storage molecules and building blocks for cellular membranes, lipids now are known to play integral roles as cellular messengers. Generally, while the results of such signaling are legion, the mechanisms by which cellular responses are initiated fall into two categories: intracellular messengers bind to protein kinases or phosphatases, and intercellular messengers bind almost exclusively to G protein-coupled receptors (GPCRs). Perhaps the most widely studied example of a kinase-binding lipid is that of DAG.³¹ Cellular levels of DAG can be rapidly increased through stimulation of phospholipase C and D (PLC and PLD) by phosphatidylinositol 4,5-bisphosphate (PIP₂) or phosphatidylcholine (PC), respectively.^{32,33} Once generated, DAG elicits its effects by binding to and activating protein kinase C (PKC), which then participates in processes as diverse as cell growth, receptor desensitization, transcription regulation, and even learning and memory.³⁴ Another important glycerolipid is lysophosphatidic acid (LPA), which binds to six different GPCRs expressed throughout the body. These LPA receptors (LPAR₁₋₆) mediate responses such as cellular growth, proliferation, and migration.³⁵ The pathophysiological roles of glycerolipids such as DAG and LPA have been extensively studied, and small-molecules that affect their synthesis or receptors may prove

therapeutically valuable.³⁶ Currently, several LPAR agonists or antagonists are in various stages of development or in clinical trials, including an LPAR_{1/3} antagonist, **VPC12249**, from our own laboratory (Figure 1.5).^{35,37}

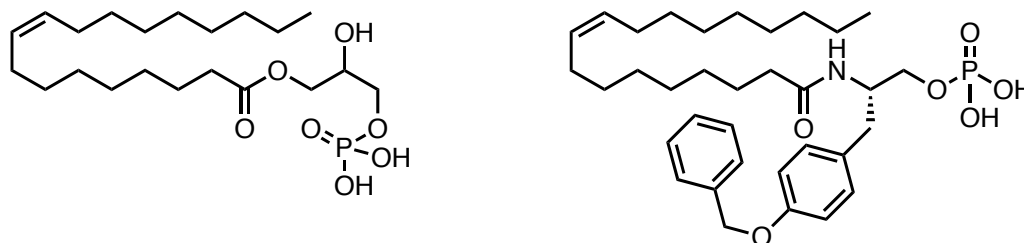


Figure 1.5. Lysophosphatidic acid (left) and LPAR_{1/3} antagonist VPC12249 (right).

1.6 The sphingolipid rheostat and the fate of cells

Like the thoroughly investigated glycerolipids described in the previous section, sphingolipids have recently been identified as critically important intra- and intercellular messengers. Sphingolipids are generally derived from sphingomyelin, another membrane lipid, in response to various physiological triggers, but can also be synthesized *de novo* from palmitoyl-CoA and serine.³⁸ The three most important sphingolipids, ceramide (Cer), sphingosine (Sph), and sphingosine 1-phosphate (S1P), are present in varying concentrations within cells, and the relative balance of these may play a fundamental role in dictating the cell survival or death; this balance, often called the sphingolipid “rheostat,” is strictly regulated by several important enzymes (Figure 1.6). This rheostat has such a profound effect on cellular fate because the lipids involved elicit dramatically different responses as messengers; Cer and Sph are generally anti-

proliferative and pro-apoptotic, while S1P is anti-apoptotic and pro-mitogenic. Briefly, the physiological regulation and effects of each sphingolipid are described here.

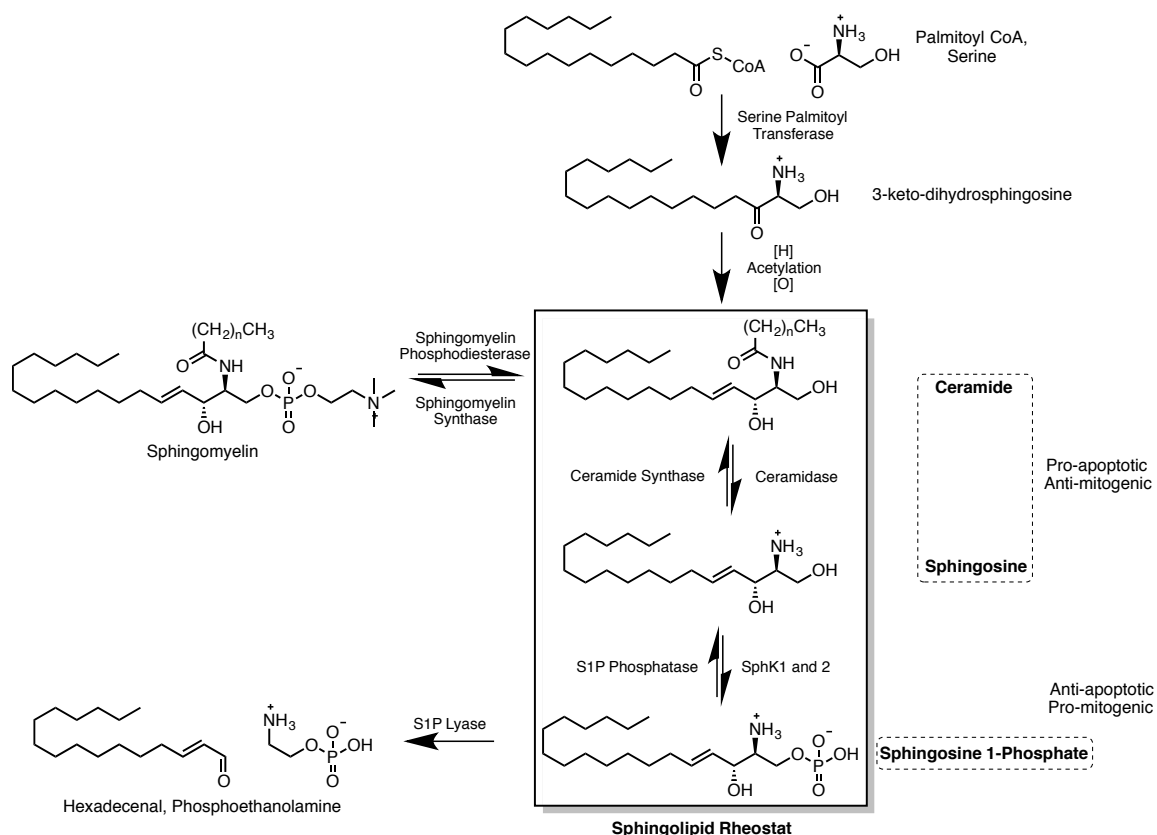


Figure 1.6. Sphingolipid metabolism and the sphingolipid rheostat. Cellular levels of Cer, Sph, and S1P are tightly regulated and influence cell fate.

As early as 1996, many of the roles of Cer as a second messenger had already been determined. Overwhelmingly, Cer production is greatly accelerated in response to cellular stress and damage; specifically, Cer accumulation through sphingomyelin hydrolysis is initiated by extracellular signals such as tumor necrosis factor- α (TNF α), endotoxin, interferon- γ , Fas ligands, chemotherapy, irradiation, heat, and nerve growth factor.³⁸ Because it is generated in response to environmental stresses, it follows that Cer signaling triggers events such as cellular senescence and apoptosis. While the exact

mechanisms of Cer-mediated apoptosis are not completely clear, several effectors have been identified, including stress-activated protein kinases (SAPKs) JNK and p38, as well as cathepsin D, an aspartic protease that mediates various apoptotic pathways.³⁹ Additionally, Cer facilitates more general intracellular responses in a unique way: Cer-dense regions of cell membranes called “lipid rafts” help to localize and amplify extracellular signals.⁴⁰

The specific cellular targets of Sph are less well defined, but its overall effects are also apoptotic. Sph is a potent inhibitor of PKC, an activator of protein kinase A (PKA), and, intracellularly, binds to certain nuclear receptors to affect gene expression.^{39,41} Sph is also the natural substrate of sphingosine kinase 1 and 2 (SphK1 and 2), the two enzymes that are solely responsible for the production of S1P.

The third lipid component of the sphingolipid rheostat, S1P, primarily elicits opposing cellular effects. Present at concentrations much lower than either Sph or Cer, S1P is an extremely potent messenger that functions both extra- and intracellularly, and is associated with increased proliferation and resistance to apoptosis. The specific functions of S1P will be explored in greater detail in the next section.

Due to their ubiquity in the body and wide range of targets and effects, sphingolipids are essential to homeostasis in all eukaryotes. This also indicates that aberrant sphingolipid signaling can have dramatic pathological consequences. Thus, biomolecular agents that influence the sphingolipid rheostat may be therapeutically valuable, particularly for the treatment of cancer and hyperproliferative diseases.

1.7 Sphingosine 1-phosphate signaling in homeostasis

If Cer and Sph are “stop” signals for cells, S1P is a definitive “go.” S1P has been identified as a driver of such cellular processes as proliferation, migration, resistance to apoptosis, inflammation, and neovascularization.^{42,43} These types of processes have been observed in both complex and simple eukaryotes, ranging from humans and other mammals to flies, worms, slime mold, plants, and yeast. The ability of S1P to influence so many aspects of physiology once seemed extraordinary and mysterious, but became clear once targets of S1P were identified.⁴⁴ S1P not only acts intracellularly, but, much like its glycerolipid counterpart, LPA, functions in an inside-out manner to stimulate a series of G protein-coupled receptors (Figure 1.7). In this way, S1P can function in either an autocrine or paracrine manner.

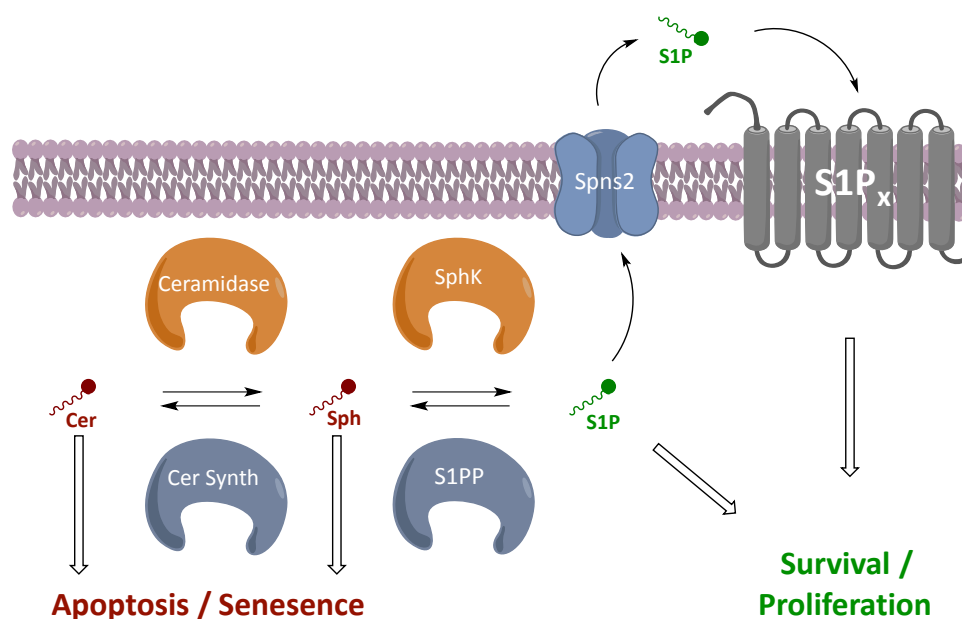


Figure 1.7. Sphingolipid metabolism and S1P signaling. S1P produced in the cell is shuttled into the extracellular milieu and binds to various S1P receptors, which initiate cell survival processes and other effects. Intracellular targets of S1P exist as well.⁴³

These widely expressed, membrane-bound GPCRs are called sphingosine 1-phosphate receptors 1-5 (S1P₁₋₅), and they mediate the vast majority of the effects of S1P. Each of S1P₁₋₅, depending on relative cell and tissue expression, as well as the specifically coupled G proteins, can elicit multiple cellular or physiological responses (Figure 1.8). The most crucial roles of S1P₁₋₅ are in regulation of vasculature, immunity, and nervous systems.⁴⁵ Specifically, these receptors mediate the development and integrity of vascular networks, influence heart rate, contribute to neuronal development, regulate lymphocyte trafficking, initiate inflammatory processes, stimulate migration, and influence various other processes.

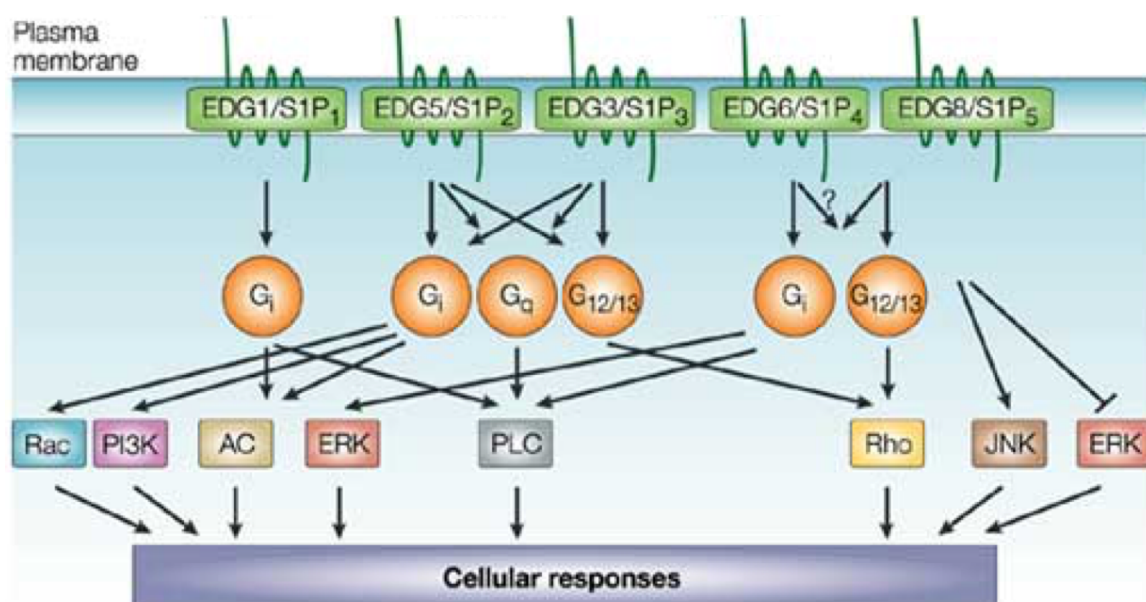


Figure 1.8. S1P receptors. S1P₁₋₅ elicit wide-ranging cellular responses through initiation of multiple enzymatic signaling cascades. Used with permission.⁴⁴

Although the existence of intracellular signaling functions of S1P has been known for the last two decades, the specific intracellular targets have not been made clear until more recently. These discoveries were made possible by advances in biotechnology, and

have revealed that S1P plays a role in mitochondrial function and assembly; affects gene expression by inhibiting histone deacetylases 1 and 2 (HDAC1 and 2); and acts as a cofactor for TRAF2 (TNF receptor-associated factor 2), which ultimately suppresses apoptosis.⁴⁶

While S1P is an essential player in the homeostasis of all eukaryotes, aberrant S1P signaling has been implicated in many different diseases.⁴⁷ Particularly, S1P has been shown to be an important contributor to the progression and onset of cancer. S1P signaling is an example of a tumor NOA, and for this reason may represent an attractive target for future cancer therapies.

1.8 Sphingosine 1-phosphate and cancer

Due to its proliferative effects as a signaling molecule, the roles of S1P in tumorigenesis are understandable, and are evidenced by increases in measured cellular levels of S1P in various types of cancer. This enrichment of S1P occurs by activation or upregulation of the SphKs, which is stimulated by a variety of growth factors, including TNF α (Figure 1.9).⁴⁸

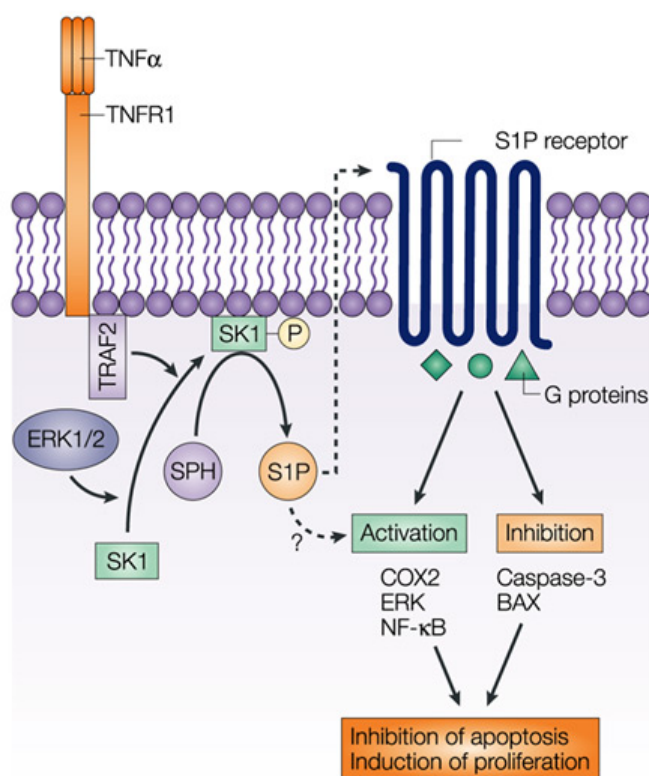


Figure 1.9. S1P production in response to growth factors. Growth factors such as TNF α facilitate ERK-catalyzed activation of SphK1 and a resultant increase in S1P signaling. Used with permission.⁴⁸

Aberrant S1P signaling has been linked to nearly every type of cancer, and feeds tumor addictions and dependencies through the promotion of processes such as cell growth, resistance to apoptosis, tumor angiogenesis, and metastasis.^{43,49} Additionally, the altered expression levels of the regulatory enzymes of S1P provide further evidence of the role of this lipid in cancer. In particular, overexpression of SphK1 appears to play a role in the onset and progression of stomach, colon, lung, brain, breast and kidney cancers, as well as non-Hodgkins lymphoma. This increased expression also correlates with lower patient survival rates.⁵⁰ The pathophysiological roles of SphK1 and SphK2 in cancer and other diseases will be examined in detail in the next chapter.

Overall, because of the constancy and prevalence S1P signaling in cancer, this pathway represents an extremely important and promising target for therapeutic modulation, and is currently an active and dynamic area of research in medicinal chemistry. The great difficulty in treating cancer, from a classical drug discovery standpoint, is the unpredictable nature of the genetic origins and drivers of the disease; the indictment and exploitation of S1P signaling is one solution to this problem, and may usher in a class of drugs that improve the survivability of numerous different types of cancer.

1.9 Conclusion

Today, cancer is the leading killer in developed countries, and is fast becoming a very serious problem all over the world. Recent decades have seen a huge increase in the scientific understanding of cancer, and with it, the promise of new and improved drugs. These drugs are targeted to the hallmarks of cancer, or, more precisely, the cellular support pathways upholding these hallmarks. S1P signaling, which involves the activity of several phosphatases, kinases, lipids, intracellular targets, and cell-surface receptors, has been implicated in numerous cancers and represents a prime target for therapeutic modulation. In the following chapter, the SphKs are described in greater detail, and specific examples of biomolecular intervention within the S1P signaling pathway are examined.

Chapter 2

Targeting Sphingolipid Signaling

The sphingolipid pathway has been identified as a critical regulator of a myriad of cellular processes including proliferation, angiogenesis, growth pathways, and ultimately cell survival and apoptosis. Several disease states in which aberrant sphingolipid signaling is implicated have been identified, including cancer, fibrosis, inflammatory diseases, and sickle cell disease. Thus, biomolecular agents that influence or alter sphingolipid signaling are therapeutically viable, and this has been proven by the success of the drug Fingolimod (FTY720), a S1P receptor agonist used to treat multiple sclerosis. However, the complexities of sphingolipid signaling present an interesting question: which enzyme or receptor in this pathway should be targeted to most effectively treat a disease? The answers may vary, but the sphingosine kinases, as the sole producers of S1P, are particularly attractive targets. Here, Fingolimod, the sphingosine kinases, and sphingosine kinase inhibitors are discussed in detail, and the early efforts to develop amidine-based SphK inhibitors are introduced.

2.1 Therapeutic validation of sphingolipid signaling: FTY720

FTY720 was synthesized in 1995 as a derivative of a fungal metabolite, myriocin (Figure 2.1), which inhibits the mixed lymphocyte reaction involved in immune responses. Indeed, FTY720 was found to suppress rejection of skin grafts in mice, but

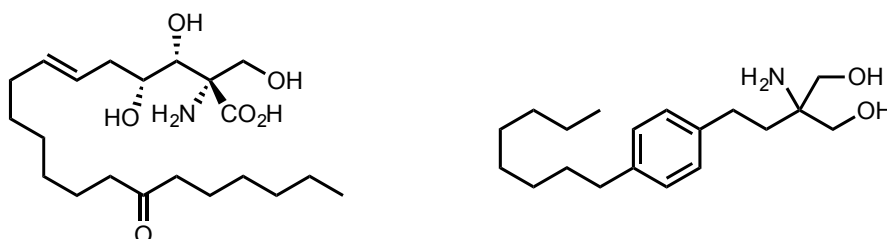


Figure 2.1. Structures of myriocin (left) and FTY720 (right).

did so at a concentration lower than the level required for *in vitro* inhibition of the mixed lymphocyte reaction. Later, FTY720 was found to deplete lymphocyte counts in blood, which was considered to be the cause of the *in vivo* efficacy of the compound in mice.⁵¹ Additionally, it was thought that this might occur through lymphocyte egress into the lymph nodes. For several years, however, the exact mechanism of this process was not known.⁵²

Soon, it was determined that activity of unspecified GPCRs was required for FTY720-stimulated lymphocyte trafficking. A study found that in lymphocytes pretreated with *Pertussis* toxin (PTX) to block all GPCR-G α i activity, FTY720 did not promote T-cell egress into lymph nodes.⁵³ The specific GPCRs were identified as S1P receptors, and the SphKs were indicated as activators of FTY720 (the drug is phosphorylated *in vivo* to yield FTY720-P),⁵⁴ but the drug was already in clinical trials for renal transplantation and multiple sclerosis before the specific SphK isoform responsible for its bioactivation was elucidated. The generation of both SphK1 and SphK2 null mice were essential to this discovery, as it was shown that no FTY720-induced lymphopenia was observed in SphK2 null mice.⁵⁵ This was sufficient to prove that FTY720 is phosphorylated to FTY720-P by SphK2 *in vivo* before it acts as a S1P receptor agonist.

The ability of FTY720 to act as a S1P₁ antagonist is essential to its success in treating relapsing-remitting multiple sclerosis (RRMS). The phosphorylated FTY720-P displays extremely high potency (0.3-0.6 nM) at S1P₁, S1P₄, and S1P₅; lesser potency at S1P₃ (3.1 nM); and no activity whatsoever at S1P₂. However, FTY720-P is a functional antagonist of S1P₁, causing lymph node-internalization and subsequent degradation of this receptor in lymphocytes; this effectively diminishes S1P-induced pro-inflammatory and immune responses that lead to neuronal demyelination in RRMS (Figure 2.2).⁵⁶

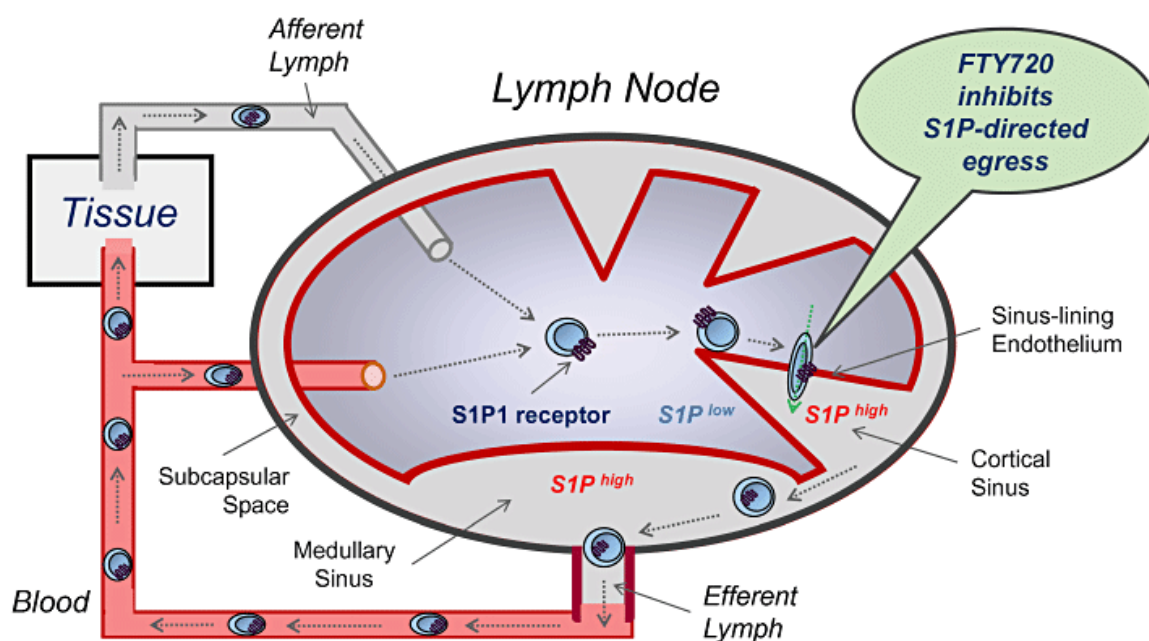


Figure 2.2. FTY720 mechanism of action. FTY720-P binds to S1P₁, causing receptor internalization and degradation. This limits S1P-induced lymphocyte egress from lymph nodes, reducing the levels of T-cells that damage neuronal myelin and lead to symptoms of multiple sclerosis. Used with permission.⁵⁶

The success of FTY720 demonstrates the therapeutic validity in targeting the S1P signaling pathway. FTY720 has inspired several other promiscuous and subtype-selective S1P receptor modulators that may improve upon the activity of FTY720 or prove useful in treating diseases other than RRMS. However, S1P receptors represent just one cog in

the sphingolipid signaling machinery. As the sole physiological producers of S1P, the two SphKs are an obvious target for therapeutic intervention. The biological roles and current inhibitors for these kinases are described in the following sections.

2.2 Sphingosine kinase 1: properties and roles in physiology and disease

Of the two sphingosine kinases, SphK1 is the more extensively studied. The clear importance of sphingolipids in regulating a host of cellular functions led researchers to identify, purify, and later clone this kinase, in order to study its roles more completely. In 1998, SphK1 was isolated and purified to homogeneity from rat kidney, allowing for some fundamental biological information to be determined. Namely, SphK1 is ~49 kDa in mass; the active form is a monomer; SphK1 shows substrate specificity for Sph and does not phosphorylate similar lipids such as phosphatidylinositol, DAG, Cer, DL-threo-dihydrosphingosine (DHS), or N,N-dimethylsphingosine (DMS); the K_M values for both Sph and ATP were identified as 5 and 93 μ M, respectively (though a more accurate value of 10 μ M would later be found for Sph); and the first competitive inhibitors of the kinase, DHS and DMS were identified.⁵⁷ This work from the laboratory of Sarah Spiegel provided much-needed fundamental information about SphK1, including the peptide sequence, which allowed for the cloning of the kinase in rats, *S. Cerevisiae*, and humans in later studies.⁵⁷⁻⁵⁹ Database searches have revealed that the SphK1 gene is highly conserved in eukaryotes, providing further evidence of the widespread importance of the enzyme. Other fundamental properties of SphK1 were identified relatively early.

SphK1 tissue distribution is widespread, but levels are highest in lung, liver, and spleen. Finally, the enzyme is located primarily in the cytosol, but upon phosphorylation by PKC, is activated and translocated to the plasma membrane.^{60,61}

Cloning of SphK1 has allowed for investigation of the enzyme in various physiological states. Overexpression of SphK1 in various cell types results in greater intracellular concentration of S1P, with levels of S1P in membrane and cytosol increasing equally. This suggests an ability of S1P to cross cellular membranes and enter various cell microdomains or organelles. Overexpression also stimulates cell growth, as evidenced by shortened doubling times.⁵⁹ Overwhelmingly, the effects of SphK1 are summarized in terms of growth, proliferation, and survival. This may be due, in large part, to the subcellular location of SphK1, because the S1P it produces is in proximity to S1P transport proteins; ultimately, this facilitates interaction with and stimulation of S1P receptors responsible for many of the effects of S1P. The compartmentalization of SphK2 is quite different, and the consequences of this special differentiation will be described in the next section.

Finally, SphK1 in particular has been implicated as an important contributor to cancer as well as several different diseases involving inflammation, immunity, or hyperproliferation. In several different types of cancer, high expression levels of SphK1 are observed and correlate with lowered patient survival rates. Further, evidence of SphK1 contributing to inflammation is provided by siRNA knockdown of SphK1 in mouse models of arthritis, in which a reduction in inflammation is observed.⁵⁰ While the

complexities of S1P signaling shroud the specifics of the roles of SphK1, it is clear that this kinase is an active contributor to human pathological conditions, and thus, an important target for biochemical modulation.

2.3 Sphingosine kinase 2: different by sub-cellular localization

In an investigation similar to the one done for SphK1, the laboratory of Sarah Spiegel first characterized and cloned both mouse and human SphK2 in 2000.⁵⁸ The enzyme was identified when database searches revealed sequences conserved in SphK1 that were present in other distinct genes. Cloning of SphK2 revealed that it is much larger than SphK1, with 618 residues to the 384 of SphK1. Tissue distribution is also different; SphK2 is ubiquitously expressed, but highest levels are found in cardiac and liver tissues. Kinetic constants vary as well, with the K_M values of SphK2 for Sph and ATP being approximately 5 μM and 80 μM , respectively.^{58,62} Interestingly, SphK2 and SphK1 displayed different substrate and inhibitor specificities: DHS is a better substrate of SphK2 than Sph; DMS inhibited SphK2, but did so in a non-competitive manner. DMS was the first identified and is still one of the best dual inhibitors of the SphKs. Overall, this study elucidated important, foundational biological characteristics of SphK2, and provided a method for the cloning of this kinase.

Key insights into SphK2 biology are gleaned by examining DNA sequence similarity and divergence from SphK1. The two kinases are largely similar, sharing 80% similarity and 45% overall sequence identity; additionally, there are five domains (C1-

C5) that are highly conserved in all SphKs, and are likely involved in substrate binding and catalysis. SphK2 differs from SphK1 in two discrete regions, one extending from the N-terminus that has been identified as a nuclear-localization sequence (NLS),⁶³ and one proline-rich region near the center (Figure 2.3.)⁶⁴

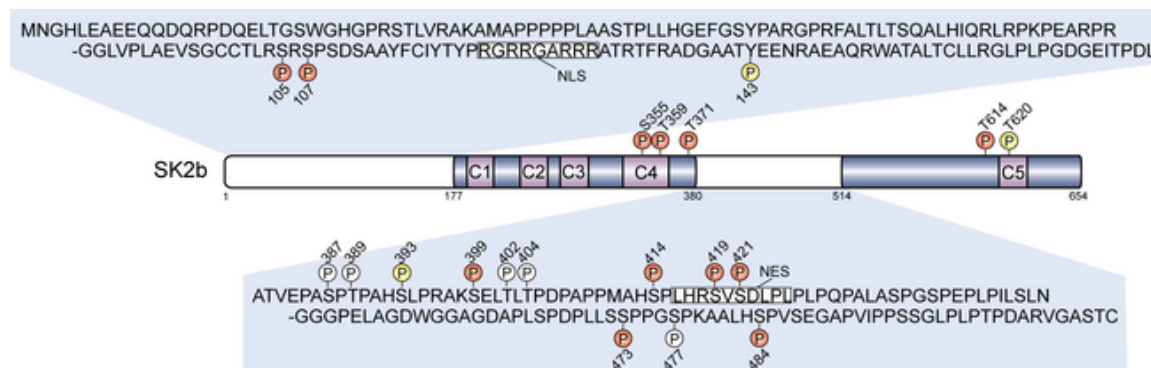


Figure 2.3. SphK2 functional domains. SphK2 shares five (C1-C5) highly conserved domains with SphK1. Shaded regions are largely similar to SphK1. The white regions are unique to SphK2, and include an NLS in the N-terminus, and a proline-rich region near the center. Used with permission.⁶⁴

This non-conserved NLS has profound effects on the cellular roles of SphK2 in physiology and disease; because they each produce S1P, the provenance of the differing effects of SphK1 and SphK2 largely stem from sub-cellular localization. The predominance of SphK2 in the nucleus was confirmed in 2003; several cell lines (COS7, HeLa, NIH 3T3) were transiently expressed with hSphK2, stained with anti-hSphK2 antibody, and analyzed by confocal microscopy. Additionally, this was the first study to identify a curious and seemingly contrary effect of overexpression of SphK2—it can actually cause apoptosis through inhibition of DNA synthesis. This effect is completely different from any SphK1-induced cellular response, and is completely dependent upon nuclear localization of the protein. When the NLS is deleted from SphK2, the protein cannot enter the nucleus and inhibit DNA synthesis; notably, appendage of the NLS

sequence to SphK1 causes this protein to enter the nucleus and initiate apoptosis and growth arrest as well.⁶³ The mechanism of this process was elucidated in 2009, when S1P generated by SphK2 was found to directly bind to and inhibit the enzymatic activity of HDAC1 and HDAC2. This results in increased transcription of cyclin-dependent kinase inhibitor p21 and c-fos, which likely contributes to the growth-arresting effects of SphK2 (Figure 2.4).^{64–66}

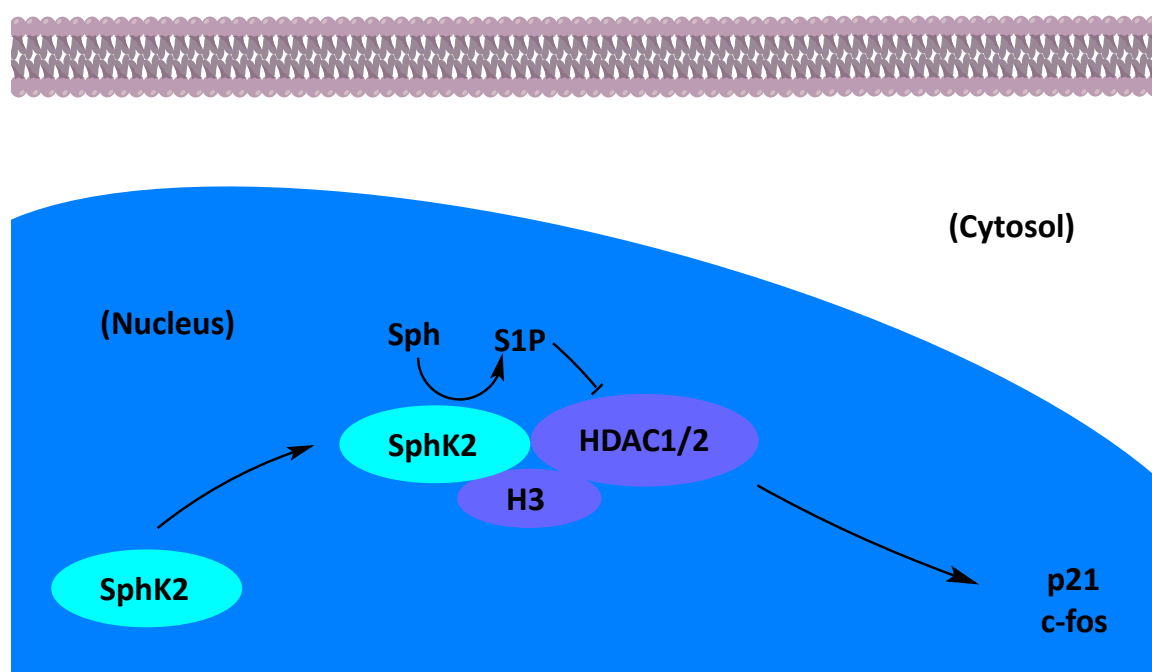


Figure 2.4. Nuclear S1P inhibits HDAC1/2, influences gene-expression. S1P produced by SphK2 in the nucleus is a direct inhibitor of HDAC1/2 enzymatic activity. This leads to higher expression levels of p21 and c-fos, and ultimately leads to apoptosis. Nuclear S1P thus elicits dramatically different effects than cytosolic S1P.⁶⁶

This ability to elicit pro-apoptotic effects makes ascribing concrete physiological roles to SphK2 exceedingly difficult. Interestingly, there is evidence of SphK2 contributing to apoptosis from other mechanisms. Specifically, siRNA knockdown studies of SphK2 in HEK 293 or mouse fibroblast cells prevented apoptosis by $\text{TNF}\alpha$, and

cells taken from SphK2^{-/-} mice displayed greater resistance to staurosporine-induced apoptosis than wild type cells, or even cells from SphK1^{-/-} mice.⁶⁴ These capabilities are highly unexpected for an enzyme that produces S1P.

Finally, while SphK2 is a clear contributor to apoptosis, it also displays traits that are similar to those of SphK1 and S1P in general (Figure 2.5). This is made clear in studies of SphK knockout mice, which have shown that the absence of either kinase can be compensated for by the other, but the absence of both is fatal; SphK1^{-/-} or SphK2^{-/-} mice are viable, fertile, and without obvious abnormal phenotype, but mice lacking both enzymes die in the embryonic stage due to insufficient formation of vasculature and neurologic systems.⁶⁷ There is also substantial evidence of SphK2 contributing to cancer, inflammation, sickle cell disease, immune disorders, and osteoarthritis.⁶⁴ The

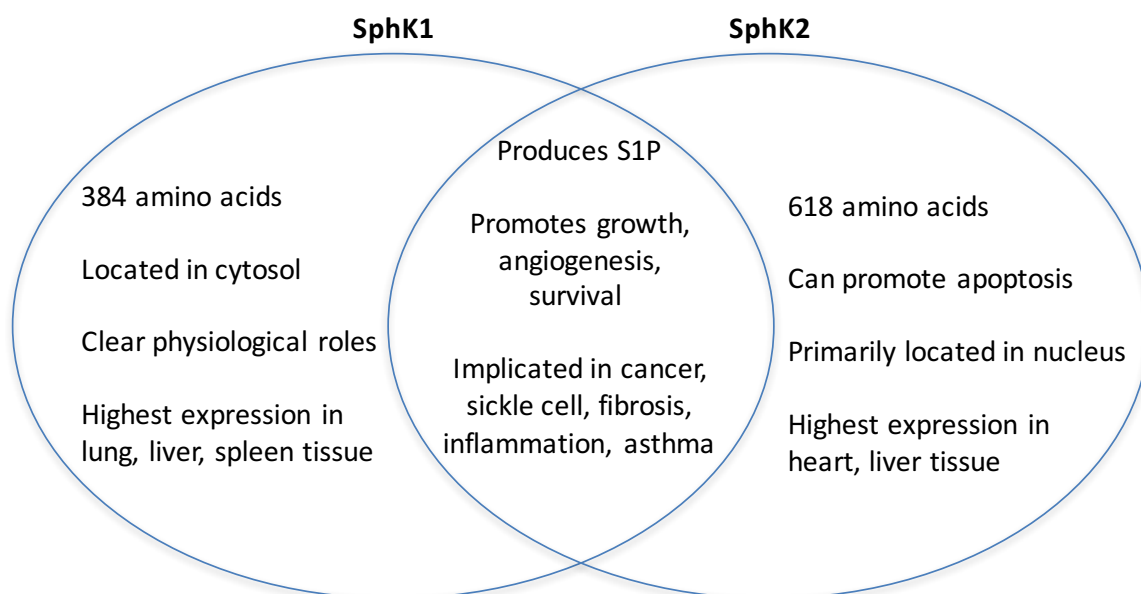


Figure 2.5. Shared and differing traits of SphK1 and SphK2. While different in several clear ways, each SphK can compensate for the absence of the other under normal physiological conditions, but a genotype lacking both kinases is fatal.

contradictory nature of SphK2 in both physiology and pathology warrants greater investigation into the mechanisms behind SphK2-specific S1P signaling. The following section will describe the successes and shortcomings in the development of a powerful class of tools used to probe and understand both of the SphKs, and ultimately, treat diseases in which they are implicated.

2.4 Sphingosine kinase inhibitors

FTY720 demonstrated the therapeutic viability in targeting S1P signaling through modulation of the S1P receptors. SphK inhibitors are used to intervene earlier in this metabolic and signaling pathway, by limiting S1P biosynthesis by the two SphKs. The earliest SphK inhibitors included lipid-based inhibitors such as DMS and DHS, as well as structurally unique compounds such as SKI-II and ABC294640 (Figure 2.6). All of these molecules were only moderately potent, but proved essential in the elucidation of

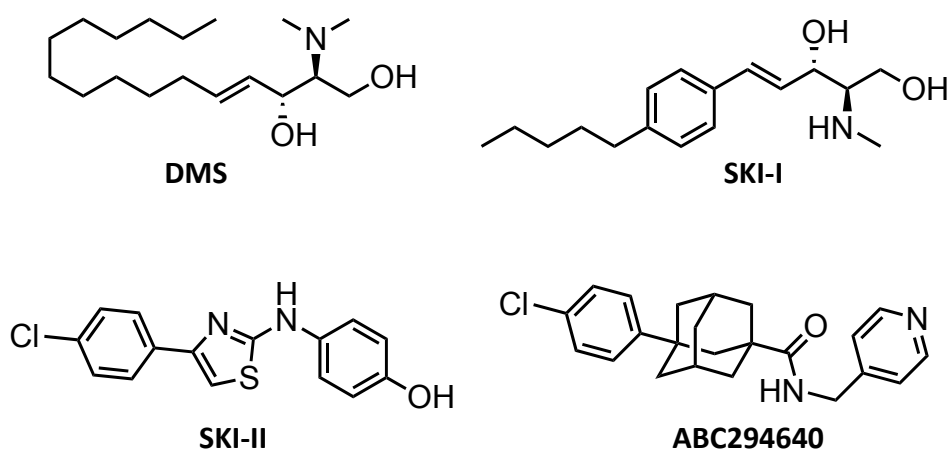


Figure 2.6. Early SphK inhibitors. These molecules were moderately potent (low micromolar range), and proved effective in several different animal disease models. However, their lack of selectivity for the SphKs limits diagnostic viability.

effects of SphK inhibition. DMS in particular has been used extensively, and has shown efficacy in inducing apoptosis in cancer cells through SphK1 inhibition. Additionally, DMS has been employed in animal inflammatory disease models such as asthma and arthritis, to good effect. Similar results have been observed for other early SphK inhibitors.⁶⁸ However, these molecules are relatively non-selective, and show inhibitory activity at other enzymes including PKC, Cer kinase, SRC kinases, and MAPKs.⁶⁹ For this reason the efficacy of these molecules cannot be specifically attributed to SphK inhibition.

Later inhibitors have improved greatly on the early generation, both in terms of potency and selectivity, and are refined enough to even distinguish one SphK over the other. Particular success has been achieved in targeting SphK1. Early efforts from our own laboratory produced a class of amidine-based inhibitors such as **1a** (Figure 2.7) that were the first to achieve double-digit nanomolar potency at SphK1 and high selectivity

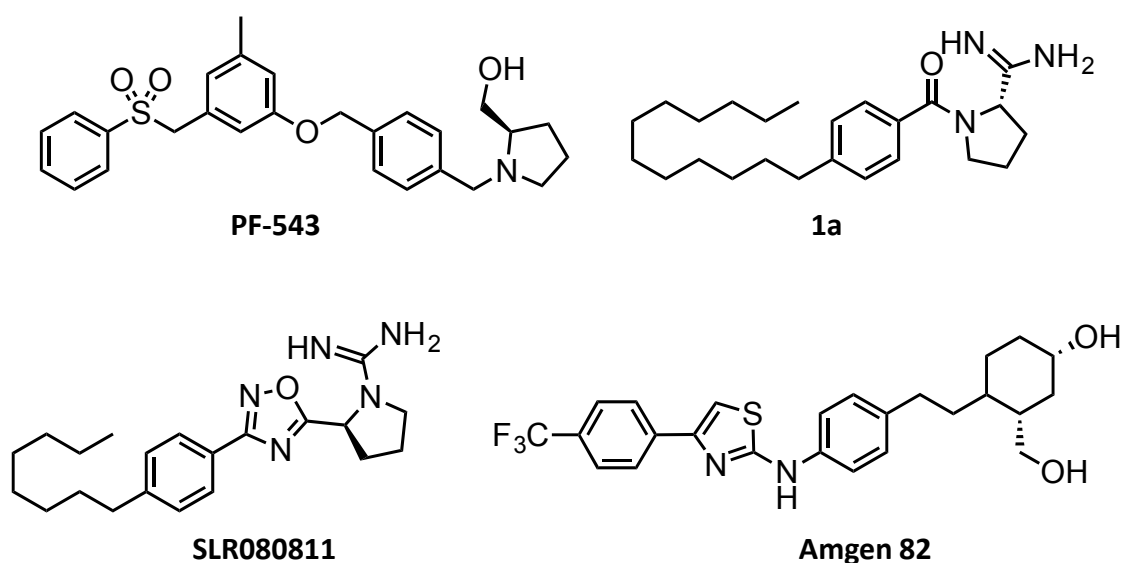


Figure 2.7. New and improved SphK inhibitors. SphK1-selective inhibitors (top) are highly potent and selective. SphK2-selective compounds (bottom) are less so, but in the last few years have seen significant improvements.

over SphK2 (these studies are summarized in the following section).^{70,71} The state of the art inhibitor, in terms of potency, is PF-543, which is the only inhibitor of either SphK to exhibit single-digit nanomolar potency.⁷² An inhibitor of comparable potency for SphK2 has yet to be identified. However, compounds such as the recently discovered **SLR080811** represent a significant advancement of the field. Developed in the Santos laboratory at Virginia Tech, **SLR080811** has a K_i of roughly 1 μ M, with 10-fold selectivity for SphK2 over SphK1.⁷³ Finally, with the aid of the newly characterized crystal structure of SphK1,⁷⁴ Amgen 82 was recently designed as a dual inhibitor of SphK1 and 2, with IC_{50} values at each kinase of 0.02 and 0.11 μ M, respectively.⁷⁵ At this time, Amgen 82 is the most potent dual inhibitor of the SphKs, and displays good pharmacokinetic properties.

This newer generation of inhibitors has allowed for more accurate interrogation of each SphK in cells and animal disease models, and some of the results have been, to put it mildly, highly unexpected. Unfortunately, PF-543, the most potent and selective SphK1 inhibitor, was completely ineffective in inducing apoptosis in cancer cells, even though S1P levels were significantly reduced.⁷² Similar results were observed for Amgen 82 and amidine-based compound 1a.^{76,77} This is not what was predicted by the sphingolipid rheostat model, but there are several possible explanations: (1) SphK1 degradation may be necessary in addition to inhibition (as occurs with administration of SKI-II),⁷⁸ (2) S1P reduction alone may be insufficient to reduce growth, and a buildup up of Cer and Sph may also be required, and (3) more *in vivo* studies with murine disease models may be necessary; the above studies were all done with cultured cancer cells.⁷⁹

Concerning SphK2, it must be repeated that the understanding of this kinase has been limited by inhibitor efficacy, and there are conflicting data regarding the role of SphK2 in cancer. Also, while the SphK2-selective compound SLR080811 effectively reduced S1P concentration in cells, it (and related SphK2-selective inhibitors⁸⁰) actually *raised* levels of S1P in blood when administered to mice.⁷³ This effect is the opposite of that observed for SphK1 inhibition, but matches the observed effect in SphK2 knockout mice. In any case, the effect of increasing blood S1P is now viewed as a useful biomarker of SphK2 inhibition, and may itself prove therapeutically useful for certain diseases.⁸¹

In summary, while the last decade has witnessed profound gains in the potency and selectivity of SphK inhibitors, the apparent complexity of S1P signaling has increased as well. Small-molecule inhibitors have been valuable tools in beginning to uncover the roles of SphK1 and SphK2, and more advanced molecules will continue to do so in the near future. The ideal “pharmacological probe” of the SphKs will have the following characteristics: (1) single-digit nanomolar potency, (2) greater than 100-fold selectivity for either SphK, and (3) sufficient safety and stability to be deployed in animal disease models.⁸¹ These qualities will likely be important for any clinical drugs as well. For these reasons, the development of SphK inhibitors remains an active, relevant, and important avenue in medicinal chemistry today.

2.5 Early amidine-based inhibitors of SphK1

Our own laboratory provided some of the first potent and selective inhibitors of SphK1. The lead molecule from this series was derived from a S1P receptor agonist and selective substrate of SphK2, (*R*)-**VPC45129**. With the goal of converting this substrate into an inhibitor, we attempted to synthesize a derivative in which the hydroxyl moiety that is phosphorylated by SphK2 was deleted. However, as a result of an unexpected reductive cleavage of the oxadiazole during this synthesis, an amidine-based compound, **VPC94075**, was isolated instead. Fortunately, this molecule displayed slight inhibition of both SphKs (K_i of 55 μ M and 20 μ M for SphK1 and SphK2, respectively), so provided an ideal lead molecule that was subsequently divided into four discrete regions for structure-activity relationship (SAR) investigation (Figure 2.8). These regions were optimized to identify a pharmacophore comprised of an amidine head group, a cyclopropyl linker substituent, an amide bond, and a phenyl ring with a 12-carbon, *para*-substituted aliphatic tail.⁷⁰ Later, with the aid of a SphK1 homology model, derivatives with rigidified tails were synthesized that granted these compounds potency in the double-digit nanomolar range and high selectivity for SphK1.⁷¹ At the time, these were the most potent and selective inhibitors developed for this kinase, and they revealed key SAR information that informed the design of later compounds.

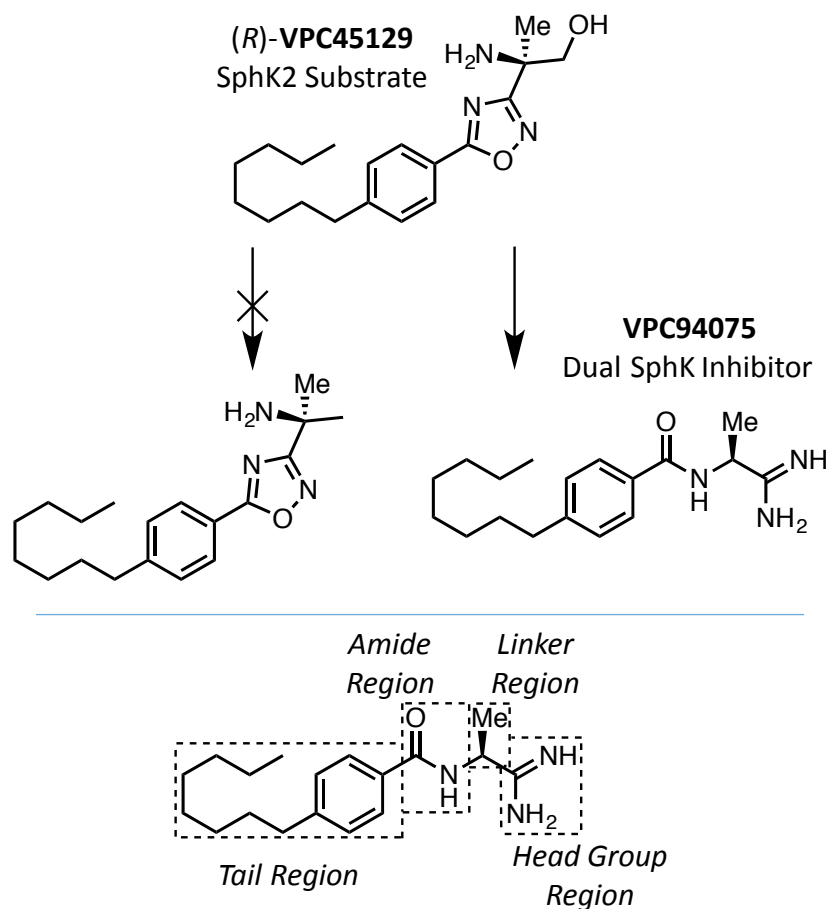


Figure 2.8. Design and SAR strategy of early SphK inhibitors. VPC94075, a derivative of the SphK2-selective substrate VPC45129, was a weak inhibitor of both SphKs. SAR studies led to the identification of highly potent amidine-based SphK1 inhibitors.

While our amidine-based compounds remain among the most potent inhibitors available today, they have yet to be optimized. The most significant limitation of these compounds is their half-life *in vivo*. Intraperitoneal injection of compound **5** in mice revealed rapid clearance or metabolism, and a half-life of less than two hours (Figure 2.9). This is likely due to hydrolysis of the amide bond, a key component of the scaffold of these inhibitors. In the following chapter, the work done to circumvent this issue will be described.

Half-life *in vivo* of compound 5

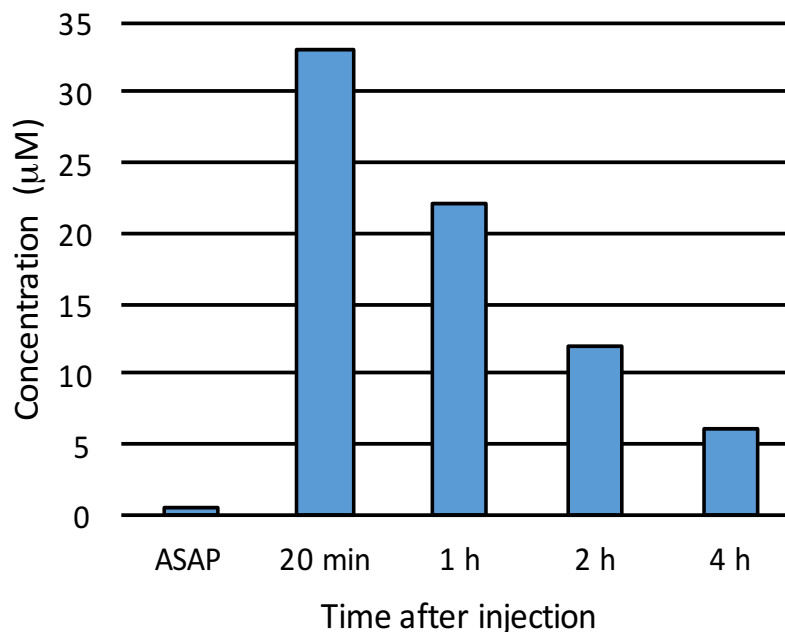


Figure 2.9. Metabolism of compound 5. In vivo studies in mice revealed rapid metabolism of our compounds.

2.6 Conclusion

Due to the complex roles of sphingolipid signaling in human physiology and disease, biomolecular agents that modulate this pathway are valuable investigative tools, and have potential as drug candidates. The S1P receptor agonist, FTY720, is an effective drug used to treat RRMS and a great example of the utility in targeting this pathway. Other enzymes involved in sphingolipid biosynthesis are viable targets as well, and the two SphKs, as the sole producers of S1P, are of particular interest. These enzymes are similar in many ways, but differ significantly in size and subcellular localization; for these and other reasons, deciphering the complex roles of the SphKs is

difficult. The development of SphK dual and subtype-selective inhibitors is a rapidly advancing area of research, and promises to clarify SphK biology and potentially identify a drug to improve the treatment of a myriad of debilitating diseases. Our laboratory has identified a class of highly potent, SphK1-selective amidine-based inhibitors, but these compounds are limited by a short half-life *in vivo*. The following chapter describes the strategy employed to improve these molecules, reveal key inhibitor-enzyme interactions, and ultimately identify the most selective inhibitor of SphK1 reported to date.

Chapter 3

Amide Bioisosteres in Amidine-Based SphK1 Inhibitors

In an effort to improve the half-life of our earlier amidine-based compounds, a new series was explored in which the amide functionality was replaced. The most effective substitution was a 1,2,4-oxadiazole, but several other moieties were explored. This led to significant gains in potency and selectivity for SphK1, but came at the expense of certain pharmacological properties, namely blood concentration and cellular uptake. The design, synthesis, and evaluation of these molecules is described, as well as the methods employed to mitigate their pharmacological deficiencies.

3.1 Structural requirements and docking analysis of amidine-based sphingosine kinase 1 inhibitors containing oxadiazoles

Note: Section 3.1 has been published in an issue of *ACS Medicinal Chemistry Letters*.⁸²

Joseph Daniel Houck, Thomas Keith Dawson, Andrew John Kennedy, Yugesh Kharel, Neils D. Naimon, Sandra Denise Field, Kevin R Lynch, and Timothy L. MacDonald

ACS Medicinal Chemistry Letters **Article ASAP**

DOI: 10.1021/acsmedchemlett.6b00002

Publication Date (Web): March 1, 2016

Copyright © 2016 American Chemical Society

ABSTRACT: Sphingosine 1-phosphate (S1P) is a potent growth-signaling lipid that has been implicated in cancer progression, inflammation, sickle cell disease, and fibrosis. Two sphingosine kinases (SphK1 and 2) are the source of S1P, thus inhibitors of the SphKs have potential as targeted cancer therapies and will help to clarify the roles of

S1P and the SphKs in other hyperproliferative diseases. Recently, we reported a series of amidine-based inhibitors with high selectivity for SphK1 and potency in the nanomolar range. However, these inhibitors display a short half-life. With the goal of increasing metabolic stability and maintaining efficacy, we designed an analogous series of molecules containing oxadiazole moieties. Generation of a library of molecules resulted in the identification of the most selective inhibitor of SphK1 reported to date (705-fold selectivity over SphK2) and we found that potency and selectivity vary significantly depending on the particular oxadiazole isomer employed. The best inhibitors were subjected to *in silico* molecular dynamics docking analysis, which revealed key insights into the binding of amidine-based inhibitors by SphK1. Herein, the design, synthesis, biological evaluation, and docking analysis of these molecules are described.

Sphingosine 1-phosphate (S1P) is a potent signaling lipid that acts on five membrane-bound receptors (S1P1-5)⁸³ and various intracellular targets.⁴³ S1P has been shown to regulate a host of processes that affect the growth and fate of cells,⁸⁴ and aberrant S1P signaling has been linked to numerous diseases including cancer,^{43,68} asthma,⁸⁵ fibrosis,⁸⁶ and sickle cell disease.⁸⁷ Cellular synthesis of S1P is exclusively dependent on the action of two sphingosine kinases (SphK1 and 2) that directly phosphorylate sphingosine (Sph).⁸⁴ As the sole sources of cellular S1P, the SphKs influence cell survival,^{42,66} and have been identified as targets of interest in pharmacology and the pharmaceutical industry.^{68,81} Therefore, SphK inhibitors, by

affecting S1P levels, have therapeutic potential and are necessary to clarify the many roles of S1P and each SphK in physiology and disease.^{69,81,88}

S1P signaling is complex, and the roles of SphK1 and 2 in various pathways differ significantly. These differences are due, in large part, to subcellular compartmentalization; SphK2 possesses an N-terminal nuclear localization sequence not present in SphK1.⁶³ Indeed, SphK2 is located primarily in the nucleus and other organelles, and may influence gene expression through S1P-dependent inhibition of histone deacetylase 1 and 2 (HDAC1 and 2).⁶⁵ Additionally, S1P produced by SphK2 in the endoplasmic reticulum and mitochondria has the effect of stimulating apoptosis.⁶⁴ In contrast, SphK1 is located primarily in the cytosol, and SphK1-derived S1P generally elicits pro-survival and proliferative effects through interactions with S1P1-5. Upon phosphorylation by the extracellular-regulated kinases, SphK1 is activated and translocated to the inner leaflet of the plasma membrane.⁸⁹ Then, in an inside-out signaling mechanism, S1P is shuttled outside the cell by the membrane-spanning spinster 2 protein (or by members of the ABC transport family), where it may bind with any of the G protein-coupled S1P1-5. Agonism at these receptors initiates a cascade of signaling events affecting growth, motility, immune cell trafficking, metastasis, and angiogenesis.⁶⁹

Because of the complexity of S1P signaling, a large and diverse set of pharmacological tools is necessary to probe the underlying physiological pathways and conclusively validate both SphK1 and 2 in different disease models. Small-molecule SphK

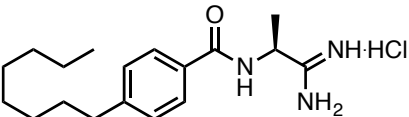
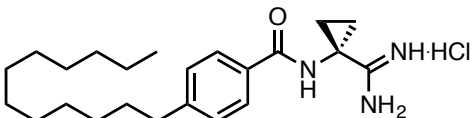
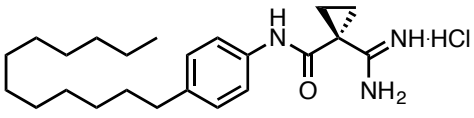
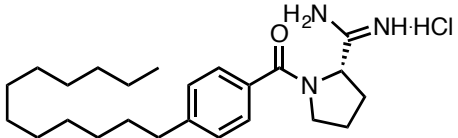
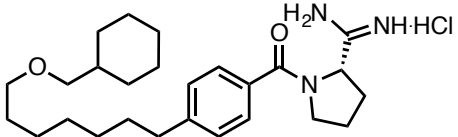
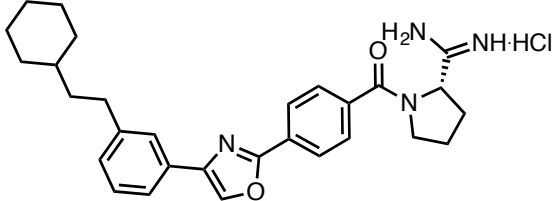
inhibitors are an important example of such a tool, and ideally should have the following characteristics: single-digit nanomolar potency, at least 100-fold selectivity for either of the SphK isoforms, and high metabolic stability.⁸¹ Currently, no single molecule fulfills each criterion simultaneously, but a new generation of inhibitors is nearing this mark. In particular, recent efforts to improve our highly potent (but unstable) amidine-based inhibitors have yielded a class of very effective guanidine-based, oxadiazole-containing molecules.^{80,90,91} These compounds are the most potent and selective inhibitors that elicit prolonged shifts in blood S1P concentrations; the ability to lower or raise blood S1P levels is an important biomarker for inhibition of SphK1 or 2, respectively.⁹²

To further improve SphK inhibitors, particularly regarding potency, it is necessary to continue to probe the Sph-binding pockets of SphK1 and 2 with structurally diverse sets of molecules. To this end, we have developed and characterized a small library of molecules combining an amidine head group with various oxadiazole linkers, elaborating on our earlier studies.^{70,71} Herein, we report an inhibitor with double-digit nanomolar potency and 705-fold selectivity for SphK1 over SphK2. Additionally, we reveal two key insights into the structure-activity relationships governing SphK1 inhibition, namely that potency and selectivity are greatly affected by oxadiazole subtypes and alkyl tail positioning.

Our previous work yielded a series of amidine-based molecules displaying high potency and selectivity for SphK1. The lead molecule, **1**, was modified to optimize tail length, amide orientation, and head group identity (**2-4**, Table 3.1).⁷⁰ Further

improvements were the result of *in silico* screening of a library of molecules with varied, rigidified tails. This analysis was carried out with a SphK1 homology model based on diacylglycerol kinase beta, and yielded **6**, a SphK1 inhibitor with a K_i of 47 nM and 180-fold selectivity over SphK2 (Table 3.1).⁷¹

Table 3.1. Previously described amidine-based SphK inhibitors.^{70,71}

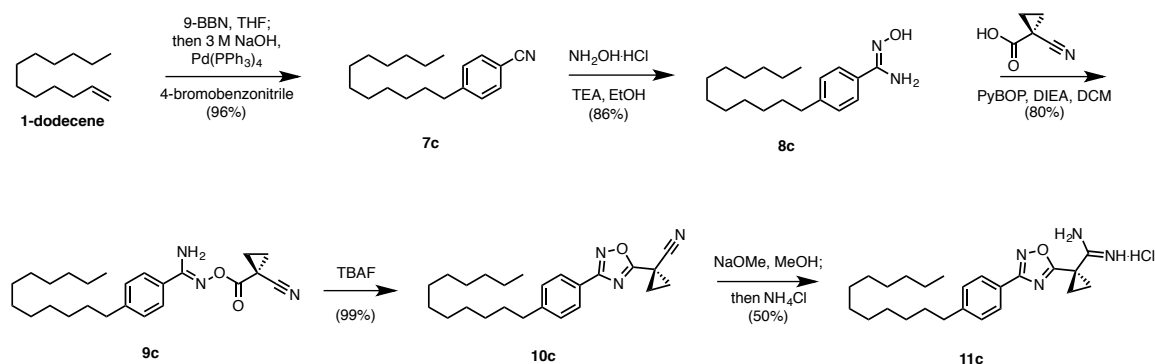
Compound	Structure	K_i (μ M) ^a		SphK1 Selectivity ^b
		SphK1	SphK2	
1 (VPC94075)		55	20	0.7
2		0.2	0.5	5
3		0.3	6	40
4		0.125	1.5	24
5		0.075	3.0	80
6		0.047	4.2	180

^a $K_i = [I] / (K_M / K_M - 1)$; K_M of sphingosine at SphK1 = 10 μ M; K_M of sphingosine at SphK2 = 5 μ M

^b Selectivity = $(K_i / K_M)^{\text{SphK2}} / (K_i / K_M)^{\text{SphK1}}$

In the work described presently, we followed a similar approach by optimizing a lead molecule with a library of synthetic variants and then following with *in silico* modeling. In this new series, the amide moiety was replaced with three distinct oxadiazoles; the reasoning for this is threefold: (1) our previous inhibitors have displayed poor half-lives *in vivo* and oxadiazoles are well-documented amide surrogates,^{93–97} (2) oxadiazoles have been effective structural subunits in our previous work with SphK2 substrates,⁹⁸ and (3) oxadiazole linkers improved the efficacy of guanidine-based SphK1 inhibitors.⁸⁰

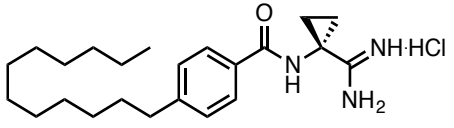
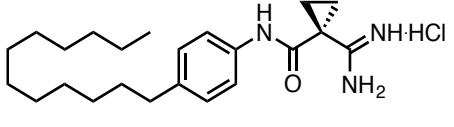
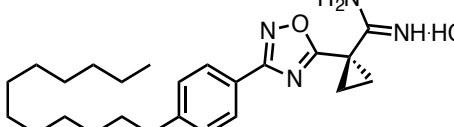
As a starting point, **11c**, an analogue of **2** and **3**, was synthesized as follows (Scheme 3.1). First, 1-dodecene was reduced to the alkyl borane with 9-BBN and coupled to 4-bromobenzonitrile using Suzuki conditions to p-alkylbenzonitrile **7c**. Next, conversion to aryl amidoxime **8c** was achieved using hydroxylamine hydrochloride and triethylamine in ethanol. PyBOP-mediated coupling of the amidoxime to 1-cyano-1-cyclopropanecarboxylic acid yielded **9c**. Cyclization of the coupled amidoxime with TBAF⁹⁹ gave oxadiazole **10c**, and was subjected to base-catalyzed Pinner conditions¹⁰⁰ to yield amidine **11c**.



Scheme 3.1. Synthesis of oxadiazole amidine **11c.**

K_i values were determined by a [γ - 32 P] ATP *in vitro* assay of SphK enzymatic activity (Table 3.2).⁶² **11c** maintains potency and SphK1 selectivity, validating the oxadiazole as a suitable replacement for the amide group.

Table 3.2. K_i values of oxadiazole **11c** compared to amides **2** and **3**.

Compound	Structure	K_i (μ M) ^a		SphK1 Selectivity ^b
		SphK1	SphK2	
2		0.2	0.5	5
3		0.3	6	40
11c		0.32	8	50

^a $K_i = [I] / (K_M / K_M - 1)$; K_M of sphingosine at SphK1 = 10 μ M; K_M of sphingosine at SphK2 = 5 μ M

^b Selectivity = $(K_i / K_M)^{\text{SphK2}} / (K_i / K_M)^{\text{SphK1}}$

The incorporation of an oxadiazole into the molecular scaffold significantly alters the angle between the tail and head groups. With this in mind, a variant of **11c** was synthesized with *meta*-substitution about the phenyl ring. Interestingly, upon attaching the tail at the *meta* position, potency and selectivity increased dramatically, with **11g** displaying a K_i of 40 nM and 705-fold selectivity for SphK1 over SphK2. As a control, a *meta*-substituted analog of our amide compounds, **13**, was synthesized (Scheme 3.2). **13** was quickly synthesized by coupling of 3-dodecylbenzoic acid directly to the amino

nitrile head group to give nitrile **12**, and then Pinner conditions deliver the final amidine product, **13**. This compound lost potency proportionately at both kinases (Table 3.3). *Meta*-substituted analogs present the amidine to the γ -phosphate of ATP such that the amidine is no longer perpendicular to the aromatic ring. Deletion of the cyclopropane ring alpha to the amidine resulted in a loss of activity in oxadiazole **15** (Scheme 3.3, Table 3.3). This compound was also rapidly synthesized, beginning with PyBOP mediated coupling to the *des*-cyclopropyl head group and spontaneous cyclization to give 1,2,4-oxadiazole **14**. Pinner condition then gave amidine **15**. This compound was not potent, however, and we hypothesized that the unique torsional angle of the cyclopropane ring provides improved presentation of the amidine in the active site.

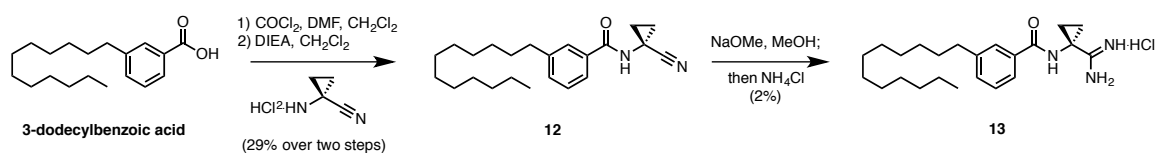
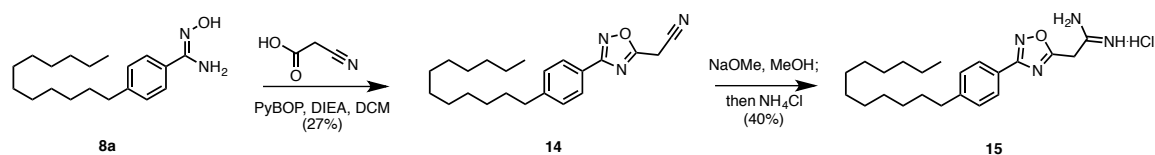
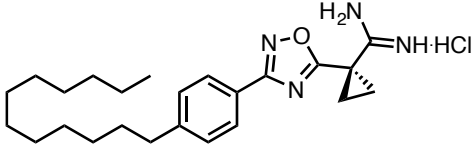
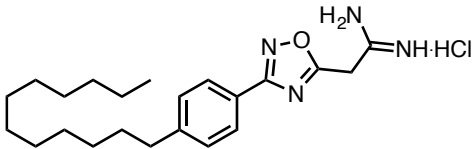
Scheme 3.2. Synthesis of **13**.Scheme 3.3. Synthesis of **15**.

Table 3.3. K_i of compound 15 compared to 11c.

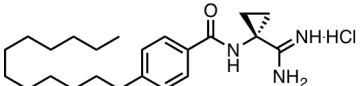
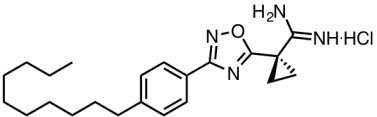
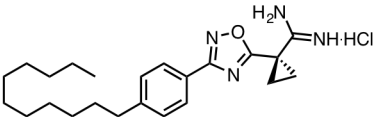
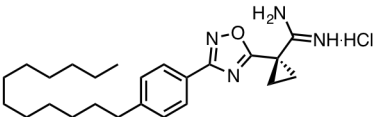
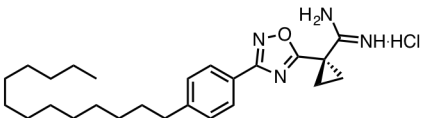
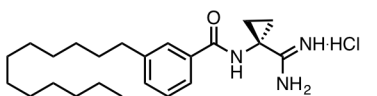
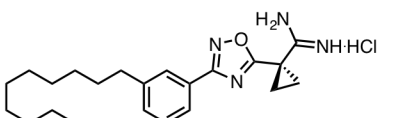
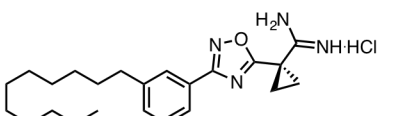
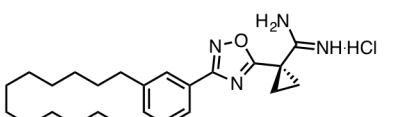
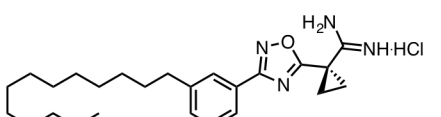
Compound	Structure	K_i (μ M) ^a		SphK1 Selectivity ^b
		SphK1	SphK2	
11c		0.32	6	40
15		13	15	2.3

^a $K_i = [I] / (K_M / K_M - 1)$; K_M of sphingosine at SphK1 = 10 μ M; K_M of sphingosine at SphK2 = 5 μ M

^b Selectivity = $(K_i / K_M)^{\text{SphK2}} / (K_i / K_M)^{\text{SphK1}}$

Because the incorporation of oxadiazoles increases the overall molecular length, we altered the length of the alkyl tail to accommodate this change. Compounds with tails ranging from 10 to 13 carbons in length, both *para*- and *meta*-substituted, were synthesized through the same methods illustrated in Scheme 3.1 (K_i values summarized in Table 3.4). The tail derivatives follow the same trend as our previous amidine-based inhibitors.^{70,71} Potency increases with tail length before dropping off at a length of 13 carbons. Tail substitution at the *para* position reaches a maximum potency and selectivity for SphK1 at a length of 11 carbons, with a K_i of 0.26 μ M (**11b**). Because an oxadiazole is one atom longer than an amide, it is expected that the 11-carbon tail fills out the sphingosine-binding pocket similarly to a 12-carbon tail on an amide analog.

Table 3.4. K_I values of para- and meta-substituted oxadiazoles 11a-h compared to amide analogs 2 and 13.

Compound	Structure	K_I (μM) ^a		SphK1 Selectivity ^b
		SphK1	SphK2	
2		0.2	0.5	5
11a		0.44	6	27
11b		0.26	43	330
11c		0.32	8	50
11d		2.5	11	9
13		4.6	10.9	4.7
11e		0.10	10.3	206
11f		0.070	9.9	283
11g		0.04	14.1	705
11h		0.98	11.7	24

^a $K_I = [I] / (K_M / K_M - 1)$; K_M of sphingosine at SphK1 = 10 μM ; K_M of sphingosine at SphK2 = 5 μM

^b Selectivity = $(K_I / K_M)^{\text{SphK2}} / (K_I / K_M)^{\text{SphK1}}$

By integrating our previous work in the development of a SphK1 homology model⁷¹ with the recently determined SphK1 crystal structure,⁷⁴ we have identified several key binding interactions between **11g** and SphK1. On docking compounds **11g** and **13** into a SphK1 model (generated with the crystal structure, PDB 4L02), one can see that *meta* amide (**13**) and *meta* oxadiazole (**11g**) adopt very different configurations (Figure 3.1). The oxadiazole inhibitor fills out the tail-binding region of the pocket to a greater extent than the amide. Further analysis reveals three cationic attractions of the amidine head group: to the γ -phosphate of ATP (as previously reported), and to Asp 81 and Asp178. Additionally, π -stacking between the oxadiazole and Phe192, which forms the roof of the pocket above the linker region, contributes to binding, as well as a favorable arene-H interaction between the phenyl ring and Ile-174.

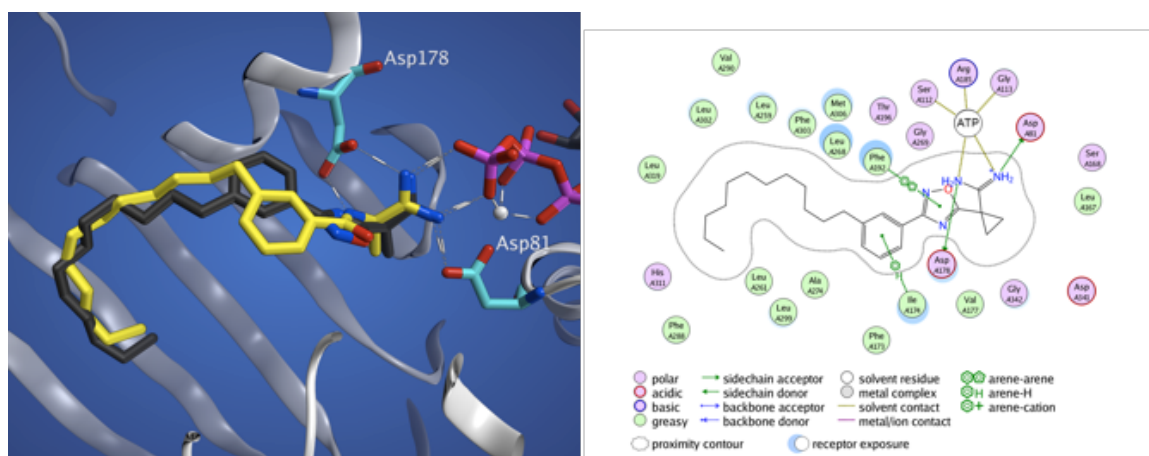
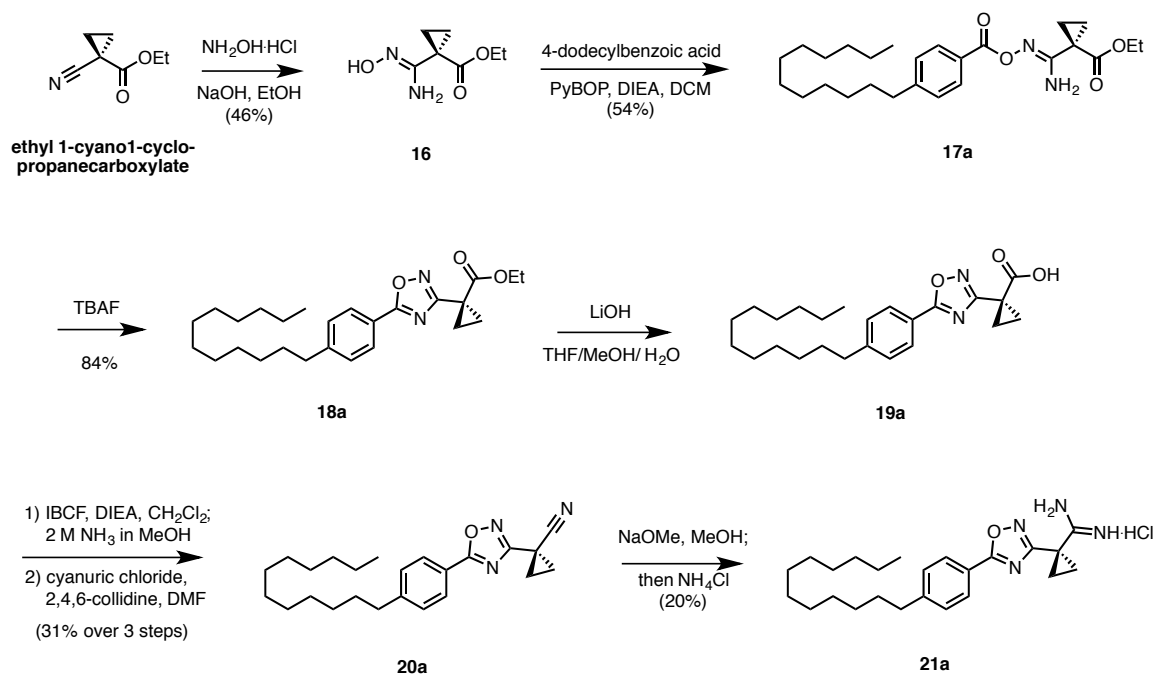


Figure 3.1. Docking studies with SphK1. *Left:* *Meta* substituted oxadiazole (**11g**, black) and amide (**13**, yellow) derivatives docked into the crystal structure of SphK1. *Right:* 2D representation of **11g** and its sidechain interactions.

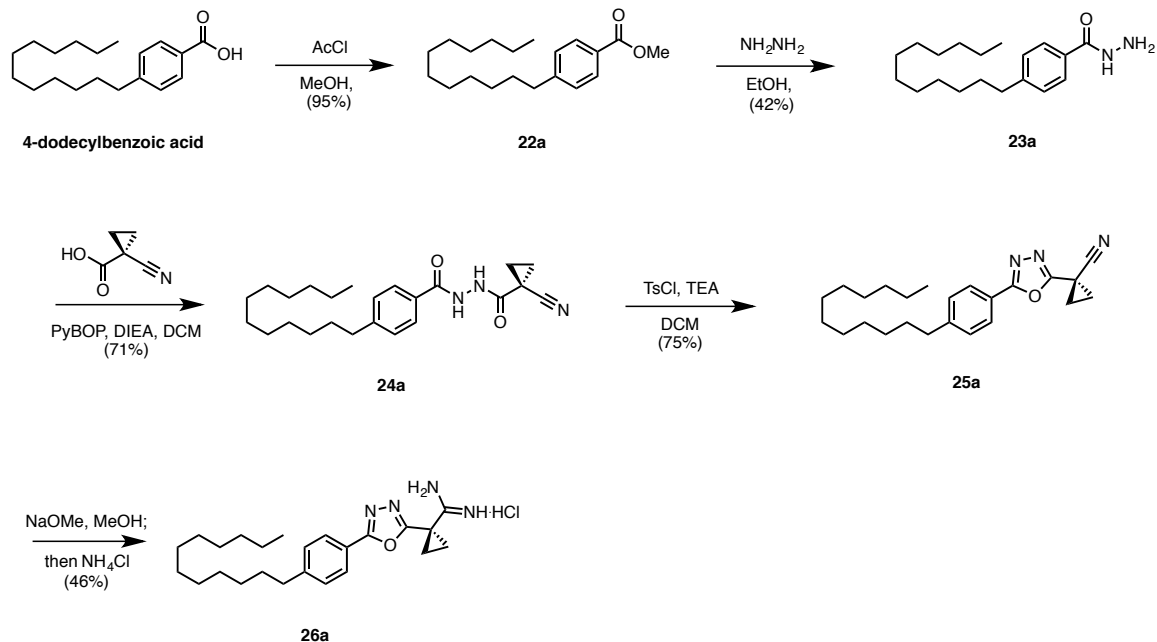
Following the evaluation of **11c** and **11g**, four additional compounds were synthesized to determine the relative efficacy of the three oxadiazole subtypes, as it has been reported in the literature that each individual regioisomer exhibits unique physical and pharmacological properties.¹⁰¹ For each oxadiazole subtype, both *meta*- and *para*-substituted variants were synthesized.

The synthesis of **21a** (Scheme 3.4) began with conversion of ethyl 1-cyano-1-cyclopropanecarboxylate to the amideoxime **16**, followed by PyBOP mediated coupling to 4-dodecylbenzoic acid. **17a** was then cyclized in high yield using TBAF as a weak base and catalyst. Next, saponification, amidation, and subsequent dehydration of **18a** yielded nitrile **20a**, whereupon Pinner conditions again mediate conversion to the corresponding amidine.

To synthesize **26a**, (Scheme 3.5) 4-dodecylbenzoic acid was esterified using methanolic HCl, then reaction with hydrazine yielded hydrazide **23a**. PyBOP coupling to the head group yielded the coupled dihydrazide product **24a**, at which point cyclization with *p*-toluenesulfonic acid and triethylamine in dichloromethane complete the 1,3,4-thiadiazole moiety. Pinner conditions yield the amidine **26a** in 46% yield.



Scheme 3.4. Synthesis of 1,2,4-oxadiazole 21a.



Scheme 3.5. Synthesis of 1,3,4-oxadiazole 26a.

Biological evaluation revealed substantial differences in the inhibitory qualities of molecules containing isomeric oxadiazoles (Table 3.5). Surprisingly, the largest distinction occurred between compounds containing the 3-aryl (**11c** and **11g**) and 5-aryl (**21a** and **21b**) 1,2,4-oxadiazole isomers. Inhibitors **11c** and **11g** display significantly higher potency and selectivity for SphK1 than do **21a** and **21b**. Compounds containing 1,3,4-oxadiazoles (**26a** and **26b**) display intermediate potency. Substitution about the phenyl ring again proved to be a very important factor, and all compounds with *meta*-

Table 3.5. K_i values of oxadiazole isomers with *meta* and *para*-substituted tails.

Compound	Structure	K_i (μM) ^a		SphK1 Selectivity ^b
		SphK1	SphK2	
11c		0.32	6	50
21a		3	3.4	2.3
26a		1.6	1.2	-
11g		0.04	14.1	705
21b		0.40	10.2	51
26b		0.2	8.1	81

^a $K_i = [I] / (K_M / K_M - 1)$; K_M of sphingosine at SphK1 = 10 μM ; K_M of sphingosine at SphK2 = 5 μM

^b Selectivity = $(K_i / K_M)^{\text{SphK2}} / (K_i / K_M)^{\text{SphK1}}$

substituted alkyl tails are much more potent and selective than *para*-substituted analogues.

These marked differences in *in vitro* activity between oxadiazole subtypes can be rationalized, in part, with additional *in silico* analyses. Compounds **11g**, **21b**, and **26b** were docked into the substrate-binding domain of SphK1, where the respective heterocycles appear to adopt different binding orientations (Figure 3.2). Most notably, electrostatic repulsion between the non-bonding electrons of the oxadiazole isomers and the backbone carbonyl of Leu268 destabilizes binding of compounds **21b** and **26b**. This interaction alters the positioning of the amidine head group, limiting binding interactions with the γ -phosphate of kinase-bound ATP. Furthermore, nitrogen atoms on the oxadiazoles of **21b** and **26b** likely undergo a repulsive interaction with the Asp81 residue.

These simulations suggest that, relative to isoforms present in other compounds, the particular 1,2,4-oxadiazole of **11g** is subjected to minimal repulsive interactions in the SphK1 active site. This favorable binding orientation, coupled with *meta*-substitution about the phenyl ring, results in a significantly enhanced inhibitory profile. **11g** is not

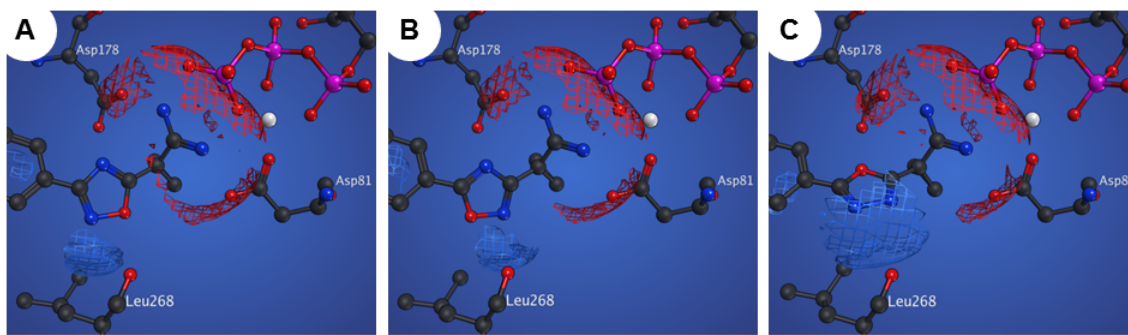


Figure 3.2. *In silico* docking of **11g** (A), **21b** (B), and **26b** (C). White sphere = Mg²⁺.

only highly potent, but with 705-fold selectivity for SphK1, is the most selective SphK1 inhibitor reported to date.

In summary, we have generated a library of amidine-based SphK1 inhibitors with *in vitro* potencies in the nanomolar range. Surprisingly, different oxadiazole subtypes elicited dramatically different effects regarding potency and selectivity; also, *meta*-substitution about the phenyl ring increased efficacy for all isomers. Docking analysis revealed important interactions between **11g** and specific amino acid residues in the SphK1 active site, and provided justification for the favorable binding of this compound. This study contributes to the growing understanding of the structural requirements for SphK1 inhibition, and compounds such as **11g** provide the ideal scaffold for future inhibitors. Simultaneous optimization of potency, selectivity, and pharmacokinetic properties will be necessary to further interrogate both SphKs in pathophysiology, and to identify suitable therapeutic candidates in the fight against cancer and hyperproliferative diseases.

3.2 Low blood concentration and poor cellular uptake

The work described in this chapter was part of a larger effort to optimize multiple drug-like properties of amidine-based inhibitors. However, while the potency, selectivity, and half-life of our molecules did improve, we were faced with two new pharmacological problems.

First, the concentration of drug observed in blood after murine IP injection was much lower than what had been observed for our earlier amide series (Figure 3.3). The cause of this low blood concentration was never determined, and remains a source of confusion.

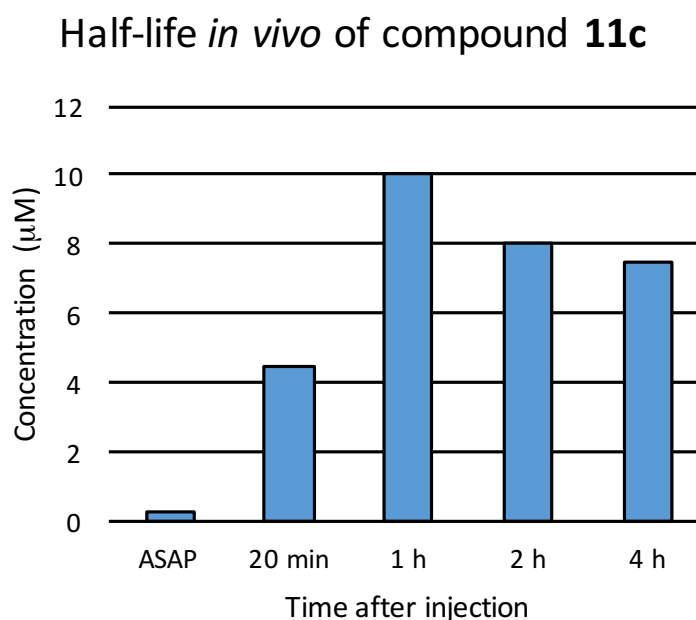
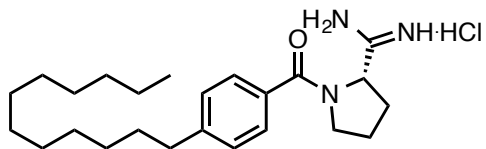
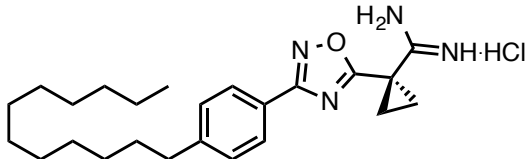
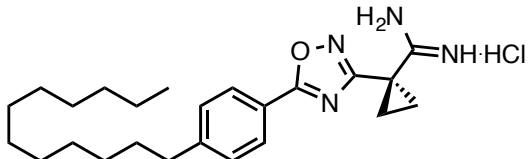
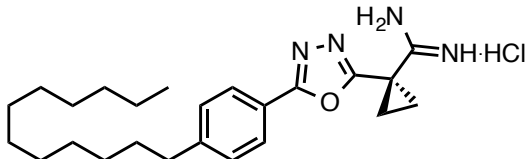
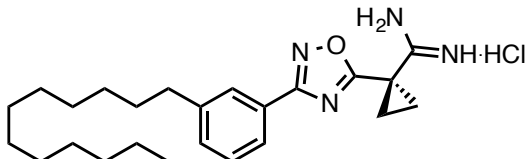
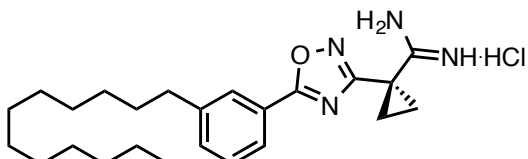
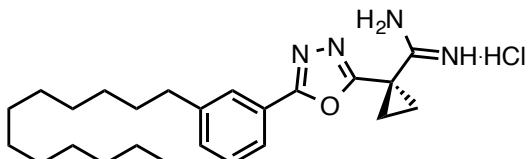


Figure 3.3. Metabolism of 11c. Oxadiazole **11c** displayed a much-improved half-life, but did not reach blood concentration levels comparable to the amide analogues.

The second problem with this series was that unfavorable results were seen in cellular assays. IC_{50} values represent the concentration of inhibitor required to bring about a fifty percent reduction in S1P in a cell-based assay. Ideally, this value should be similar to the K_i value, because Sph is present at cellular concentrations near the K_M . But when we determined IC_{50} values for each oxadiazole, we saw discrepancies that depended on tail positioning and oxadiazole subtype; it appeared that *para* positioning of the tail improved IC_{50} values, and that the 1,3,4-oxadiazole did so as well (Table 3.6).

Table 3.6. K_I and IC_{50} values of oxadiazoles and amide 3. Large discrepancies in K_I and IC_{50} values were observed for differing oxadiazole subtypes.

Compound	Structure	K_I (μM) ^a		
		SphK1	SphK2	IC_{50} (μM)
4		0.13	1.5	0.03
11c		0.32	6	1
21a		3	3.4	28
26a		1.6	1.2	0.2
11g		0.04	14.1	4
21b		0.40	10.2	1.2
26b		0.2	8.1	0.2

^a $K_I = [I] / (K_M / K_M - 1)$; K_M of sphingosine at SphK1 = 10 μM ; K_M of sphingosine at SphK2 = 5 μM

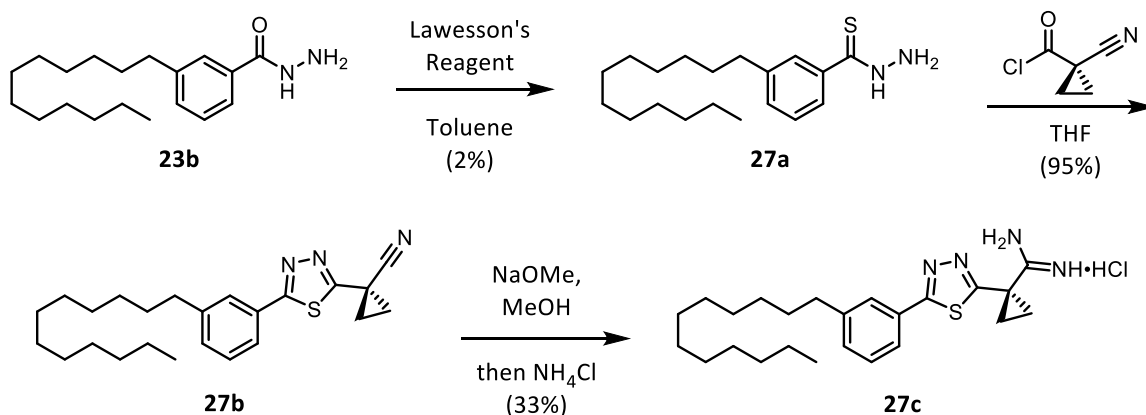
^b Selectivity = $(K_I / K_M)^{SphK2} / (K_I / K_M)^{SphK1}$

This was interesting, but unfortunate, because *meta* tail positioning and the 1,2,4-oxadiazole isomer of **11g** were required to maximize potency *in vitro*. This type of difficulty is common in drug discovery—the optimization of one parameter (potency) may arbitrarily and adversely affect another (cellular efficacy).

3.3 Synthesis, and evaluation of additional bioisosteres

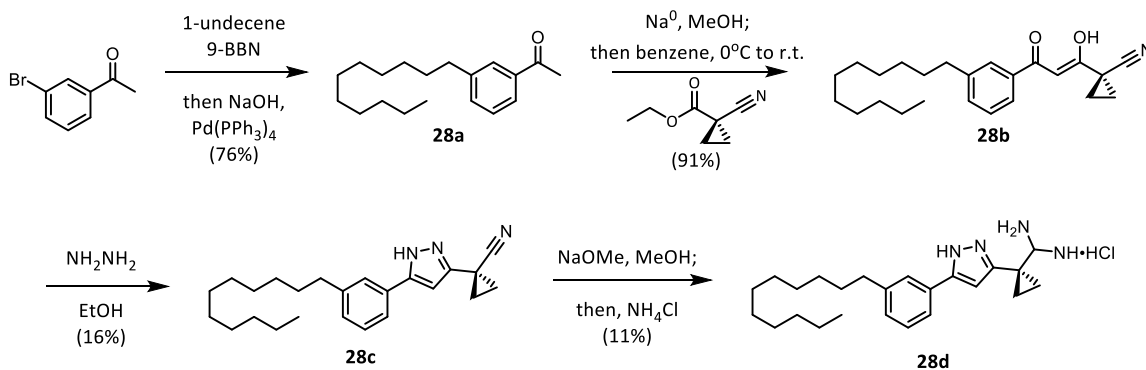
The disconnect between K_i and IC_{50} values for our oxadiazoles is likely caused by an issue of cellular uptake. We believed that this might be dependent on the action of membrane transport proteins that do not recognize the oxadiazole unit to allow our compounds to enter, or by efflux proteins that rapidly eject them. Whatever the mechanism, it is clear that this series does not reach effective concentrations in cells, as our amide compounds do (IC_{50} of amide **4** is 0.03 μ M, Table 3.5). For this reason, several other amide bioisosteres were synthesized, again with the goal of maintaining potency while increasing metabolic stability, but now with the additional aim of improved cellular efficacy.

Three additional heterocycles were proposed, beginning with thiadiazole **27c**. The synthetic route (Scheme 3.6) began by refluxing hydrazide **23b** with Lawesson's reagent in toluene to yield thiohydrazide **27a**. Coupling and subsequent cyclization of **27a** to the acid halide head group in refluxing THF gave the 1,3,4-thiadiazole, which was converted to amidine **27c** under Pinner conditions in the final step.



Scheme 3.6. Synthesis of thiadiazole 27c.

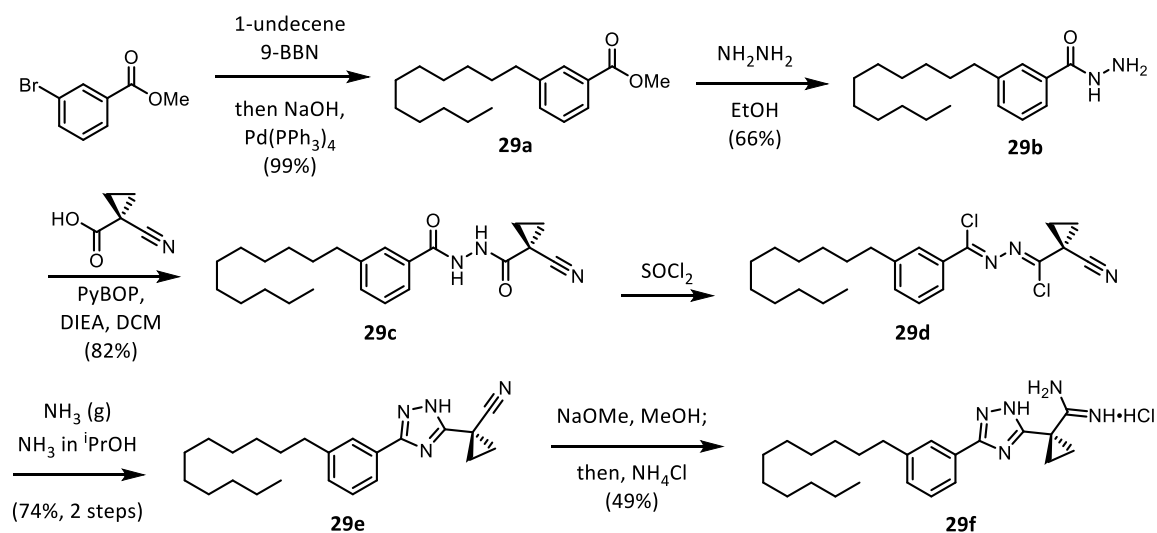
Next, synthesis of pyrazole **28d** (Scheme 3.7) began with a Suzuki coupling of the alkyl tail to 3-bromoacetophenone. A mixed Claisen condensation with ethyl 1-cyanocyclopropanecarboxylate followed to yield the 1,3-diketone **28b** (depicted in enol form). This molecule was then refluxed with hydrazine in ethanol to cyclize and construct the pyrazole group, and Pinner conditions furnished the final amidine **28d**.



Scheme 3.7. Synthesis of pyrazole 28d.

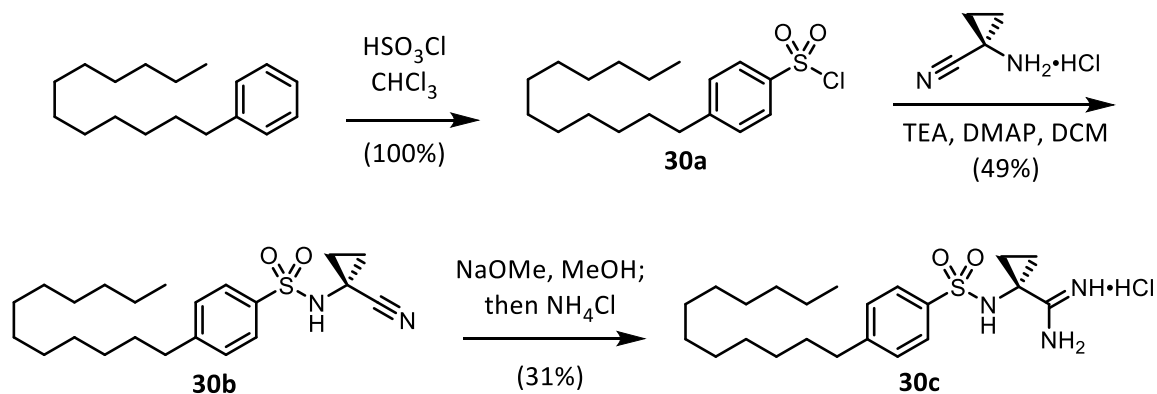
The last heterocycle proposed was a triazole, and was made (Scheme 3.8) by Suzuki coupling of the alkyl tail to methyl 3-bromo-benzoate, hydrazide formation, and then PyBOP coupling to 1-cyclopropanecarboxylic acid to yield coupled hydrazide **29c**.

Next, reaction with thionyl chloride followed by cyclization with ammonia yielded the triazole group. Pinner conditions yield the corresponding amidine **29f** in 49% yield.



Scheme 3.8. Synthesis of triazole 29f.

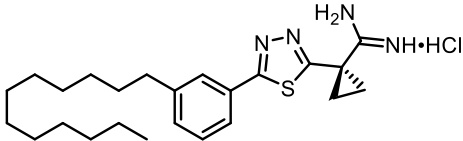
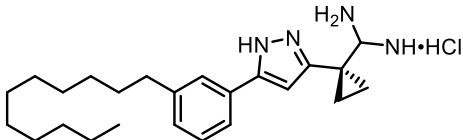
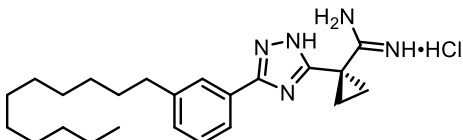
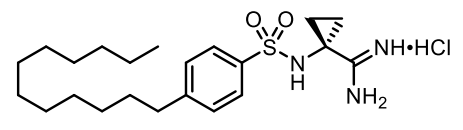
Finally, a non-heterocyclic amide isostere, a sulfonamide, was synthesized as follows (Scheme 3.9). First, reaction of dodecylbenzene with chlorosulfonic acid in chloroform produced the sulfonyl chloride in quantitative yield. Then, this was coupled to the amino head group to furnish the sulfonamide, which was converted to the amidine under Pinner conditions to yield **30c** in 31% yield.



Scheme 3.9. Synthesis of sulfonamide 30c.

These molecules each provided a unique isostere that would potentially provide a solution to the problems we were experiencing regarding blood concentration and cellular uptake. Unfortunately, none of the four molecules inhibited SphK1 with sufficient potency to warrant further use as a new lead compound (Table 3.7). For this reason, the project was ultimately discontinued.

Table 3.7. K_i values of other amide isosteres at SphK1.

Compound	Structure	K_i (micromolar), SphK1
27c		0.3
28d		>10
29f		0.37
30c		>10

$$K_i = [I] / (K_M / K_M - 1); K_M \text{ of sphingosine at SphK1} = 10 \mu\text{M}$$

3.4 Conclusion

Overall, this project proved to be highly successful in terms of elucidating structural requirements for SphK1 inhibition, developing highly potent and selective compounds, and identifying specific amino acid residues responsible for key kinase-

inhibitor interactions. This information will be highly valuable in the design and optimization of future inhibitors. But while molecules with better inhibitory properties were identified, they were limited as drug candidates by low concentration in blood following IP injection and poor cellular uptake as evidenced by IC_{50} values. Other amide isosteres were synthesized with the hope of resolving this issue, but none were sufficiently potent to warrant further derivatization.

Chapter 4

Targeting SphK2 with Substrate-Based Inhibitors

As described in Chapter 2, SphK2 has proved to be a highly elusive target for small-molecule inhibitors; several inhibitors have been discovered, but the best of these are only moderately potent ($\sim 1 \mu\text{M}$) and slightly selective (20-fold for SphK1 over SphK2). This lack of effective inhibitors is unfortunate for two reasons: (1) a highly potent small-molecule may be efficacious in any of the myriad of diseases in which SphK2 is implicated, and (2) extremely selective inhibitors (greater than 100-fold for SphK2) would be invaluable in the clarification and characterization of the unique roles of this kinase in homeostasis and pathology. However, while inhibitors of SphK2 are relatively rare, many synthetic substrates are known that are extensively and almost exclusively phosphorylated by SphK2. In order to ultimately identify SphK2-selective inhibitors, we first developed a “super substrate” of SphK2, a thiadiazole-containing compound, **34g**. Subsequently, structural modifications were built in to disrupt the phosphorylation of this molecule, with the goal of converting the substrate into an inhibitor. In this chapter, the design, synthesis, and evaluation of this substrate and its derivatives are described.

4.1 A lack of inhibitors and a plethora of substrates for SphK2

When described in literature review articles, SphK2 is often referred to as “enigmatic” or “less understood” when compared to SphK1. This is partly due to the seemingly contradictory biological processes in which this kinase is a contributor. However, perhaps the greatest limiting factor in the characterization of the roles of SphK2 is the lack of effectual inhibitors available. The utility of nanomolar potent, 100-fold selective pharmacological probes has been observed in studies of SphK1, in which compounds such as PF-543 have revealed important insights into the pathophysiology of SphK1.^{72,79} The need for improved SphK2-selective inhibitors is well known, and several compounds have been identified. Unfortunately, the best of these only achieve potency in the micromolar range (Figure 4.1).

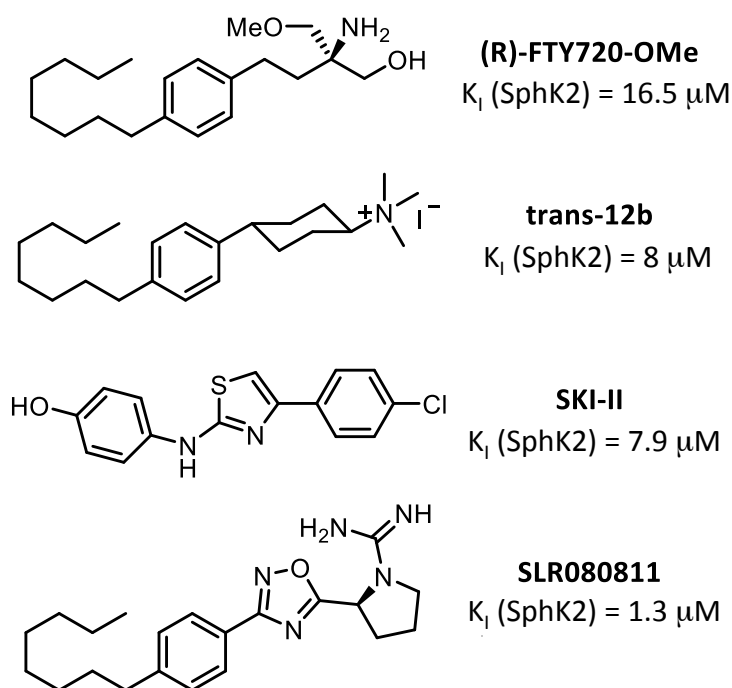


Figure 4.1. Examples of SphK2 inhibitors. The most potent compounds only achieve potency near the single-digit micromolar range.

Interestingly, when available substrates are considered, the above trend is reversed; many more substrates are known for SphK2 than for SphK1. The most famous of these is FTY720, which is phosphorylated exclusively by SphK2 before acting as a S1P receptor agonist, but others include AAL(R), an FTY720 structural variant;¹⁰² **VPC92153**, an oxazole-containing amino alcohol;⁹⁸ GSK1842799, a thiadiazole-containing amino alcohol;¹⁰³ and the lipids phytosphingosine, ω -biotinyl D-erythro-sphingosine, and D,L-threo-dihydrosphingosine.⁶⁴ Clearly, substrate-recognition by SphK1 and SphK2 is significantly different; to identify SphK2-selective inhibitors, we sought to exploit this tendency by first identifying and later modifying substrates of SphK2.

4.2 Optimizing substrates of SphK2

Generally, SphK inhibition projects progress via optimization of a molecule that is either found in a large combinatorial screen or otherwise identified as a moderately potent inhibitor. These types of studies have identified many SphK1 inhibitors, but as described above, few SphK2 inhibitors, and none that are highly potent. For unclear reasons, it is extremely difficult to target SphK2 in this way. To avoid this difficulty, we devised a different strategy: first build in selectivity for SphK2 by optimizing a selective substrate, and then modify this molecular scaffold to yield a selective inhibitor. This approach was employed successfully to identify FTY720-OMe, an FTY720 variant in which the phosphate-accepting hydroxyl moiety is capped with a methyl group. FTY720-OMe is a selective inhibitor of SphK2 with double-digit micromolar potency;¹⁰⁴ we

hypothesized that an even more potent inhibitor may result by beginning with an even more active, selective substrate.

To identify such a substrate, we designed a small library of compounds to determine the SAR of SphK2 phosphorylation. The derivatives were based on the scaffold of **VPC92153**, an FTY720 variant and substrate of SphK2 with moderate activity.⁹⁸ S1P receptor agonists like **VPC92153** have contributed significantly to the understanding of substrate recognition by SphK2, as nearly all are prodrugs phosphorylated by this kinase. To maximize this activity, four compounds were synthesized to determine the effects of the following structural modifications: (1) deletion of the methyl group at the amino carbon, (2) inversion of stereochemistry at the amino carbon, and (3) replacement of the oxazole ring with a 1,3,4-thiadiazole (Figure 4.2).

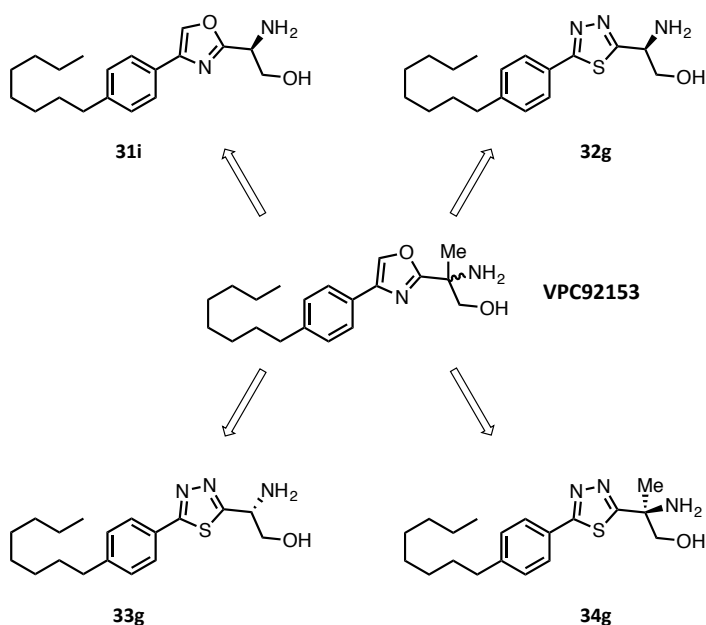
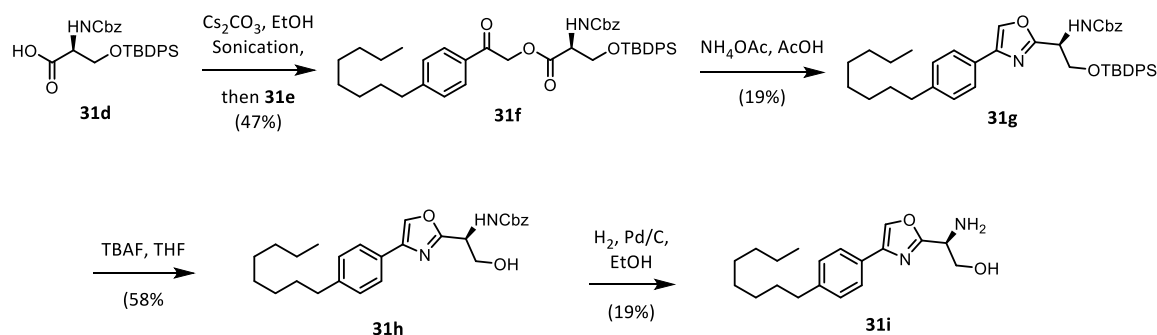


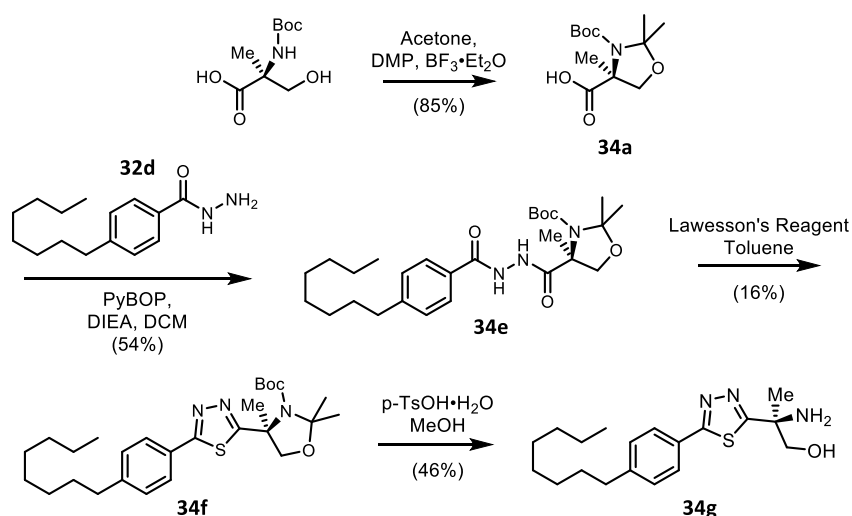
Figure 4.2. SphK2 substrate lead series. Derivatives of VPC92153 were synthesized to optimize substrate activity at SphK2.

Oxazole **31i** was synthesized as follows (Scheme 4.1). **31d** was suspended in EtOH with Cs₂CO₃ and sonicated until homogeneity was reached. Then the alpha-bromo ketone **31e** was added to afford the coupled product **31f** in 47% yield. Cyclization to construct the oxazole moiety was achieved with NH₄OAc in AcOH, then the silyl protecting group was removed using TBAF to give **31h** in 58% yield. Finally, removal of the carboxybenzyl protecting group gave the final product in 19% yield.



Scheme 4.1. Synthesis of 31i.

The syntheses of the three thiadiazoles were completely analogous, and carried out as shown in Scheme 4.2. First, the Boc-protected serine derivative was cyclized and acetonide-protected in one step to yield **34a**. This intermediate was coupled to hydrazide **32d**, and then thionated and cyclized in one step to furnish the thiadiazole group. Finally, the acetonide and Boc groups were removed in the final step to afford the product in 46% yield.



Scheme 4.2. Synthesis of 34g.

Each of these four derivatives was tested for phosphorylation by SphK2, and striking results were observed (Figure 4.3). First, deletion of the methyl group at the amino carbon in **31i** nearly abolished substrate activity, when we had hoped this change would result in increased activity. Now, in hindsight this methyl group is clearly essential, and a similar alpha-methyl amino alcohol head group was used to great effect in the *des*-hydroxy FTY720 variant, AAL-(R).¹⁰² Similarly, the enantiomeric *des*-methyl thiadiazoles **32g** and **33g** were poor substrates, and again revealed the importance of the methyl group. Finally, the thiadiazole **34g** displayed drastically improved activity; this compound is one of the most active substrates of SphK2 known today. Recouping the SAR from the study that identified GSK1842799,¹⁰³ we observed that a 1,3,4-thiadiazole, as well as methyl substitution and *S*-stereochemistry at the amino carbon, provided the optimum substrate activity. **34g**, strikingly, is phosphorylated at a level nearing that of the natural substrate, Sph.

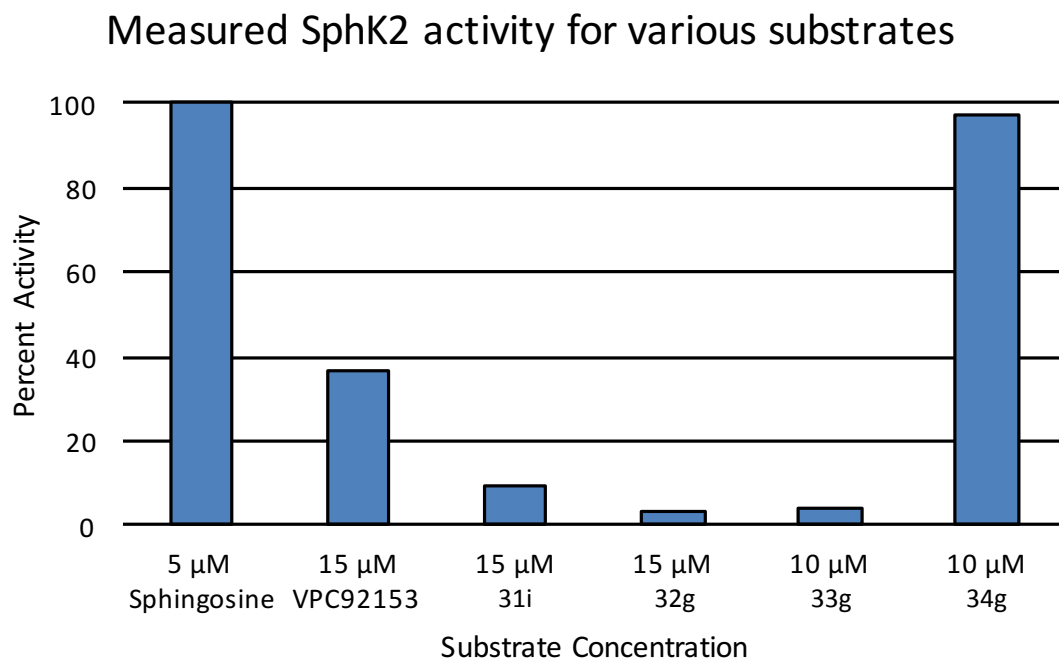


Figure 4.3. SphK2 activity as measured for various substrates. Sph, VPC92153, and four derivatives were tested for phosphorylation by SphK2. **34g** is one of the most active substrates known for SphK2.

Compound **34g** represented an ideal molecular scaffold to subject to medicinal chemistry optimization; it is one of the most active synthetic substrates known, and is completely selective for SphK2. The first objective of this project—to develop a “super substrate” with extreme selectivity for SphK2—had been achieved, so efforts shifted to the final objective of converting this substrate into an inhibitor.

4.3 Substrate-based inhibitors of SphK2

In the most germane sense, the SphK2-mediated transfer of the γ -phosphate of ATP to a substrate is a nucleophilic substitution, and in **34g** the primary hydroxyl group serves as the nucleophile (Figure 4.4).

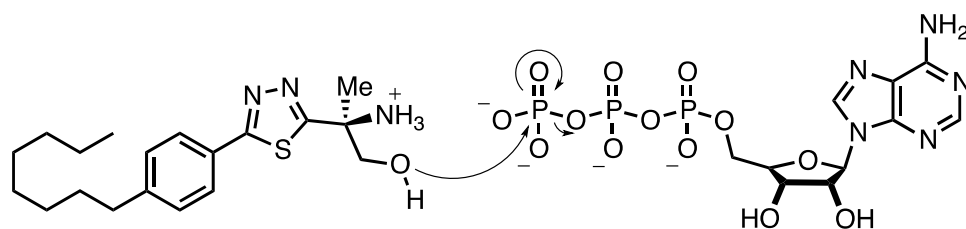


Figure 4.4. Phosphorylation of 34g. The primary hydroxyl group of **34g** serves as a nucleophile and displaces the γ -phosphate of ATP in SphK2-mediated phosphorylation.

By slowing or limiting the extent of this reaction, while at the same time retaining favorable hydrostatic interactions with the substrate-binding site, inhibition of SphK2 would be possible. To do this, a straightforward approach was taken in which structural modifications were introduced to interfere with phosphorylation of **34g**. Several derivatives were synthesized (Figure 4.5) in which the hydroxyl group was deleted (**35c**), capped (**38d** and **39e**), sterically hindered (**36d**), or spatially altered by introducing reversed stereochemistry at the amino carbon (**37d**).

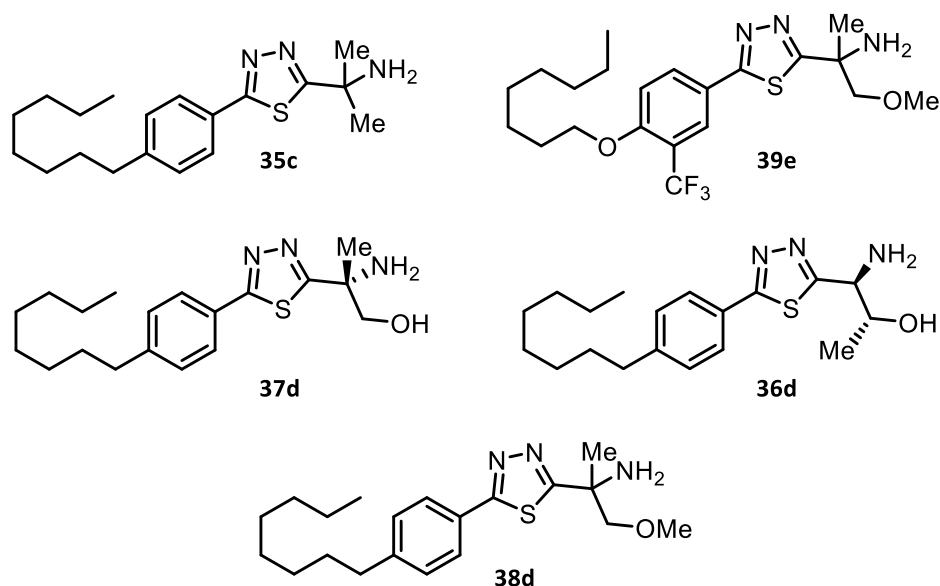


Figure 4.5. Substrate-based inhibitors. Derivatives of **34g** were synthesized with structural modifications designed to interfere with or eliminate phosphorylation.

Disappointingly, these molecules displayed quite poor inhibition when tested for activity at SphK2 (Figure 4.6); the two best compounds, **35c** and **36d**, only achieved 14% and 15% inhibition, respectively, when dosed at 1 μ M concentration.

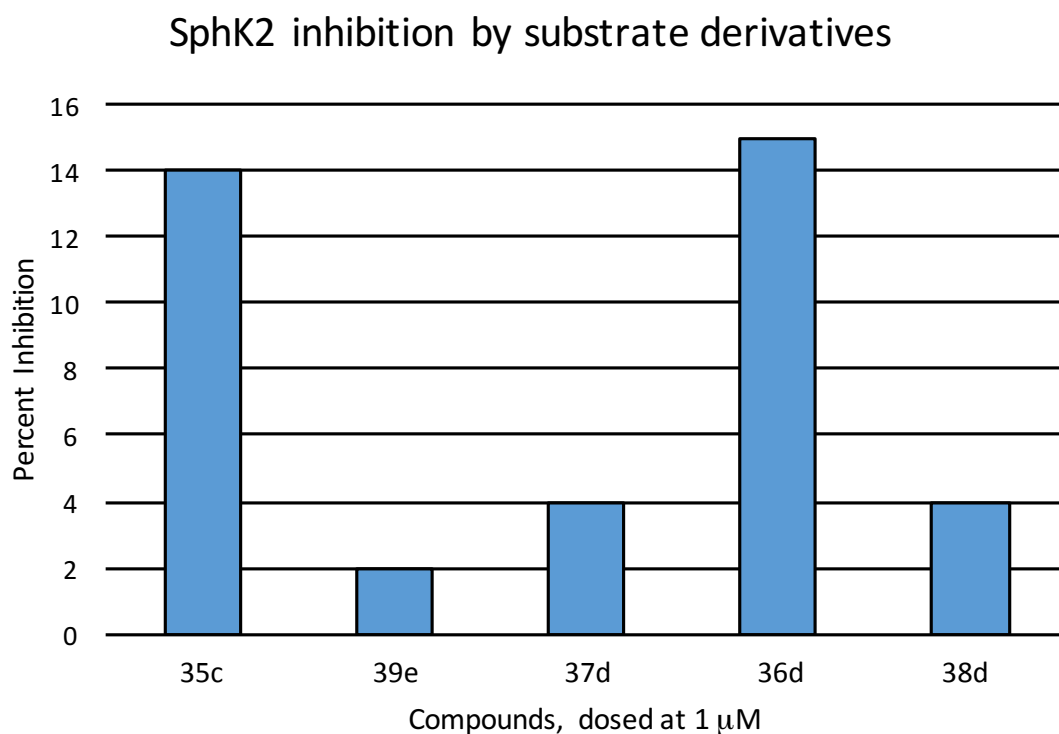


Figure 4.6. Inhibition of SphK2 by derivatives of **34g.** Weak inhibition was observed for these substrate-based compounds.

Strangely, the compounds in which the hydroxyl group was capped with a methyl substituent (**38d** and **39e**) exhibited extremely poor inhibition. This was completely bewildering because this small change was sufficient to convert FTY720 into an SphK2-selective inhibitor with potency in the low micromolar range. Moreover, **34g** was a much more active substrate than FTY720 for SphK2—we completely expected the methylated version to be at least as potent as FTY720-OMe, if not significantly more so.

Ultimately, methylation or any of the other transformations were not sufficient to beget inhibition, and for this reason this particular molecular scaffold was abandoned.

Although we were unable to derive potent inhibitors from the “super substrate” **34g**, this approach may yet be effective for a different class of molecules. Again, the efficacy of FTY720-OMe provides evidence of the utility of hydroxyl methylation,¹⁰⁴ but to fully investigate the scope of this alteration it would be necessary to incorporate it into other scaffolds. Two structures of immediate interest are AAL-(R)-OMe, and VPC92153-OMe (Figure 4.7). Compound AAL-(R) was found to be phosphorylated much more rapidly than FTY720 in human cells and whole blood,¹⁰² and due to its structural similarity to FTY720 may be an ideal structure for hydroxyl methylation. Additionally, the unique oxazole-containing scaffold of VPC92153 would provide further structural diversity and may yield effective substrate-based inhibitors.

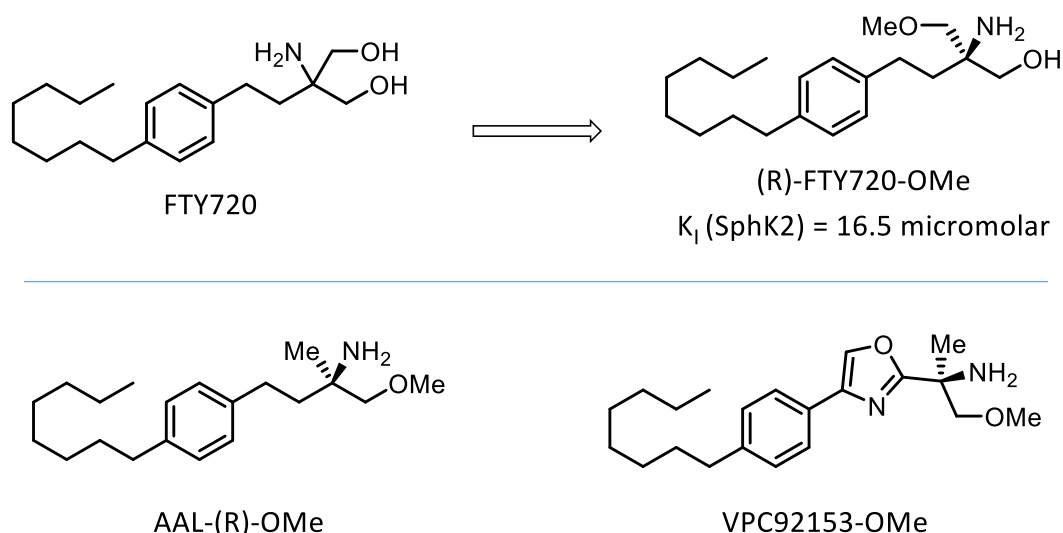


Figure 4.7. FTY720-OMe and potential substrate-based inhibitors. The efficacy of methylation of FTY720 may be recapitulated in methylated AAL-(R) and VPC92153.

4.4 Conclusion

The urgent need for potent and selective inhibitors of SphK2 has been difficult to meet—the most potent inhibitors have only achieved single-digit micromolar potency. Interestingly, nearly all synthetic substrates are phosphorylated by SphK2 exclusively, and do not associate with SphK1. We sought to exploit this tendency of substrate specificity through a two-part approach. First, we designed a “super substrate” with very high activity and complete selectivity for SphK2. Then, we sought to convert the resultant molecule into an inhibitor through the incorporation of structural modifications of and around the nucleophilic hydroxyl moiety that accepts a phosphate from ATP. We were very successful in identifying an ideal substrate, **34g**, but unfortunately could not determine the necessary alterations to beget inhibition. However, this substrate-based approach to inhibitor design may yet succeed if a suitable substrate scaffold is defined. Ultimately, although this study did not yield potent inhibitors, it provided the inspiration for the completely novel class of compounds described in the following chapter.

Chapter 5

Bisubstrate and Irreversible Inhibitors of SphK2

SphK2 remains an extremely attractive target for pharmacological inhibition; this kinase is implicated not only in cancer, but also in sickle cell disease, asthma, inflammation, Alzheimer's, diabetic retinopathy, and arthritis. Again, inhibitors of SphK2 may be useful in treating these conditions, and are essential tools in the investigation of SphK2 biology and pathology. However, the attractiveness of SphK2 as a drug target is matched by its elusiveness. To overcome the difficulty in targeting this kinase through conventional methods, we attempted two novel approaches. First, a series of bisubstrate inhibitors was developed; these molecules simultaneously target the Sph- and ATP-binding domains of SphK2. Next, in an attempt to exploit a nucleophilic amino acid residue unique to SphK2, we synthesized and evaluated three putative irreversible inhibitors. In this chapter, the design, synthesis, and biological evaluation of these molecules is described.

5.1 Bifunctional inhibitors of SphK2: born of necessity

Perhaps the most enigmatic aspects of the SphKs are their greatly differing substrate and inhibitor specificities. As mentioned in earlier chapters, several potent inhibitors of SphK1 have been identified, but none with better than single-digit micromolar potency have been found for SphK2. Conversely, synthetic substrates

abound for SphK2, and are extremely rare for SphK1. While homology models and inhibitor SAR have revealed certain clues about the character of the SphK2 active site, very little is yet known of specific kinase/inhibitor interactions that influence binding. Understanding these details would greatly accelerate inhibitor development, and could help explain the preferences of SphK2 for certain inhibitors and substrates.

Because relatively little is known about small-molecule recognition by SphK2, gains in inhibitor potency and selectivity have been very slow. To identify the next generation of highly effective SphK2 inhibitors, a drug discovery breakthrough will likely be required. Three possible manifestations of such an advancement are (1) the discovery of a completely novel and effective inhibitor pharmacophore, (2) the characterization of a SphK2 crystal structure, or (3) the development of compounds that operate through unusual modes of inhibition. We have begun to pursue the third of these possibilities by synthesizing two series of molecules: one designed to operate via bisubstrate inhibition, and the other to bind to SphK2 irreversibly. For each series, the ultimate goal was the same: exploit multiple binding sites to maximize both potency and selectivity for SphK2.

5.2 Design, synthesis, and evaluation of bisubstrate inhibitors of SphK2

The use of bisubstrate inhibitors to target SphK2 is indeed novel, but the essence of this approach is a natural extension of the work outlined in Chapter 4; ultimately, the goal was to convert a substrate into a selective, potent inhibitor. The key difference,

however, is that bisubstrate inhibitors are not limited to a single binding domain of an enzyme. Rather, these molecules consist of two distinct and spatially disparate structural subunits that are connected by a linker of some kind. In the case of bisubstrate inhibitors targeted to SphK2, the scaffold consists of an ATP-mimetic covalently linked to a Sph-mimetic (Figure 5.1).

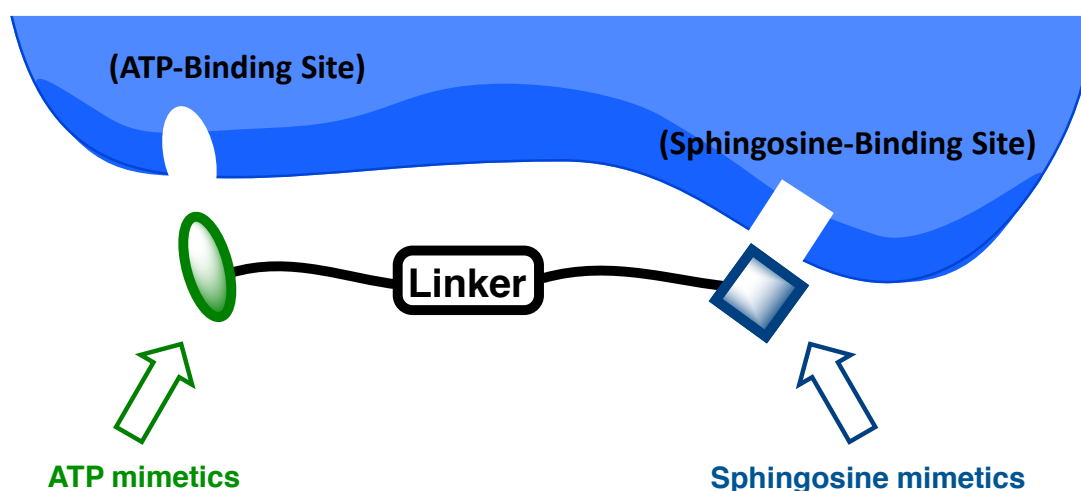


Figure 5.1. Structural components of SphK2 bisubstrate inhibitors. An ATP-mimetic is coupled to a Sph-mimetic by an alkyl linker.

Bisubstrate inhibitors in general are not completely new, and they have been successfully employed in the inhibition of certain protein kinases. In these studies, peptide substrates have been converted into inhibitors as follows. First, the hydroxyl moiety that accepts the phosphate group from ATP is either methylated or deleted, a step that requires knowledge of the specific amino acid residue involved. Next, a linker of some sort is covalently attached to the substrate. While several factors influence linker efficacy, the most important is the identification of an ideal length. Finally, the

linker is attached to an ATP-mimetic of some kind, the identity of which can be critically important.^{105,106}

Above all, bisubstrate inhibition offers the undeniably beneficial prospect of additive binding affinities, which can result in greatly enhanced potency and selectivity. The K_i of a traditional inhibitor is of course proportional to the free energy of binding: $\Delta G_{\text{binding}} = RT \ln K_i$. In bisubstrate inhibitors, the K_i is proportional to the sum of the *separate* free energies of binding for each of the two substrates, plus an additional entropic gain from the chelate effect: $\Delta G_{\text{Subs1}} + \Delta G_{\text{Subs2}} + \Delta G_{\text{chelate}} = RT \ln K_i$. The impact of additive free energies of binding is undeniable, as linear decreases in binding energy result in exponential decreases in K_i values. For instance, under ideal conditions, combining two substrates or inhibitors with millimolar potency could result in a bisubstrate inhibitor with nanomolar potency.¹⁰⁶ For this reason, this application is perfect for the inhibition of SphK2, and could finally yield effective inhibitors.

We developed a lead series of putative bisubstrate inhibitors of SphK2 with the initial goal of optimizing molecular length. Attaining an ideal length is critically important to allow each of the two substrates to interact with the active sites of the kinase as they do in their unlinked state. ATP- and Sph-mimetics were chosen and kept constant, and were linked by alkyl chains designed to afford lengths near that of the transition state for Sph-phosphorylation (Figure 5.2). After identifying the length required for maximal potency, we planned to design a library of compounds with additional, structurally diverse substrate subunits.

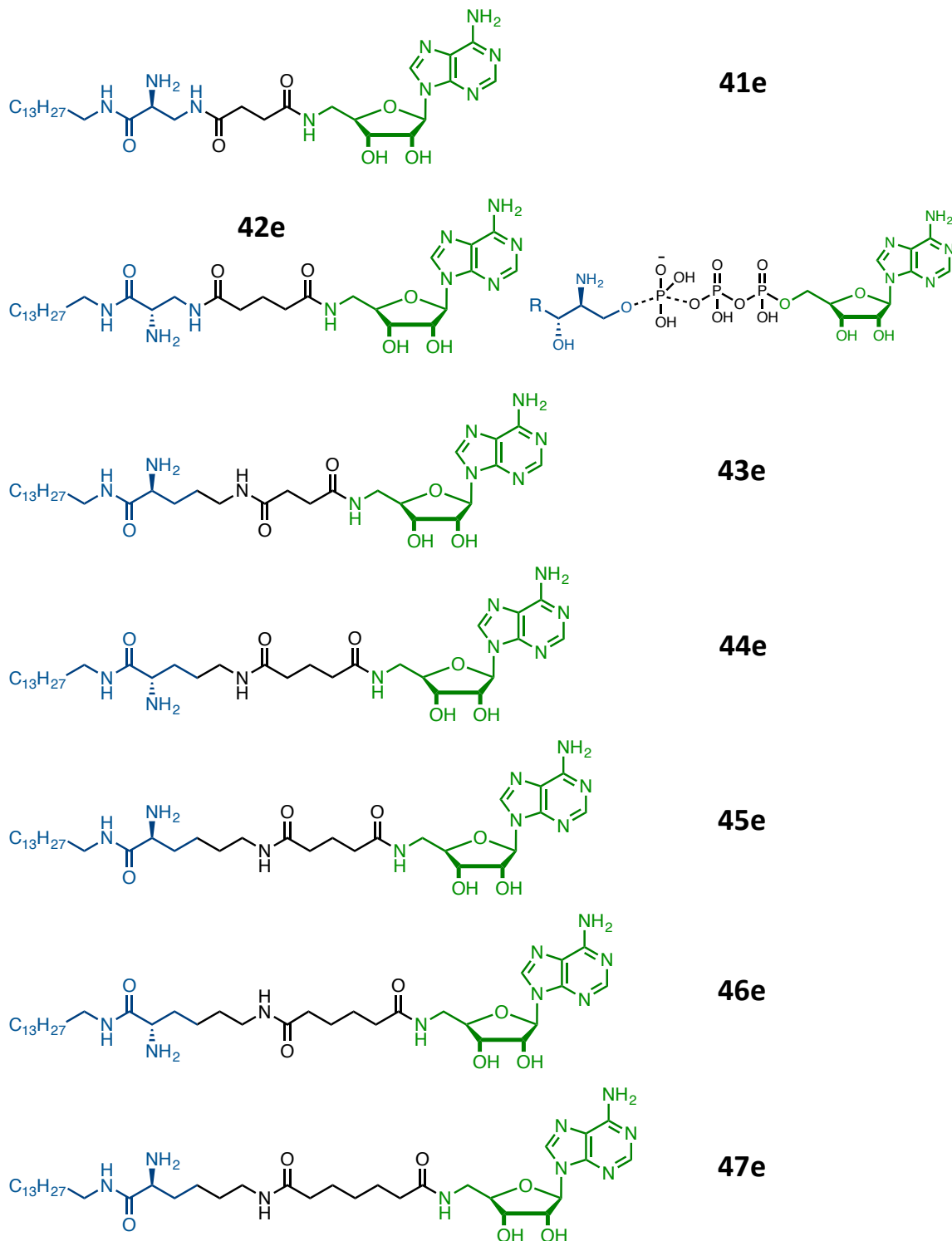
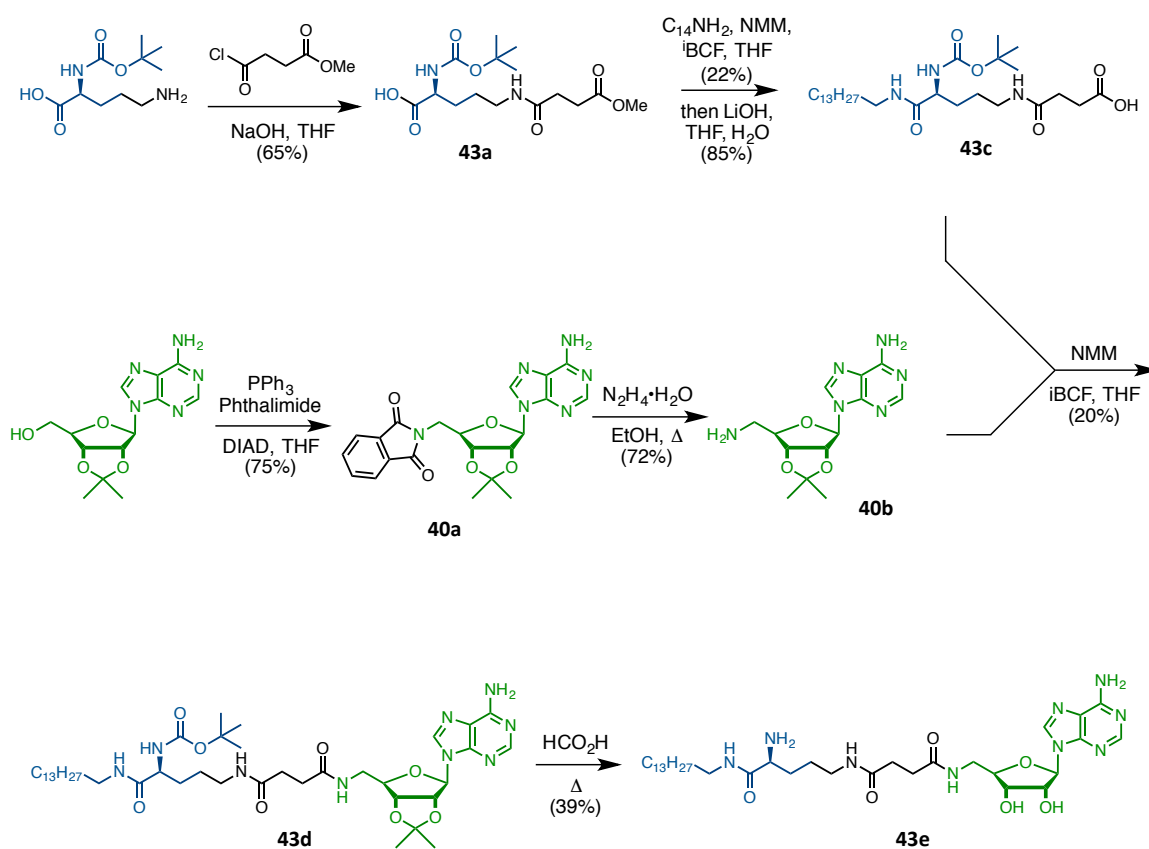


Figure 5.2. Bisubstrate inhibitor lead series. Each compound consists of a Sph-mimetic (blue), an ATP-mimetic (green), and an alkyl linker (black). This series was designed to optimize overall molecular length. We suspected that a length near that of the transition state for Sph-phosphorylation would be required.

The synthetic route for compound **43e** proceeded as follows (Scheme 5.1). First, Boc-protected ornithine was coupled to 3-(methoxycarbonyl)propanoyl chloride to yield **42a** in 65% yield. Next, tetradecylamine was coupled via iBCF-mediated activation of **42a**, and then the methyl ester was saponified using LiOH in THF and water to afford **43c** in 85% yield. This intermediate was then coupled to **40b** (synthesized previously from acetonide-protected adenosine via a Gabriel amine synthesis) in 20% yield. Finally, simultaneous deprotection of the Boc and acetonide groups afforded the final product, **43e**, in 39% yield. Each of the six molecules in the bisubstrate series was synthesized analogously, using different amino acids and linkers to provide the desired lengths.



Scheme 5.1. Synthesis of **43e**.

Following synthesis, each of the molecules in this series was submitted for inhibitory evaluation at both SphK1 and SphK2. Regrettably, no overall trend was observed regarding length; again, we had hoped to identify an ideal length that allowed for maximum inhibition. Moreover, this series showed a distinct selectivity for SphK1 (Figure 5.3) rather than SphK2, which was not inhibited at all.

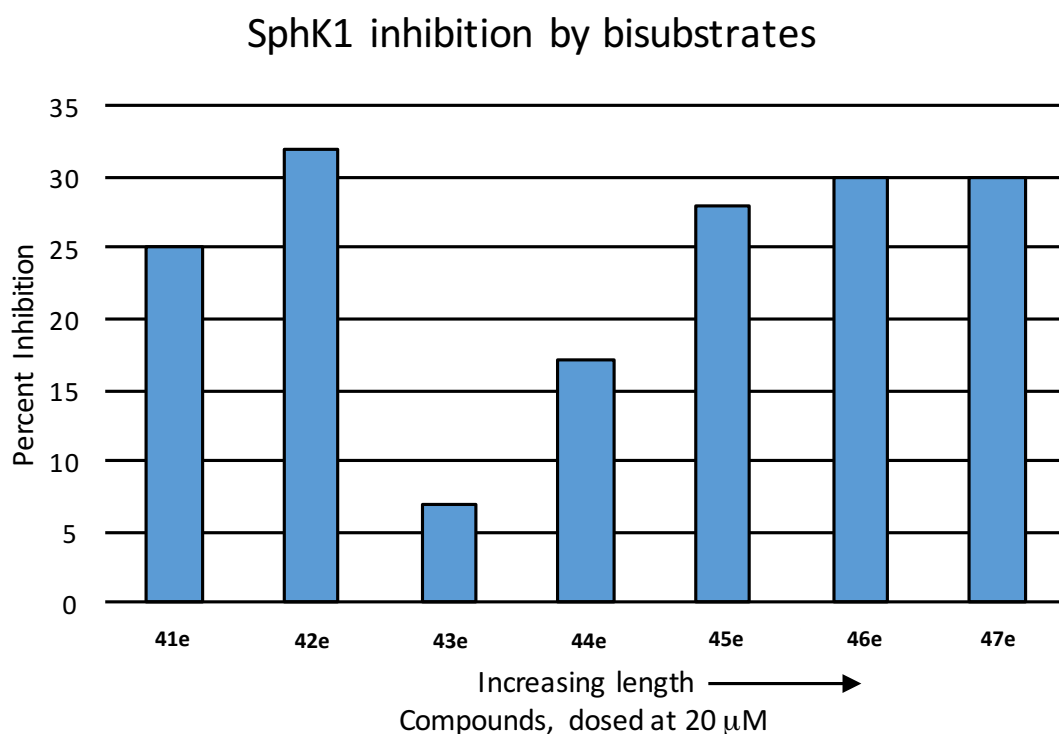


Figure 5.3. Selectivity for SphK1 by bisubstrate inhibitors. The compounds in this series did not inhibit SphK2 at all, and instead showed selectivity for SphK1. Unfortunately, potency was low and did not correlate with length.

The lack of inhibition of SphK2 is somewhat surprising, but it is possible that different initial substrates may improve potency. The particular substrate analogues employed in this series were selected based on synthetic attainability, not inherent activity at SphK2. To build in initial selectivity for SphK2, future bisubstrate inhibitors could employ our extremely active substrate, **34g**, in place of a more generic Sph-

mimetic (Figure 5.4). Additionally, more potent ATP analogues may be required to raise initial attraction for SphK2. With more suitable molecular components in place from the start, a new bisubstrate series could be synthesized and optimized for length.

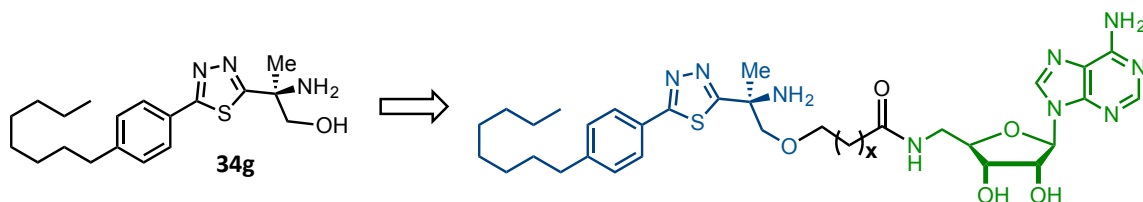


Figure 5.4. Building in SphK2 selectivity in bisubstrate inhibitors. To raise initial reactivity at SphK2, it may be necessary to begin with better substrates, such as 34g.

Overall, the bisubstrate series did not achieve the desired effect, as no inhibition of SphK2 was observed. However, the selectivity of these molecules for SphK1 was an interesting result, and potency could possibly be enhanced by substitution with different substrate analogues. Ultimately, due to synthetic constraints and the lack of correlation between length and potency, the bisubstrate approach was not pursued further.

But while the initial bisubstrate lead series was not effective against SphK2, the utility of this and related types of bifunctional inhibitors remains a definite possibility. Specifically, irreversible kinase inhibitors retain the benefits of bisubstrate inhibitors (namely, increased potency and improved selectivity) but can also display longer residence times in the active site, non-ATP-competitive modes of action, and the ability to inhibit enzymes with residence mutations.¹⁰⁷ In the following section, the design and synthesis of three putative irreversible inhibitors of SphK2 is described.

5.3 Irreversible inhibitors of SphK2: preliminary efforts

In medicinal chemistry, covalently reactive electrophilic moieties have historically been avoided due to the possibility of adverse off-target effects,¹⁰⁸ and many promising molecular scaffolds containing such functional groups have been rejected out of hand. Most drugs operate reversibly, under equilibrium conditions, and are designed to maximize intermolecular attractions to a target protein;¹⁰⁹ the potency and selectivity of the drug are the direct result of these non-covalent electrostatic interactions. Drugs with covalently reactive electrophiles, on the other hand, have the potential to bind irreversibly to any endogenous nucleophile, and have been viewed as dangerous and non-selective.^{110,111}

However, the anxieties of the drug discovery community notwithstanding, the reality is that covalent inhibitors have a rich and successful history, and that many molecules operate by an irreversible mechanism. For instance, aspirin, perhaps the world's most well known drug, covalently inhibits cyclooxygenase-2 (COX-2) by acetylation of a specific amino acid residue, Ser530.¹¹² In total, almost 30% of marketed drugs function through covalent inhibition.¹¹³ Why, then, has there been such reluctance to actively develop these types of compounds? The majority of concerns can be traced back to studies carried out in the 1970s that profiled the generation and effects of reactive drug metabolites, moieties that react covalently and indiscriminately, and are indeed cytotoxic. These were landmark works in toxicology and pharmacology,

but caused the unfortunate side-effect of blanket mistrust of drug scaffolds containing covalently reactive functional groups.^{109,110,113}

But despite early concerns, the last few years have seen a welcome trend emerge in which irreversible inhibitors are viewed much more favorably;¹⁰⁹ between 2010 and 2014, over sixty patents were granted or pending for applications of covalent inhibitors.¹⁰⁸ Researchers now know that a covalent mechanism does not inherently result in off-target effects. Instead, high selectivity can be conferred if the following three criteria are met: (1) the molecular scaffold employed is already a selective, reversible inhibitor of the target, (2) the nucleophilic residue of the target is relatively non-conserved, and (3) the reactivity of the appended electrophile is carefully tuned.¹¹⁰ When these conditions are met, the resultant “targeted covalent inhibitors” do not react irreversibly until positioned in proximity to the targeted nucleophilic residue in the enzyme active site.¹¹⁴ This approach has been effective in selectively inhibiting several notable targets including c-Src,¹⁰⁷ JAK3,¹¹⁵ EGFR-T790M,¹¹⁶ and BTK,¹¹⁷ among others.

In addition to increased potency and selectivity, irreversible inhibitors have many other benefits. These include greater efficiency (due to high potency) that allows a smaller dose, decreased risk of drug resistance, decreased sensitivity to pharmacokinetic parameters, and, because enzyme activity is only restored upon new biosynthesis, a greatly lengthened period of inhibition.^{118,119} Another interesting advantage, from a pharmacological perspective, is the option of generating an inhibitor-resistant mutant form of the targeted enzyme by deletion of the nucleophilic amino acid

residue. This would allow for a very effective control experiment in which enzymatic activity was restored even in the presence of a covalent inhibitor.¹²⁰ In many cases, these remarkable benefits outweigh potential risks, and have fueled the revival of irreversible inhibitors over the last several years.

The clear advantages of covalent inhibition have led us to develop the first putative irreversible inhibitors of SphK2. We believe this approach may overcome the great difficulty in targeting this kinase, and finally yield potent and selective inhibitors. However, for this to be possible, a prerequisite is that SphK2 contain a suitably positioned nucleophilic amino acid residue. Fortuitously, when we examined the active site of this kinase with the aid of a homology model, we found a cysteine residue in the Sph-binding domain, near the end of the hydrophobic region that accommodates the aliphatic tail of Sph. Crucially, this particular cysteine is not present in the corresponding location in the active site of SphK1. For this reason, it may be possible to inhibit SphK2 with complete selectivity by targeting this residue with irreversible inhibitors.

As an initial effort in exploiting this non-conserved cysteine residue, we synthesized three putative inhibitors. The scaffold for two of these, compounds **49** and **50**, was based on SLR080811, a SphK2-selective inhibitor with micromolar potency. SLR080811 was chosen because, again, irreversible inhibitors must first be targeted to the kinase in a traditional, reversible manner in order to position the reactive electrophile near the nucleophilic amino acid. The electrophiles employed for these compounds were a traditional Michael acceptor, an acrylamide, in **49**, and an α -chloro

amide in **50** (Figure 5.5). The use of these groups did not simply provide molecular diversity, but afforded slightly different “reactive lengths”—the acrylamide group in **49** reacts with nucleophiles at the terminal carbon atom, and the α -chloro amide of **50** does so at the carbon directly adjacent to the carbonyl. Just as in bisubstrate inhibitors, optimizing length is critical in irreversible inhibitors.

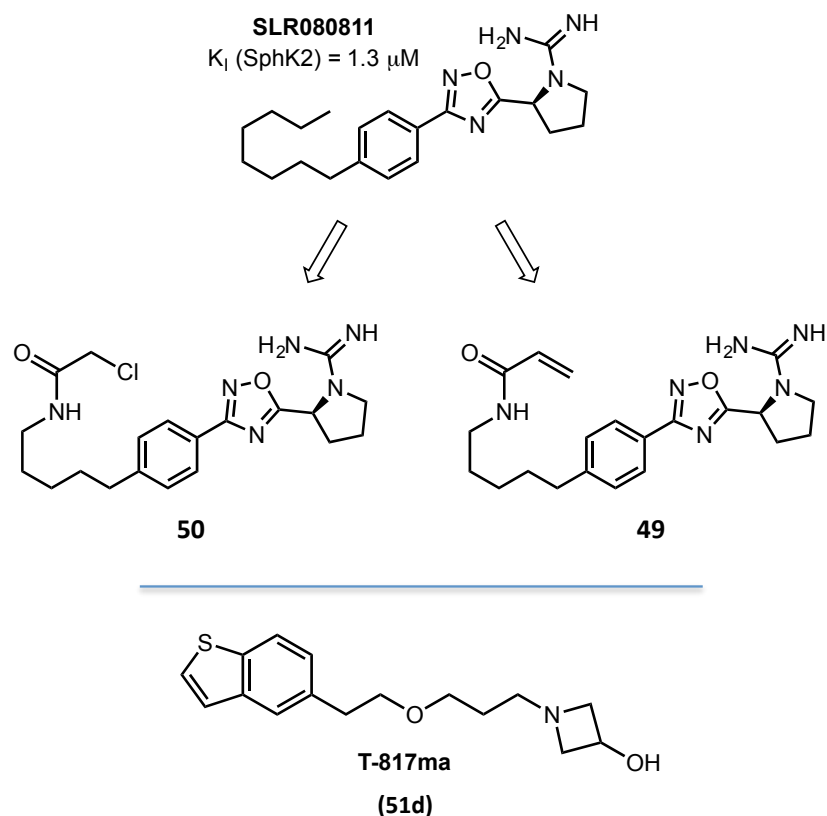
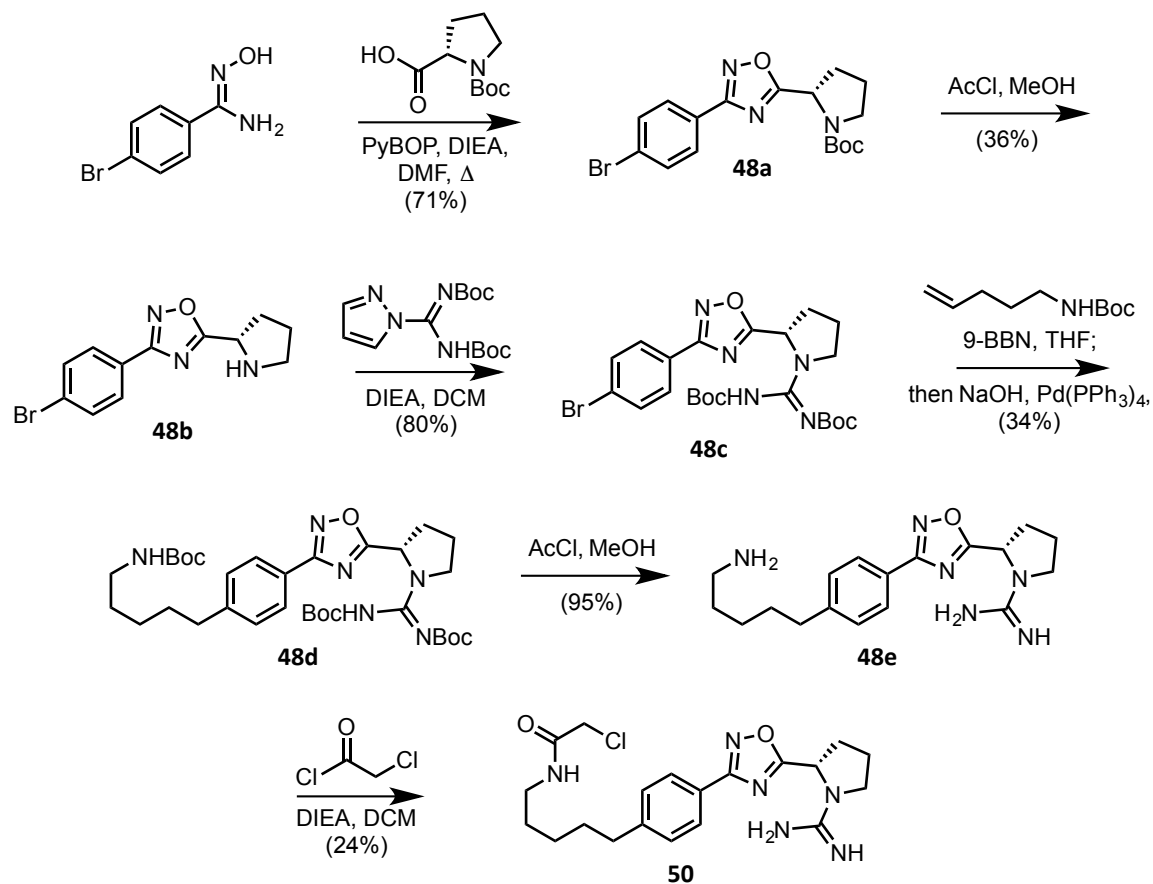


Figure 5.5. SLR080811 and potential irreversible inhibitors of SphK2. An α -halo amide and acrylamide were appended to SLR080811 to generate irreversible inhibitors. T-817ma is an experimental drug that may interact in some way with the SphKs.

Next, a sample of T-817ma was synthesized (**51d**, Figure 5.5). T-817ma is currently in Phase II clinical trials for the treatment of Alzheimer’s disease,¹²¹ and notably, its specific mechanism of action is unknown. Because of the remarkable resemblance of T-817ma to many SphK inhibitors and substrates, we believed that this

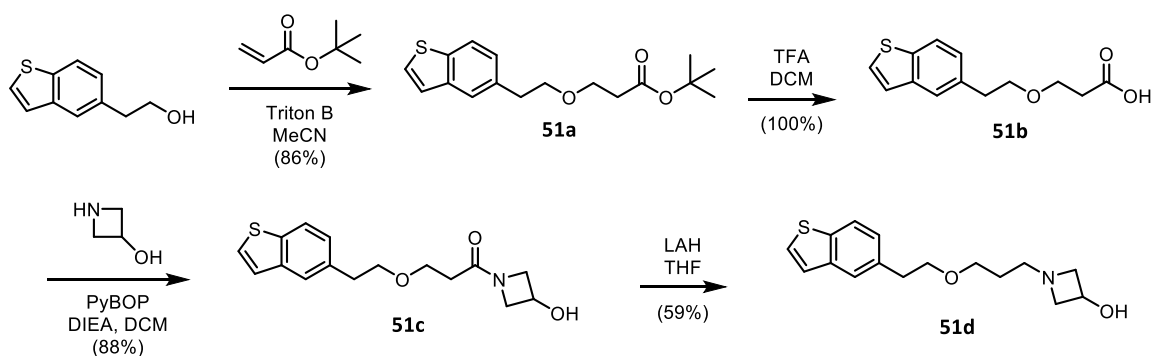
drug might operate through a SphK-dependent mechanism. Furthermore, it is very likely that the molecule's benzothiophene moiety reacts irreversibly following a bioactivation step. In the antiplatelet prodrug clopidogrel, a similar thienopyridine functionality is converted by CYP2C19 and PON1 to yield the active metabolite, which then covalently inhibits the target ADP receptor;¹²² we believe that T-817ma reacts similarly, and thus might prove effective in targeting and exploiting the non-conserved cysteine in the SphK2 active site. For these reasons, T-817ma was a highly suitable candidate to test for conventional inhibition of either SphK, and for irreversible inhibition of SphK2 in particular.

The syntheses of the two inhibitors based on SLR080811 (**49** and **50**, Scheme 5.2) were identical until the final step, at which point the electrophiles were appended. First, 4-bromobenzamidoxime was coupled to Boc-proline, mediated by PyBOP. Then, following deprotection by methanolic HCl, **48b** was coupled to N,N'-Di-Boc-1H-pyrazole-1-carboxamide in 80% yield. A Suzuki coupling was used to append the protected tail in the fourth step in 34% yield. Finally, following deprotection, **48e** was coupled to chloroacetylchloride to afford the final product in 24% yield.



Scheme 5.2. Synthesis of 50.

T-817ma (**51d**) was synthesized in four steps (Scheme 5.3), beginning with the Michael addition of Benzo[b]thiophene-5-ethanol to *tert*-butyl acrylate in acetonitrile with catalytic Triton B. Next, the *tert*-butyl ester was hydrolyzed in trifluoroacetic acid to provide the carboxylic acid **51b** in quantitative yield, whereupon PyBOP-mediated coupling to 4-hydroxyazetidine hydrochloride gave the amide **51c**. Lastly, the amide was reduced to an amine to afford the final product in 59% yield.



Scheme 5.3. Synthesis of T-817ma (51d).

Directly following synthesis, these inhibitors were submitted for evaluation of inhibitory activity at SphK1 and SphK2, and unfortunately, no inhibition was observed at either kinase. However, this result does not delegitimize this method of targeting SphK2. Many additional molecules will need to be synthesized and tested in order to determine the ideal tail length and electrophile identity. The optimization of such molecules would be significantly accelerated if guided by *in silico* modeling with a SphK2 homology model.

Moreover, regarding T-817ma, additional *in vivo* experiments will be necessary to confirm or rule out efficacy. For the benzothiophene moiety of this molecule to react as an electrophile (as the thienopyridine group does in clopidogrel) it will first require bioactivation by a cytochrome P450. A possible mechanism of this activation begins with epoxidation of the thiophene ring followed by spontaneous rearrangement to a thiolactone. This species may immediately react irreversibly with any nucleophilic residues, or may, after hydrolysis, react with cysteine residues to form disulfide linkages (Figure 5.6). Bioactivation is impossible in an *in vitro* SphK assay, but *in vivo* murine

studies may be used to determine whether T-817ma interacts with either SphK in this manner.

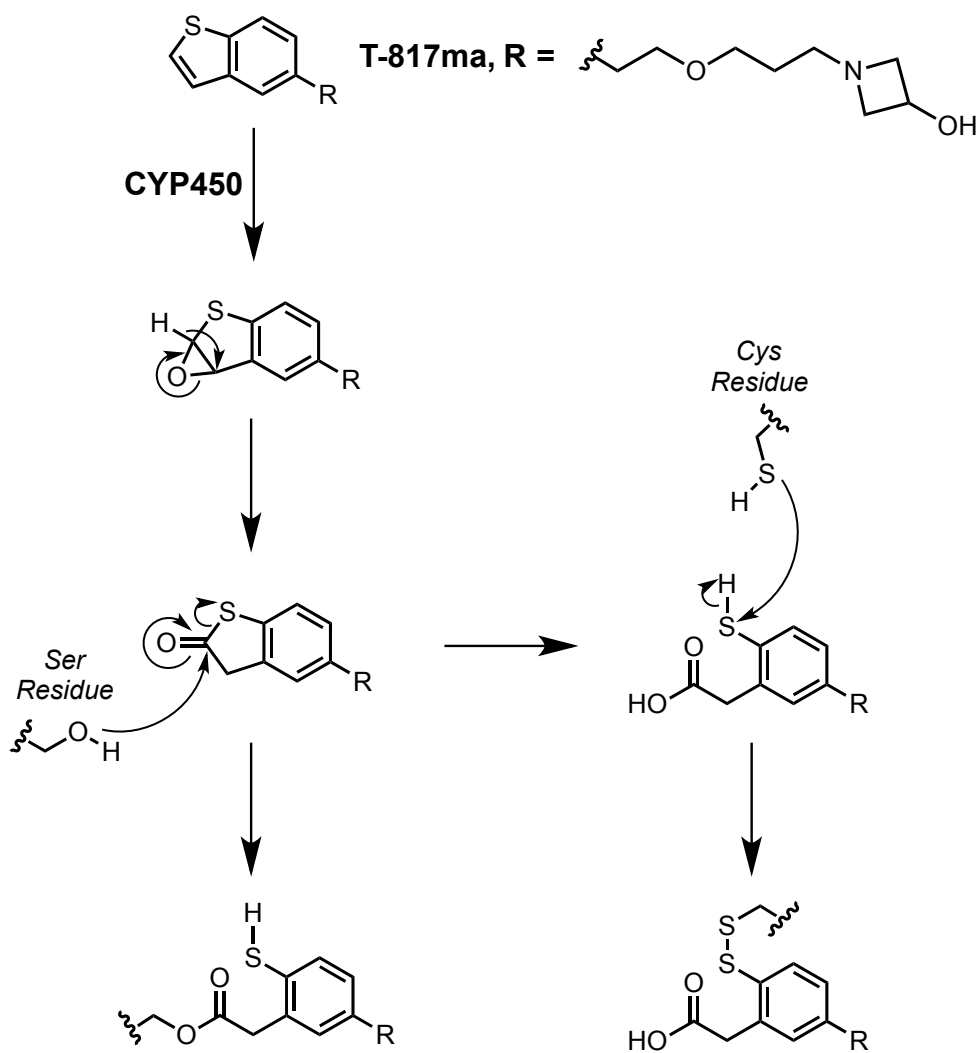


Figure 5.6. Possible mechanism of T-817ma bioactivation. T-817ma was inactive in an in vitro SphK assay, but may require bioactivation before reacting. In vivo experiments are necessary to confirm or rule out any interaction of T-817ma with the SphKs.

5.4 Conclusion

Currently, the demand for effective SphK2 inhibitors has not been met, as the best compounds only achieve potency near the single-digit micromolar range. The

difficulty in designing SphK2 inhibitors drove us to attempt two unique approaches. In the first, bisubstrate inhibitors were designed that consisted of Sph- and ATP-mimetic subunits connected by an alkyl chain of varying length. Interestingly, this series showed selectivity for SphK1, but potency was limited and did not correlate with length. In the next approach, we synthesized and tested three potential irreversible inhibitors, aiming to exploit a non-conserved nucleophilic cysteine in the active site of SphK2. This series did not inhibit either SphK, but a larger library of compounds containing various electrophiles and tail lengths will be required to validate or rule out this approach. For T-817ma, *in vivo* investigations will be required to determine whether or not this molecule interacts with SphK1 or SphK2 in a covalent manner.

These two approaches are the first of their kind to be applied in a SphK inhibition project. Both bisubstrate and irreversible inhibitors offer significant advantages over conventional inhibitors, and their efficacy against SphK2 in particular remains a definite possibility. Larger synthetic libraries guided by *in silico* design will likely be required to identify bifunctional molecules, but this labor could result in the first SphK2 inhibitors with potency in the nanomolar range.

Chapter 6

Supplementary Information

6.1 Biological methods

Sphingosine Kinase Assay. Human SphK1 and mouse SphK2 cDNAs were used to generate mutant baculoviruses that encoded these proteins. Infection of Sf9 insect cells with the viruses for 72 h resulted in >1000-fold increases in SphK activity in 10000g supernatant fluid from homogenized cell pellets. The enzyme assay conditions were exactly as described,⁶² except infected Sf9 cell extract containing 2-3 µg of protein was used as a source of enzyme.

Pharmacokinetic Analysis. Groups of 8-12-week-old mice (strain C57BL/6J) were injected (intraperitoneally) with either compounds (at a dose of 10 mg/kg) or an equal volume of vehicle [2% solution of hydroxypropyl-β-cyclodextrin (Cargill Cavitron 82004)]. After injection, animals were bled at the specified time points [ASAP (as soon as possible) time points were 1-2 min after dosing]. Whole blood was processed immediately for LC-MS analysis as described below.

U937 Cell Culture Assay. U937 cells were grown according to a previously described literature procedure.¹²³ In general, cells were grown in RPMI 1640 medium enriched with L-glutamine, 10% penicillin and streptomycin, and 10% fetal bovine serum (FBS). Twenty-four hours before dosing with SphK inhibitors, the medium was replaced

with medium containing 2% FBS. All cell cultures were grown at a stable temperature of 37 °C, and the SphK inhibitors were dosed for 2 h.

S1P Extraction and LCMS Quantification. Extraction protocols and LCMS procedures were adapted from a previously reported study.¹²⁴ Samples of pelleted cells (approximately 4 million) were taken up in 2 mL of 3:1 methanol/chloroform mixture and transferred to a capped glass vial. To this suspension was added 10 µL of internal standard solution containing 1 µM C17 S1P (purchased from Avanti Polar Lipids). The mixture was homogenized via sonication for 10 min and immediately incubated at 48 °C for 16 h. After this time, the mixture was cooled to ambient temperature and 200 µL of 1 M KOH in methanol was added to the suspension. The samples were again sonicated and incubated at 37 °C for an additional 2 h. After this time, the samples were neutralized through the addition of 30 µL of glacial acetic acid and transferred to 2 mL microcentrifuge tubes. Samples were then centrifuge at 10000g for 10 min at 4 °C. The supernatant fluid was collected in a separate glass vial, and the pellets were discarded. The resulting solution was evaporated (to a solid) with a stream of nitrogen. Immediately prior to LCMS analysis, the solid material was taken up in 300 µL of methanol and centrifuged at 12000g for 12 min at 4 °C. An autosampler vial was loaded with 150 µL of the resulting supernatant for LCMS analysis. S1P analysis from cellular extracts was performed on an Applied Biosystems 4000 QTrap LC/MS/MS instrument. Chromatographic resolution of analytes was achieved with a Shimadzu LC-20AD system. A binary solvent gradient with a flow rate of 1 mL/min was used to separate sphingolipid

analytes by reverse phase chromatography (Supelco Discovery C18 column; 50 mm, 2.1 mm (length, i.d.); 5 μ m bead size). Mobile phase A consisted of water/methanol/formic acid (79:20:1), and mobile phase B consisted of methanol/formic acid (99:1). The run started with 100% A for 0.5 min. Solvent B was then increased linearly for 5.1 min to 100% of the total solvent composition and held at 100% for an additional 4.3 min. The column was finally reequilibrated to 100% for 0.1 min and held for an additional 1 min. The following analytes (and fragmentation patterns) were monitored simultaneously for identification. C17S1P (366.4, 250.4); S1P (380.4, 264.4).

6.2 General synthetic materials and methods

All nonaqueous reactions were carried out in oven or flame-dried glassware under an argon or nitrogen atmosphere with dry solvents and magnetic stirring, unless otherwise stated. The argon and nitrogen were dried by passing through a tube of Drierite. Anhydrous diethyl ether (Et_2O), chloroform (CHCl_3), Dimethyl sulfoxide (DMSO), toluene (PhMe), dichloromethane (CH_2Cl_2), methanol (MeOH), ethanol (EtOH), and tetrahydrofuran (THF) and *N,N*-dimethylformamide (DMF) were purchased from Aldrich or VMR Chemicals and used as received. THF was dried over activated molecular sieves (4 Å) prior to use. All other reagents were purchased from Acros chemicals and Aldrich chemicals. Except as indicated otherwise, reactions were monitored by thin layer chromatography (TLC) using 0.25 mm Whatman precoated silica gel plates. Flash chromatography was performed with the indicated solvents and Dynamic Adsorbents

silica gel (particle size 0.023 – 0.040 mm). Proton (^1H) and carbon (^{13}C) NMR spectra were recorded on a Varian UnityInova 500/51 or Varian UnityInova 300/54 at 300K unless otherwise noted. Chemical shifts are reported in ppm (δ) values relative to the solvent as follows: CDCl_3 (δ 7.24 for proton and δ 77.0 for carbon NMR), DMSO-d_6 (δ 2.50 for proton and δ 39.5 for carbon NMR) CD_3OD (δ 3.31 for proton and δ 47.6 for carbon NMR). All high-resolution mass spectrometry was carried out by the Mass Spectrometry Laboratory in the School of Chemical Sciences at the University of Illinois Urbana-Champaign (Urbana, IL).

Other abbreviations: 1,1'-bis(diphenylphosphino)ferrocene (dppf), 4-dimethylaminopyridine (DMAP), 9-borabicyclo[3.3.1]nonane (9-BBN), acetic acid (AcOH), benzotriazol-1-yl-oxytripyrrolidinophosphonium hexafluorophosphate (PyBOP), di-tert-butyl dicarbonate (Boc_2O), ethyl acetate (EtOAc), N,N -diisopropylethylamine (DIEA), tert-butanol (tBuOH), triethylamine (TEA), trifluoroacetic acid (TFA), trifluoroacetic anhydride (TFAA), tetrabutylammonium fluoride (TBAF).

Liquid Chromatography and Mass Spectrometry for Evaluation of Chemical Purity. All compounds submitted for biological evaluation were determined to be > 95% pure by LCMS evaluation performed by the Mass Spectrometry Laboratory in the School of Chemical Sciences at the University of Illinois Urbana-Champaign (Urbana, IL). High performance liquid chromatography - mass spectrometry (LCMS) was carried out using an Agilent 2.1x50 mm C-18 column and a Micromass Q-tof Ultima mass spectrometer. Mobile phase A consisted of HPLC grade H_2O and 0.01% TFA; mobile phase B consisted

of MeCN and 0.01% TFA. LCMS identification and purity utilized a binary gradient starting with 90% A and 10% B and linearly increasing to 100% B over the course of 6 min, followed by an isocratic flow of 100% B for an additional 3 min. A flow rate of 0.5 mL / min was maintained throughout the HPLC method. The purity of all products was determined by integration of the total ion count (TIC) spectra and integration of the ultraviolet (UV) spectra at 214 nm. Retention times are abbreviated as t_R ; mass to charge ratios are abbreviated as m/z .

General Procedure A: Conversion of Nitriles to Amidines. To a solution of a nitrile (1.0 eq.) in MeOH (0.10 M) was added a 0.5 M solution of sodium methoxide in MeOH (0.50 eq.) at rt and then heated to 50 °C for 24 h. The intermediate imidate was detectable by TLC; however, being in equilibrium with the nitrile, full conversion does not occur. Ammonium chloride (4.0 eq.) was then added in one portion at that temperature and allowed to react until the imidate was completely consumed by TLC analysis. The reaction was then cooled to rt and evacuated to dryness to yield a crude solid. The solid was reconstituted with CHCl_3 and filtered through a fine glass fritted funnel in order to remove excess ammonium chloride, and the filtrate was again evacuated to dryness. The material was then recrystallized in Et_2O to yield the pure amidine hydrochloride salt. The yields varied greatly depending upon substrate, because amidine formation is dependent upon the equilibrium ratio between nitrile and imidate established under the sodium methoxide conditions.

General Procedure B: PyBOP Mediated Couplings of Amines, Anilines, and Amideoximes to Carboxylic Acids. To a suspension of an amine or aniline (1.0 eq.), carboxylic acid (1.0 eq.), and PyBOP (1.0 eq.), in CH₂Cl₂ at rt was added DIEA (4.0 eq.) and was stirred for 4 h unless otherwise stated. The reaction was then evaporated to dryness and immediately purified by flash chromatography. In the case of amideoximes, a small amount of oxadiazole was formed in the reaction.

General Procedure C: Suzuki Coupling. To a solution of alkene (1.5 eq.) at rt was added a 0.5 M solution of 9-BBN in THF (1.5 eq.) and was stirred until consumption of the alkene was evident by TLC analysis (4 h unless otherwise stated). The reaction was then treated with 3 M NaOH, and diluted with THF (0.2 M relative to the starting alkene). The aryl bromide (1.0 eq.) and Pd(PPh₃)₄ were then sequentially added and the reaction was heated to reflux and was stirred for 4 h. The reaction was reduced to a dark oil, diluted with EtOAc and washed 1x with sat. NaHCO₃. The organic layer was then dried with MgSO₄, evaporated to a dark oil, and immediately purified by flash chromatography.

General Procedure D: Pinnick Oxidation. To a solution of an aldehyde (1.0 eq.), NaH₂PO₄ (8.0 eq.), and 2-methyl-2-butene (10 eq.) in THF, water, and tBuOH (4:4:1) (0.04 M) at rt was added sodium chlorite (4 eq.) and was stirred for 1 h. The reaction was diluted with EtOAc (10x the volume of the reaction's mixture of solvents), and washed 3x with 1 N HCl (5x the volume of the reaction's mixture of solvents). The organic layer

was then dried with MgSO_4 , and evaporated to a white solid. No further purification was necessary.

General procedure E: Deprotection of N-Boc and O-tBu Ester Protecting Groups.

To a solution of either a N-Boc or O-tBu protecting group (1.0 eq.) in CH_2Cl_2 (0.2 M) at rt was added TFA (0.2 M) and the reaction was reacted until judged complete by TLC analysis (30 min unless otherwise stated). The reaction was then evaporated to dryness and taken on crude.

General Procedure F: Conversion of Nitriles to Amideoximes. To a solution of nitrile (1 eq.) and hydroxylamine hydrochloride (5 eq.) in EtOH (0.2 M) was added TEA (10 eq.). The reaction was heated to 50 °C for 5 h. The EtOH was evaporated and the crude white solid was immediately purified via flash chromatography.

General Procedure G: Synthesis of 3,5-disubstituted-1,2,4-oxadiazoles Using Tetrabutylammonium Fluoride from Acylated Amideoximes. To a solution of O-acyl amidoxime (1.0 eq.) in THF (0.1 M) at rt was added a 1.0 M solution of TBAF in THF (1.0 eq.) and was stirred for 1 h. The reaction was evaporated to dryness and immediately purified by flash chromatography.

General Procedure H: Coupling of Amines to N,N'-Di-Boc-1H-pyrazole-1-carboxamidine. To a solution of amine (1.0 eq.) and N,N'-Di-Boc-1H-pyrazole-1-carboxamidine (1.1 eq.) in MeOH (0.1 M) was added a catalytic amount of DMAP followed by DIEA (3.0 eq.). The reaction was heated to 50 °C overnight, cooled to rt, and evaporated. The resulting solid was immediately purified via flash chromatography.

General Procedure I: Esterification of Benzoic Acids to Methyl Benzoates. A 2 M solution of HCl in MeOH was prepared by adding acetyl chloride dropwise to MeOH (1.0 M relative to the benzoic acid) at 0 °C. This mixture was removed from the ice bath and stirred for 15 min. A benzoic acid (1 eq.) was added neat and the mixture was heated to reflux for 14 h. The mixture was then cooled to room temperature and evaporated to a yellow oil and immediately purified by flash chromatography.

General Procedure J: Benzohydrazide Formation. To a solution of a methyl benzoate (1 eq.) in EtOH (0.6 M) at room temperature was added hydrazine (3 eq.), and the mixture was heated to reflux for 14 h. The mixture was then cooled to room temperature, evaporated to a white solid, and immediately purified by flash chromatography.

General Procedure K: Conversion of N-acylbenzohydrazides to 1,3,4-oxadiazoles. To a solution of a N-acylbenzohydrazide (1.0 eq.) and *p*-toluenesulfonylchloride (2.0 eq.) in CH₂Cl₂ (0.2 M) was added TEA (3.0 eq.) dropwise. The mixture was allowed to stir at room temperature for 12 h. The reaction was evaporated to dryness and immediately purified by flash chromatography.

General Procedure L: Acid Chloride Formation. To a solution of a carboxylic acid (1.0 eq.) and DMF (0.05 eq.) in CH₂Cl₂ (0.1 M) at 0 °C was added oxalyl chloride (2.0 eq.) dropwise and let warm to rt. The reaction progresses to a yellow green color and after 3 h the reaction was evaporated to dryness, and then immediately purified by flash chromatography.

General Procedure M: Acid Chloride and Amine Coupling. To a solution of an acid chloride (1.0 eq.) in CH_2Cl_2 (0.3 M) at rt was added DIEA (4.0 eq.) followed by an amine HCl salt (1.5 eq.) and the reaction was left stirring for 12 h. The reaction was then evaporated to dryness and immediately purified by flash chromatography.

General Procedure N: Williamson Ether Synthesis. To a solution of an alcohol (2 eq.) in DMF (0.3 M) at 0 °C was added 60 % sodium hydride dispersed in mineral oil (2.0 eq.) at 0 °C, then let warm to rt, and then let react for 45 min. The alkyl bromide was then added in one portion and the reaction was stirred for 12 h. The reaction was quenched with sat. NaHCO_3 (100x the volume of DMF) and extracted into EtOAc (100x the volume of DMF). The organic layer was washed 3x with neat water (100x the volume of DMF), dried with Na_2SO_4 , evaporated to a yellow oil, and immediately purified by flash chromatography.

General Procedure O: Cyclization of a Dihydrazide to Form a Thiadiazole. A couple hydrazide product (1.0 eq.) was dissolved in toluene (0.08 M) and Lawesson's reagent (3.0 eq., recrystallized from boiling toluene) was added. The mixture stirred at reflux until dissolution, then another 2 h. The reaction mixture was directly purified by flash chromatography, followed by preparatory TLC if necessary.

General Procedure P: One-pot Deprotection of Boc and Acetonide Groups. The protected amino alcohol (1.0 eq.) was dissolved in MeOH (0.05 M); para-toluenesulfonic acid monohydrate (5.0 eq.) was added. The reaction mixture stirred at 70 °C or until for 2 h or until complete by TLC. After cooling, the MeOH was evaporated and the residue

taken up in DCM. This was washed 3 times with K_2CO_3 and once with brine, then dried over Na_2SO_4 , and purified by preparatory TLC.

General Procedure Q: Acetonide Protection and Cyclization of Serine or Threonine Amino Acid Derivatives. A Boc-protected serine or threonine (1 eq) was dissolved in acetone (0.4 M). Dimethoxypropane (1.3 eq.) was added, followed by $BF_3 \cdot Et_2O$ (cat. eq.), and the mixture stirred 3.5 h at rt. The liquids were evaporated and the residue taken up in EtOAc, which was washed 3 times with sat. NH_4Cl and once with brine, dried over Na_2SO_4 , concentrated, and carried on crude.

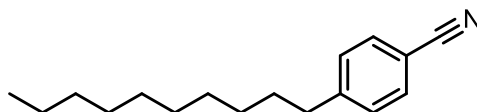
General Procedure R: Coupling of Amines or Hydrazides to Carboxylic Acids using ⁱButyl chloroformate. The carboxylic acid (1.0 eq.) was dissolved in THF (0.15 M), then NMM (1.0 eq.) and isobutyl chloroformate (1.0 eq., added dropwise) were added and the solution stirred for 0.5 h. The amine or hydrazide (1.0 eq.) was added in one portion and the reaction stirred for 2 h. The reaction mixture was filtered and the filtrate concentrated. The resultant residue was taken up in EtOAc, washed 3 times with water and once with brine, dried over Na_2SO_4 , and purified by flash chromatography.

General Procedure S: Saponification of a Methyl Ester. The methyl ester (1.0 eq.) was dissolved in a 3:1 solution of THF:Water (0.13M). $LiOH \cdot H_2O$ (5.0 eq) was added and the solution stirred overnight at rt. The THF was then evaporated; the solution was diluted slightly with water and acidified using 10% HCl. This was extracted 3 times with EtOAc and these organic layers dried over Mg_2SO_4 .

General Procedure T: Coupling of Acid Halides to Boc-protected Amino Acids.

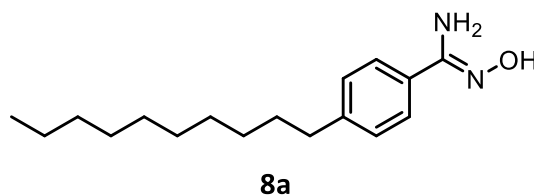
The acid halide (1.0 eq.) and Boc-protected amino acid (1.0 eq.) were dissolved in a 1:1 solution of 1 M NaOH:THF (0.2 M). This solution stirred overnight at rt, then was cooled to 0 degrees C, washed once with cold Et₂O, acidified to pH 4 with 1 M HCl, and extracted 3 times with EtOAc. The combined organics were dried over Na₂SO₄, concentrated, and carried on crude.

6.3 Syntheses and NMR data

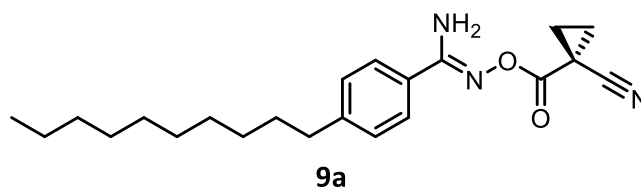


7a

4-decylnitrile (7a). General procedure C was used to couple 1-decene (1.20 mL, 6.16 mmol) and 4-bromobenzonitrile (750 mg, 4.11 mmol) to yield the title product. 98%. Clear and colorless oil. R_f = 0.47 (5% EtOAc in hexanes). ¹H NMR (300 MHz, CDCl₃) δ 7.51 (d, J = 8.1, 2H), 7.24 (d, J = 8.0, 2H), 2.62 (t, J = 7.6, 2H), 1.68 – 1.48 (m, 2H), 1.37 – 1.13 (m, 14H), 0.85 (t, J = 6.6, 3H). ¹³C NMR (75 MHz, CDCl₃) δ 148.77, 132.24, 129.38, 119.31, 109.68, 36.31, 32.12, 31.20, 29.81, 29.77, 29.65, 29.55, 29.40, 22.91, 14.33.

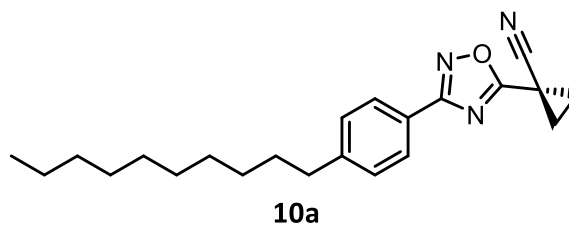


(Z)-4-decyl-*N'*-hydroxybenzimidamide (8a). General procedure F was used to convert 7a (0.98 g, 4.03 mmol) to the title product. 90%. R_f = 0.48 (50% EtOAc in hexanes). ^1H NMR (300 MHz, CDCl_3) δ 7.54 (d, J = 8.3, 2H), 7.20 (d, J = 8.3, 2H), 4.93 (s, 2H), 2.62 (t, J = 7.5, 2H), 1.72 – 1.50 (m, 2H), 1.42 – 1.14 (m, 14H), 0.88 (t, J = 6.6, 3H). ^{13}C NMR (75 MHz, CDCl_3) δ 152.94, 145.42, 129.82, 128.91, 126.00, 36.00, 32.13, 31.54, 29.82, 29.72, 29.56, 29.51, 22.92, 14.36.



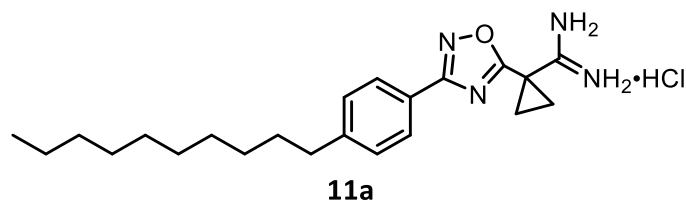
(Z)-*N'*-((1-cyanocyclopropanecarbonyl)oxy)-4-decylbenzimidamide (9a).

General procedure B was used to couple 8a (150 mg, 0.54 mmol) and 1-cyano-1-cyclopropanecarboxylic acid (60 mg, 0.54 mmol) to yield the title product. 91%. White solid. R_f = 0.32 (25% EtOAc in hexanes). ^1H NMR (300 MHz, CDCl_3) δ 7.57 (d, J = 8.1, 2H), 7.19 (d, J = 8.1, 2H), 5.31 (s, 2H), 2.61 (t, J = 7.7, 2H), 1.78 (dd, J = 4.7, 8.3, 2H), 1.66 (dd, J = 4.7, 8.3, 2H), 1.58 (m, 2H), 1.24 (m, 14H), 0.86 (t, J = 6.2, 3H). ^{13}C NMR (75 MHz, CDCl_3) δ 164.82, 157.95, 146.89, 129.04, 127.88, 126.92, 118.98, 36.02, 32.11, 31.45, 29.80, 29.68, 29.54, 29.43, 22.91, 19.38, 14.36, 12.65.



1-(3-(4-decylphenyl)-1,2,4-oxadiazol-5-yl)cyclopropanecarbonitrile (10a).

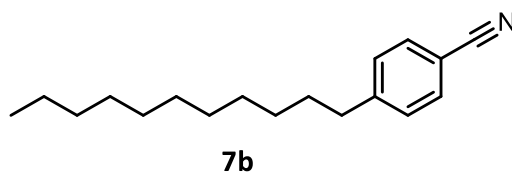
General procedure G was used to convert 9a (182 mg, 0.49 mmol) to the title product. 73%. White solid. R_f = 0.43 (25% EtOAc in hexanes). ^1H NMR (300 MHz, CDCl_3) δ 7.93 (d, J = 8.2, 2H), 7.27 (d, J = 8.1, 2H), 2.65 (t, J = 7.5, 2H), 2.01 (s, 4H), 1.63 (m, 2H), 1.25 (m, 18H), 0.88 (t, J = 6.7, 3H). ^{13}C NMR (75 MHz, CDCl_3) δ 174.84, 169.02, 147.23, 129.19, 127.70, 123.48, 117.79, 36.21, 32.15, 31.43, 29.88, 29.71, 29.60, 29.50, 23.33, 22.94, 19.50, 14.38, 9.10.



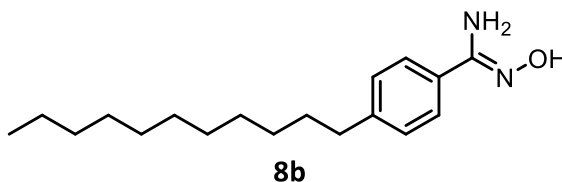
1-(3-(4-decylphenyl)-1,2,4-oxadiazol-5-yl)cyclopropanecarboximidamide

hydrochloride (11a). General procedure A was used to convert 10a (126 mg, 0.36 mmol) to the title product. In this example, the solid was purified via flash chromatography. The hydrochloride salt was prepared by the dropwise addition of 2 M HCl in ether to the purified amidine. The ether was evaporated, reconstituted in ether, and again evacuated to dryness to yield the title product. 66%. Tan solid. R_f = 0.42 (15% MeOH in CHCl_3). ^1H NMR (500 MHz, DMSO) δ 9.54 (s, 2H), 9.39 (s, 2H), 7.87 (d, J = 5.8, 2H), 7.36

(d, $J = 5.9$, 2H), 2.62 (s, 2H), 1.94 (s, 2H), 1.83 (s, 2H), 1.56 (s, 2H), 1.23 (m, 14H), 0.83 (s, 3H). ^{13}C NMR (126 MHz, DMSO) δ 177.73, 168.18, 166.02, 147.06, 129.70, 127.50, 123.50, 35.50, 31.74, 31.09, 29.43, 29.27, 29.14, 29.08, 22.61, 22.56, 18.67, 14.44. LCMS: $t_R = 5.22$; $m/z = 369.2$. HRMS m/z calcd for $\text{C}_{22}\text{H}_{33}\text{N}_4\text{O}$ ($M + H$), 369.2654; found 369.2644.

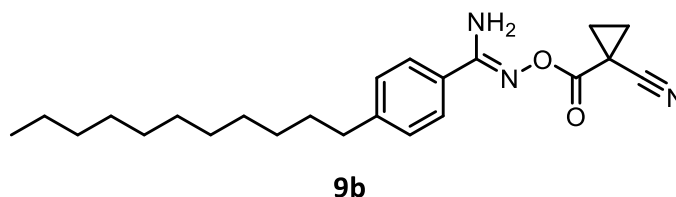


4-undecylbenzonitrile (7b). General procedure C was used to couple undecene (2.40 mL, 11.66 mmol) and 4-bromobenzonitrile (1.40 g, 7.70 mmol) to yield the title product. 99%. Colorless oil. $R_f = 0.50$ (10% EtOAc in hexanes). ^1H NMR (300 MHz, CDCl_3) δ 7.48 (d, $J = 8.2$, 2H), 7.21 (d, $J = 8.1$, 2H), 2.60 (t, $J = 7.5$, 2H), 1.57 (m, 2H), 1.22 (m, 16H), 0.84 (t, $J = 6.3$, 3H). ^{13}C NMR (75 MHz, CDCl_3) δ 148.67, 132.17, 129.35, 119.15, 109.75, 36.28, 32.14, 31.19, 29.86, 29.78, 29.65, 29.58, 29.42, 22.91, 14.30.



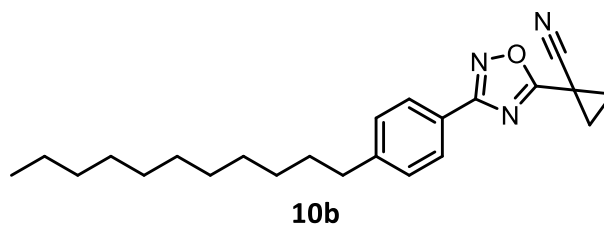
(Z)-N'-hydroxy-4-undecylbenzimidamide (8b). General procedure F was used to convert 7b (2.00 g, 7.77 mmol) to the title product. 95%. White solid. $R_f = 0.51$ (50% EtOAc in hexanes). ^1H NMR (300 MHz, CDCl_3) δ 7.54 (d, $J = 8.2$, 2H), 7.19 (d, $J = 8.2$, 2H), 4.93 (s, 2H), 2.61 (t, $J = 7.5$ 1H), 1.73 – 1.50 (m, 2H), 1.45 – 1.19 (m, 16H), 0.89 (t, $J = 6.7$,

3H). ^{13}C NMR (75 MHz, CDCl_3) δ 152.90, 145.36, 129.91, 128.90, 126.01, 36.00, 32.16, 31.55, 29.84, 29.75, 29.59, 29.53, 22.93, 14.37.



(Z)-N'-((1-cyanocyclopropanecarbonyl)oxy)-4-undecylbenzimidamide (9b).

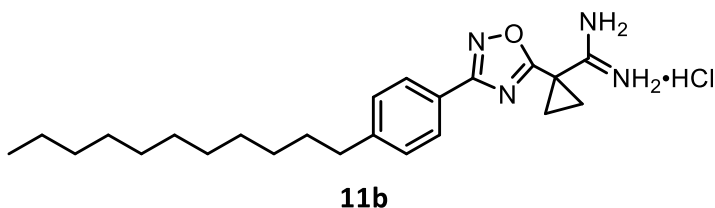
General procedure B was used to couple 8b (150 mg, 0.52 mmol) and 1-cyano-1-cyclopropanecarboxylic acid (57 mg, 0.52 mmol) to yield the title product. 82%. White solid. R_f = 0.63 (50% EtOAc in hexanes). ^1H NMR (300 MHz, CDCl_3) δ 7.58 (d, J = 8.2, 2H), 7.20 (d, J = 8.1, 2H), 5.29 (s, 2H), 2.61 (t, J = 7.5, 2H), 1.79 (dd, J = 4.6, 8.4, 2H), 1.67 (dd, J = 4.8, 8.3, 2H), 1.58 (m, 2H), 1.24 (m, 16H), 0.87 (t, J = 6.5, 3H). ^{13}C NMR (75 MHz, CDCl_3) δ 164.81, 157.94, 146.92, 130.21, 129.06, 127.88, 126.92, 118.99, 36.03, 32.14, 31.46, 29.85, 29.80, 29.69, 29.57, 29.43, 22.92, 19.39, 14.37, 12.66.



1-(3-(4-undecylphenyl)-1,2,4-oxadiazol-5-yl)cyclopropanecarbonitrile (10b).

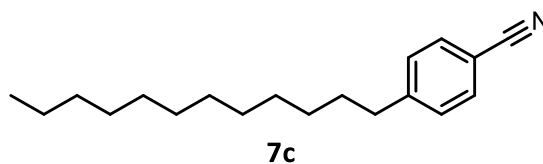
General procedure G was used to convert 9b (163 mg, 0.43 mmol) to the title product. 81%. White solid. R_f = 0.64 (25% EtOAc in hexanes). ^1H NMR (300 MHz, CDCl_3) δ 7.93 (d, J = 8.3, 2H), 7.27 (d, J = 8.3, 2H), 2.65 (t, J = 7.5, 2H), 2.02 (d, J = 7.9, 4H), 1.63 (m, 2H),

1.28 (m, 16H), 0.88 (t, $J = 6.7$, 3H). ^{13}C NMR (75 MHz, CDCl_3) δ 174.85, 169.01, 147.24, 129.18, 127.69, 123.51, 117.78, 36.20, 32.15, 31.43, 29.87, 29.71, 29.58, 29.50, 22.93, 20.89, 18.90, 14.37, 9.08.

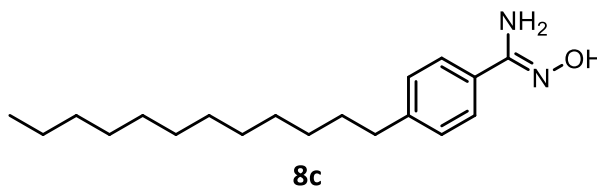


1-(3-(4-undecylphenyl)-1,2,4-oxadiazol-5-yl)cyclopropanecarboximidamide

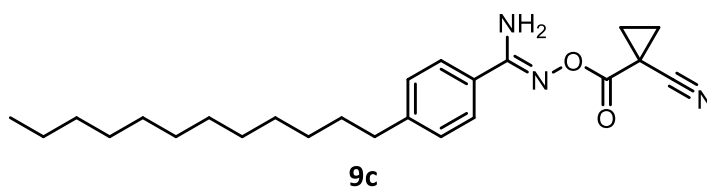
hydrochloride (11b). General procedure A was used to convert 10b (127 mg, 0.35 mmol) to the title product. In this example, the solid was purified via flash chromatography. The hydrochloride salt was prepared by the dropwise addition of 2 M HCl in ether to the purified amidine. The ether was evaporated, reconstituted in ether, and again evacuated to dryness to yield the title product. 32%. Tan solid. $R_f = 0.49$ (15% MeOH in CHCl_3). ^1H NMR (500 MHz, DMSO) δ 9.56 (s, 2H), 9.42 (s, 2H), 7.88 (d, $J = 7.5$, 2H), 7.37 (d, $J = 7.5$, 2H), 2.62 (t, $J = 7.1$, 3H), 1.95 (s, 2H), 1.85 (s, 2H), 1.57 (s, 2H), 1.24 (m, 16H), 0.83 (t, $J = 6.4$, 3H). ^{13}C NMR (126 MHz, DMSO) δ 177.72, 168.18, 166.04, 147.05, 129.68, 127.50, 123.50, 35.49, 31.74, 31.08, 29.44, 29.27, 29.16, 29.07, 22.60, 22.55, 18.66, 14.42. LCMS: $t_R = 5.22, 6.08$; $m/z = 383.2$. HRMS m/z calcd for $\text{C}_{23}\text{H}_{35}\text{N}_4\text{O}$ ($M + \text{H}$), 383.2811; found 383.2805.



4-dodecylbenzonitrile (7c). General procedure C was used to couple 1-dodecene (3.64 mL, 16.4 mmol) and 4-iodobenzonitrile (2.5 g, 10.9 mmol) to yield the title product. 99%. Colorless oil. $R_f = 0.52$ (10% EtOAc in hexanes). ^1H NMR (300 MHz, CDCl_3) δ 7.56 (d, $J = 8.1$, 2H), 7.26 (d, $J = 8.1$, 2H), 2.71 – 2.59 (m, 2H), 1.60 (m, 2H), 1.38 – 1.16 (m, 18H), 0.88 (t, $J = 6.7$, 3H).

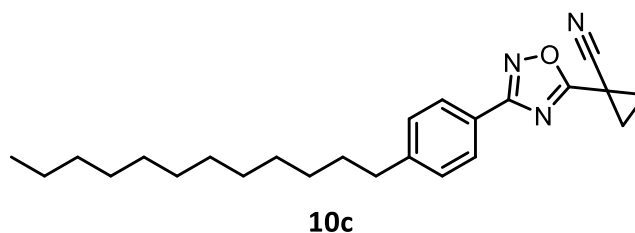


(Z)-4-dodecyl-N'-hydroxybenzimidamide (8c). General procedure F was used to convert 7c (1.17 g, 4.31 mmol) to the title product. 86%. White solid. $R_f = 0.52$ (50% EtOAc in hexanes). ^1H NMR (300 MHz, CDCl_3) δ 7.53 (d, $J = 8.3$, 2H), 7.20 (d, $J = 8.3$, 2H), 4.88 (s, 2H), 2.61 (t, $J = 7.5$, 2H), 1.60 (m, 2H), 1.25 (m, 18H), 0.88 (t, $J = 6.7$, 3H). ^{13}C NMR (151 MHz, CDCl_3) δ 153.57, 145.82, 128.78, 128.44, 126.04, 35.81, 31.95, 31.28, 29.71, 29.70, 29.67, 29.63, 29.52, 29.39, 29.34, 22.72, 14.16.



(Z)-N'-((1-cyanocyclopropanecarbonyl)oxy)-4-dodecylbenzimidamide (9c).

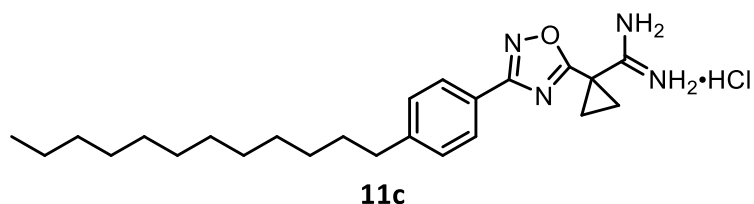
General procedure B was used to couple 8c (200 mg, 0.66 mmol) and 1-cyano-1-cyclopropanecarboxylic acid (311 mg, 0.60 mmol) to yield the title product. 80%. White solid. R_f = 0.21 (25% EtOAc in hexanes). ^1H NMR (300 MHz, CDCl_3) δ 7.58 (d, J = 8.0, 2H), 7.21 (d, J = 7.9, 2H), 5.28 (s, 2H), 2.62 (t, J = 7.6, 2H), 1.80 (dd, J = 4.8, 8.2, 2H), 1.68 (dd, J = 4.6, 8.4, 2H), 1.64 – 1.52 (m, 2H), 1.25 (m, 18H), 0.87 (t, J = 6.5, 3H). ^{13}C NMR (75 MHz, CDCl_3) δ 164.81, 157.93, 146.98, 129.09, 127.85, 126.93, 118.99, 36.03, 32.14, 31.47, 29.87, 29.81, 29.69, 29.58, 29.43, 22.92, 19.41, 14.37, 12.65.



1-(3-(4-dodecylphenyl)-1,2,4-oxadiazol-5-yl)cyclopropanecarbonitrile (10c).

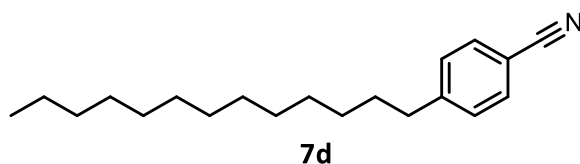
General procedure G was used to convert 9c (190 mg, 0.48 mmol) to the title product. 99%. White solid. R_f = 0.56 (25% EtOAc in hexanes). ^1H NMR (300 MHz, CDCl_3) δ 7.94 (d, J = 8.2, 2H), 7.27 (d, J = 8.1, 2H), 2.65 (t, J = 7.5, 2H), 2.01 (s, 4H), 1.63 (m, 2H), 1.25 (m, 18H), 0.88 (t, J = 6.7, 3H). ^{13}C NMR (75 MHz, CDCl_3) δ 174.83, 169.02, 147.25, 129.19,

127.70, 123.48, 117.80, 36.21, 32.15, 31.45, 29.88, 29.71, 29.60, 29.50, 23.33, 22.94, 20.90, 14.38, 9.10.

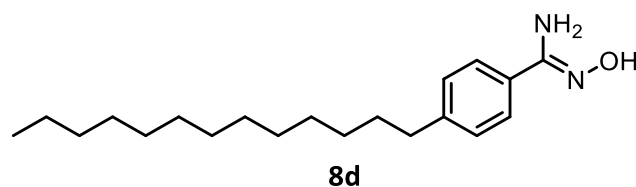


1-(3-(4-dodecylphenyl)-1,2,4-oxadiazol-5-yl)cyclopropanecarboximidamide

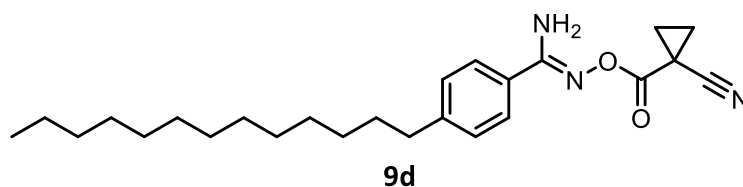
hydrochloride (11c). General procedure A was used to convert 10c (190 mg, 0.50 mmol) to the crude amidine. In this example, the solid was purified via flash chromatography. The hydrochloride salt was prepared by the dropwise addition of 2 M HCl in ether to the purified amidine. The ether was evaporated, reconstituted in ether, and again evacuated to dryness to yield the title product. 50%. Yellow solid. $R_f = 0.28$ (15% MeOH in CHCl_3). ^1H NMR (500 MHz, DMSO) δ 9.56 (s, 1H), 9.43 (s, 1H), 7.88 (d, $J = 7.1$, 2H), 7.37 (d, $J = 7.2$, 2H), 2.62 (m, 2H), 1.96 (s, 2H), 1.84 (s, 2H), 1.57 (s, 2H), 1.24 (m, 18H), 0.83 (t, $J = 5.9$, 2H). ^{13}C NMR (126 MHz, DMSO) δ 177.73, 168.17, 166.03, 147.04, 129.67, 127.50, 123.51, 35.50, 31.75, 31.09, 29.46, 29.27, 29.17, 29.08, 22.60, 22.56, 18.66, 14.42. LCMS: $t_R = 6.65$; $m/z = 397.3$. HRMS m/z calcd for $\text{C}_{24}\text{H}_{37}\text{N}_4\text{O}$ ($M + \text{H}$), 397.2967; found 397.2967.



4-tridecylbenzonitrile (7d). General procedure C was used to couple 1-tridecene (1.95 mL, 8.24 mmol) and 4-bromobenzonitrile (1.0 g, 5.49 mmol) to yield the title product. 97%. Clear and colorless oil. R_f = 0.56 (5% EtOAc in hexanes). ^1H NMR (300 MHz, CDCl_3) δ 7.54 (d, J = 8.0, 2H), 7.26 (d, J = 8.0, 2H), 2.65 (t, J = 7.7, 2H), 1.71 – 1.51 (m, 2H), 1.41 – 1.17 (m, 20H), 0.87 (t, J = 6.6, 3H). ^{13}C NMR (75 MHz, CDCl_3) δ 148.67, 132.15, 129.26, 119.24, 109.54, 36.20, 32.01, 31.06, 29.74, 29.61, 29.49, 29.27, 22.78, 14.20.

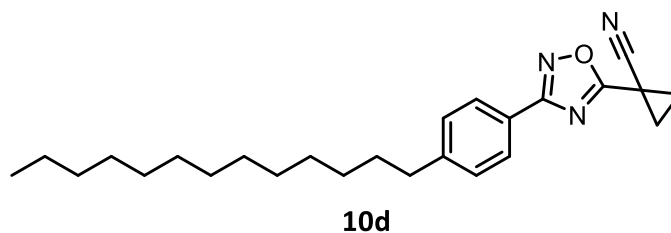


(Z)-N'-hydroxy-4-tridecylbenzimidamide (8d). General procedure F was used to convert 7d (1.53 g, 5.36 mmol) to the title product. 90%. White solid. R_f = 0.50 (40% EtOAc in hexanes). ^1H NMR (300 MHz, CDCl_3) δ 7.54 (d, J = 8.0, 2H), 7.20 (d, J = 8.1, 2H), 4.87 (s, 2H), 2.62 (t, J = 7.7, 2H), 1.71 – 1.51 (m, 2H), 1.39 – 1.16 (m, 20H), 0.88 (t, J = 6.5, 3H). ^{13}C NMR (75 MHz, CDCl_3) δ 152.79, 145.27, 129.91, 128.82, 125.85, 35.91, 32.07, 31.46, 29.81, 29.64, 29.50, 29.42, 25.45, 22.84, 14.27, 0.81.



(Z)-N'-((1-cyanocyclopropanecarbonyl)oxy)-4-tridecylbenzimidamide (9d).

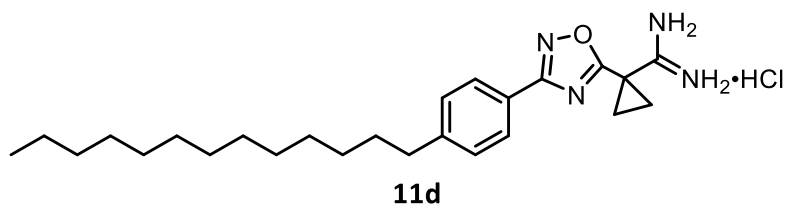
General procedure B was used to couple 8d (193 mg, 0.61 mmol) and 1-cyano-1-cyclopropanecarboxylic acid (67 mg, 0.61 mmol) to yield the title product. 82%. White solid. R_f = 0.20 (25% EtOAc in hexanes). ^1H NMR (300 MHz, CDCl_3) δ 7.59 (d, J = 8.3, 2H), 7.22 (d, J = 8.2, 2H), 5.24 (s, 2H), 2.56 (t, J = 7.7, 2H), 1.81 (dd, J = 4.6, 8.4, 2H), 1.68 (dd, J = 4.6, 8.4, 2H), 1.65 – 1.52 (m, 2H), 1.39 – 1.17 (m, 20H), 0.87 (t, J = 6.6, 3H). ^{13}C NMR (75 MHz, CDCl_3) δ 164.66, 157.78, 146.81, 128.94, 127.76, 126.79, 118.86, 35.90, 32.01, 31.32, 29.75, 29.56, 29.45, 29.30, 22.79, 19.25, 14.22, 12.53.



1-(3-(4-tridecylphenyl)-1,2,4-oxadiazol-5-yl)cyclopropanecarbonitrile (10d).

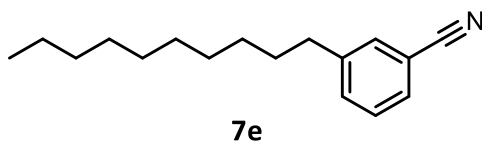
General procedure G was used to convert 9d (205 mg, 0.50 mmol) to the title product. 88%. White solid. R_f = 0.59 (25% EtOAc in hexanes). ^1H NMR (300 MHz, CDCl_3) δ 7.93 (d, J = 8.1, 2H), 7.27 (d, J = 8.1, 2H), 2.56 (t, J = 7.7, 2H), 2.00 (s, 4H), 1.70 – 1.51 (m, 2H), 1.41 – 1.19 (m, 20H), 0.88 (t, J = 6.5, 3H). ^{13}C NMR (75 MHz, CDCl_3) δ 174.70, 168.84,

147.05, 129.01, 127.52, 123.35, 117.61, 36.03, 32.00, 31.27, 29.73, 29.65, 29.55, 29.44, 29.34, 22.77, 20.72, 14.20, 8.91.



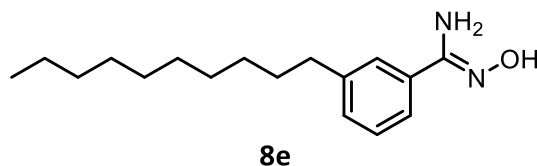
1-(3-(4-tridecylphenyl)-1,2,4-oxadiazol-5-yl)cyclopropanecarboximidamide

hydrochloride (11d). General procedure A was used to convert 10d (198 mg, 0.50 mmol) to the title product. 36%. Yellow solid. R_f = 0.23 (15% MeOH in CHCl_3). ^1H NMR (600 MHz, DMSO) δ 9.56 (s, 2H), 9.44 (s, 2H), 7.88 (d, J = 8.1, 2H), 7.37 (d, J = 8.1, 2H), 2.57 (t, J = 7.6, 2H), 2.03 – 1.78 (m, 4H), 1.70 – 1.48 (m, 2H), 1.36 – 1.12 (m, 20H), 0.84 (t, J = 6.6, 3H). ^{13}C NMR (151 MHz, DMSO) δ 177.09, 167.59, 165.51, 146.43, 129.07, 126.91, 122.93, 34.92, 31.15, 30.47, 28.89, 28.86, 28.82, 28.67, 28.56, 28.48, 21.99, 21.95, 18.12, 13.82. LCMS: t_R = 7.44 m/z = 411.3. HRMS m/z calcd for $\text{C}_{25}\text{H}_{39}\text{N}_4\text{O}$ ($M + \text{H}$), 411.3124; found 411.3119.

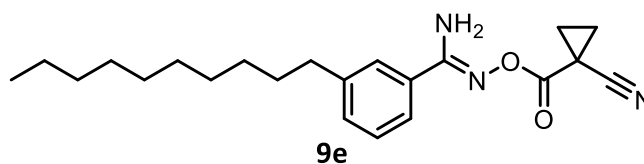


3-decylnitrile (7e). General procedure C was used to couple 1-decene (1.6 mL, 8.33 mmol) and 3-bromobenzonitrile (1.0 g, 5.56 mmol) to yield the title product. 99%. Clear and colorless oil. R_f = 0.35 (5% EtOAc in hexanes). ^1H NMR (300 MHz, CDCl_3) δ 7.51 – 7.30 (m, 4H), 2.62 (t, J = 7.7, 2H), 1.71 – 1.54 (m, 2H), 1.40 – 1.18 (m, 14H), 0.88

(t, $J = 6.7$, 3H). ^{13}C NMR (75 MHz, CDCl_3) δ 144.35, 133.13, 132.04, 129.57, 129.11, 112.34, 35.63, 32.01, 31.22, 29.69, 29.65, 29.52, 29.43, 29.23, 22.80, 14.24.



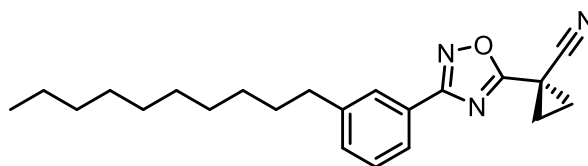
(Z)-3-decyl-*N'*-hydroxybenzimidamide (8e). General procedure F was used to convert 7e (1.38 g, 5.67 mmol) to the title product. 89%. White solid. $R_f = 0.48$ (40% EtOAc in hexanes). ^1H NMR (300 MHz, CDCl_3) δ 7.55 – 7.41 (m, 2H), 7.37 – 7.19 (m, 2H), 4.97 (s, 2H), 2.57 (t, $J = 7.7$, 2H), 1.72 – 1.56 (m, 2H), 1.48 – 1.09 (m, 14H), 0.91 (t, $J = 6.5$, 3H). ^{13}C NMR (75 MHz, CDCl_3) δ 152.90, 143.44, 132.44, 130.09, 128.54, 126.05, 123.32, 35.99, 31.99, 31.54, 29.70, 29.60, 29.42, 22.77, 14.20.



(Z)-*N'*-((1-cyanocyclopropanecarbonyl)oxy)-3-decylbenzimidamide (9e).

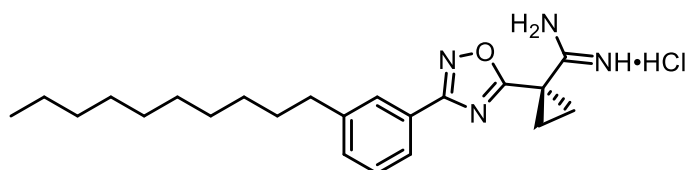
General procedure B was used to couple 8e (178 mg, 0.64 mmol) and 1-cyano-1-cyclopropanecarboxylic acid (72 mg, 0.64 mmol) to yield the title product. 64%. White solid. $R_f = 0.25$ (25% EtOAc in hexanes). ^1H NMR (300 MHz, CDCl_3) δ 7.54 – 7.40 (m, 2H), 7.32 – 7.25 (m, 2H), 5.34 (s, 2H), 2.59 (t, $J = 7.7$, 2H), 1.77 (dd, $J = 4.6$, 8.4, 2H), 1.65 (dd, $J = 4.8$, 8.2, 2H), 1.62 – 1.52 (m, 2H), 1.40 – 1.13 (m, 14H), 0.86 (t, $J = 6.5$, 3H). ^{13}C NMR

(75 MHz, CDCl₃) δ 164.66, 157.97, 143.76, 131.45, 130.34, 128.68, 126.89, 124.05, 118.75, 35.82, 31.92, 31.42, 29.62, 29.50, 29.34, 22.71, 19.20, 14.16, 12.45.

**10e**

1-(3-(3-decylphenyl)-1,2,4-oxadiazol-5-yl)cyclopropanecarbonitrile (10e).

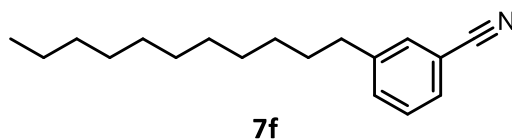
General procedure G was used to convert 9e (152 mg, 0.41 mmol) to the title product. 72%. White solid. R_f = 0.63 (25% EtOAc in hexanes). ¹H NMR (300 MHz, CDCl₃) δ 7.87 – 7.81 (m, 2H), 7.41 – 7.28 (m, 2H), 2.65 (t, J = 7.7, 2H), 2.01 (s, 4H), 1.71 – 1.56 (m, 2H), 1.42 – 1.19 (m, 14H), 0.87 (t, J = 6.7, 3H). ¹³C NMR (75 MHz, CDCl₃) δ 174.78, 168.98, 143.86, 131.81, 128.85, 127.46, 125.85, 124.93, 117.59, 35.87, 31.96, 31.47, 29.65, 29.54, 29.36, 22.75, 20.73, 14.18, 8.91.

**11e**

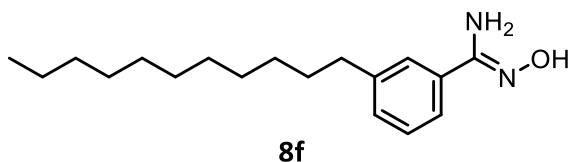
1-(3-(3-decylphenyl)-1,2,4-oxadiazol-5-yl)cyclopropanecarboximidamide

hydrochloride (11e). General procedure A was used to convert 10e (170 mg, 0.48 mmol) to the title product. 35%. Yellow solid. R_f = 0.31 (15% MeOH in CHCl₃). ¹H NMR (300 MHz, DMSO) δ 9.57 (s, 2H), 9.43 (s, 2H), 7.89 – 7.72 (m, 2H), 7.54 – 7.36 (m, 2H), 2.66 (t, J = 7.4, 2H), 2.03 – 1.80 (m, 4H), 1.67 – 1.48 (m, 2H), 1.37 – 1.12 (m, 14H), 0.84

(t, $J = 6.3$, 3H). ^{13}C NMR (151 MHz, DMSO) δ 177.20, 167.74, 165.58, 143.52, 131.73, 129.19, 126.62, 125.50, 124.43, 34.79, 31.18, 30.86, 28.88, 28.87, 28.72, 28.57, 28.50, 21.99, 18.19, 13.86. LCMS: $t_{\text{R}} = 5.44$; $m/z = 369.2$. HRMS m/z calcd for $\text{C}_{22}\text{H}_{33}\text{N}_4\text{O}$ ($\text{M} + \text{H}$), 369.2654; found 369.2656.

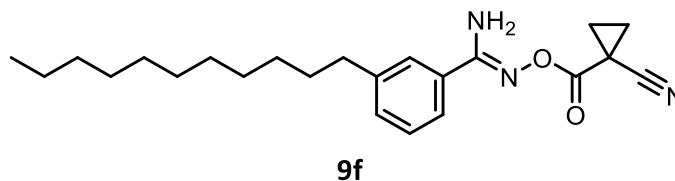


3-undecylbenzonitrile 7f). General procedure C was used to couple 1-undecene (1.71 mL, 8.33 mmol) and 3-bromobenzonitrile (1.0 g, 5.56 mmol) to yield the title product. 99%. Clear and colorless oil. $R_{\text{f}} = 0.38$ (5% EtOAc in hexanes). ^1H NMR (300 MHz, CDCl_3) δ 7.51 – 7.30 (m, 4H), 2.63 (t, $J = 7.7$, 2H), 1.70 – 1.48 (m, 2H), 1.47 – 1.15 (m, 16H), 0.88 (t, $J = 6.7$, 3H). ^{13}C NMR (75 MHz, CDCl_3) δ 144.35, 133.14, 132.06, 129.57, 129.12, 119.27, 112.35, 35.63, 32.03, 31.23, 29.74, 29.65, 29.53, 29.46, 29.24, 22.81, 14.25.



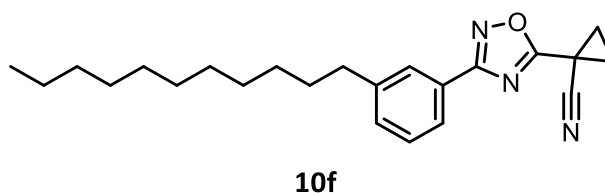
(Z)-N'-hydroxy-3-undecylbenzimidamide (8f). General procedure F was used to convert 7f (1.41 g, 5.5 mmol) to the title product. 90%. White solid. $R_{\text{f}} = 0.49$ (40% EtOAc in hexanes). ^1H NMR (300 MHz, CDCl_3) δ 7.45 (d, $J = 8.7$, 2H), 7.35 – 7.20 (m, 2H), 4.92 (s, 2H), 2.57 (t, $J = 7.7$, 2H), 1.72 – 1.51 (m, 2H), 1.44 – 1.06 (m, 16H), 0.88 (d, $J =$

6.9, 3H). ^{13}C NMR (75 MHz, CDCl_3) δ 152.90, 143.56, 132.49, 130.21, 128.63, 126.05, 123.32, 36.04, 32.05, 31.59, 29.73, 29.65, 29.46, 22.82, 14.25.



(Z)-N'-((1-cyanocyclopropanecarbonyl)oxy)-3-undecylbenzimidamide (9f).

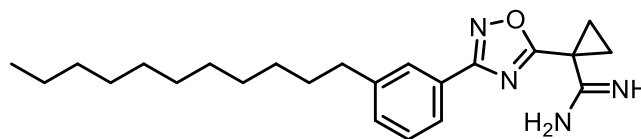
General procedure B was used to couple 8f (192 mg, 0.66 mmol) and 1-cyano-1-cyclopropanecarboxylic acid (73 mg, 0.66 mmol) to yield the title product. 64%. White solid. R_f = 0.24 (25% EtOAc in hexanes). ^1H NMR (300 MHz, CDCl_3) δ 7.48 (s, 1H), 7.46 – 7.39 (m, 1H), 7.29 – 7.22 (m, 2H), 5.38 (s, 2H), 2.49 (t, J = 7.7, 2H), 1.80 – 1.69 (m, 2H), 1.68 – 1.47 (m, 5H), 1.38 – 1.01 (m, 16H), 0.85 (t, J = 6.7, 3H). ^{13}C NMR (75 MHz, CDCl_3) δ 164.61, 157.94, 143.64, 131.34, 130.28, 128.58, 126.82, 124.00, 118.67, 35.75, 31.88, 31.36, 29.55, 29.44, 29.29, 22.65, 19.12, 14.10, 12.38.



1-(3-(3-undecylphenyl)-1,2,4-oxadiazol-5-yl)cyclopropanecarbonitrile (10f).

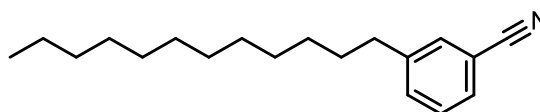
General procedure G was used to convert 9f (163 mg, 0.43 mmol) to the title product. 75%. White solid. R_f = 0.56 (20% EtOAc in hexanes). ^1H NMR (300 MHz, CDCl_3) δ 7.88 – 7.81 (m, 2H), 7.41 – 7.28 (m, 2H), 2.66 (t, J = 7.7, 2H), 2.02 (s, 4H), 1.74 – 1.58 (m, 2H), 1.48 – 1.17 (m, 16H), 0.88 (t, J = 6.6, 3H). ^{13}C NMR (75 MHz, CDCl_3) δ 174.79, 169.02,

143.91, 131.85, 128.89, 127.51, 125.87, 124.96, 117.63, 35.91, 32.00, 31.51, 29.71, 29.57, 29.39, 22.78, 20.75, 14.21, 8.94.

**11f**

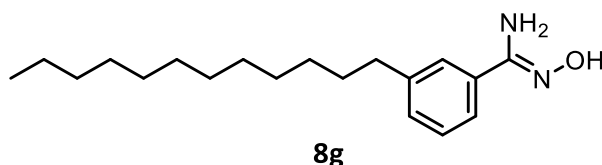
1-(3-(3-undecylphenyl)-1,2,4-oxadiazol-5-yl)cyclopropanecarboximidamide

hydrochloride (11f). General procedure A was used to convert 10f (181 mg, 0.50 mmol) to the title product. 48%. Yellow solid. $R_f = 0.35$ (15% MeOH in CHCl_3). ^1H NMR (600 MHz, DMSO) δ 9.59 (s, 2H), 9.49 (s, 2H), 7.86 – 7.76 (m, 2H), 7.51 – 7.41 (m, 2H), 2.67 (t, $J = 7.5$, 2H), 2.04 – 1.96 (m, 2H), 1.90 – 1.84 (m, 2H), 1.65 – 1.53 (m, 2H), 1.36 – 1.18 (m, 16H), 0.85 (t, $J = 6.9$, 3H). ^{13}C NMR (151 MHz, DMSO) δ 177.23, 167.77, 165.60, 143.55, 131.74, 129.20, 126.64, 125.52, 124.45, 34.81, 31.21, 30.88, 28.94, 28.90, 28.75, 28.62, 28.53, 22.03, 22.02, 18.20, 13.88. LCMS: $t_R = 5.72$; $m/z = 383.2$. HRMS m/z calcd for $\text{C}_{23}\text{H}_{35}\text{N}_4\text{O}$ ($M + H$), 383.2811; found 383.2813.

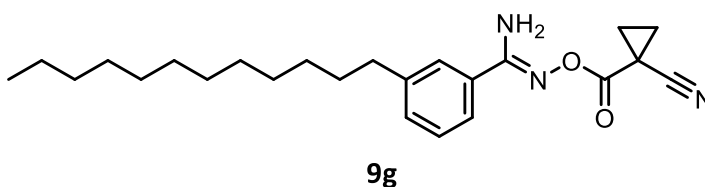
**7g**

3-dodecylbenzonitrile (7g). General Procedure C was used to couple 1-dodecene (1.83 mL, 8.24 mmol) and 3-bromobenzonitrile (1.0 g, 5.49 mmol) to yield the title product. 98%. Clear and colorless oil. $R_f = 0.40$ (5% EtOAc in hexanes). ^1H NMR (300 MHz, CDCl_3) δ 7.50 – 7.44 (m, 2H), 7.43 – 7.32 (m, 2H), 2.63 (t, $J = 6.0$, 7.5, 2H), 1.73 –

1.48 (m, 2H), 1.41 – 1.13 (m, 18H), 0.88 (t, $J = 6.7$, 3H). ^{13}C NMR (75 MHz, CDCl_3) δ 144.42, 133.21, 132.14, 129.64, 129.18, 119.34, 112.41, 77.65, 77.23, 76.81, 35.72, 32.12, 31.31, 29.84, 29.73, 29.62, 29.55, 29.32, 22.90, 14.34.



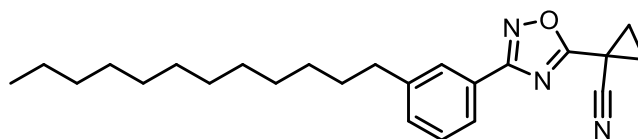
3-dodecyl-*N'*-hydroxybenzimidamide (8g). General Procedure F was used to convert 7g (1.4 g, 5.16 mmol) to the title product. 25%. White solid. $R_f = 0.60$ (50% EtOAc in hexanes). ^1H NMR (300 MHz, CDCl_3) δ 7.51 – 7.39 (m, 2H), 7.35 – 7.19 (m, 2H), 4.92 (s, 2H), 2.62 (t, $J = 7.5$, 2H), 1.71 – 1.55 (m, 2H), 1.44 – 1.20 (m, 18H), 0.89 (t, $J = 6.7$, 3H). ^{13}C NMR (75 MHz, CDCl_3) δ 152.97, 143.63, 132.56, 130.27, 128.69, 126.12, 123.39, 36.12, 32.11, 31.66, 29.87, 29.71, 29.55, 22.89, 14.33.



(*Z*)-*N'*-((1-cyanocyclopropanecarbonyl)oxy)-3-dodecylbenzimidamide (9g).

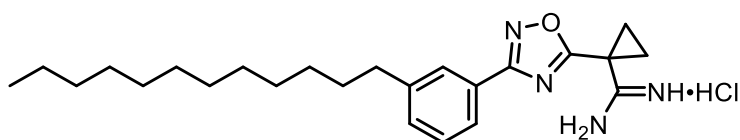
General Procedure B was used to couple 8g (438 mg, 1.43 mmol) and 1-cyano-1-cyclopropanecarboxylic acid (159 mg, 1.43 mmol) to yield the title product. 25%. White solid. $R_f = 0.25$ (25% EtOAc in hexanes). ^1H NMR (300 MHz, CDCl_3) δ 7.55 – 7.43 (m, 2H), 7.38 – 7.27 (m, 2H), 5.25 (s, 2H), 2.62 (t, $J = 7.5$, 2H), 1.82 (dd, $J = 3.1, 6.5$, 2H), 1.69 (dd, $J = 4.6, 8.4$, 2H), 1.66 – 1.53 (m, 2H), 1.41 – 1.14 (m, 18H), 0.87 (t, $J = 6.6$, 3H). ^{13}C NMR

(75 MHz, CDCl₃) δ 161.88, 158.08, 144.06, 131.71, 130.54, 128.92, 127.07, 124.21, 118.94, 36.01, 32.11, 31.60, 29.85, 29.77, 29.67, 29.51, 22.88, 19.38, 14.32, 12.62.

**10g**

1-(3-(3-dodecylphenyl)-1,2,4-oxadiazol-5-yl)cyclopropanecarbonitrile (10g).

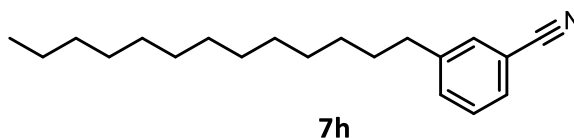
General Procedure G was used to convert 9g (100 mg, 0.25 mmol) to the title product. 69%. R_f = 0.64 (25% EtOAc in hexanes). ¹H NMR (300 MHz, CDCl₃) δ 7.95 – 7.81 (m, 2H), 7.45 – 7.29 (m, 2H), 2.83 – 2.46 (m, 2H), 2.03 (s, 4H), 1.64 (bs, 2H), 1.41 – 1.19 (m, 18H), 0.88 (t, J = 6.5, 3H). ¹³C NMR (75 MHz, CDCl₃) δ 172.21, 169.36, 144.15, 132.18, 131.97, 129.09, 127.65, 125.11, 117.74, 36.02, 34.95, 33.36, 32.93, 32.65, 32.38, 32.11, 31.62, 29.85, 29.68, 29.54, 27.76, 27.06, 25.91, 24.53, 24.24, 22.88, 20.85, 20.03, 18.76, 14.32, 9.05.

**11g**

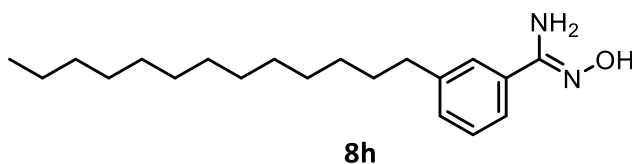
1-(3-(3-dodecylphenyl)-1,2,4-oxadiazol-5-yl)cyclopropanecarboximidamide

hydrochloride (11g). General procedure A was used to convert 10g (66 mg, 0.17 mmol) to the title product. In this example, the solid was purified via flash chromatography (15 % MeOH in CHCl₃). The hydrochloride salt was prepared by the dropwise addition of 2 M HCl in ether to the purified amidine. The ether was evaporated, reconstituted in

ether, and again evacuated to dryness to yield the title product. Yellow solid. 19%. ^1H NMR (600 MHz, DMSO) δ 9.54 (s, 2H), 9.41 (s, 2H), 7.88 – 7.74 (m, 2H), 7.52 – 7.39 (m, 2H), 2.66 (s, 2H), 1.97 (s, 2H), 1.86 (s, 2H), 1.58 (s, 2H), 1.41 – 1.09 (m, 18H), 0.84 (s, 3H). ^{13}C NMR (151 MHz, DMSO) δ 177.79, 168.30, 166.11, 144.09, 132.31, 129.77, 127.19, 126.06, 125.01, 35.38, 31.77, 31.46, 29.51, 29.50, 29.48, 29.46, 29.31, 29.18, 29.10, 22.58, 18.77, 14.45. LCMS: t_R = 5.44; m/z = 397.3. HRMS m/z calcd for $\text{C}_{24}\text{H}_{37}\text{N}_4\text{O}_2$ ($\text{M} + \text{H}$), 397.2967; found 397.2963.

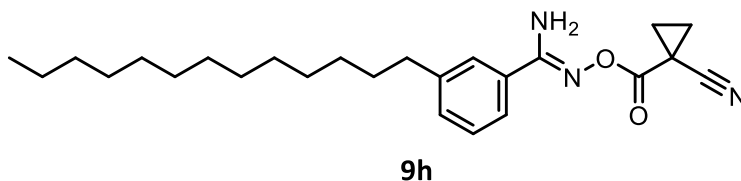


3-tridecylbenzonitrile (7h). General procedure C was used to couple 1-tridecene (1.95 mL, 8.24 mmol) and 3-bromobenzonitrile (1.0 g, 5.49 mmol) to yield the title product. 97%. Clear and colorless oil. R_f = 0.55 (5% EtOAc/hexanes). ^1H NMR (300 MHz, CDCl_3) δ 7.51 – 7.29 (m, 4H), 2.58 (t, J = 7.7, 2H), 1.69 – 1.52 (m, 2H), 1.51 – 1.11 (m, 20H), 0.87 (t, J = 6.7, 3H). ^{13}C NMR (75 MHz, CDCl_3) δ 144.35, 133.13, 132.05, 129.56, 129.10, 119.25, 112.34, 35.63, 32.04, 31.22, 29.77, 29.65, 29.53, 29.48, 29.24, 22.82, 14.24.



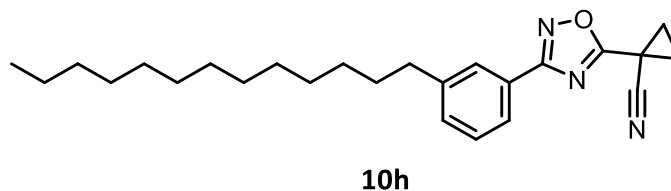
(Z)-N'-hydroxy-3-tridecylbenzimidamide (8h). General procedure F was used to convert 7h (1.53 g, 5.36 mmol) to the title product. 90%. White solid. R_f = 0.56 (40%

EtOAc in hexanes). ^1H NMR (300 MHz, CDCl_3) δ 7.48 – 7.40 (m, 2H), 7.35 – 7.19 (m, 2H), 4.89 (s, 2H), 2.54 (t, J = 7.7, 2H), 1.75 – 1.49 (m, 2H), 1.46 – 1.04 (m, 20H), 0.88 (t, J = 6.6, 3H). ^{13}C NMR (75 MHz, CDCl_3) δ 152.98, 143.63, 132.51, 130.26, 128.66, 126.03, 123.29, 36.06, 32.06, 31.60, 29.81, 29.65, 29.47, 22.83, 14.26.



(Z)-N'-((1-cyanocyclopropanecarbonyl)oxy)-3-tridecylbenzimidamide (9h).

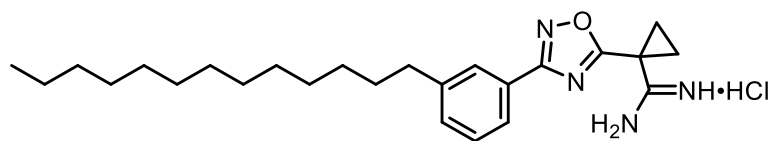
General procedure B was used to couple 8h (193 mg, 0.61 mmol) and 1-cyano-1-cyclopropanecarboxylic acid (67 mg, .61 mmol) to yield the title product. 79%. White solid. R_f = 0.24 (25% EtOAc in hexanes). ^1H NMR (300 MHz, CDCl_3) δ 7.58 – 7.43 (m, 2H), 7.38 – 7.28 (m, 2H), 5.26 (s, 2H), 2.61 (t, J = 7.7, 2H), 1.81 (dd, J = 3.1, 6.6, 2H), 1.69 (dd, J = 2.9, 6.7, 2H), 1.65 – 1.51 (m, 2H), 1.25 (s, 20H), 0.87 (t, J = 6.7, 3H). ^{13}C NMR (75 MHz, CDCl_3) δ 164.68, 158.00, 143.96, 131.61, 130.46, 128.83, 126.98, 124.12, 118.86, 35.93, 32.03, 31.52, 29.77, 29.69, 29.59, 29.47, 22.80, 19.30, 14.25, 12.53.



1-(3-(3-tridecylphenyl)-1,2,4-oxadiazol-5-yl)cyclopropanecarbonitrile (10h).

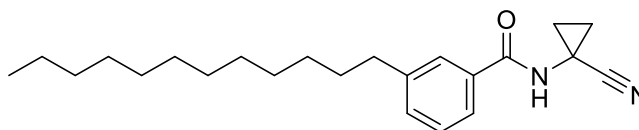
General procedure G was used to convert 9h (196 mg, 0.48 mmol) to the title product. 86%. White solid. R_f = 0.65 (25% EtOAc in hexanes). ^1H NMR (300 MHz, CDCl_3) δ 7.92 –

7.79 (m, 2H), 7.41 – 7.27 (m, 2H), 2.65 (t, $J = 7.7$, 2H), 2.01 (m, 4H), 1.71 – 1.56 (m, 2H), 1.44 – 1.16 (m, 20H), 0.88 (t, $J = 6.7$, 3H). ^{13}C NMR (75 MHz, CDCl_3) δ 174.78, 168.99, 143.89, 131.82, 128.86, 127.48, 125.87, 124.95, 117.61, 35.89, 32.00, 31.49, 29.74, 29.57, 29.43, 29.38, 22.77, 20.73, 14.20, 8.93.

**11h**

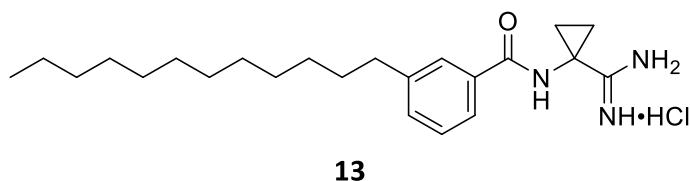
1-(3-(3-tridecylphenyl)-1,2,4-oxadiazol-5-yl)cyclopropanecarboximidamide

hydrochloride (11h). General procedure A was used to convert 10h (192 mg, 0.49 mmol) to the title product. 54%. Yellow solid. $R_f = 0.27$ (15% MeOH in CHCl_3) ^1H NMR (600 MHz, DMSO) δ 9.55 (s, 2H), 9.46 (s, 2H), 7.88 – 7.69 (m, 2H), 7.56 – 7.32 (m, 2H), 2.57 (t, $J = 7.7$, 2H), 2.05 – 1.80 (m, 4H), 1.66 – 1.48 (m, 2H), 1.38 – 1.11 (m, 20H), 0.83 (t, $J = 6.7$, 3H). ^{13}C NMR (151 MHz, DMSO) δ 176.93, 167.47, 165.31, 143.25, 131.51, 129.00, 126.37, 125.24, 124.20, 34.59, 30.96, 30.62, 28.67, 28.49, 28.36, 28.28, 21.77, 18.05, 13.68. LCMS: $t_R = 7.44$; $m/z = 411.3$. HRMS m/z calcd for $\text{C}_{25}\text{H}_{39}\text{N}_4\text{O}$ ($M + \text{H}$), 411.3124; found 411.3112.

**12**

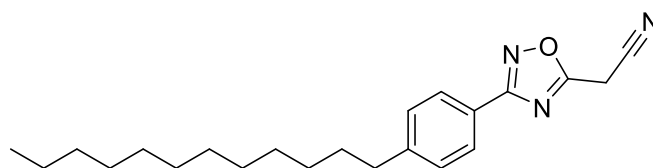
***N*-(1-cyanocyclopropyl)-3-dodecylbenzamide (12).** General procedure L was used to convert 3-dodecylbenzoic acid (7.34 mmol) to the corresponding acyl chloride.

After standard work-up procedures, the acyl chloride was coupled to 1-amino-1-cyclopropylcarbonitrile hydrochloride (1.0 g, 3.0 mmol) using general procedure M. 76%. White solid. $R_f = 0.48$ (30% EtOAc in hexanes). ^1H NMR (300 MHz, CDCl_3) δ 7.56 (m, 2H), 7.34 (m, 2H), 6.78 (m,), 2.68 – 2.56 (m, 2H), 1.68 – 1.50 (m, 4H), 1.41 – 1.11 (m, 20H), 0.88 (t, $J = 5.7$, 3H). ^{13}C NMR (75 MHz, CDCl_3) δ 168.43, 143.92, 132.72, 129.04, 128.72, 127.59, 124.55, 120.28, 35.91, 32.06, 31.51, 29.78, 29.47, 22.84, 21.01, 20.41, 17.05, 14.26.



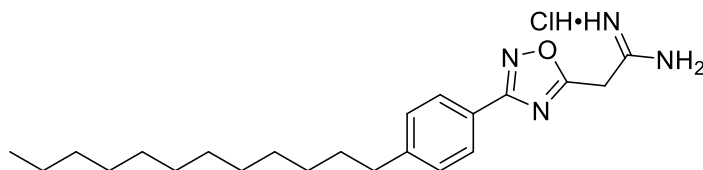
***N*-(1-carbamimidoylcyclopropyl)-3-dodecylbenzamide hydrochloride (13).**

General procedure A was used to convert **12** (2.15 mmol) to the title product. 9%. Yellow solid. ^1H NMR (500 MHz, DMSO) δ 9.10 (s, 1H), 8.75 (s, 2H), 8.54 (s, 2H), 7.75 – 7.62 (m, 2H), 7.40 – 7.33 (m, 3H), 2.54 (t, $J = 7.6$, 2H), 1.66 (dd, $J = 5.7$, 7.4, 2H), 1.62 – 1.50 (m, 2H), 1.38 (dd, $J = 5.8$, 7.7, 2H), 1.35 – 1.16 (m, 18H), 0.83 (t, $J = 6.7$, 3H). ^{13}C NMR (126 MHz, DMSO) δ 172.14, 167.98, 144.33, 132.98, 129.56, 128.84, 127.88, 124.97, 35.97, 32.20, 31.58, 29.98, 29.76, 23.04, 21.41, 20.72, 18.01, 14.45. LCMS: $t_R = 5.44$; $m/z = 372.3$. HRMS m/z calcd for $\text{C}_{23}\text{H}_{38}\text{N}_3\text{O}$ ($M + H$), 372.3015; found 372.3017.

**14**

2-(3-(4-dodecylphenyl)-1,2,4-oxadiazol-5-yl)acetonitrile (14). General procedure

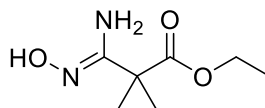
B was used to couple **8a** (200 mg, 0.66 mmol) and cyanoacetic acid (51 mg, 0.60 mmol) to yield the oxadiazole product. 27%. White solid. R_f = 0.50 (25% EtOAc in hexanes). ^1H NMR (300 MHz, CDCl_3) δ 7.97 (d, J = 8.2, 2H), 7.30 (d, J = 8.2, 2H), 4.12 (s, 2H), 2.64 (t, J = 7.6, 2H), 1.63 (m, 2H), 1.28 (m, 18H), 0.87 (t, J = 6.6, 3H). ^{13}C NMR (75 MHz, CDCl_3) δ 169.33, 168.94, 147.50, 129.30, 127.71, 123.23, 115.45, 67.39, 36.22, 32.15, 31.44, 29.89, 29.81, 29.71, 29.60, 29.51, 22.94, 17.38, 14.37.

**15**

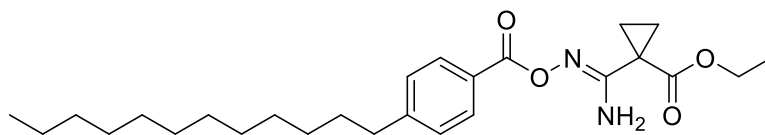
2-(3-(4-dodecylphenyl)-1,2,4-oxadiazol-5-yl)acetimidamide hydrochloride (15).

General procedure A was used to convert **14** (61 mg, 0.16 mmol) to the title product. In this example, the solid was purified via flash chromatography. The hydrochloride salt was prepared by the dropwise addition of 2 M HCl in ether to the purified amidine. The ether was evaporated, reconstituted in ether, and again evacuated to dryness to yield the title product. 40%. Tan solid. R_f = 0.25 (15% MeOH in CHCl_3). ^1H NMR (500 MHz, DMSO) δ 9.47 (s, 2H), 9.15 (s, 2H), 7.90 (s, 2H), 7.37 (s, 2H), 4.38 (s, 2H), 2.63 (s, 2H),

1.57 (s, 2H), 1.21 (s, 18H), 0.82 (s, 3H). ^{13}C NMR (126 MHz, DMSO) δ 173.81, 168.25, 163.97, 147.06, 129.72, 127.48, 123.56, 35.50, 31.75, 31.09, 30.63, 29.46, 29.27, 29.16, 29.08, 22.56, 14.43. LCMS: t_R = 6.46; m/z = 371.54. HRMS m/z calcd for $\text{C}_{22}\text{H}_{35}\text{N}_4\text{O}$ (M + H), 371.2811; found 371.2814.

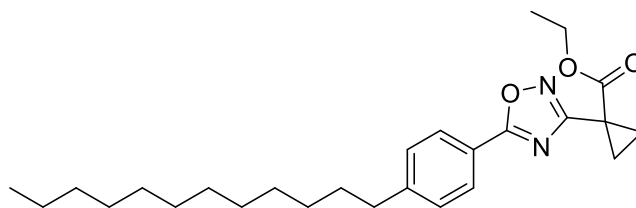
**16**

(Z)-ethyl 1-(N'-hydroxycarbamimidoyl)cyclopropanecarboxylate (16). Sodium hydroxide (0.33 g, 8.26 mmol) and hydroxylamine hydrochloride (0.55 g, 7.91 mmol) were stirred in EtOH (7.19 mL, 1 M) at room temperature for 2 h. The mixture was filtered through a fine frit and ethyl 1-cyano-1-cyclopropanecarboxylate (1.0 g, 7.19 mmol) was added and the reaction heated to 50 °C overnight. The mixture was then cooled to room temperature, evaporated to a white solid, and immediately purified by flash chromatography. 46%. White solid. R_f = 0.37 (75% EtOAc in hexanes). ^1H NMR (300 MHz, CDCl_3) δ 5.01 (s, 2H), 4.11 (q, 7.1, 2H), 1.37 (dd, J = 4.2, 7.2, 2H), 1.29 (dd, J = 4.0, 7.1, 2H), 1.20 (t, J = 7.1, 3H). ^{13}C NMR (75 MHz, CDCl_3) δ 172.40, 152.34, 61.41, 25.02, 15.65, 14.11.

**17a**

(Z)-ethyl-1-(N'-((4-dodecylbenzoyl)oxy)carbamimidoyl)cyclopropanecarboxylate

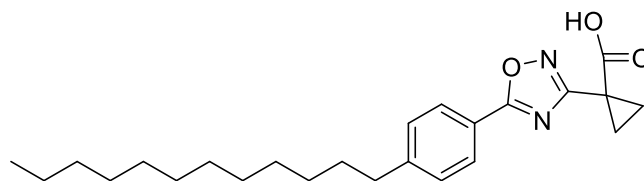
(17a). General procedure B was used to couple 16 (0.23 g, 1.35 mmol) and 4-dodecylbenzoic acid (0.39 g, 1.35 mmol) to yield the title product. 54%. White solid. R_f = 0.27 (25% EtOAc in hexanes). ^1H NMR (300 MHz, CDCl_3) δ 7.88 (d, J = 8.2, 2H), 7.17 (d, J = 8.2, 2H), 5.61 (s, 2H), 4.08 (q, J = 7.1, 2H), 2.40 (t, J = 7.7, 2H), 1.60 – 1.44 (m, 6H), 1.28 – 1.18 (m, 21H), 0.82 (t, J = 6.6, 3H). ^{13}C NMR (75 MHz, CDCl_3) δ 171.76, 163.88, 157.45, 148.49, 129.38, 128.41, 126.86, 61.39, 35.92, 31.83, 31.05, 29.56, 29.49, 29.38, 29.27, 29.19, 28.67, 24.83, 22.60, 16.60, 14.03, 13.99.

**18a**

Ethyl 1-(5-(4-dodecylphenyl)-1,2,4-oxadiazol-3-yl)cyclopropanecarboxylate

(18a). General procedure G was used to convert 17a (325 mg, 0.73 mmol) to the title product. 84%. R_f = 0.56 (20% EtOAc in hexanes). ^1H NMR (300 MHz, CDCl_3) δ 7.98 (d, J = 8.2, 2H), 7.26 (d, J = 8.2, 2H), 4.16 (q, J = 7.1, 2H), 2.62 (t, J = 7.7, 2H), 1.68 (dd, J = 4.3, 7.6, 2H), 1.64 – 1.54 (m, 2H), 1.50 (dd, J = 4.3, 7.6, 2H), 1.36 – 1.12 (m, 21H), 0.82 (t, J = 6.6, 3H). ^{13}C NMR (75 MHz, CDCl_3) δ 175.61, 170.94, 169.68, 148.39, 129.09, 128.07,

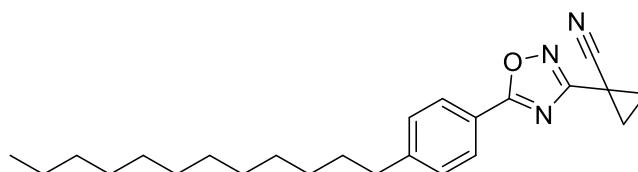
121.61, 61.58, 36.04, 31.91, 31.09, 29.63, 29.56, 29.45, 29.35, 29.22, 22.68, 21.27, 16.65, 14.09.



19a

1-(5-(4-dodecylphenyl)-1,2,4-oxadiazol-3-yl)cyclopropanecarboxylic acid (19a).

To a mixture of 18a (261 mg, 0.61 mmol) and LiOH (3.0 eq.) were added THF (2 mL), *t*BuOH (2 mL), and H₂O (2 mL). The mixture was stirred at room temperature for 4 h. The mixture was diluted with EtOAc (100 mL) and washed with 1 M HCl (3 x 10 mL). The organic layer was washed with brine, dried over MgSO₄, evaporated to a white solid and carried on crude.

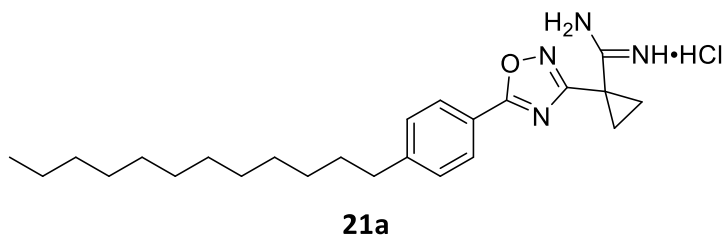


20a

1-(5-(4-dodecylphenyl)-1,2,4-oxadiazol-3-yl)cyclopropanecarbonitrile (20a).

Crude acid, 19a (244 mg, 0.61 mmol) was dissolved in CH₂Cl₂ (0.3 M) at 0 °C and treated with TEA (3.0 eq.) and then isobutyl chloroformate (1.1 eq.). The mixture turned turbid after the addition and was allowed to warm to room temperature. After 1 h at room temperature, the mixture was treated with 2 M NH₃ in MeOH (2.0 eq.) and allowed to

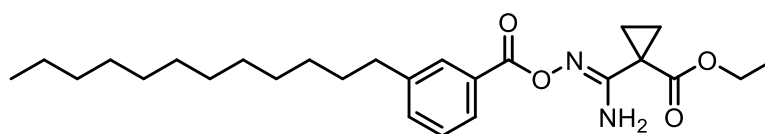
stir 8 h. The mixture was then evaporated and taken on crude. The crude amide (168 mg, 0.42 mmol) was dissolved in DMF (0.1 M) and 2,4,6-collidine (8 eq.) at 0 °C and then treated with cyanuric chloride (3.15 eq.) and allowed to warm to room temperature. The reaction turned a deep red color and was allowed to stir for 12 h. The mixture was then extracted with EtOAc (20 x volume of DMF) and washed 3 x with saturated NaHCO₃ (10 x the volume of DMF), 3 x with 1 M HCl (10 x the volume of DMF), and once with brine (10 x the volume of DMF). The organic layer was then dried with MgSO₄, evaporated to a yellow oil and immediately purified with flash chromatography to yield the title compound. 31% (over 3 steps). R_f = 0.34 (15% EtOAc in hexanes). ¹H NMR (300 MHz, CDCl₃) δ 7.98 (d, J = 8.3, 2H), 7.31 (d, J = 8.4, 2H), 2.67 (t, J = 7.7, 2H), 1.84 (s, 4H), 1.70 – 1.56 (m, 2H), 1.43 – 1.19 (m, 18H), 0.87 (t, J = 6.7, 3H). ¹³C NMR (75 MHz, CDCl₃) δ 176.78, 168.09, 149.17, 129.32, 128.30, 121.03, 119.08, 36.18, 32.00, 31.15, 29.73, 29.64, 29.53, 29.45, 29.31, 22.78, 18.29, 14.22, 7.87.



1-(5-(4-dodecylphenyl)-1,2,4-oxadiazol-3-yl)cyclopropanecarboximidamide

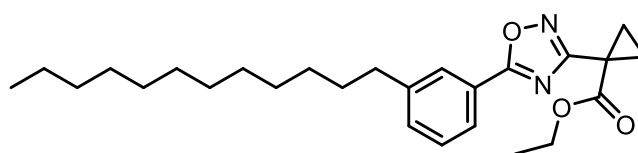
hydrochloride (21a). General procedure A was used to convert 20a (71 mg, 0.19 mmol) to the title product. 20%. Yellow solid. R_f = 0.42 (15% MeOH in CHCl₃). ¹H NMR (600 MHz, DMSO) δ 9.27 (s, 4H), 7.77 (d, J = 8.2, 2H), 7.28 (d, J = 8.2, 2H), 2.58 (t, J = 7.6, 2H), 1.86 – 1.44 (m, 6H), 1.41 – 0.95 (m, 18H), 0.83 (t, J = 6.6, 2H). ¹³C NMR (151 MHz,

DMSO) δ 175.28, 169.33, 166.96, 148.58, 129.38, 127.74, 124.37, 34.97, 31.10, 30.30, 28.82, 28.61, 28.51, 28.40, 21.90, 20.93, 15.87, 13.81. LCMS: t_R = 5.15; m/z = 397.3. HRMS m/z calcd for $C_{24}H_{37}N_4O$ (M + HCl), 397.2967; found 397.2949.

**17b**

(Z)-ethyl 1-(N'-((3-dodecylbenzoyl)oxy)carbamimidoyl)cyclopropanecarboxylate

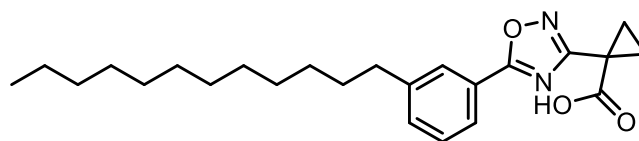
(17b). General procedure C was used to couple amidoxime 16 (1.4 mmol) to 3-dodecylbenzoic acid (1.4 mmol) to yield the title product. 72%. 1H NMR (600 MHz, $CDCl_3$) δ 7.89-7.77 (m, 2H), 7.45-7.31 (m, 2H), 5.59 (s, 2H), 4.18 (q, J = 3Hz, 2H), 2.65 (t, J = 3Hz, 2H), 1.65-1.60 (m, 2H), 1.34-1.21 (m, 18H), 0.88 (t, 3H). ^{13}C NMR (125 MHz, DMSO) δ 167.35, 159.52, 153.20, 138.91, 128.61, 124.99, 124.91, 123.81, 122.17, 57.03, 31.27, 27.41, 26.89, 25.15, 25.07, 24.98, 24.84, 24.78, 20.23, 18.18, 12.49, 9.59.

**18b**

Ethyl 1-(5-(3-dodecylphenyl)-1,2,4-oxadiazol-3-yl)cyclopropanecarboxylate

(18b). General procedure G was used to convert 17b (1.01 mmol) to the title product. 89%. White solid. R_f = 0.51 (20% EtOAc in hexanes). 1H NMR (300 MHz, $CDCl_3$) δ 7.98-7.90 (m, 2H), 7.45-7.37 (m, 2H), 4.21 (q, J = 7.1 Hz, 2H), 2.68 (t, 2H), 1.70-1.60 (m, 2H), 1.37-1.18 (m, 25H), 0.87 (t, J = 6.7 Hz, 3H). ^{13}C NMR (75 MHz, $CDCl_3$) δ 175.97, 171.19,

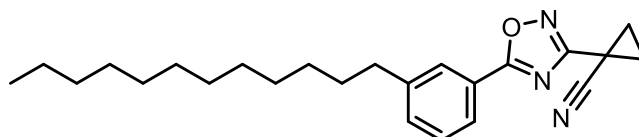
169.95, 144.29, 133.17, 129.18, 128.22, 125.63, 124.22, 61.86, 35.97, 32.13, 31.59, 29.86, 29.78, 29.69, 29.57, 29.47, 22.90, 21.47, 16.87, 14.33.



19b

1-(5-(3-dodecylphenyl)-1,2,4-oxadiazol-3-yl)cyclopropanecarboxylic acid (19b).

To a solution of 17b (0.90 mmol) in 1.65 mL each of MeOH, THF, and H₂O were added LiOH (2.7 mmol). This mixture was allowed to stir 15 h at room temperature. The mixture was then taken up in 100 mL EtOAc, washed with three 10 mL portions of 1 M HCl, one portion of brine (10 mL), and then dried over Na₂SO₄. 92%. White solid.

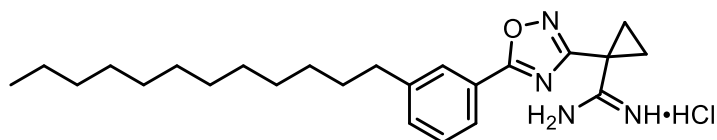


20b

1-(5-(3-dodecylphenyl)-1,2,4-oxadiazol-3-yl)cyclopropanecarbonitrile (20b).

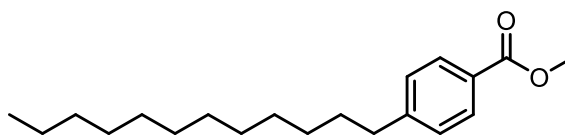
To a solution of 19b (0.83 mmol) in DCM (1.66 mL) was added *i*-butyl chloroformate (0.91 mmol) and TEA (0.35 mL). After this solution stirred 1 h, NH₃ in MeOH (1.25 mL) were added dropwise, and the mixture stirred and additional 15 h at rt. The solvent was then evaporated and the crude product purified by flash chromatography (silica gel, 20% EtOAc in Hexanes). 76%. White solid. ¹H NMR (600 MHz, CDCl₃) δ 8.23 (s, 2H), 7.96-7.89 (m, 2H), 7.47-7.39 (m, 2H), 2.69 (t, *J* = 4.5 Hz, 2H), 1.69-1.62 (m, 2H), 1.38-1.21 (m, 22H), 0.88 (t, *J* = 7.1 Hz, 3H). To an ice-cold stirring solution of 2,4,6-collidine (5.03 mmol) and

cyanuric chloride (1.98 mmol) in DMF (6.3 mL) was added the 1,2,4-oxadiazole amide (0.63 mmol). This mixture was allowed to warm to room temperature and stirred for 15 h. At this time, the reaction was slowly quenched with a saturated NaHCO_3 solution and then extracted with three portions of 25 mL EtOAc. The combined organic layers were then washed with three 10 mL portions of 1 N HCl and one 10 mL portion of brine, and then dried over Na_2SO_4 . 66%. White solid. ^1H NMR (300 MHz, CDCl_3) δ 7.98-7.87 (m, 2H), 7.47-7.38 (m, 2H), 2.74-2.64 (m, 2H), 1.70-1.60 (m, 2H), 1.37-1.16 (m, 22H), 0.88 (t, J = 6.7 Hz, 3H).

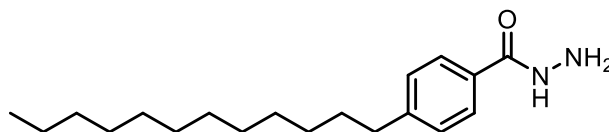
**21b**

1-(5-(3-dodecylphenyl)-1,2,4-oxadiazol-3-yl)cyclopropanecarboximidamide

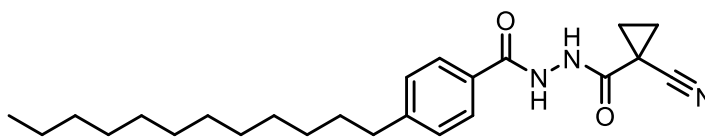
hydrochloride (21b). General procedure A was used convert nitrile 20b (0.42 mmol) to the title product. Additional purification through flash chromatography was required (silica gel, 15% MeOH in CHCl_3). 13%. Yellow solid. ^1H NMR (600 MHz, DMSO) δ 9.32 (s, 2H), 9.11 (s, 2H), 7.94-7.90 (m, 2H), 7.60-7.54 (m, 2H), 2.52 (t, J = 1.8 Hz, 2H), 1.64-1.56 (m, 2H), 1.33-1.18 (m, 22H), 0.86 (t, J = 9 Hz, 3H). ^{13}C NMR (151 MHz, DMSO) δ 176.08, 170.09, 168.54, 167.40, 166.01, 144.60, 134.16, 130.11, 127.97, 125.83, 123.35, 65.39, 35.19, 31.76, 31.34, 29.48, 29.47, 22.57, 21.69, 16.44, 15.65, 14.44. LCMS: t_R = 5.15; m/z = 397.3. HRMS m/z calcd for $\text{C}_{24}\text{H}_{37}\text{N}_4\text{O}$ ($\text{M} + \text{HCl}$), 397.2967; found 397.2957.

**22a**

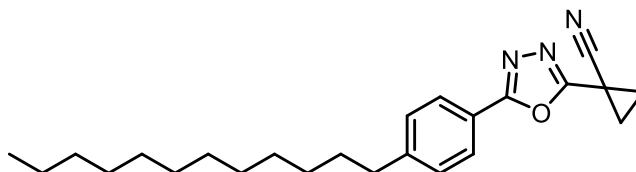
Methyl 4-dodecylbenzoate (22a). General procedure I was used to convert 4-dodecylbenzoic acid (1.2 g, 4.13 mmol) to the title product. 95%. Clear and colorless oil. R_f = 0.45 (5% EtOAc in hexanes). ^1H NMR (600 MHz, CDCl_3) δ 7.94 (d, J = 8.1, 2H), 7.23 (d, J = 8.1, 2H), 3.89 (s, 3H), 2.61 (t, J = 7.7, 2H), 1.67 – 1.55 (m, 2H), 1.37 – 1.17 (m, 18H), 0.88 (t, J = 7.0, 3H). ^{13}C NMR (151 MHz, CDCl_3) δ 167.31, 148.62, 129.73, 128.54, 127.75, 60.68, 36.14, 32.05, 31.25, 29.76, 29.68, 29.58, 29.47, 29.37, 29.33, 22.81, 14.23.

**23a**

4-dodecylbenzohydrazide (23a). General procedure J was used to convert 22a (1.2 g, 3.94 mmol) to the title product. 42%. White solid. R_f = 0.31 (75% EtOAc in hexanes). ^1H NMR (300 MHz, CDCl_3) δ 7.65 (d, J = 8.2, 2H), 7.22 (d, J = 8.3, 2H), 4.92 (s, 2H), 2.62 (t, J = 7.7, 2H), 1.66 – 1.54 (m, 2H), 1.37 – 1.17 (m, 18H), 0.86 (t, J = 6.6, 3H). ^{13}C NMR (75 MHz, CDCl_3) δ 168.92, 147.51, 130.12, 129.74, 128.86, 127.00, 36.00, 32.04, 31.73, 31.32, 29.77, 29.70, 29.59, 29.48, 29.38, 22.79, 14.24.

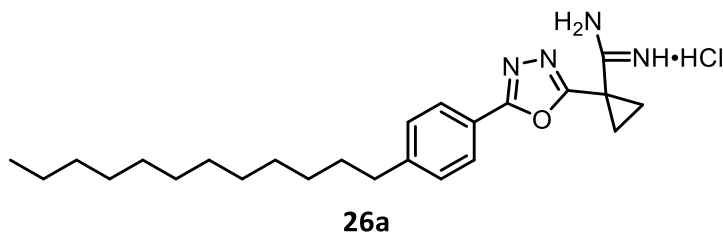
**24a**

***N'*-(1-cyanocyclopropanecarbonyl)-4-dodecylbenzohydrazide (24a).** General procedure B was used to couple 23a (250 mg, 0.82 mmol) and 1-cyano-1-cyclopropanecarboxylic acid (91 mg, 0.82 mmol) to yield the title product. 71%. White solid. R_f = 0.57 (50% EtOAc in hexanes). ^1H NMR (300 MHz, CDCl_3) δ 7.73 (d, J = 8.3, 2H), 7.19 (d, J = 8.3, 2H), 2.55 (t, J = 7.7, 2H), 1.68 (dd, J = 4.6, 8.3, 2H), 1.64 – 1.48 (m, 4H), 1.41 – 1.18 (m, 18H), 0.87 (t, J = 6.7, 3H). ^{13}C NMR (75 MHz, CDCl_3) δ 165.68, 164.69, 148.31, 128.83, 128.44, 127.60, 118.89, 36.02, 32.02, 31.25, 29.76, 29.57, 29.45, 29.39, 22.79, 18.56, 14.23, 12.64.

**25a**

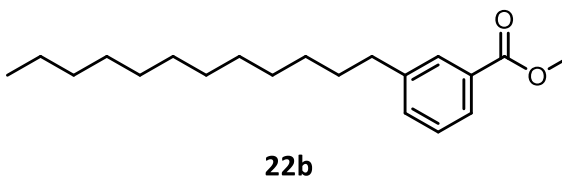
1-(5-(4-dodecylphenyl)-1,3,4-oxadiazol-2-yl)cyclopropanecarbonitrile (25a). General procedure K was used to convert 24a (230 mg, 0.58 mmol) to the title product. 75%. White solid. R_f = 0.46 (25% EtOAc in hexanes). ^1H NMR (300 MHz, CDCl_3) δ 7.91 (d, J = 8.3, 2H), 7.29 (d, J = 8.3, 2H), 2.64 (t, J = 7.7, 2H), 1.93 (s, 4H), 1.73 – 1.50 (m, 2H), 1.48 – 1.16 (m, 18H), 0.85 (t, J = 6.2, 3H). ^{13}C NMR (75 MHz, CDCl_3) δ 165.64, 162.07,

147.79, 129.21, 126.96, 120.53, 117.91, 36.03, 31.95, 31.14, 29.67, 29.60, 29.49, 29.38, 29.27, 22.72, 19.17, 14.16, 7.14.



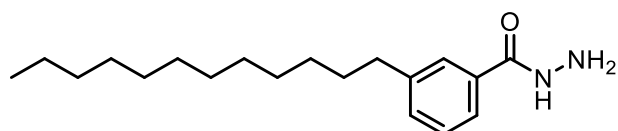
1-(5-(4-dodecylphenyl)-1,3,4-oxadiazol-2-yl)cyclopropanecarboximidamide

hydrochloride (26a). General procedure A was used to convert 25a (164 mg, 0.43 mmol) to the title product. 46%. Tan solid. $R_f = 0.36$ (15% MeOH in CHCl_3). ^1H NMR (600 MHz, DMSO) δ 9.39 (d, $J = 11.1$, 4H), 7.91 (d, $J = 7.5$, 2H), 7.42 (d, $J = 7.6$, 2H), 2.66 (t, $J = 7.1$, 2H), 1.96 – 1.81 (m, 4H), 1.64 – 1.54 (m, 2H), 1.33 – 1.19 (m, 18H), 0.85 (t, $J = 6.7$, 3H). ^{13}C NMR (151 MHz, DMSO) δ 166.68, 164.11, 163.69, 146.93, 129.22, 126.53, 120.55, 34.97, 31.20, 30.51, 28.94, 28.91, 28.88, 28.72, 28.62, 28.50, 22.01, 20.26, 16.81, 13.88. LCMS: $t_R = 4.86$; $m/z = 397.3$. HRMS m/z calcd for $\text{C}_{24}\text{H}_{37}\text{N}_4\text{O}$ ($M + \text{HCl}$), 397.2967; found 397.2956.

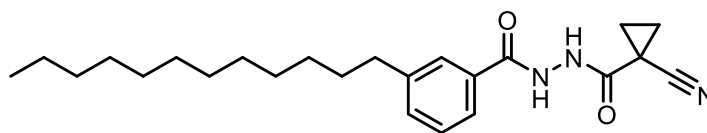


Methyl 3-dodecylbenzoate (22b). Acetyl chloride (15.5 mmol) was added dropwise over 10 minutes to ice-cold MeOH (12 mL), and this solution was allowed to stir 5 min. 3-dodecylbenzoic acid (5.2 mmol) was then added to the solution in one

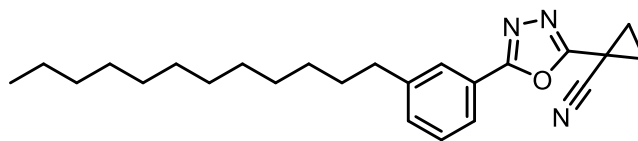
portion. This solution was heated to reflux with stirring for 2 h. At this point solid NaHCO_3 was added to neutralize the solution, which was then filtered through a fine fritted funnel. The solvent was evaporated from the filtrate to yield the title product. 96%. Amber oil. $R_f = 0.87$ (15% EtOAc in hexanes). ^1H NMR (300 MHz, CDCl_3) δ 7.89-7.80 (m, 2H), 7.35 (d, $J = 7.7$ Hz, 2H), 3.91 (s, 3H), 2.64 (t, $J = 7.5$ Hz, 2H), 1.32 – 1.14 (m, 18H), 0.88 (t, $J = 6.6$ Hz, 3H). ^{13}C NMR (151 MHz, CDCl_3) δ 167.33, 143.23, 133.08, 130.08, 129.51, 128.25, 126.93, 52.02, 35.78, 31.96, 31.42, 29.70, 29.68, 29.67, 29.60, 29.51, 29.39, 29.28, 22.73, 14.14.

**23b**

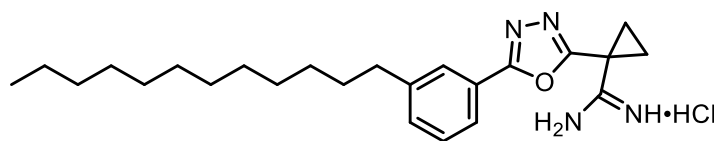
3-dodecylbenzohydrazide (23b). General procedure J was used to convert 22b (5.0 mmol) to the title product. 58%. White solid. $R_f = 0.62$ (10% MeOH in CHCl_3). ^1H NMR (300 MHz, DMSO) δ 9.69 (bs, 1H), 7.66 – 7.59 (m, 2H), 7.33-7.26 (m, 2H), 2.52-2.45 (m, 2H), 1.97 (s, 2H), 1.25-1.10 (m, 18H), 0.82 (t, $J = 6.8$ Hz, 3H). ^{13}C NMR (151 MHz, DMSO) δ 166.46, 142.93, 133.72, 131.46, 128.62, 127.35, 124.73, 35.49, 31.77, 31.30, 29.51, 29.48, 29.46, 29.33, 29.19, 29.10, 22.58, 14.44.

**24b**

***N'*-(1-cyanocyclopropanecarbonyl)-3-dodecylbenzohydrazide (24b).** General procedure B was used to couple 23b (2.86 mmol) to 1-cyano-1-cyclopropanecarboxylic acid (2.86 mmol). 56%. White solid. R_f = 0.52 (50% EtOAc in hexanes). ^1H NMR (300 MHz, CHCl_3) δ 8.88-8.78 (bs, 1H), 8.34-8.30 (s, 1H), 7.65-7.57 (m, 2H), 7.42-7.35 (m, 2H), 2.71-2.59 (m, 2H), 1.85-1.74 (m, 2H), 1.29-1.22 (m, 18H), 0.87 (t, J = 7.0 Hz, 3H). ^{13}C NMR (151 MHz, CDCl_3) δ 165.34, 163.83, 143.95, 132.90, 130.99, 128.73, 127.39, 124.49, 118.80, 35.81, 31.94, 31.37, 29.69, 29.67, 29.66, 29.59, 29.49, 29.37, 29.30, 22.71, 19.90, 18.50, 14.15, 12.54.

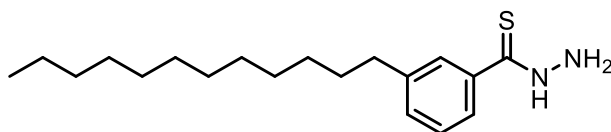
**25b**

1-(5-(3-dodecylphenyl)-1,3,4-oxadiazol-2-yl)cyclopropanecarbonitrile (25b). General procedure K was used to convert 24b (1.6 mmol) to the title product. R_f = 0.51 (20% EtOAc in hexanes). ^1H NMR (300 MHz, CDCl_3) δ 7.90-7.80 (m, 2H), 7.48-7.32 (m, 2H), 2.68 (t, J = 7.5 Hz, 2H), 1.34-1.22 (m, 18H), 0.87 (t, J = 6.6 Hz, 3H). ^{13}C NMR (75 MHz, CDCl_3) δ 165.98, 165.98, 144.44, 132.62, 129.28, 127.08, 124.56, 123.17, 118.13, 36.02, 32.14, 31.62, 29.88, 29.81, 29.70, 29.59, 29.50, 22.93, 19.45, 14.36, 7.31.

**26b**

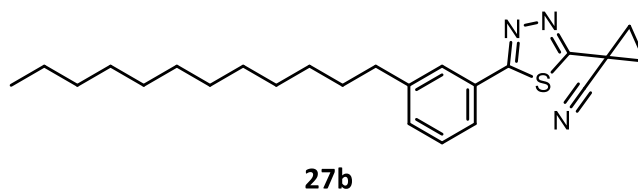
1-(5-(3-dodecylphenyl)-1,3,4-oxadiazol-2-yl)cyclopropanecarboximidamide

hydrochloride (26b). General procedure A was used to convert 25b (0.92 mmol) to the title product. 42%. Yellow solid. ^1H NMR (600 MHz, DMSO) δ 9.31 (s, 2H), 9.16 (s, 2H), 7.82 (dd, J = 6.8, 1.4 Hz, 2H), 7.55-7.46 (m, 2H), 2.69 (t, J = 3 Hz, 2H), 1.64-1.58 (m, 2H), 1.32-1.2 (m, 18H), 0.87 (t, J = 7.0 Hz, 3H). ^{13}C NMR (600 MHz, DMSO) δ 166.45, 164.20, 163.98, 143.80, 64.89, 40.06, 34.80, 31.26, 30.86, 28.99, 28.98, 28.97, 28.96, 28.88, 28.67, 28.57, 22.07, 20.43, 16.73, 15.15, 13.93. LCMS: t_R = 5.15; m/z = 397.3. HRMS m/z calcd for $\text{C}_{24}\text{H}_{37}\text{N}_4\text{O}$ ($M + \text{HCl}$), 397.2967; found 397.2957.

**27a**

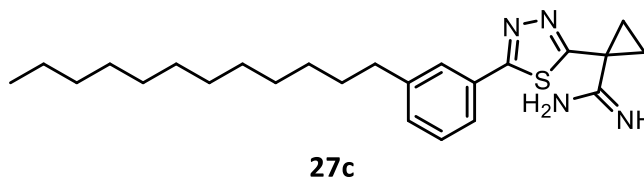
3-dodecylbenzothiohydrazide (27a). Compound 23b (17.4 mmol) was dissolved in toluene (102 mL). Lawesson's reagent (17.4 mmol) was added and the solution stirred at reflux until complete by TLC. Upon completion, toluene was evaporated. The residue was dissolved in ethyl acetate, washed with water, sat. NaHCO_3 , brine, and the organic layer dried over Na_2SO_4 . Purified by flash chromatography (25% EtOAc/Hexanes). Collected fractions were allowed to sit for 72 h, at which point solid crystals began to form. These were collected by filtration, then recrystallized in EtOAc to afford the title

product in 2% yield. Yellow solid. R_f = 0.47, 50% EtOAc/Hexanes. ^1H NMR (300 MHz, $\text{DMSO}-d_6$) δ 7.52-7.46 (m, 2H), 7.27 (d, J = 7.0 Hz, 2H), 2.57 (t, J = 7.0 Hz, 2H), 1.60-1.50 (m, 2H), 1.29-1.17 (m, 18H), 0.82 (t, J = 6.9 Hz, 3H).



1-(5-(3-dodecylphenyl)-1,3,4-thiadiazol-2-yl)cyclopropanecarbonitrile (27b).

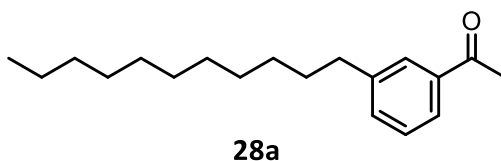
Compound 27a (0.29 mmol) was dissolved in THF (4.0 mL). The acyl chloride (0.45 mmol) was dissolved in 2.0 mL THF and added dropwise. The solution stirred at reflux for 4 h. After cooling, the reaction mixture was concentrated and purified by flash chromatography (15% EtOAc/ Hexanes) to afford the title product in 95% yield. R_f = 0.57, 15% EtOAc/Hexanes. ^1H NMR (600 MHz, $\text{Chloroform}-d$) δ 7.76-7.73 (m, 2H), 7.36 (d, J = 7.8 Hz, 2H), 2.13 (q, J = 3.9 Hz, 2H), 1.99 (d, J = 3.6 Hz, 2H), 1.71-1.65 (m, 2H), 1.40-1.25 (m, 18H), 0.91 (t, J = 7.1 Hz, 3H). ^{13}C NMR (151 MHz, CDCl_3) δ 170.84, 169.44, 144.32, 131.71, 129.20, 127.78, 125.36, 60.42, 35.79, 31.94, 31.34, 29.69, 29.67, 29.66, 29.58, 29.49, 29.37, 29.27, 22.71, 21.31, 14.22, 14.15, 11.19.



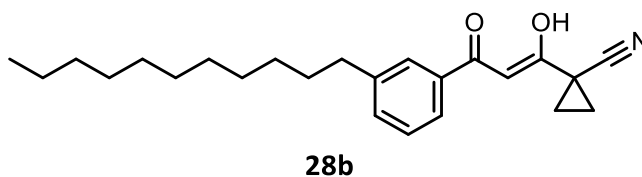
1-(5-(3-dodecylphenyl)-1,3,4-thiadiazol-2-yl)cyclopropanecarboximidamide

hydrochloride (27c). General procedure A was used to convert the 27b to the title

product. 33% yield. $R_f = 0.45$, 15% MeOH/ CHCl_3 . ^1H NMR (497 MHz, $\text{DMSO}-d_6$) δ 9.44 (s, 2H), 9.24 (s, 2H), 7.82-7.75 (m, 2H), 7.51-7.40 (m, 2H), 2.67 (t, $J = 7.0$ Hz, 2H), 1.93-1.89 (m, 2H), 1.75-1.70 (m, 2H), 1.64-1.58 (m, 2H), 1.33-1.20 (m, 18H), 0.86 (t, $J = 6.1$ Hz, 3H).

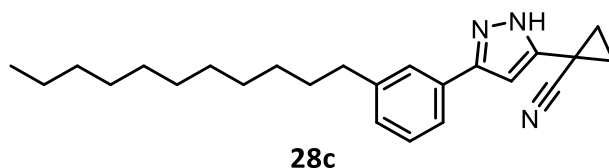


1-(3-undecylphenyl)ethanone (28a). General procedure C was used to couple 3-bromoacetophenone (5.02 mmol) to 1-undecene (7.54 mmol) to afford the title compound. 76% yield. $R_f = 0.34$ (25% EtOAc/Hexanes). ^1H NMR (300 MHz, CDCl_3) δ 7.77 (dd, $J = 5.2, 2.2$ Hz, 2H), 7.37 (dd, $J = 5.9, 1.0$ Hz, 2H), 2.67 (t, $J = 7.5$ Hz, 2H), 2.60 (s, 3H), 1.62 (dd, $J = 8.7, 5.0$ Hz, 2H), 1.30-1.25 (m, 16H), 0.88 (t, $J = 6.6$ Hz, 3H). ^{13}C NMR (75 MHz, CDCl_3) δ 182.90, 133.44, 128.57, 128.26, 126.00, 35.98, 32.06, 31.60, 29.77, 29.72, 29.63, 29.49, 29.41, 26.88, 22.84, 14.29.

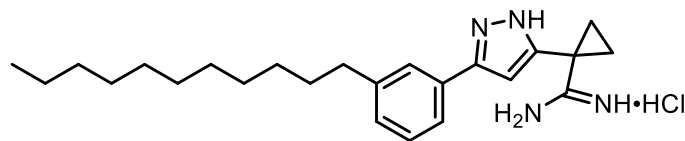


(Z)-1-(1-hydroxy-3-oxo-3(3-undecylphenyl)prop-1-en-1-yl)cyclopropanecarbonitrile (28b). To a stirring solution of 28a (1.97 mmol) and ethyl 1-cyanocyclopropanecarboxylate in benzene (0.22 M) was added sodium metal (2.37 mmol) dissolved in anhydrous MeOH (0.33M) dropwise. The reaction was warmed to rt and stirred overnight. Once complete, the reaction was quenched with 1 M HCl and the

solvent evaporated. The solid was dissolved in DCM and the salts removed by filtration, then the solvent evaporated to yield the title product. 91% yield. ^1H NMR (300 MHz, CDCl_3) δ 10.51 (bs, 1H), 7.83-7.66 (m, 2H), 7.45-7.27 (m, 2H), 6.81 (s, 1H), 2.71-2.61 (t, J = 7.5 Hz, 5H), 1.78-1.70 (m, 2H), 1.70, 1.50 (m, 4H), 1.29-1.25 (m, 16H), 0.87 (t, J = 6.4 Hz, 3H).

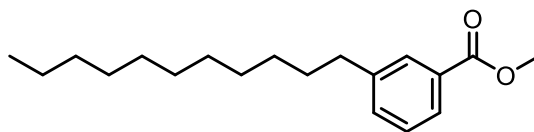


1-(3-(3-undecylphenyl)-1H-pyrazol-5-yl)cyclopropanecarbonitrile (28c). To a stirring solution of 28b (1.8 mmol) in EtOH (0.16 M) was added hydrazine (14.37 mmol). The reaction stirred at reflux overnight. After cooling, the solvent was evaporated and the residue purified by preparative TLC to afford the title product in 16% yield. R_f = 0.43 (25% EtOAc/Hexanes). ^1H NMR (600 MHz, Acetone) δ 7.57 (s, 1H), 7.17 (t, J = 7.6 Hz, 1H), 7.13 (t, J = 7.7 Hz, 1H), 7.07 (d, J = 7.5 Hz, 1H), 6.50 (s, 1H), 2.49-2.45 (t, 2H), 1.51-1.42 (m, 2H), 1.23-1.02 (m, 20H), 0.70 (t, J = 6.9 Hz, 3H). ^{13}C NMR (151 MHz, Acetone) δ 157.99, 143.61, 139.75, 130.35, 129.03, 127.38, 124.86, 100.95, 36.64, 32.74, 32.47, 30.49, 30.45, 30.45, 30.34, 30.31, 30.18, 30.10, 18.13, 15.12, 14.56, 14.48.

**28d**

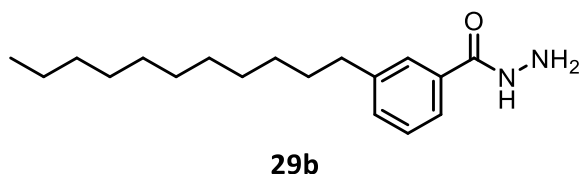
1-(3-(3-undecylphenyl)-1H-pyrazol-5-yl)cyclopropanecarboximidamide

hydrochloride (28d). General procedure A was used to convert 28c to the title product in 11% yield. ^1H NMR (600 MHz, DMSO) δ : two tautomers = 13.28 (bs, 1H), 9.01 (bs, 1H), 8.92 (bs, 1H), 8.92 (bs 1H), 7.98 (dd, J = 7.9, 1.0 Hz, 1H), 7.70 (dd, 7.7, 1.7 Hz, 1H), 7.48 (td, J = 7.6, 1.2 Hz, 1H), 7.27-7.19 (m, 1H), 6.65 (s, 1H), 2.61-2.57 (t, J = 6.0 Hz, 2H), 1.62-1.53 (m, 4H), 1.42 (bs, 2H), 1.28-1.23 (m, 16H), 1.14 (dd, J = 7.1, 4.7 Hz, 2H), 0.93 (dd, J = 7.1, 4.7 Hz, 2H), 0.84 (t, J = 7.0 Hz, 3H). ^{13}C NMR (151 MHz, DMSO) δ 180.23, 180.08, 180.01, 179.95, 140.48, 132.41, 130.02, 128.15, 99.53, 94.12, 63.89, 31.30, 29.97, 29.05, 29.01, 29.00, 29.89, 28.72, 28.70, 22.11, 13.98, 12.42, 11.21.

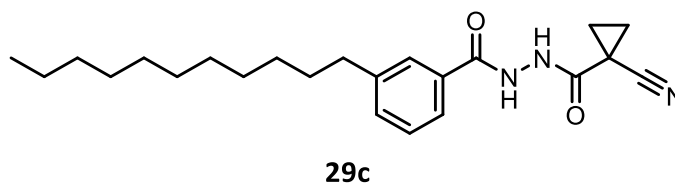
**29a**

Methyl 3-undecylbenzoate (29a). General procedure C was used to couple methyl 3-bromobenzoate to 1-undecene to afford title product in 69% yield. R_f = 0.44, 5% EtOAc/Hexanes. ^1H NMR (300 MHz, CDCl_3) δ 7.90-7.81 (m, 2H), 7.35 (dd, J = 5.7, 4.0 Hz, 2H), 3.91 (t, J = 7.5 Hz, 3H), 2.69-2.61 (m, 2H), 1.62 (dt, J = 13.7, 6.7, 2H), 1.40-1.15 (m, 16H), 0.88 (t, 6.7 Hz, 3H). ^{13}C NMR (75 MHz, CDCl_3) δ 167.53, 143.38, 133.23, 129.64,

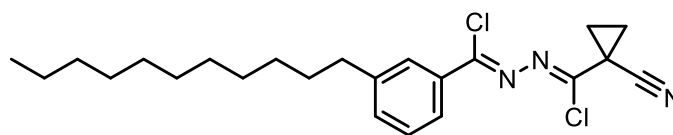
128.38, 127.05, 52.20, 51.42, 35.90, 32.06, 31.55, 29.78, 29.71, 29.62, 29.49, 29.39, 22.84, 14.28.



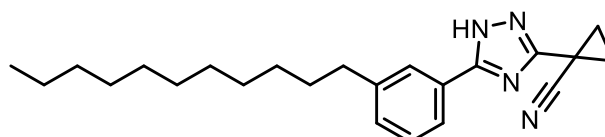
3-undecylbenzohydrazide (29b). To a stirring solution of 29a (1.93 mmol) in EtOH (0.6 M) was added hydrazine (5.78 mmol). The solution was stirred at reflux overnight. After cooling, solvent was evaporated and the residue purified by flash chromatography to afford the title product in 66% yield. R_f = 0.32 (75% EtOAc/Hexanes).



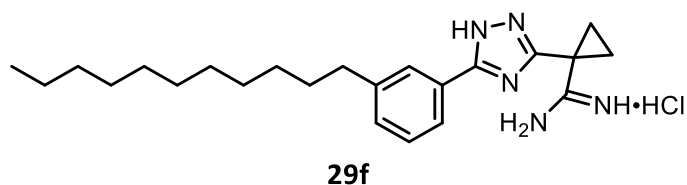
***N'*-(1-cyanocyclopropanecarbonyl)-3-undecylbenzohydrazide (29c).** General procedure B was used to couple 29b (1.27 mmol) to cyanocyclopropanecarboxylic acid (1.27 mmol) to afford the title product in 82% yield. R_f = 0.62 (50% EtOAc/Hexanes). ^1H NMR (300 MHz, CDCl_3) δ 9.27 (s, 1H), 9.00 (s, 1H), 7.65 (s, 1H), 7.64-7.59 (m, 1H), 7.32 (d, J = 7.2 Hz, 2H), 2.67-2.52 (m, 2H), 1.71 (dd, J = 8.3, 4.6 Hz, 2H), 1.56 (dd, J = 8.2, 4.6 Hz, 4H), 1.24 (bs, 16H), 0.87 (t, 6.7 Hz, 3H). ^{13}C NMR (75 MHz, CDCl_3) δ 165.77, 164.48, 143.89, 132.89, 131.02, 128.73, 127.63, 124.68, 118.89, 51.38, 35.89, 32.03, 31.46, 29.78, 29.75, 29.70, 29.59, 29.46, 29.42, 22.80, 18.62, 14.26, 12.64.

**29d**

(1Z,N'Z)-N'-chloro(1-cyanocyclopropyl)methylene)-3-undecylbenzohydrazonoyl chloride (29d). A solution of 29c (1.04 mmol) in SOCl_2 (20.78 mmol) was refluxed for 24 h. The solvent was removed and co-evaporated twice with ether. The product was carried on crude.

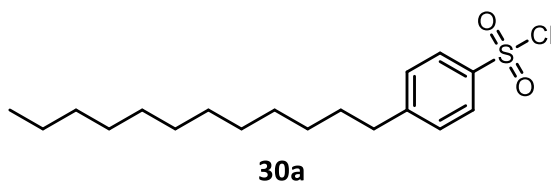
**29e**

1-(5-(3-undecylphenyl)-1H-1,2,4-triazol-3-yl)cyclopropanecarbonitrile (29e). A solution of 29d (1.04 mmol) in i-PrOH saturated with NH_3 (0.02 M) was stirred under NH_3 overnight, then refluxed for 30 h. The reaction was cooled, the solvent evaporated, and the residue purified by flash chromatography to afford the title product in 74% yield. R_f = 0.40 (25% EtOAc/Hexanes). ^1H NMR (300 MHz, Acetone) δ 7.87 (s, 1H), 7.85-7.80 (m, 1H), 7.50 (t, J = 5.7 Hz, 1H), 7.47 (d J = 2.1 Hz, 1H), 2.77-2.63 (m, 1H), 2.03 (qd, J = 3.5, 2.2 Hz, 2H), 1.73-1.59 (m, 1H), 1.40-1.22 (m, 6H), 0.86 (t, J = 6.7 Hz, 3H). ^{13}C NMR (75 MHz, Acetone) δ 165.93, 163.61, 145.16, 133.08, 130.18, 127.46, 125.09, 124.57, 118.97, 47.08, 36.33, 32.74, 32.32, 30.48, 30.28, 30.03, 23.44, 19.26, 14.48, -2.97, -6.84.



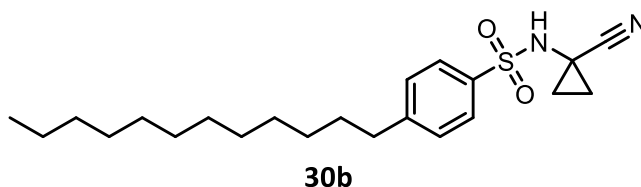
1-(5-(3-undecylphenyl)-1H-1,2,4-triazol-3-yl)cyclopropanecarboximidamide

hydrochloride (29f). General procedure A was used to convert 29e to the corresponding amidine in 49% yield. $R_f = 0.24$ (10% MeOH/ CHCl_3). ^1H NMR (600 MHz, DMSO) δ 9.44 (d, 2H), 7.80 (d, $J = 6.0$ Hz, 1H), 7.47 (dd, $J = 7.3$ Hz, 1H), 2.65 (d, $J = 6.9$ Hz, 2H), 1.95 (d, $J = 4.6$ Hz, 2H), 1.85 (d, $J = 4.5$ Hz, 2H), 1.58 (s, 2H), 1.25 (bs, 16 H), 0.83 (t, $J = 7.0$ Hz, 3H). ^{13}C NMR (151 MHz, DMSO) δ 166.90, 164.22, 163.87, 143.71, 132.04, 129.29, 126.19, 124.06, 123.12, 34.81, 31.25, 30.84, 28.99, 28.95, 28.80, 28.66, 28.57, 22.05, 20.27, 16.93, 13.89.

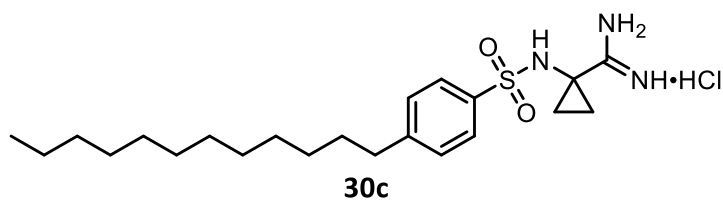


4-dodecylbenzenesulfonyl chloride (30a). Dodecylbenzene (15.7 mmol) was dissolved in CHCl_3 (0.62 M) at 0°C . HSO_3Cl (47.1 mmol) was added carefully, dropwise, keeping temperature at 0°C . The reaction mixture stirred overnight at rt, then was poured over 100 mL of crushed ice. The mixture melted, then was extracted three times with EtOAc; the combined organics were washed once with water, sat. NaHCO_3 , again with water, dried over Na_2SO_4 , and then concentrated. The reaction was carried on crude. ^1H NMR (600 MHz, Chloroform- d) δ 7.96 (d, $J = 8.7$ Hz, 2H), 7.43 (d, $J = 8.5$ Hz,

2H), 2.75 (d, $J = 7.3$ Hz, 2H), 1.67 (p, $J = 7.7$ Hz, 2H), 1.39-1.25 (m, 18H), 0.90 (t, $J = 7.0$ Hz, 3H). ^{13}C NMR (151 MHz, CDCl_3) δ 171.10, 151.69, 141.79, 129.59, 127.08, 60.38, 36.07, 31.92, 30.94, 29.65, 29.63, 29.62, 29.51, 29.39, 29.35, 29.20, 22.69, 21.03, 14.20, 14.12.

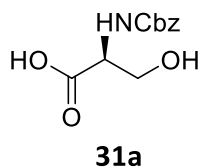


N-(1-cyanocyclopropyl)-4-dodecylbenzenesulfonamide (30b). The amine (1.81 mmol), TEA (7.22 mmol), and DMAP (0.09 mmol) were dissolved in DCM (8.0 mL). The reaction was cooled to 0°C and then 30a was added dropwise, transferred with 1 mL DCM. After stirring 16 h at rt, the reaction was quenched with sat. NH_4Cl . The mixture was then diluted with EtOAc and the organic layer washed with brine, then dried over Na_2SO_4 . The product was purified by flash chromatography to yield the title product in 48.9% yield. $R_f = 0.33$ (10% EtOAc/Hexanes). ^1H NMR (300 MHz, Chloroform- d) δ 7.85 (d, $J = 9.2$ Hz, 2H), 7.35 (d, $J = 8.5$ Hz, 2H), 2.70 (t, $J = 7.2$ Hz, 2H), 1.95-1.88 (m, 2H), 1.75-1.69 (m, 2H), 1.68-1.58 (m, 2H), 1.37-1.21 (m, 18H), 0.88 (t, $J = 6.6$ Hz, 3H). ^{13}C NMR (75 MHz, CDCl_3) δ 151.14, 135.77, 129.44, 129.14, 118.70, 36.25, 32.16, 31.22, 29.89, 29.78, 29.67, 29.60, 29.45, 27.14, 22.93, 20.13, 14.37.

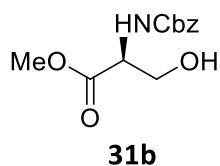


1-((4-dodecylphenyl)sulfonamide)cyclopropanecarboximidamide hydrochloride

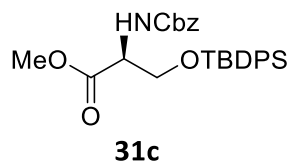
(30c). General procedure A was used to afford the title product in 31.2% yield. ^1H NMR (300 MHz, DMSO- d_6) δ 7.48 (d, J = 8.1 Hz, 2H), 7.10 (d, J = 8.0 Hz, 2H), 2.52 (t, J = 7.3 Hz, 2H), 1.57 – 1.46 (m, 2H), 1.21 (s, 18H), 0.87 – 0.79 (m, 3H). ^{13}C NMR (75 MHz, DMSO) δ 143.35, 128.12, 126.17, 46.75, 35.51, 31.99, 31.62, 29.70, 29.55, 29.41, 29.28, 22.79, 14.65.



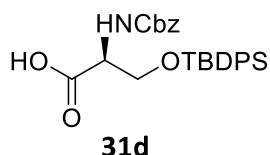
((Benzyloxy)carbonyl)-L-serine (31a). L-serine (14.25 mmol) was dissolved in 10% Na_2CO_3 (0.37 M, aq.). Dioxanes (0.5 M) and Cbz-succinamide (28.5 mmol) were added and the reaction stirred at rt for 24 h. The mixture was washed 3 times with Et_2O ; the aqueous layer was acidified with HCl, then extracted 5 times with EtOAc. The combined EtOAc layers were washed twice with brine, dried over Na_2SO_4 , concentrated, then the product was carried on crude.



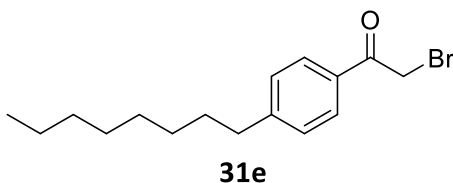
Methyl ((benzyloxy)carbonyl)-L-serinate (31b). The protected amine 31a (14.25 mmol) was dissolved in 40.8 mL MeOH and 244.7 mL benzene. TMS-diazomethane (14.25 mmol) was added dropwise and the solution stirred 2.5 h. The reaction was quenched with glacial AcOH, then evaporated. The residue was dissolved in EtOAc, washed with water followed by brine, dried over Na₂SO₄, then carried on crude.



Methyl N-((benzyloxy)carbonyl)-O-(tert-butyldiphenylsilyl)-L-serinate (31c). Compound 31b (12.2 mmol) was dissolved in DMF (24.4 mL), whereupon imidazole (26.7 mmol) and TBDPSCI (18.2 mmol) were added. The reaction stirred 16 h, then was diluted extensively with EtOAc; washed with water, then brine; then the residue was purified by flash chromatography (15% EtOAc/Hexanes) to afford the title product in 64% yield. ¹H NMR (600 MHz, Chloroform-d) δ 7.65 – 7.60 (m, 5H), 7.49 – 7.43 (m, 3H), 7.43 – 7.36 (m, 7H), 5.69 (d, J = 8.5 Hz, 2H), 5.16 (dd, J = 12.4, 0.1 Hz, 1H), 4.51 – 4.47 (m, 1H), 4.13 (dd, J = 10.1, 2.6 Hz, 1H), 3.94 (dd, J = 10.2, 2.9 Hz, 1H), 3.78 (s, 3H), 1.06 (s, 9H). ¹³C NMR (151 MHz, CDCl₃) δ 170.88, 155.89, 135.54, 135.49, 132.82, 132.70, 129.93, 129.91, 128.57, 128.21, 128.14, 127.82, 127.79, 67.04, 64.50, 55.95, 52.44, 26.73, 19.28, 14.23.

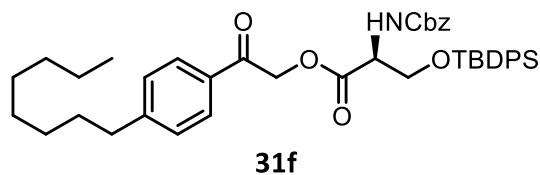


N-((benzyloxy)carbonyl)-O-(tert-butyldiphenylsilyl)-L-serine (31d). The ester 31c (7.84 mmol) was dissolved in iPrOH (0.05M), then NaOH (15.7 mmol, dissolved in 52 mL H₂O) was added. The solution stirred at 60 °C for 2.5 h, then was diluted with water, acidified to pH 3 using conc. HCl, and extracted 4 times with EtOAc. The combined organics were washed with brine, dried over Na₂SO₄, and concentrated to afford the title product in 100% yield. ¹H NMR (600 MHz, Methanol-d₄) δ 7.75 (s, 2H), 7.67 (s, 4H), 7.37 (s, 9H), 5.20 – 4.95 (m, 2H), 4.62 (s, 1H), 4.40 (s, 1H), 4.01 (d, J = 59.2 Hz, 2H), 1.10 – 0.98 (m, 9H). ¹³C NMR (151 MHz, CDCl₃) δ 171.99, 156.76, 135.32, 135.27, 135.18, 134.58, 132.85, 132.73, 111.32, 66.39, 63.89, 56.02, 25.96, 23.99, 18.80.



2-bromo-1-(4-octylphenyl)ethan-1-one (31e). Aluminum trichloride (46 mmol) was dissolved in DCE (24 mL), and the solution was cooled to 0 °C. Bromoacetyl bromide (48 mmol) was added dropwise, followed by phenyl octane (20 mmol) added dropwise. The mixture was warmed to rt and stirred for 4 h, then was carefully quenched at 0 °C using water. The organic layer was isolated, dried over Na₂SO₄, and purified by flash chromatography (10% EtOAc/Hexanes) to give the title product in 82% yield. ¹H NMR

(600 MHz, Chloroform-d) δ 7.90 – 7.85 (m, 2H), 7.25 (d, J = 8.4 Hz, 2H), 4.40 (s, 2H), 2.64 (d, J = 7.9 Hz, 2H), 1.62 (p, J = 7.6 Hz, 2H), 1.39 – 1.21 (m, 10H), 0.89 (t, J = 7.1 Hz, 3H). ^{13}C NMR (151 MHz, CDCl_3) δ 190.63, 149.74, 131.67, 129.06, 128.85, 36.09, 31.92, 31.31, 31.06, 29.49, 29.35, 29.30, 22.73, 14.18.

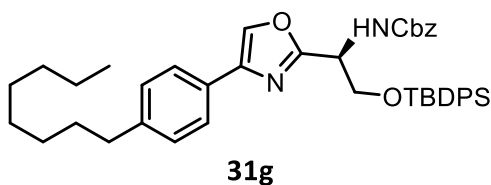


2-(4-octylphenyl)-2-oxoethyl

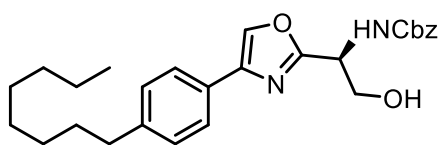
N-((benzyloxy)carbonyl)-O-(tert-

butyldiphenylsilyl)-L-serinate (31f). Carboxylic acid 31d (8.1 mmol) was dissolved in EtOH (26 mL); Cs_2CO_3 (4.31 mmol) was added and the suspension was sonicated for 15 minutes. The EtOH was evaporated and the residue dissolved in DMF (25 mL), then 31e (11.0 mmol) was added, dissolved in DMF (25 mL). The solution stirred overnight, then was diluted with EtOAc, washed extensively with water, washed once with brine, dried over Na_2SO_4 , and purified by flash chromatography (5 to 20% EtOAc/Hexanes) to afford the title product in 47% yield. ^1H NMR (300 MHz, Chloroform-d) δ 7.83 (d, J = 8.1 Hz, 2H), 7.71 – 7.62 (m, 5H), 7.41 (dq, J = 12.7, 6.2 Hz, 10H), 7.30 (d, J = 8.3 Hz, 2H), 5.74 (d, J = 8.5 Hz, 2H), 5.15 (d, J = 3.3 Hz, 2H), 4.75 – 4.66 (m, 1H), 4.25 (dd, J = 10.3, 3.2 Hz, 1H), 4.05 (dd, J = 10.4, 3.1 Hz, 1H), 2.68 (t, J = 7.7 Hz, 2H), 1.72 – 1.60 (m, 2H), 1.40 – 1.28 (m, 10H), 1.07 (s, 9H), 0.95 – 0.86 (m, 3H). ^{13}C NMR (75 MHz, CDCl_3) δ 190.81, 170.20, 156.05, 150.11, 135.90, 135.81, 133.09, 132.02, 130.13, 129.17, 128.78, 128.36, 128.16,

128.05, 67.24, 66.84, 64.52, 60.63, 56.25, 36.34, 32.11, 31.33, 29.67, 29.49, 27.02, 22.93, 21.31, 19.54, 14.46, 14.39.

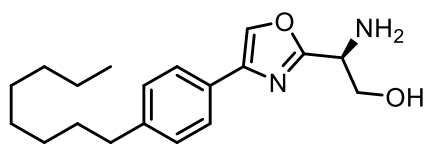


Benzyl (S)-2-((tert-butyldiphenylsilyl)oxy)-1-(4-(4-octylphenyl)oxazol-2-yl)ethyl carbamate (31g). Compound 31h (3.8 mmol) was dissolved in glacial AcOH, then NH₄OAc (9.4 mmol) was added and the mixture stirred at 100 °C overnight. The liquids were evaporated and the residue taken up in EtOAc, which was washed five times with sat. NaHCO₃, washed once with brine, dried over Na₂SO₄, and purified by flash chromatography (15 to 25% EtOAc/Hexanes) to afford the title product in 19% yield. ¹H NMR (600 MHz, Chloroform-d) δ 7.86 (d, J = 7.9 Hz, 1H), 7.73 – 7.67 (m, 4H), 7.49 – 7.37 (m, 13H), 7.34 (t, J = 9.4 Hz, 2H), 5.77 (d, J = 8.5 Hz, 2H), 5.18 (q, J = 12.3 Hz, 1H), 4.76 – 4.71 (m, 1H), 4.29 (dd, J = 10.4, 3.3 Hz, 1H), 4.09 (dd, J = 10.4, 3.2 Hz, 1H), 2.71 (t, J = 7.7 Hz, 2H), 1.68 (p, J = 7.5 Hz, 2H), 1.40 – 1.32 (m, 10H), 1.11 (s, 9H), 0.94 (t, J = 7.0 Hz, 3H). ¹³C NMR (151 MHz, CDCl₃) δ 190.60, 171.11, 169.97, 155.84, 149.87, 135.69, 135.59, 132.86, 131.85, 129.91, 128.96, 128.56, 128.17, 128.13, 127.95, 127.85, 127.82, 67.02, 66.63, 64.32, 60.40, 56.06, 36.13, 31.90, 31.10, 29.45, 29.28, 29.26, 26.82, 22.71, 21.06, 19.34, 14.25, 14.16.

**31h**

Benzyl (S)-(2-hydroxy-1-(4-(4-octylphenyl)oxazol-2-yl)ethyl)carbamate (31h).

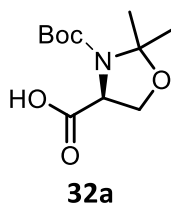
Compound 31 g (0.72 mmol) was dissolved in a 1 M solution of TBAF in THF (1.56 mmol) and stirred overnight at rt. The reaction was evaporated and the residue dissolved in EtOAc, which was washed 4 times with NH_4Cl , washed once with water and once with brine, dried over Na_2SO_4 , and purified by flash chromatography (50% EtOAc/Hexanes) to afford the title product in 58% yield. ^1H NMR (300 MHz, Chloroform- d) δ 7.81 (s, 1H), 7.58 (d, J = 8.1 Hz, 2H), 7.34 (d, J = 7.7 Hz, 5H), 7.21 (d, J = 8.2 Hz, 2H), 5.94 (d, J = 8.5 Hz, 2H), 5.15 (s, 1H), 5.10 – 5.03 (m, 1H), 4.16 (dd, J = 11.5, 3.2 Hz, 1H), 3.97 (dd, J = 11.5, 3.9 Hz, 1H), 3.16 (s, 1H), 2.62 (t, J = 7.3 Hz, 2H), 1.69 – 1.55 (m, 2H), 1.29 (d, J = 9.9 Hz, 10H), 0.88 (t, J = 6.7 Hz, 3H). ^{13}C NMR (75 MHz, CDCl_3) δ 162.48, 143.66, 133.84, 129.08, 128.79, 128.49, 128.41, 127.73, 125.71, 67.55, 64.00, 50.89, 36.00, 32.12, 31.65, 29.72, 29.52, 22.91, 14.37.

**31i**

(S)-2-amino-2-(4-(4-octylphenyl)oxazol-2-yl)ethan-1-ol (31i). Compound 31h

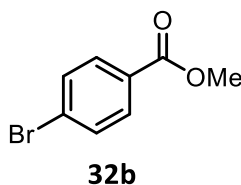
(0.42 mmol) was dissolved in EtOH (0.05 M). A catalytic amount of Pd/C was added, and the mixture stirred under hydrogen atmosphere overnight. The suspension was filtered

through Celite, using EtOH and MeOH to wash the solid. The filtrate was concentrated and purified by flash chromatography followed by preparatory TLC (50% EtOAc/Hexanes) to afford the title product in 18.7% yield. ^1H NMR (600 MHz, DMSO- d_6) δ 8.50 (s, 1H), 7.68 (d, J = 7.3 Hz, 2H), 7.25 (d, J = 7.3 Hz, 2H), 4.09 (s, 1H), 3.71 (dd, J = 17.4, 5.3 Hz, 1H), 3.40 (s, 1H), 2.59 (t, J = 7.5 Hz, 2H), 1.58 (s, 2H), 1.41-1.15 (m, 10H), 0.86 (t, J = 14.0, 6.4 Hz, 3H). ^{13}C NMR (151 MHz, CDCl_3) δ 165.53, 142.51, 139.98, 134.84, 129.09, 128.90, 125.51, 64.50, 52.03, 35.38, 31.75, 31.33, 29.31, 29.15, 22.56, 14.43.

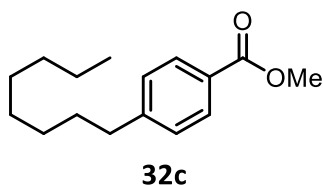


(S)-3-(tert-butoxycarbonyl)-2,2-dimethyloxazolidine-4-carboxylic acid (32a).

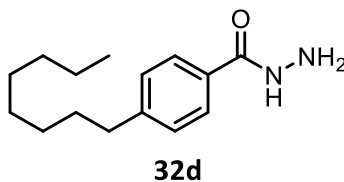
General procedure Q was used to convert Boc-L-serine to the title product.



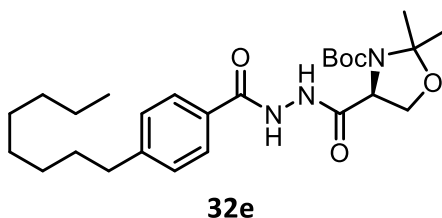
Methyl 4-bromobenzoate (32b). General procedure I was used to convert 4-bromobenzoic acid to the title product in 96% yield. R_f = 0.63, 5% EtOAc/Hexanes. ^1H NMR (600 MHz, Chloroform- d) δ 7.93 – 7.84 (m, 2H), 7.61 – 7.52 (m, 2H), 3.90 (s, 3H). ^{13}C NMR (151 MHz, CDCl_3) δ 168.84, 134.22, 133.62, 131.55, 130.55, 54.81.



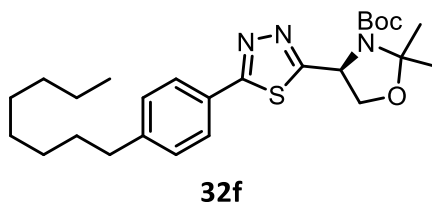
Methyl 4-octylbenzoate (32c). General procedure C was used to couple 1-octene to 32b to yield the title product in 56% yield. R_f = 0.57, 5% EtOAc/Hexanes. ^1H NMR (600 MHz, Chloroform- d) δ 7.95 (d, J = 8.9 Hz, 2H), 7.23 (d, J = 8.0 Hz, 2H), 3.90 – 3.88 (m, 3H), 2.64 (t, J = 6.3 Hz, 2H), 1.62 (p, J = 7.6 Hz, 2H), 1.36 – 1.21 (m, 10H), 0.88 (t, J = 7.1 Hz, 3H). ^{13}C NMR (151 MHz, CDCl_3) δ 169.68, 151.01, 132.13, 130.93, 130.13, 54.43, 38.54, 34.39, 33.67, 31.96, 31.80, 31.76, 25.19, 16.62.



4-octylbenzohydrazide (32d). General procedure J was used to convert 32b to the title product in 53% yield. R_f = 0.38, 5% MeOH/ CHCl_3 . ^1H NMR (600 MHz, Methanol- d_4) δ 7.72 (d, J = 7.2 Hz, 2H), 7.30 (d, J = 7.0 Hz, 2H), 3.34 (s, 1H), 2.68 (t, J = 7.1 Hz, 2H), 1.65 (s, 2H), 1.40 – 1.27 (m, 10H), 0.91 (t, J = 6.5 Hz, 3H). ^{13}C NMR (151 MHz, CDCl_3) δ 173.53, 146.94, 128.23, 126.94, 35.36, 31.63, 31.06, 29.16, 29.00, 28.92, 22.33, 13.05.

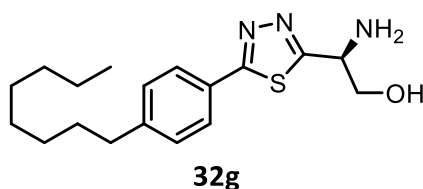


Tert-butyl (S)-2,2-dimethyl-4-(2-(4-octylbenzoyl)hydrazine-1-carbonyl)oxazolidine-3-carboxylate (32e). General procedure B was used to couple 32a and 32d to afford the title product in 56% yield. R_f = 0.49, 40% EtOAc/Hexanes. ^1H NMR (600 MHz, Chloroform- d) δ 10.32 – 10.02 (m, 1H), 9.97 – 9.71 (m, 1H), 7.72 (s, 2H), 7.12 (d, J = 7.5 Hz, 2H), 4.57 (d, J = 26.1 Hz, 1H), 4.24 (s, 1H), 4.02 (d, J = 22.9 Hz, 1H), 2.56 (t, J = 7.7 Hz, 2H), 1.65 (d, J = 15.4 Hz, 2H), 1.50 (s, 6H), 1.47 – 1.34 (m, 9H), 1.31 – 1.17 (m, 10H), 0.84 (s, 3H). ^{13}C NMR (151 MHz, CDCl_3) δ 171.05, 151.38, 128.48, 127.50, 95.09, 81.51, 60.30, 35.84, 31.82, 31.10, 29.38, 29.22, 29.19, 28.19, 22.60, 20.93, 14.12, 14.03.

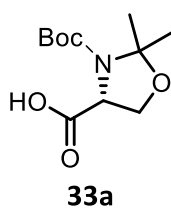


Tert-butyl (S)-2,2-dimethyl-4-(5-(4-octylphenyl)-1,3,4-thiadiazol-2-yl)oxazolidine-3-carboxylate (32f). General procedure O was used to convert 32e to the title product in 41% yield. R_f = 0.72, 40% EtOAc/Hexanes. ^1H NMR (300 MHz, Chloroform- d) δ 7.85 – 7.76 (m, 2H), 7.26 – 7.16 (m, 2H), 5.35 (dd, J = 16.5, 4.5 Hz, 1H), 4.29 (d, J = 6.2 Hz, 1H), 4.16 (d, J = 9.1 Hz, 1H), 2.59 (t, J = 7.4 Hz, 2H), 1.78 – 1.72 (m, 2H), 1.55 (s, 9H), 1.47 (s, 6H), 1.35 – 1.16 (m, 10H), 0.82 (t, J = 6.3 Hz, 3H). ^{13}C NMR (75

MHz, CDCl₃) δ 172.81, 169.15, 151.47, 146.84, 129.39, 128.00, 95.39, 94.91, 81.62, 81.24, 69.11, 68.33, 57.36, 36.05, 32.06, 31.40, 29.63, 29.43, 28.45, 27.47, 26.72, 24.44, 23.23, 22.86, 14.33.

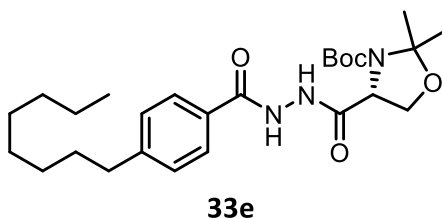


(S)-2-amino-2-(5-(4-octylphenyl)-1,3,4-thiadiazol-2-yl)ethan-1-ol (32g). General procedure P was used to convert 32f to the title product in 12% yield. R_f = 0.42, 10% MeOH/EtOAc. ¹H NMR (600 MHz, DMSO-*d*₆) δ 7.86 (d, *J* = 8.3 Hz, 2H), 7.36 (d, *J* = 8.4 Hz, 2H), 5.15 (s, 1H), 4.31 (dd, *J* = 6.3, 4.7 Hz, 1H), 3.76 – 3.70 (m, 1H), 3.65 – 3.58 (m, 1H), 3.36 (s, 2H), 2.67 – 2.62 (m, 2H), 1.60 (p, *J* = 7.2 Hz, 2H), 1.34 – 1.19 (m, 10H), 0.86 (t, *J* = 7.1 Hz, 3H). ¹³C NMR (151 MHz, DMSO) δ 176.66, 168.20, 146.19, 129.75, 128.06, 127.80, 66.45, 54.21, 35.42, 31.75, 31.13, 29.13, 29.13, 22.57, 14.44.

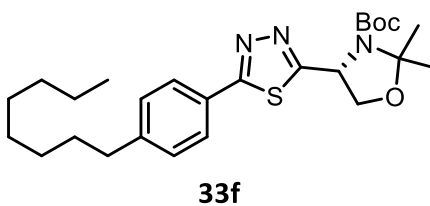


(R)-3-(tert-butoxycarbonyl)-2,2-dimethyloxazolidine-4-carboxylic acid (33a).

General procedure Q was used to convert Boc-R-serine to the title product in 29% yield. R_f = 0.61, 5% MeOH/ CHCl₃).

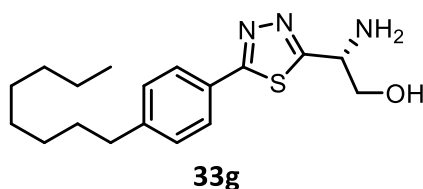


Tert-butyl (R)-2,2-dimethyl-4-(2-(4-octylbenzoyl)hydrazine-1-carbonyl)oxazolidine-3-carboxylate (33e). General procedure B was used to couple 33a and 32d and afford the title product in 70% yield. R_f = 0.46, 40% EtOAc/Hexanes. ^1H NMR (300 MHz, Chloroform- d) δ 10.49 – 10.14 (m, 1H), 10.01 – 9.80 (m, 1H), 7.70 (s, 2H), 7.08 (d, J = 6.9 Hz, 2H), 4.56 (s, 1H), 4.23–4.14 (m, 1H), 4.09 – 3.88 (m, 1H), 2.53 (t, J = 7.2 Hz, 2H), 1.61 (s, 2H), 1.55 – 1.11 (m, 25H), 0.82 (t, J = 5.8 Hz, 3H). ^{13}C NMR (75 MHz, CDCl_3) δ 168.84, 164.87, 153.06, 151.56, 148.00, 128.70, 127.77, 95.18, 94.88, 81.65, 80.91, 66.91, 65.87, 59.02, 36.08, 32.06, 31.35, 29.63, 29.44, 28.41, 26.52, 25.51, 24.86, 24.23, 22.84, 14.30.

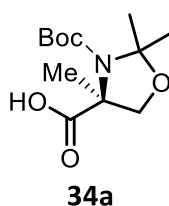


Tert-butyl (R)-2,2-dimethyl-4-(5-(4-octylphenyl)-1,3,4-thiadiazol-2-yl)oxazolidine-3-carboxylate (33f). General procedure O was used to convert 33e to the title product in 39% yield. R_f = 0.57, 40% EtOAc/Hexanes. ^1H NMR (300 MHz, Chloroform- d) δ 7.82 (d, J = 8.1 Hz, 2H), 7.24 (d, J = 7.9 Hz, 2H), 5.37 (dd, J = 16.0, 4.5 Hz, 1H), 4.37 – 4.16 (m, 1H), 3.18 – 3.09 (m, 1H), 2.69 – 2.55 (m, 2H), 1.83 – 1.11 (m, 27H),

0.92 – 0.76 (m, 3H). ¹³C NMR (75 MHz, CDCl₃) δ 172.90, 171.70, 152.49, 151.52, 146.92, 146.53, 129.41, 128.03, 127.67, 95.43, 94.96, 81.33, 69.15, 68.35, 60.60, 57.38, 36.09, 32.08, 31.43, 29.65, 29.46, 28.47, 26.75, 23.24, 14.34.

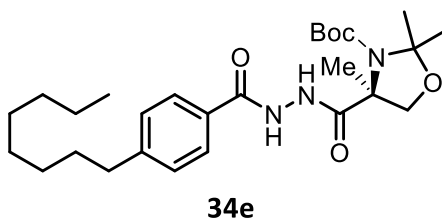


(R)-2-amino-2-(5-(4-octylphenyl)-1,3,4-thiadiazol-2-yl)ethan-1-ol (33g). General procedure P was used to convert 33f to the title product in 16% yield. *R*_f = 0.40, 10% MeOH/EtOAc. ¹H NMR (600 MHz, DMSO-*d*₆) δ 7.88 – 7.83 (m, 2H), 7.35 (d, *J* = 8.3 Hz, 2H), 5.18 (s, 2H), 4.32 (dd, *J* = 6.3, 4.7 Hz, 1H), 3.73 (dd, *J* = 10.7, 4.7 Hz, 1H), 3.62 (dd, *J* = 10.7, 6.4 Hz, 1H), 2.64 (t, *J* = 8.1 Hz, 2H), 2.48 (s, 1H), 1.60 (p, *J* = 7.3 Hz, 2H), 1.34 – 1.20 (m, 10H), 0.85 (t, *J* = 7.0 Hz, 3H). ¹³C NMR (151 MHz, DMSO) δ 176.62, 168.18, 146.13, 129.69, 128.08, 127.78, 66.45, 54.23, 35.44, 31.76, 31.13, 29.31, 29.15, 22.57, 14.40.

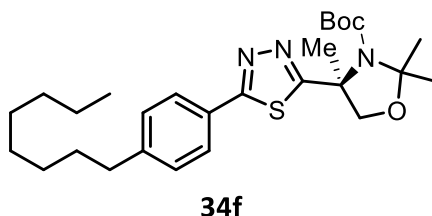


(S)-3-(tert-butoxycarbonyl)-2,2,4-trimethyloxazolidine-4-carboxylic acid (34a).

General procedure Q was used to convert N-Boc-2-methyl serine to the title product. *R*_f = 0.43, 5% MeOH/CHCl₃.

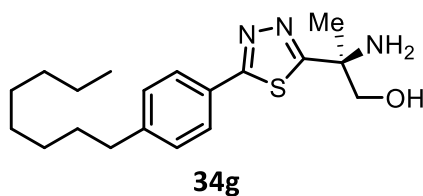


Tert-butyl (S)-2,2,4-trimethyl-4-(2-(4-octylbenzoyl)hydrazine-1-carbonyl)oxazolidine-3-carboxylate (34e). General procedure B was used to couple 34a and 32d to afford the title product in 54% yield. R_f = 0.59, 40% EtOAc/Hexanes. ^1H NMR (300 MHz, Chloroform- d) δ 10.22 – 9.60 (m, 1H), 9.15 (s, 1H), 7.69 (d, J = 8.0 Hz, 2H), 7.07 (d, J = 8.1 Hz, 2H), 4.44 – 4.06 (m, 1H), 3.59 (d, J = 8.0 Hz, 1H), 2.50 (t, J = 7.2 Hz, 2H), 1.91 (s, 3H), 1.61 – 1.44 (m, 8H), 1.35 (s, 9H), 1.26 – 1.06 (m, 10H), 0.77 (t, J = 6.5 Hz, 3H). ^{13}C NMR (75 MHz, CDCl_3) δ 170.50, 164.81, 147.58, 128.96, 128.60, 127.70, 96.15, 81.50, 74.03, 73.29, 65.75, 60.45, 36.01, 32.00, 31.30, 29.57, 29.36, 28.43, 25.51, 22.79, 21.08, 14.23.



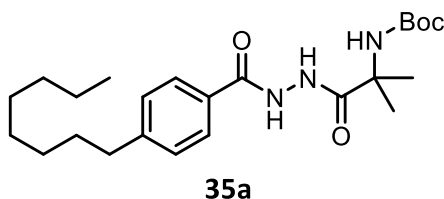
Tert-butyl (S)-2,2,4-trimethyl-4-(5-(4-octylphenyl)-1,3,4-thiadiazol-2-yl)oxazolidine-3-carboxylate (34f). General procedure O was used to convert 34e to the title product in 16% yield. R_f = 0.63, 25% EtOAc/Hexanes. ^1H NMR (300 MHz, Chloroform- d) δ 7.83 (d, J = 7.2 Hz, 2H), 7.30 – 7.20 (m, 2H), 4.37 (s, 1H), 4.11 (dd, J = 35.2, 8.9 Hz, 1H), 2.62 (t, J = 7.5 Hz, 2H), 1.99 (s, 3H), 1.75 (s, 2H), 1.62 (d, J = 10.9 Hz,

6H), 1.47 (s, 9H), 1.29 (d, $J = 22.0$ Hz, 10H), 0.84 (t, $J = 7.0$ Hz, 3H). ^{13}C NMR (75 MHz, CDCl_3) δ 175.32, 169.45, 153.62, 146.88, 129.42, 128.02, 127.76, 96.67, 95.39, 81.27, 64.06, 61.25, 55.66, 36.09, 32.07, 31.43, 29.65, 29.45, 28.49, 25.67, 25.34, 23.90, 22.88, 14.35.



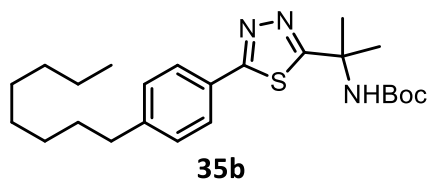
(S)-2-amino-2-(5-(4-octylphenyl)-1,3,4-thiadiazol-2-yl)propan-1-ol (34g).

General procedure P was used to convert 34f to the title product in 46% yield. $R_f = 0.49$, 15% MeOH/EtOAc. ^1H NMR (600 MHz, $\text{DMSO}-d_6$) δ 7.84 (d, $J = 8.1$ Hz, 2H), 7.34 (d, $J = 8.0$ Hz, 2H), 5.22 (s, 1H), 3.69 (d, $J = 10.0$ Hz, 1H), 3.52 (d, $J = 10.2$ Hz, 1H), 2.62 (t, $J = 7.6$ Hz, 2H), 2.48 (s, 1H), 1.63 – 1.55 (m, 2H), 1.45 (s, 3H), 1.34 – 1.18 (m, 10H), 0.85 (t, $J = 6.9$ Hz, 3H). ^{13}C NMR (151 MHz, DMSO) δ 180.56, 168.45, 146.03, 129.70, 129.67, 128.17, 127.75, 70.58, 57.38, 35.44, 31.75, 31.13, 29.30, 29.14, 26.60, 22.57, 14.41.



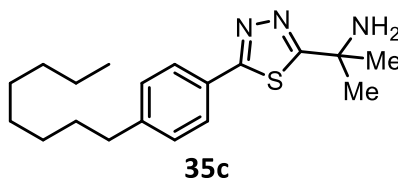
Tert-butyl (2-methyl-1-(2-(4-octylbenzoyl)hydrazinyl)-1-oxopropan-2-yl)carbamate (35a). General procedure B was used to couple 32d and Boc- α -methylalanine to afford the title product in 77% yield. $R_f = 0.46$, 40% EtOAc/Hexanes. ^1H NMR (600 MHz, $\text{Chloroform}-d$) δ 9.54 (s, 1H), 7.76 (d, $J = 7.9$ Hz, 2H), 7.26 – 7.18 (m, 2H),

2.67 – 2.60 (m, 2H), 1.66 – 1.60 (m, 2H), 1.60 – 1.56 (m, 6H), 1.49 – 1.43 (m, 9H), 1.36 – 1.23 (m, 10H), 0.92 – 0.87 (m, 3H). ¹³C NMR (151 MHz, CDCl₃) δ 171.17, 154.92, 128.60, 128.58, 127.38, 56.21, 35.90, 31.86, 31.15, 29.43, 29.25, 28.31, 22.66, 21.04, 14.21, 14.10.



Tert-butyl (2-(5-(4-octylphenyl)-1,3,4-thiadiazol-2-yl)propan-2-yl)carbamate

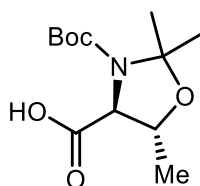
(35b). General procedure O was used to convert 35a to the title product in 59% yield. *R*_f = 0.59, 20% EtOAc/Hexanes. ¹H NMR (600 MHz, Chloroform-*d*) δ 7.81 (d, *J* = 8.1 Hz, 2H), 7.21 (d, *J* = 8.1 Hz, 2H), 5.72 (s, 1H), 2.59 (t, *J* = 8.1 Hz, 2H), 1.78 (s, 6H), 1.58 (p, *J* = 7.6 Hz, 2H), 1.38 (d, *J* = 28.3 Hz, 9H), 1.30 – 1.16 (m, 10H), 0.83 (t, *J* = 7.1 Hz, 3H). ¹³C NMR (151 MHz, CDCl₃) δ 177.02, 168.86, 154.27, 146.17, 129.05, 127.82, 127.75, 79.74, 54.56, 35.82, 31.83, 31.16, 29.40, 29.20, 28.29, 22.62, 14.09.



2-(5-(4-octylphenyl)-1,3,4-thiadiazol-2-yl)propan-2-amine (35c). General

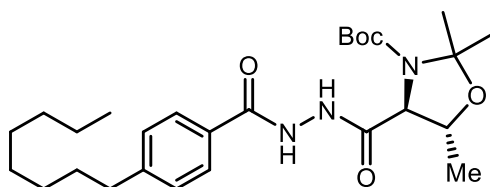
procedure P was used to convert 35b to the title product in 75% yield. *R*_f = 0.46, 10% MeOH/EtOAc. ¹H NMR (600 MHz, DMSO-*d*₆) δ 9.42 (s, 3H), 7.86 (d, *J* = 8.2 Hz, 2H), 7.34 (d, *J* = 8.2 Hz, 2H), 2.59 (t, *J* = 7.6 Hz, 2H), 1.85 (s, 6H), 1.54 (p, *J* = 7.1 Hz, 2H), 1.28 – 1.13

(m, 10H), 0.80 (t, $J = 7.0$ Hz, 3H). ^{13}C NMR (151 MHz, DMSO) δ 171.84, 169.93, 146.91, 129.86, 129.76, 128.17, 128.03, 127.13, 54.71, 35.49, 31.76, 31.09, 29.32, 29.16, 28.03, 27.66, 27.52, 22.57, 14.36.

**36a**

(4S,5R)-3-(tert-butoxycarbonyl)-2,2,5-trimethyloxazolidine-4-carboxylic acid

(36a). General procedure Q was used to convert Boc-L-threonine to the title product.

**36b**

Tert-butyl (4S,5R)-2,2,5-trimethyl-4-(2-(4-octylbenzoyl)hydrazine-1-

carbonyl)oxazolidine-3-carboxylate (36b). General procedure B was used to couple 36a

and 32d to afford the title product in 31% yield. ^1H NMR (600 MHz, Chloroform- d) δ

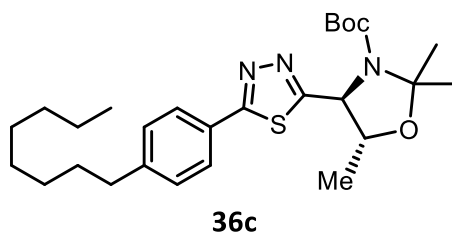
10.28 – 9.86 (m, 1H), 9.69 – 9.10 (m, 1H), 7.69 (s, 2H), 7.16 (s, 2H), 4.34 – 4.16 (m, 1H),

4.05 (d, $J = 7.3$ Hz, 1H), 2.59 (t, $J = 7.0$ Hz, 2H), 1.68 – 1.52 (m, 11H), 1.50 – 1.19 (m, 19H),

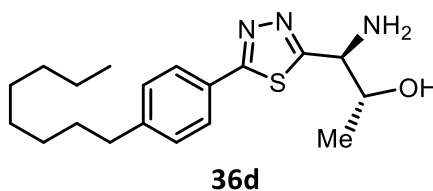
0.85 (d, $J = 7.3$ Hz, 3H). ^{13}C NMR (151 MHz, CDCl_3) δ 173.69, 132.17, 131.28, 131.18,

130.84, 129.91, 122.70, 111.91, 87.61, 71.71, 68.18, 66.52, 62.92, 38.41, 34.37, 33.65,

31.93, 31.78, 31.74, 30.78, 25.16, 16.61.

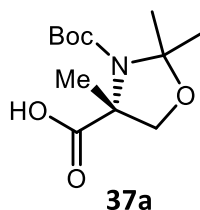


Tert-butyl (4S,5R)-2,2,5-trimethyl-4-(5-(4-octylphenyl)-1,3,4-thiadiazol-2-yl)oxazolidine-3-carboxylate (36c). General procedure O was used to convert 36b to the title product in 42% yield. ¹H NMR (600 MHz, Chloroform-d) δ 7.67 (s, 2H), 7.09 (s, 2H), 4.64 (s, 1H), 4.04 (s, 1H), 2.46 (s, 2H), 1.61 – 1.38 (m, 14H), 1.26 (s, 6H), 1.20 – 0.96 (m, 10H), 0.68 (s, 3H). ¹³C NMR (151 MHz, CDCl₃) δ 173.65, 171.28, 153.68, 149.27, 131.74, 131.60, 130.31, 130.25, 97.88, 83.42, 66.22, 34.35, 33.69, 31.92, 31.72, 30.64, 25.15, 16.60.



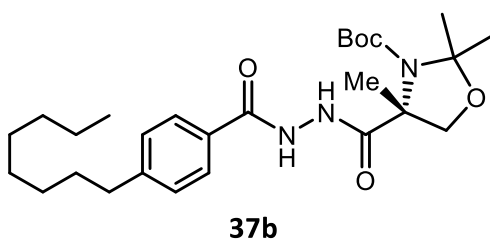
(1S,2R)-1-amino-1-(5-(4-octylphenyl)-1,3,4-thiadiazol-2-yl)propan-2-ol (36d).

General procedure P was used to convert 36c to the title product in 30% yield. ¹H NMR (600 MHz, DMSO-d₆) δ 7.88 – 7.80 (m, 2H), 7.38 – 7.29 (m, 2H), 5.06 (s, 2H), 4.09 (d, J = 4.7 Hz, 1H), 3.92 (s, 1H), 2.64 – 2.58 (m, 2H), 2.44 (s, 1H), 1.57 (s, 2H), 1.35 – 1.17 (m, 10H), 1.12 (t, J = 5.9 Hz, 3H), 0.83 (t, J = 6.9 Hz, 3H). ¹³C NMR (151 MHz, CDCl₃) δ 179.43, 170.74, 148.63, 132.26, 132.15, 130.61, 130.35, 130.21, 72.69, 60.61, 37.93, 34.26, 31.80, 31.65, 25.07, 22.75, 16.92.



(R)-3-(tert-butoxycarbonyl)-2,2,4-trimethyloxazolidine-4-carboxylic acid (37a).

General procedure Q was used to convert *N*-[(1,1-dimethylethoxy)carbonyl]-2-methyl-D-serine to afford the title product.



Tert-butyl

(R)-2,2,4-trimethyl-4-(2-(4-octylbenzoyl)hydrazine-1-

carbonyl)oxazolidine-3-carboxylate (37b). General procedure B was used to couple 37a

and 32d to afford the title product. *R*_f = 0.49, EtOAc/Hexanes. ¹H NMR (300 MHz,

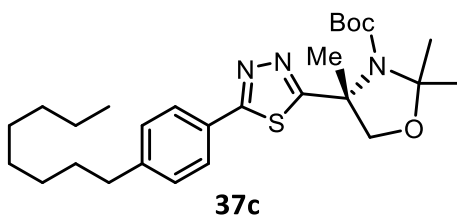
Chloroform-*d*) δ 9.78 (s, 1H), 9.13 (s, 1H), 7.70 (d, *J* = 8.0 Hz, 2H), 7.10 (d, *J* = 8.0 Hz, 2H),

4.02 (q, *J* = 7.1 Hz, 2H), 2.53 (t, *J* = 7.9 Hz, 2H), 1.94 (s, 3H), 1.64 – 1.54 (m, 2H), 1.49 (s,

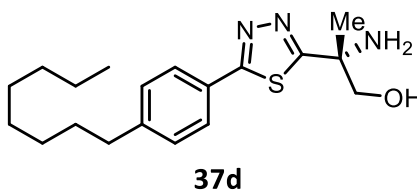
6H), 1.38 (d, *J* = 18.8 Hz, 9H), 1.29 – 1.08 (m, 10H), 0.79 (t, *J* = 6.6 Hz, 3H). ¹³C NMR (75

MHz, CDCl₃) δ 171.22, 170.40, 164.69, 147.69, 128.97, 128.66, 127.66, 96.17, 81.61,

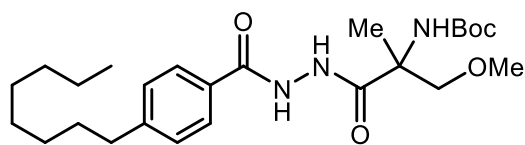
60.49, 36.03, 32.02, 31.31, 29.58, 29.38, 28.46, 22.80, 21.11, 14.32, 14.24.



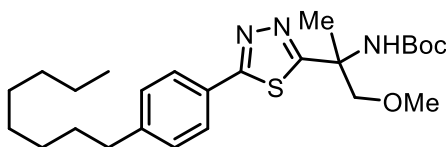
Tert-butyl (R)-2,2,4-trimethyl-4-(5-(4-octylphenyl)-1,3,4-thiadiazol-2-yl)oxazolidine-3-carboxylate (37c). General procedure O was used to convert 37b to the title product in 10% yield. ¹H NMR (600 MHz, Chloroform-d) δ 7.04 (s, 2H), 6.76 (s, 2H), 4.08 (s, 1H), 3.96 (s, 1H), 2.38 (t, J = 30.9 Hz, 2H), 1.79 (s, 2H), 1.68 (s, 6H), 1.57 – 1.49 (m, 3H), 1.45 (s, 9H), 1.34 – 1.23 (m, 10H), 0.89 (t, J = 7.0 Hz, 3H). ¹³C NMR (151 MHz, CDCl₃) δ 163.64, 160.07, 139.63, 99.99, 54.47, 48.07, 31.92, 29.70, 29.68, 29.67, 29.66, 29.62, 29.57, 29.36, 29.32, 22.69, 14.13.



(R)-2-amino-2-(5-(4-octylphenyl)-1,3,4-thiadiazol-2-yl)propan-1-ol (37d). General procedure P was used to convert 37c to the title product in 22% yield. ¹H NMR (600 MHz, Methanol-d₄) δ 8.30 – 8.26 (m, 2H), 7.98 – 7.92 (m, 2H), 5.49 – 5.44 (m, 1H), 3.64 – 3.57 (m, 1H), 3.53 – 3.46 (m, 1H), 2.20 (t, J = 3.9 Hz, 2H), 1.57 – 1.48 (m, 2H), 1.46 (s, 3H), 1.37 – 1.26 (m, 10H), 0.92 (t, J = 7.1 Hz, 3H). ¹³C NMR (151 MHz, MeOD) δ 174.69, 174.27, 148.81, 140.67, 119.48, 114.32, 90.48, 84.62, 83.46, 82.10, 35.32, 31.70, 29.43, 29.41, 29.10, 27.39, 26.19, 24.25, 22.37, 13.12.

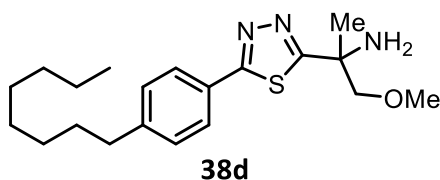
**38a**

Tert-butyl (3-methoxy-2-methyl-1-(2-(4-octylbenzoyl)hydrazinyl)-1-oxopropan-2-yl)carbamate (38a). *N*-[(1,1-dimethylethoxy)carbonyl]-2-methyl-serine (0.64 mmol) was dissolved in THF (0.15 M); NMM (1.0 eq.) was added, then BCF (1.0 eq.) was added and the solution stirred for 0.5 h. Next, 32d (2.0 eq.) was added and the solution stirred for 2 h. The reaction mixture was filtered and the filtrate diluted with EtOAc. This was washed 3 times with water and once with brine, dried over Na₂SO₄, and purified by flash chromatography to afford the title product in 39% yield. *R*_f = 0.48, 40% EtOAc/Hexanes. ¹H NMR (800 MHz, Chloroform-*d*) δ 9.72 (s, 1H), 9.49 (s, 1H), 7.75 (d, *J* = 7.7 Hz, 2H), 7.19 (d, *J* = 7.7 Hz, 2H), 5.53 (s, 1H), 3.78 (s, 1H), 3.67 (d, *J* = 9.1 Hz, 1H), 3.43 (s, 3H), 2.61 (t, *J* = 7.6 Hz, 2H), 1.59 (s, 5H), 1.44 (s, 9H), 1.33 – 1.22 (m, 10H), 0.88 (t, *J* = 7.0 Hz, 3H). ¹³C NMR (201 MHz, CDCl₃) δ 170.57, 164.34, 154.90, 147.58, 128.87, 128.56, 127.36, 59.37, 35.88, 31.85, 31.12, 29.40, 29.21, 28.30, 22.64, 14.09.

**38b**

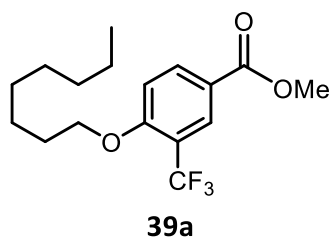
Tert-butyl (1-methoxy-2-(5-(4-octylphenyl)-1,3,4-thiadiazol-2-yl)propan-2-yl)carbamate (38b). General procedure O was used to convert 38a to the title product in

32% yield. R_f = 0.56, 25% EtOAc/Hexanes. ^1H NMR (800 MHz, Chloroform- d) δ 7.86 (d, J = 7.7 Hz, 2H), 7.28 (d, J = 7.6 Hz, 2H), 5.78 (s, 1H), 3.85 (s, 1H), 3.77 – 3.65 (m, 1H), 3.40 (s, 3H), 2.67 (t, J = 7.6 Hz, 2H), 1.91 (s, 3H), 1.72 – 1.61 (m, 2H), 1.45 (s, 9H), 1.39 – 1.22 (m, 10H), 0.90 (t, J = 6.9 Hz, 3H). ^{13}C NMR (201 MHz, CDCl_3) δ 174.18, 169.36, 154.51, 146.33, 129.15, 129.05, 127.82, 127.78, 59.37, 59.30, 57.71, 35.88, 31.87, 29.44, 29.25, 29.24, 28.36, 28.32, 23.59, 23.48, 14.15.

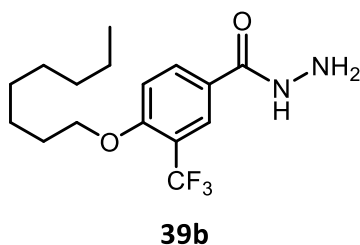


1-methoxy-2-(5-(4-octylphenyl)-1,3,4-thiadiazol-2-yl)propan-2-amine (38d).

General procedure P was used to convert 38b to the title product in 75% yield. R_f = 0.70, 20% MeOH/EtOAc. ^1H NMR (800 MHz, Methanol- d_4) δ 7.87 (d, J = 8.1 Hz, 2H), 7.37 (d, J = 8.0 Hz, 2H), 3.74 (d, J = 9.0 Hz, 1H), 3.58 (d, J = 9.0 Hz, 1H), 3.41 (s, 3H), 3.34 (s, 2H), 2.71 (t, J = 7.7 Hz, 2H), 1.68 (h, J = 6.9, 6.5 Hz, 2H), 1.61 (s, 3H), 1.41 – 1.27 (m, 10H), 0.92 (t, J = 7.1 Hz, 3H). ^{13}C NMR (201 MHz, MeOD) δ 177.98, 169.80, 146.69, 129.13, 129.01, 127.37, 127.31, 80.17, 58.14, 55.85, 35.37, 31.63, 31.02, 29.15, 28.99, 28.93, 25.07, 22.32, 13.09.

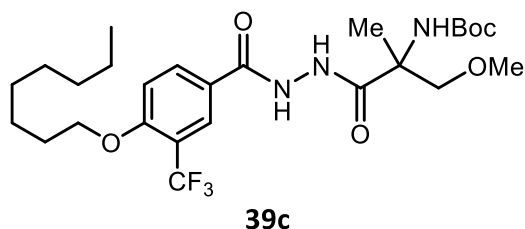


Methyl 4-(octyloxy)-3-(trifluoromethyl)benzoate (39a). 4-hydroxy-3-(trifluoromethyl)-methyl benzoate (4.5 mmol) was added to a suspension of K_2CO_3 (2.0 eq.) in acetonitrile (0.14 M) and stirred for 0.5 h. 1-bromooctane was added (1.0 eq.) and the solution stirred for 12 h. The reaction was then filtered and the filtrate concentrated. The residue was taken up in EtOAc, washed with H_2O and brine, dried over Na_2SO_4 , and concentrated to afford the title product in 83% yield. 1H NMR (598 MHz, Chloroform- d) δ 8.33 – 8.10 (m, 2H), 7.03 (dt, J = 18.0, 8.1 Hz, 1H), 4.13 (qd, J = 12.2, 7.2, 6.7 Hz, 2H), 3.98 – 3.86 (m, 3H), 1.92 – 1.76 (m, 2H), 1.59 – 1.43 (m, 2H), 1.31 (s, 8H), 0.97 – 0.82 (m, 3H). ^{13}C NMR (150 MHz, $cdCl_3$) δ 165.84, 160.61, 135.02, 128.99, 121.77, 112.17, 69.13, 52.12, 31.75, 29.15, 28.84, 28.82, 25.73, 22.63, 14.05.

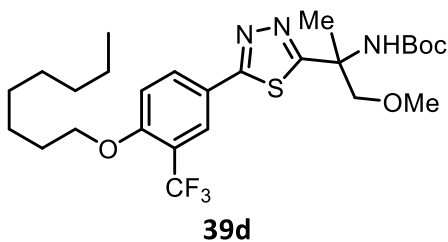


4-(octyloxy)-3-(trifluoromethyl)benzohydrazide (39b). General procedure J was used to afford the title product in 84% yield. 1H NMR (800 MHz, Chloroform- d) δ 8.09 (s, 1H), 8.02 (d, J = 8.6 Hz, 1H), 7.76 (s, 2H), 7.11 (d, J = 8.7 Hz, 2H), 4.18 (t, J = 6.3 Hz, 2H), 1.92 (p, J = 6.5 Hz, 2H), 1.57 (p, J = 7.4 Hz, 2H), 1.47 – 1.33 (m, 8H), 0.98 (t, J = 6.7 Hz,

3H). ¹³C NMR (201 MHz, CDCl₃) δ 167.29, 159.82, 132.32, 132.27, 126.16, 124.00, 112.64, 112.52, 69.14, 31.75, 29.16, 28.84, 22.65, 14.05.

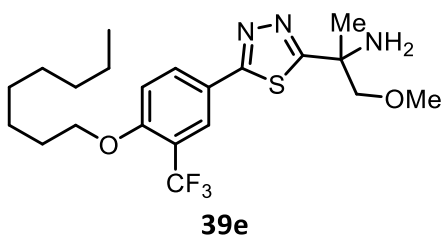


Tert-butyl (3-methoxy-2-methyl-1-(2-(4-(octyloxy)-3-(trifluoromethyl)benzoyl)hydrazinyl)-1-oxopropan-2-yl)carbamate (39c). General procedure R was used to couple 39b to *N*-[(1,1-dimethylethoxy)carbonyl]-2-methylserine to afford the title product in 60% yield. ¹H NMR (800 MHz, Chloroform-*d*) δ 10.25 (s, 1H), 9.63 (s, 1H), 8.15 (s, 1H), 8.03 (d, *J* = 8.3 Hz, 1H), 6.94 (d, *J* = 8.8 Hz, 1H), 5.64 (s, 1H), 4.08 (t, *J* = 6.3 Hz, 2H), 3.85 (s, 1H), 3.74 (d, *J* = 9.2 Hz, 1H), 3.48 (s, 3H), 1.86 (p, *J* = 6.5 Hz, 2H), 1.66 (s, 3H), 1.50 (d, *J* = 27.5 Hz, 11H), 1.43 – 1.29 (m, 8H), 0.94 (t, *J* = 7.0 Hz, 3H). ¹³C NMR (201 MHz, CDCl₃) δ 172.28, 163.57, 159.77, 154.84, 132.58, 127.22, 122.80, 112.14, 68.96, 59.28, 31.71, 29.12, 29.11, 28.79, 28.22, 25.68, 22.59, 14.02.

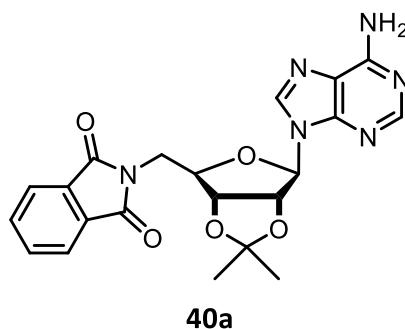


Tert-butyl (1-methoxy-2-(5-(4-(octyloxy)-3-(trifluoromethyl)phenyl)-1,3,4-thiadiazol-2-yl)propan-2-yl)carbamate (39d). General procedure O was used to convert 39c to the title product in 71% yield. ¹H NMR (598 MHz, Chloroform-*d*) δ 8.11 – 8.01 (m,

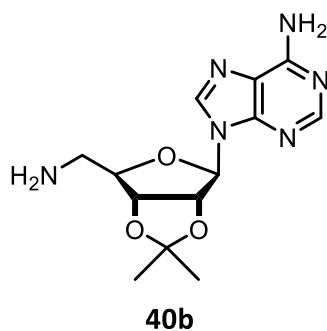
2H), 7.07 – 6.94 (m, 1H), 5.72 (s, 1H), 4.11 – 4.05 (m, 2H), 3.84 (s, 3H), 3.78 (s, 1H), 3.67 (d, J = 9.0 Hz, 1H), 1.86 (s, 3H), 1.81 (dt, J = 14.5, 6.4 Hz, 2H), 1.46 (dt, J = 15.3, 7.3 Hz, 2H), 1.40 (s, 9H), 1.35 – 1.20 (m, 8H), 0.89 – 0.83 (m, 3H). ¹³C NMR (150 MHz, CDCl₃) δ 174.35, 167.69, 164.15, 158.93, 154.46, 134.41, 134.01, 132.52, 126.85, 122.24, 114.05, 113.12, 78.16, 69.08, 60.31, 59.27, 57.65, 55.52, 31.70, 29.11, 28.83, 28.27, 25.70, 23.44, 22.58, 14.02.



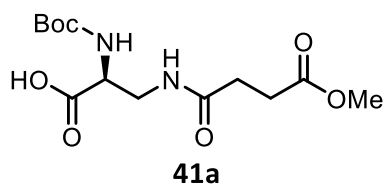
1-methoxy-2-(5-(4-(octyloxy)-3-(trifluoromethyl)phenyl)-1,3,4-thiadiazol-2-yl)propan-2-amine (39e). General procedure P was used to convert 39d to the title product in 67% yield. ¹H NMR (800 MHz, Chloroform-d) δ 8.12 (d, J = 2.1 Hz, 1H), 8.08 (dd, J = 8.7, 2.2 Hz, 1H), 7.06 (d, J = 8.7 Hz, 1H), 4.11 (t, J = 6.3 Hz, 2H), 3.77 (d, J = 9.0 Hz, 1H), 3.55 (d, J = 9.1 Hz, 1H), 3.40 (s, 3H), 2.13 (s, 2H), 1.88 – 1.82 (m, 2H), 1.54 (s, 3H), 1.49 (dt, J = 15.2, 7.4 Hz, 2H), 1.39 – 1.24 (m, 8H), 0.89 (t, J = 7.1 Hz, 3H). ¹³C NMR (201 MHz, CDCl₃) δ 178.12, 167.73, 158.90, 132.40, 126.92, 122.57, 113.28, 113.12, 80.77, 69.18, 59.30, 56.32, 31.73, 29.14, 28.91, 28.72, 27.04, 26.94, 25.75, 13.95.



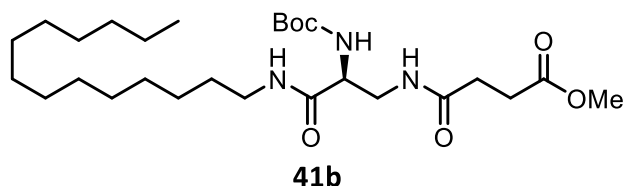
2-(((4R,6R)-6-(6-amino-9H-purin-9-yl)-2,2-dimethyltetrahydrofuro[3,4-d][1,3]dioxol-4-yl)methyl)isoindoline-1,3-dione (40a). Acetonide-protected adenosine (12.5 mmol), phthalimide (12.9 mmol), and triphenylphosphine (12.5 mmol) were dissolved in THF (0.3 M). DIAD (12.5 mmol) was added dropwise, and the solution turned orange in color. The reaction mixture stirred for 2.5 h at rt, then was filtered. The solids were washed with dry Et₂O (140 mL), then collected and dried under vacuum to afford the product in 75% yield. ¹H NMR (600 MHz, Methanol-d₄) δ 8.24 (s, 1H), 7.96 (s, 1H), 7.80 – 7.77 (m, 4H), 6.20 (d, J = 1.6 Hz, 1H), 5.58 (dd, J = 6.3, 1.7 Hz, 1H), 5.30 (dd, J = 6.2, 3.7 Hz, 1H), 4.90 (s, 2H), 4.52 (td, J = 6.0, 3.7 Hz, 1H), 4.00 (dd, J = 6.0, 4.5 Hz, 2H), 1.59 (s, 3H), 1.40 (s, 3H). ¹³C NMR (151 MHz, MeOD) δ 170.69, 158.30, 154.89, 151.25, 143.44, 136.49, 134.25, 125.22, 121.77, 116.59, 92.56, 87.45, 86.46, 84.80, 41.63, 28.53, 26.66.



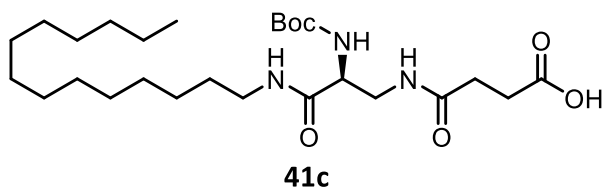
9-((4R,6R)-6-(aminomethyl)-2,2-dimethyltetrahydrofuro[3,4-d][1,3]dioxol-4-yl)-9H-purin-6-amine (40b). Compound 40a (9.43 mmol) was dissolved in EtOH (0.033 M) and hydrazine monohydrate (150 mmol) was added. The solution refluxed overnight, then was cooled and filtered, and the filtrate concentrated. The residue was dissolved in water and acidified to pH = 4 using glacial AcOH, then filtered and the filtrate collected. The pH was increased to 10 using 3 M NaOH, then extracted 4 times using DCM. The organics were dried over Na₂SO₄ and then concentrated to afford the title product in 72% yield. ¹H NMR (600 MHz, Methanol-d₄) δ 8.30 (s, 1H), 8.24 (s, 1H), 6.17 (d, J = 3.1 Hz, 1H), 5.50 (dd, J = 6.4, 3.1 Hz, 1H), 5.03 (dd, J = 6.4, 3.4 Hz, 1H), 4.86 (s, 2H), 4.25 (td, J = 5.7, 5.3, 3.5 Hz, 1H), 2.91 (dd, J = 5.7, 2.8 Hz, 2H), 1.62 (s, 3H), 1.41 (s, 3H). ¹³C NMR (151 MHz, MeOD) δ 158.54, 155.08, 151.44, 143.07, 121.82, 116.78, 92.71, 89.61, 85.99, 84.37, 45.73, 28.61, 26.68.



(S)-2-((tert-butoxycarbonyl)amino)-3-(4-methoxy-4-oxobutanamido)propanoic acid (41a). General procedure T was used to couple (2S)-3-amino-2-[(tert-butoxycarbonyl)amino]propanoic acid and methyl 4-chloro-4-oxobutyrates to afford the title product.

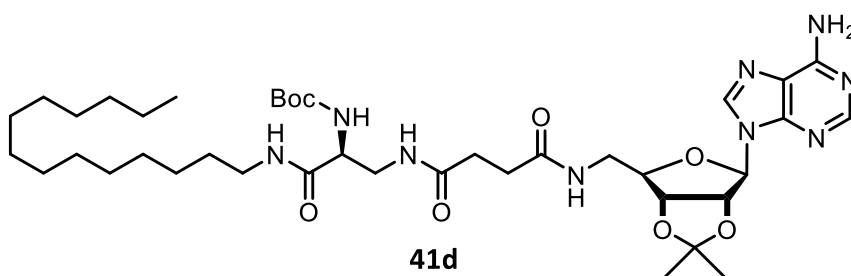


Methyl (S)-4-((2-((tert-butoxycarbonyl)amino)-3-oxo-3-(tetradecylamino)propyl)amino)-4-oxobutanoate (41b). General procedure R was used to couple tetradecylamine and 41a to afford the title product in 17% yield. $R_f = 0.61$, 5% MeOH/EtOAc. ^1H NMR (600 MHz, Methanol- d_4) δ 8.17 – 8.11 (m, 1H), 8.00 (s, 2H), 3.80 (d, $J = 6.7$ Hz, 2H), 3.70 (s, 3H), 3.26 – 3.15 (m, 2H), 2.73 – 2.69 (m, 1H), 2.64 (dt, $J = 9.7$, 6.9 Hz, 2H), 2.51 (dt, $J = 9.1$, 7.0 Hz, 2H), 1.57 – 1.50 (m, 2H), 1.47 (s, 9H), 1.39 – 1.27 (m, 22H), 0.93 (t, $J = 7.0$ Hz, 3H). ^{13}C NMR (151 MHz, MeOD) δ 178.29, 173.40, 172.76, 169.30, 100.02, 79.45, 79.38, 50.89, 50.81, 31.74, 29.47, 29.14, 27.72, 27.35, 27.30, 26.63, 22.40, 13.15.



(S)-4-((2-((tert-butoxycarbonyl)amino)-3-oxo-3-

(tetradecylamino)propyl)amino)-4-oxobutanoic acid (41c). General procedure S was used to convert 41b to the title product in 93% yield. R_f = 0.45, 5% MeOH/EtOAc. ^1H NMR (600 MHz, Methanol- d_4) δ 8.12 (s, 1H), 8.04 (s, 1H), 7.98 (s, 1H), 4.91 (s, 1H), 3.50 (dd, J = 13.8, 5.0 Hz, 2H), 3.22 – 3.14 (m, 2H), 2.63 – 2.58 (m, 2H), 2.50 – 2.44 (m, 2H), 1.50 (dd, J = 15.4, 8.6 Hz, 2H), 1.45 (s, 9H), 1.37 – 1.25 (m, 22H), 0.91 (t, J = 7.0 Hz, 3H). ^{13}C NMR (151 MHz, MeOD) δ 177.29, 176.54, 176.29, 175.46, 173.85, 158.71, 81.92, 50.59, 43.38, 41.78, 41.65, 34.24, 32.60, 31.97, 31.95, 31.93, 31.91, 31.88, 31.64, 31.52, 31.33, 29.86, 29.12, 24.90, 21.94, 15.65.



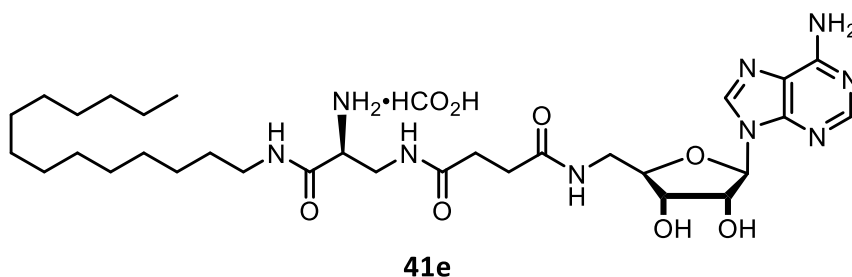
Tert-butyl

((2S)-3-(4-((((4R,6R)-6-(6-amino-9H-purin-9-yl)-2,2-

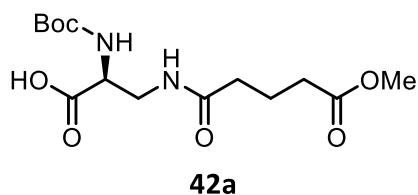
dimethyltetrahydrofuro[3,4-d][1,3]dioxol-4-yl)methyl)amino)-4-oxobutanamido)-1-

oxo-1-(tetradecylamino)propan-2-yl)carbamate (41d). General procedure R was used to

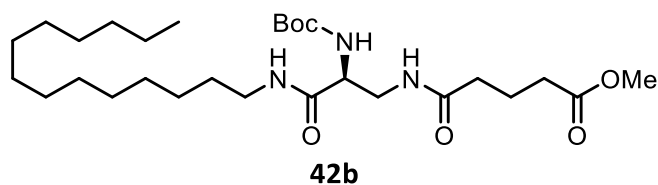
couple 40b and 41c to afford the title product 42% yield. R_f = 0.63, 20% MeOH/EtOAc.



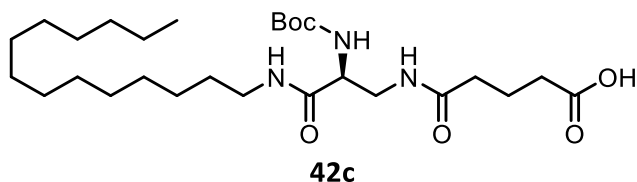
N1-((S)-2-amino-3-oxo-3-(tetradecylamino)propyl)-N4-(((2R,5R)-5-(6-amino-9H-purin-9-yl)-3,4-dihydroxytetrahydrofuran-2-yl)methyl)succinamide methanoic acid (41e). General procedure P was used to convert 41d to the title product in 34% yield. R_f = 0.40, 20% MeOH/EtOAc. ^1H NMR (800 MHz, DMSO- d_6) δ 7.91 (d, J = 6.7 Hz, 1H), 7.43 (d, J = 7.0 Hz, 1H), 3.72 (d, J = 8.9 Hz, 1H), 3.55 (d, J = 8.9 Hz, 1H), 3.40 – 3.39 (m, 8H), 3.37 – 3.35 (m, 2H), 2.71 (t, J = 7.5 Hz, 2H), 2.59 – 2.56 (m, 3H), 1.70 – 1.63 (m, 2H), 1.55 – 1.51 (m, 2H), 1.40 – 1.27 (m, 20H), 0.93 (t, J = 6.8 Hz, 3H). ^{13}C NMR (201 MHz, DMSO) δ 180.08, 168.61, 146.18, 129.74, 128.03, 127.80, 80.99, 59.29, 56.37, 40.18, 35.40, 31.73, 31.10, 29.26, 29.10, 26.98, 22.54, 14.42.



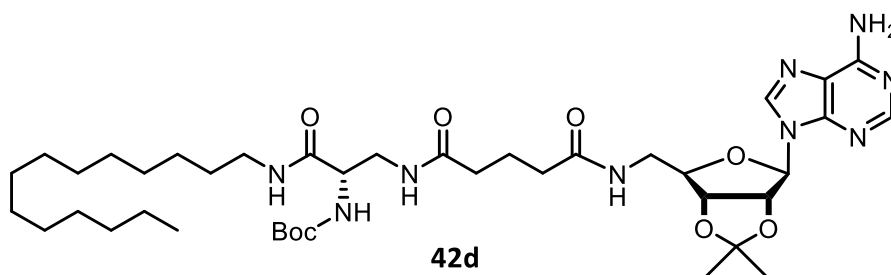
(S)-2-((tert-butoxycarbonyl)amino)-3-(5-methoxy-5-oxopentanamido)propanoic acid (42a). General procedure T was used to couple (2S)-3-amino-2-[(tert-butoxycarbonyl)amino]propanoic acid and glutaric acid monomethyl ester chloride to afford the title product.



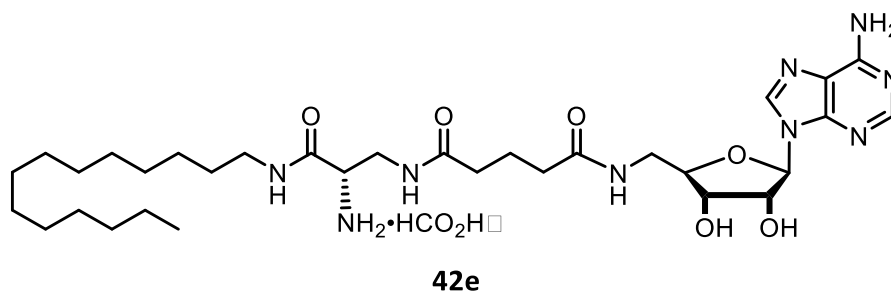
Methyl (S)-5-((2-((tert-butoxycarbonyl)amino)-3-oxo-3-(tetradecylamino)propyl)amino)-5-oxopentanoate (42b). General procedure R was used to couple tetradecylamine and 42a to afford the title product in 32% yield. R_f = 0.63, 5% MeOH/EtOAc.



(S)-5-((2-((tert-butoxycarbonyl)amino)-3-oxo-3-(tetradecylamino)propyl)amino)-5-oxopentanoic acid (42c). General procedure S was used to convert 42b to the title product in 74% yield. R_f = 0.48, 5% MeOH/EtOAc. ^1H NMR (600 MHz, Methanol- d_4) δ 4.15 (s, 1H), 3.46 (d, J = 11.2 Hz, 2H), 3.38 (s, 1H), 3.21 – 3.12 (m, 2H), 2.31 (t, J = 7.0 Hz, 2H), 2.23 (d, J = 6.7 Hz, 2H), 1.90 – 1.83 (m, 2H), 1.47 (d, J = 16.9 Hz, 2H), 1.42 (s, 9H), 1.34 – 1.25 (m, 22H), 0.88 (t, J = 7.0 Hz, 3H). ^{13}C NMR (151 MHz, MeOD) δ 179.99, 177.85, 158.71, 81.96, 57.57, 43.34, 41.62, 37.15, 35.20, 34.22, 31.95, 31.94, 31.92, 31.89, 31.87, 31.63, 31.50, 29.84, 29.09, 24.89, 23.32, 15.63.

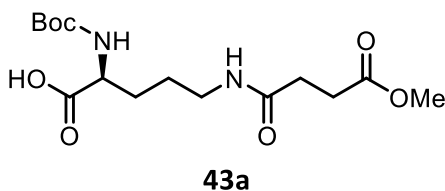


Tert-butyl ((2S)-3-(5-(((4R,6R)-6-(6-amino-9H-purin-9-yl)-2,2-dimethyltetrahydrofuro[3,4-d][1,3]dioxol-4-yl)methyl)amino)-5-oxopentanamido)-1-oxo-1-(tetradecylamino)propan-2-yl)carbamate (42d). General procedure R was used to couple 40b and 42c to afford the title product in 49% yield. $R_f = 0.69$, 20% MeOH/EtOAc.

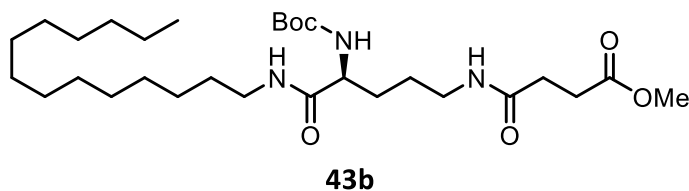


N1-((S)-2-amino-3-oxo-3-(tetradecylamino)propyl)-N5-(((2R,5R)-5-(6-amino-9H-purin-9-yl)-3,4-dihydroxytetrahydrofuran-2-yl)methyl)glutaramide methanoic acid (42e). General procedure P was used to convert 42d to the title product in 28% yield. ^1H NMR (800 MHz, DMSO- d_6) δ 8.46 – 8.23 (m, 2H), 7.43 (s, 2H), 5.93 (s, 1H), 5.82 – 4.98 (m, 3H), 4.86 – 4.67 (m, 1H), 4.09 (d, $J = 61.2$ Hz, 2H), 3.61 – 3.38 (m, 3H), 3.22 – 3.06 (m, 2H), 2.20 (d, $J = 36.7$ Hz, 4H), 1.88 – 1.76 (m, 2H), 1.52 – 1.40 (m, 2H), 1.37 – 1.22 (m, 22H), 0.97 – 0.86 (m, 3H). ^{13}C NMR (201 MHz, DMSO) δ 173.29, 172.56, 169.54, 169.27, 167.82, 156.65, 152.97, 149.65, 140.99, 120.02, 88.64, 88.23, 84.31, 83.92, 73.13, 73.00,

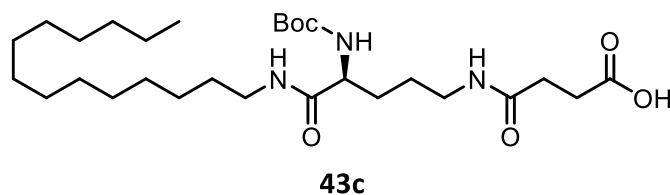
71.90, 71.52, 53.05, 41.39, 40.24, 35.21, 31.75, 29.52, 29.48, 29.22, 29.17, 26.82, 22.55, 21.66, 14.35.



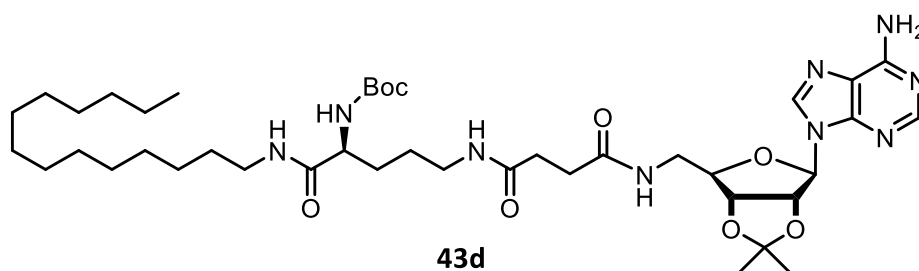
(S)-2-((tert-butoxycarbonyl)amino)-5-(4-methoxy-4-oxobutanamido)pentanoic acid (43a). General procedure T was used to couple N^2 -[(1,1-dimethylethoxy)carbonyl]-L-ornithine and methyl 4-chloro-4-oxobutyrates to afford the title product.



Methyl (S)-4-((4-((tert-butoxycarbonyl)amino)-5-oxo-5-(tetradecylamino)pentyl)amino)-4-oxobutanoate (43b). General procedure R was used to couple tetradecylamine and 43a to afford the title product in 22% yield. R_f = 0.53, 5% MeOH/EtOAc. ^1H NMR (600 MHz, Methanol- d_4) δ 7.99 (s, 1H), 7.86 (s, 1H), 4.00 – 3.95 (m, 1H), 3.65 (s, 1H), 3.64 (s, 3H), 3.21 – 3.10 (m, 2H), 2.59 (t, J = 6.9 Hz, 2H), 2.57 (s, 1H), 2.45 (t, J = 6.9 Hz, 2H), 1.69 (d, J = 8.3 Hz, 2H), 1.60 – 1.52 (m, 2H), 1.51 – 1.45 (m, 2H), 1.44 (s, 9H), 1.34 – 1.22 (m, 22H), 0.88 (t, J = 7.0 Hz, 3H). ^{13}C NMR (151 MHz, MeOD) δ 176.99, 176.10, 175.88, 175.34, 81.63, 57.27, 56.69, 53.87, 53.49, 53.33, 52.93, 41.66, 41.01, 34.27, 32.58, 32.00, 31.98, 31.93, 31.85, 31.69, 31.61, 31.36, 30.94, 30.88, 30.07, 29.85, 24.95, 15.75.

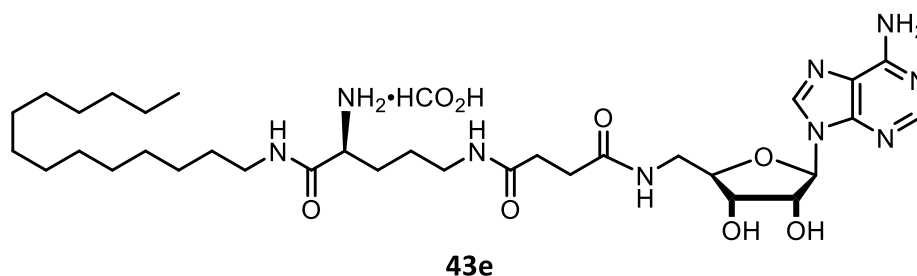


(S)-4-((4-((tert-butoxycarbonyl)amino)-5-oxo-5-(tetradecylamino)pentyl)amino)-4-oxobutanoic acid (43c). General procedure S was used to convert 43b to the title product in 85% yield. R_f = 0.57, MeOH/EtOAc. ^1H NMR (600 MHz, Methanol- d_4) δ 4.02 (s, 2H), 3.38 (s, 1H), 3.27 – 3.15 (m, 2H), 2.62 (t, J = 7.7 Hz, 2H), 2.59 (s, 1H), 2.48 (t, J = 6.7 Hz, 2H), 1.75 (s, 2H), 1.65 – 1.57 (m, 2H), 1.56 – 1.49 (m, 2H), 1.46 (s, 9H), 1.38 – 1.28 (m, 22H), 0.92 (t, J = 7.0 Hz, 3H). ^{13}C NMR (151 MHz, MeOD) δ 174.73, 173.72, 156.37, 124.71, 79.17, 54.45, 39.02, 38.48, 31.74, 30.23, 29.48, 29.46, 29.44, 29.42, 29.39, 29.15, 29.13, 29.05, 28.97, 28.47, 27.41, 26.60, 25.60, 22.41, 19.48, 13.18.



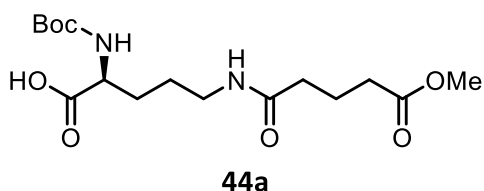
Tert-butyl ((2S)-5-(4-(((4R,6R)-6-(6-amino-9H-purin-9-yl)-2,2-dimethyltetrahydrofuro[3,4-d][1,3]dioxol-4-yl)methyl)amino)-4-oxobutanamido)-1-oxo-1-(tetradecylamino)pentan-2-yl)carbamate (43d). General procedure R was used to couple 40b and 43c to afford the title product in 20% yield. R_f = 0.53, 20% MeOH/EtOAc. ^1H NMR (600 MHz, Methanol- d_4) δ 8.34 (s, 1H), 8.30 (s, 1H), 6.13 (d, J = 3.4 Hz, 1H),

5.45 (dd, $J = 6.2, 3.6$ Hz, 1H), 4.97 (dd, $J = 6.2, 2.9$ Hz, 1H), 4.40 – 4.33 (m, 1H), 4.06 – 3.99 (m, 1H), 3.73 (dd, $J = 14.0, 4.6$ Hz, 1H), 3.41 (dd, $J = 13.9, 4.1$ Hz, 1H), 3.25 – 3.19 (m, 2H), 3.19 – 3.12 (m, 2H), 2.67 – 2.44 (m, 2H), 1.73 (d, $J = 8.7$ Hz, 2H), 1.62 (s, 3H), 1.53 – 1.47 (m, 2H), 1.45 (s, 9H), 1.39 (s, 3H), 1.29 (s, 22H), 0.92 (t, $J = 7.0$ Hz, 3H). ^{13}C NMR (151 MHz, MeOD) δ 173.66, 173.55, 173.12, 156.38, 156.12, 152.64, 148.79, 140.71, 119.49, 114.34, 90.63, 84.32, 83.26, 81.86, 79.15, 54.49, 40.80, 38.99, 38.46, 31.70, 30.83, 30.66, 29.51, 29.44, 29.41, 29.37, 29.35, 29.11, 29.09, 29.04, 27.38, 26.57, 26.24, 25.67, 24.28, 22.37, 13.13.

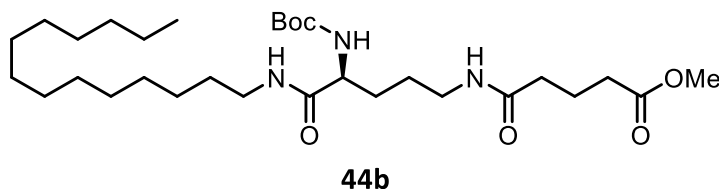


N1-((S)-4-amino-5-oxo-5-(tetradecylamino)pentyl)-N4-(((2R,5R)-5-(6-amino-9H-purin-9-yl)-3,4-dihydroxytetrahydrofuran-2-yl)methyl)succinamide methanoic acid (43e). General procedure P was used to convert 43d to the title product in 39% yield. ^1H NMR (800 MHz, DMSO- d_6) δ 8.35 (s, 1H), 8.29 (s, 3H), 8.20 (s, 1H), 7.99 – 7.92 (m, 0H), 7.35 (s, 1H), 7.12 (s, 1H), 5.85 (d, $J = 6.3$ Hz, 1H), 4.69 – 4.67 (m, 1H), 4.06 – 4.03 (m, 1H), 3.99 – 3.95 (m, 2H), 3.57 (s, 1H), 3.47 (dt, $J = 12.4, 6.4$ Hz, 1H), 3.36 – 3.31 (m, 1H), 3.14 – 3.05 (m, 2H), 3.05 – 3.00 (m, 2H), 2.43 – 2.36 (m, 2H), 2.33 (t, $J = 7.4$ Hz, 2H), 1.64 (s, 2H), 1.60 (s, 2H), 1.41 (s, 2H), 1.24 (d, $J = 4.2$ Hz, 20H), 0.86 (t, $J = 7.0, 4.0$ Hz, 3H). ^{13}C NMR (201 MHz, DMSO) δ 172.15, 171.79, 156.64, 153.00, 149.61, 140.98, 140.80,

140.79, 119.95, 99.99, 88.16, 84.35, 73.12, 72.99, 71.87, 71.44, 52.88, 39.08, 38.40, 31.22, 29.53, 29.48, 29.36, 29.18, 26.82, 25.44, 22.56, 14.38.

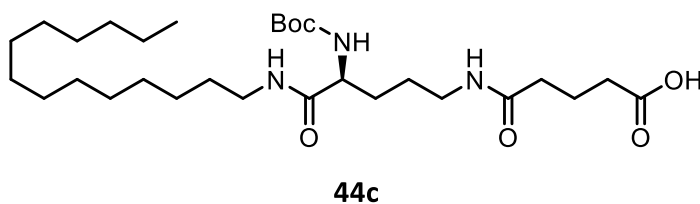


(S)-2-((tert-butoxycarbonyl)amino)-5-(5-methoxy-5-oxopentanamido)pentanoic acid (44a). General procedure T was used to couple N^2 -[(1,1-dimethylethoxy)carbonyl]-L-ornithine and glutaric acid monomethyl ester chloride to afford the title product.



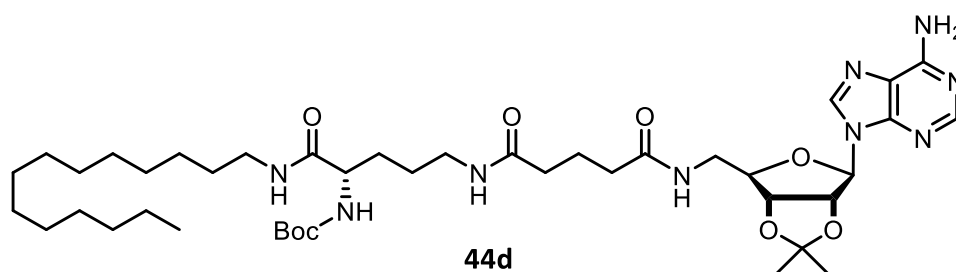
Methyl

(S)-5-((4-((tert-butoxycarbonyl)amino)-5-oxopentyl)amino)-5-oxopentanoate (44b). General procedure R was used to couple tetradecylamine and 44a to afford the title product in 35% yield. R_f = 0.42, 5% MeOH/EtOAc. ^1H NMR (600 MHz, Methanol- d_4) δ 8.01 – 7.96 (m, 1H), 7.92 – 7.86 (m, 1H), 3.64 (s, 3H), 3.22 – 3.10 (m, 5H), 2.33 (t, J = 7.4 Hz, 2H), 2.20 (t, J = 7.4 Hz, 2H), 1.92 – 1.84 (m, 2H), 1.75 – 1.65 (m, 2H), 1.61 – 1.52 (m, 4H), 1.52 – 1.45 (m, 4H), 1.42 (s, 9H), 1.34 – 1.24 (m, 18H), 0.88 (t, J = 7.0 Hz, 3H). ^{13}C NMR (151 MHz, MeOD) δ 176.25, 176.17, 176.04, 158.80, 81.60, 57.26, 56.68, 53.72, 53.34, 53.17, 52.79, 41.65, 41.00, 37.18, 35.15, 34.28, 32.24, 32.01, 31.99, 31.94, 31.70, 31.62, 29.86, 24.95, 23.39, 15.76.



(S)-5-((4-((tert-butoxycarbonyl)amino)-5-oxo-5-

(tetradecylamino)pentyl)amino)-5-oxopentanoic acid (44c). General procedure S was used to convert 44b to the title product in 82% yield. ¹H NMR (600 MHz, Methanol-d₄) δ 7.99 (s, 1H), 7.89 (s, 1H), 3.98 (s, 1H), 3.22 – 3.10 (m, 5H), 2.31 (t, J = 7.6 Hz, 2H), 2.22 (t, J = 7.4 Hz, 2H), 1.87 (p, J = 7.3 Hz, 2H), 1.70 (s, 2H), 1.61 – 1.53 (m, 4H), 1.52 – 1.46 (m, 4H), 1.42 (s, 9H), 1.27 (s, 18H), 0.88 (t, J = 7.0 Hz, 3H). ¹³C NMR (151 MHz, MeOD) δ 175.30, 173.93, 173.49, 156.32, 100.25, 79.14, 54.44, 48.59, 39.04, 38.50, 34.78, 32.80, 31.77, 29.59, 29.52, 29.50, 29.48, 29.46, 29.43, 29.19, 29.17, 29.08, 27.48, 26.64, 25.63, 22.44, 20.96, 13.26.



Tert-butyl

((2S)-5-(5-((((4R,6R)-6-(6-amino-9H-purin-9-yl)-2,2-

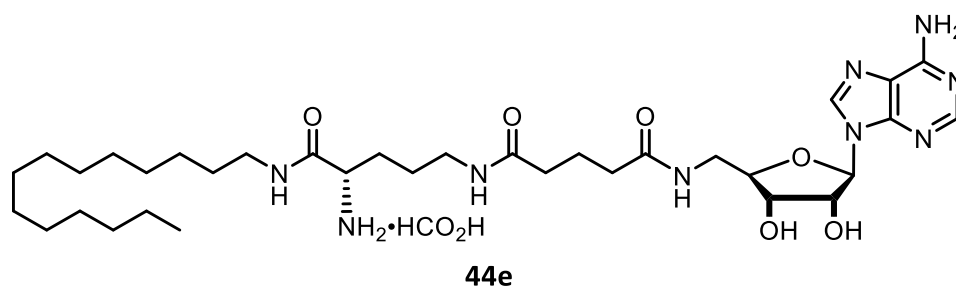
dimethyltetrahydrofuro[3,4-d][1,3]dioxol-4-yl)methyl)amino)-5-oxopentanamido)-1-

oxo-1-(tetradecylamino)pentan-2-yl)carbamate (44d). General procedure R was used to

couple 40b and 44c to afford the title product in 55% yield. R_f = 0.66, 20% MeOH/EtOAc.

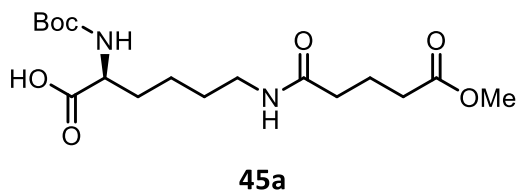
¹H NMR (600 MHz, Methanol-d₄) δ 8.30 (s, 1H), 8.27 (s, 1H), 6.16 (d, J = 2.9 Hz, 1H),

5.46 (dd, $J = 6.1, 3.0$ Hz, 1H), 4.99 (dd, $J = 6.2, 3.1$ Hz, 1H), 4.41 – 4.33 (m, 1H), 4.08 – 4.00 (m, 1H), 3.64 (dd, $J = 14.0, 5.6$ Hz, 1H), 3.47 (dd, $J = 14.0, 5.0$ Hz, 1H), 3.26 – 3.13 (m, 5H), 2.35 – 2.26 (m, 2H), 2.22 (t, $J = 7.3$ Hz, 2H), 1.92 (p, $J = 7.3$ Hz, 2H), 1.75 (s, 2H), 1.60 (d, $J = 11.3$ Hz, 3H), 1.50 (d, $J = 6.8$ Hz, 4H), 1.46 (d, $J = 6.7$ Hz, 9H), 1.39 (s, 3H), 1.29 (s, 18H), 0.92 (t, $J = 7.0$ Hz, 3H). ^{13}C NMR (151 MHz, MeOD) δ 174.21, 173.86, 173.48, 156.10, 152.63, 148.77, 140.66, 119.50, 114.32, 90.57, 84.52, 83.40, 82.05, 79.15, 40.90, 38.98, 38.48, 34.79, 34.71, 31.71, 29.44, 29.42, 29.40, 29.38, 29.35, 29.12, 29.09, 27.38, 26.58, 26.21, 25.64, 24.25, 22.38, 21.73, 13.13.



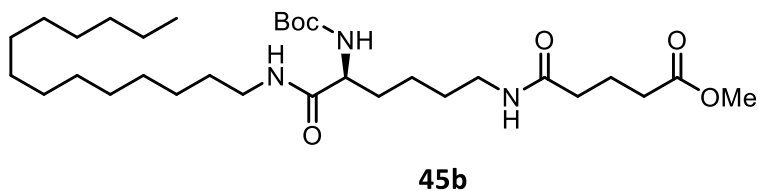
N1-((S)-4-amino-5-oxo-5-(tetradecylamino)pentyl)-N5-(((2R,5R)-5-(6-amino-9H-purin-9-yl)-3,4-dihydroxytetrahydrofuran-2-yl)methyl)glutaramide methanoic acid (44e). General procedure P was used to convert 44d to the title product in 32% yield. ^1H NMR (800 MHz, DMSO- d_6) δ 8.36 (s, 1H), 8.27 (s, 1H), 8.19 (s, 1H), 7.90 (s, 1H), 7.37 (s, 1H), 5.85 (d, $J = 6.0$ Hz, 1H), 4.74 – 4.65 (m, 1H), 4.04 (s, 1H), 3.99 – 3.96 (m, 1H), 3.68 (s, 1H), 3.50 – 3.44 (m, 1H), 3.37 – 3.32 (m, 1H), 3.13 (dd, $J = 12.9, 6.2$ Hz, 1H), 3.07 (dd, $J = 12.5, 6.0$ Hz, 1H), 3.05 – 3.00 (m, 5H), 2.15 (t, $J = 6.9$ Hz, 2H), 2.06 (t, $J = 7.3$ Hz, 2H), 1.77 – 1.70 (m, 2H), 1.65 (s, 2H), 1.41 (s, 4H), 1.23 (s, 18H), 0.85 (t, $J = 7.1$ Hz, 3H). ^{13}C NMR (201 MHz, DMSO) δ 172.51, 172.32, 168.88, 156.65, 152.97, 149.63, 140.96, 120.07,

88.61, 84.34, 73.10, 72.95, 71.89, 71.54, 52.59, 39.16, 38.26, 35.30, 31.75, 29.52, 29.47, 29.46, 29.32, 29.27, 29.21, 29.17, 29.08, 26.80, 25.38, 22.55, 21.99, 14.35.



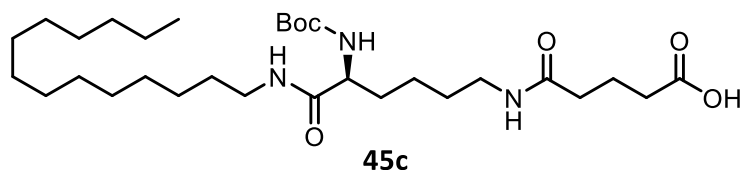
N2-(tert-butoxycarbonyl)-N6-(5-methoxy-5-oxopentanoyl)-L-lysine (45a).

General procedure T was used to couple N^2 -[(1,1-dimethylethoxy)carbonyl]-L-Lysine and and glutaric acid monomethyl ester chloride to afford the title product.

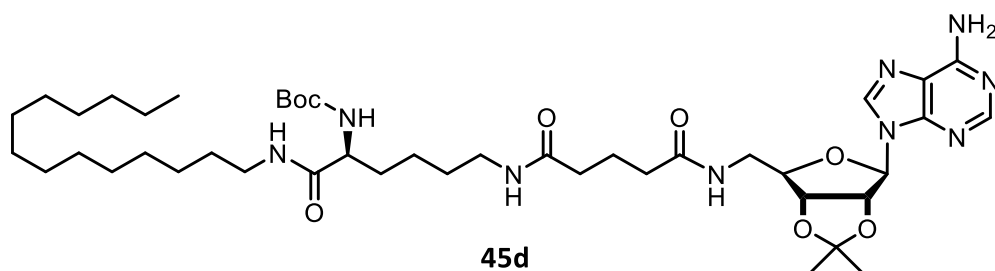


Methyl (S)-5-((5-((tert-butoxycarbonyl)amino)-6-oxo-6-

(tetradecylamino)hexyl)amino)-5-oxopentanoate (45b). General procedure R was used to couple tetradecylamine and 45a to afford the title product in 31% yield. R_f = 0.46, 5% MeOH/EtOAc. ^1H NMR (600 MHz, Chloroform- d) δ 6.90 (s, 1H), 6.58 (s, 1H), 5.65 – 5.59 (m, 1H), 4.06 – 3.96 (m, 2H), 3.59 (s, 3H), 3.18 – 3.08 (m, 5H), 2.29 (t, J = 7.3 Hz, 2H), 2.16 (t, J = 7.4 Hz, 2H), 1.91 – 1.84 (m, 2H), 1.76 – 1.67 (m, 2H), 1.62 – 1.53 (m, 2H), 1.49 – 1.38 (m, 4H), 1.35 (s, 9H), 1.31 – 1.27 (m, 2H), 1.26 – 1.12 (m, 18H), 0.80 (t, J = 7.0 Hz, 3H). ^{13}C NMR (151 MHz, CDCl_3) δ 173.62, 172.45, 172.23, 155.86, 79.54, 54.34, 51.48, 50.16, 39.44, 38.83, 35.25, 33.11, 31.84, 29.62, 29.61, 29.59, 29.57, 29.56, 29.51, 29.45, 29.28, 29.06, 28.27, 26.87, 22.60, 20.90, 14.05.

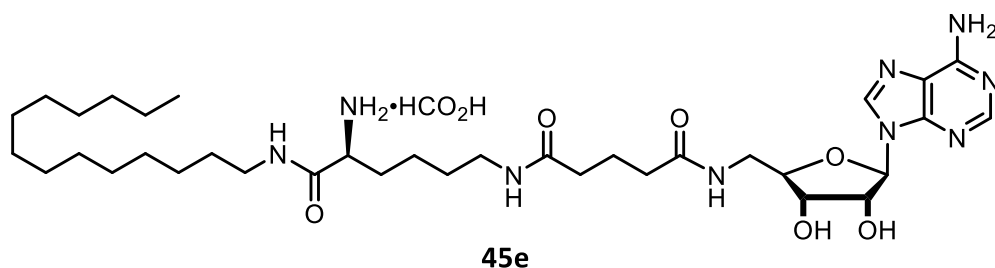


(S)-5-((5-((tert-butoxycarbonyl)amino)-6-oxo-6-(tetradecylamino)hexyl)amino)-5-oxopentanoic acid (45c). General procedure S was used to convert 45b to the title product in 84% yield. R_f = 0.48, 5% MeOH/EtOAc. ^1H NMR (600 MHz, Chloroform- d) δ 7.19 (s, 1H), 7.06 (s, 1H), 5.93 (s, 1H), 4.17 – 4.06 (m, 1H), 3.21 (s, 5H), 2.39 (s, 2H), 2.31 (s, 2H), 2.10 – 2.03 (m, 4H), 1.96 (s, 2H), 1.76 (s, 2H), 1.64 (s, 2H), 1.49 (s, 2H), 1.41 (s, 9H), 1.34 – 1.17 (m, 18H), 0.92 – 0.83 (m, 3H). ^{13}C NMR (151 MHz, CDCl_3) δ 178.61, 177.02, 175.97, 173.68, 158.55, 82.23, 62.86, 56.96, 42.08, 41.47, 37.63, 35.65, 34.35, 32.13, 32.08, 32.03, 31.79, 31.31, 30.76, 29.35, 25.11, 23.43, 16.59.



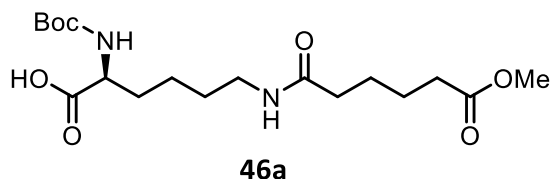
Tert-butyl ((2S)-6-(5-((((4R,6R)-6-(6-amino-9H-purin-9-yl)-2,2-dimethyltetrahydrofuro[3,4-d][1,3]dioxol-4-yl)methyl)amino)-5-oxopentanamido)-1-oxo-1-(tetradecylamino)hexan-2-yl)carbamate (45d). General procedure R was used to couple 40b and 45c to afford the title product in 16% yield. R_f = 0.40, 20% MeOH/EtOAc. ^1H NMR (600 MHz, Chloroform- d) δ 8.37 (s, 1H), 8.34 (s, 1H), 7.96 (s, 1H), 7.22 (s, 1H), 7.03 (s, 1H), 6.71 (s, 1H), 6.34 (d, J = 7.8 Hz, 1H), 5.92 (d, J = 4.1 Hz, 1H), 5.35 – 5.31 (m,

1H), 4.87 (dd, J = 6.2, 2.0 Hz, 1H), 4.51 – 4.47 (m, 1H), 4.14 (dd, J = 12.6, 5.5 Hz, 1H), 4.08 – 4.01 (m, 1H), 3.33 (d, J = 13.6 Hz, 2H), 3.27 – 3.15 (m, 5H), 2.50 – 2.42 (m, 1H), 2.42 – 2.34 (m, 1H), 2.29 (t, J = 8.5 Hz, 2H), 2.03 (t, J = 6.3 Hz, 2H), 1.84 – 1.76 (m, 2H), 1.70 – 1.64 (m, 2H), 1.62 (s, 3H), 1.55 – 1.45 (m, 4H), 1.42 (s, 9H), 1.36 (s, 3H), 1.31 – 1.21 (m, 18H), 0.88 (t, J = 7.0 Hz, 3H). ¹³C NMR (151 MHz, CDCl₃) δ 175.89, 175.17, 173.67, 158.78, 158.59, 155.29, 151.21, 142.71, 123.14, 117.16, 94.54, 86.10, 85.10, 83.94, 82.08, 71.82, 62.87, 57.05, 52.60, 43.50, 42.00, 41.51, 37.86, 37.68, 34.48, 34.36, 33.30, 32.14, 32.13, 32.11, 32.10, 32.07, 32.03, 31.95, 31.80, 31.78, 31.63, 30.83, 29.91, 29.39, 27.78, 25.55, 25.13, 24.11, 23.51, 21.48, 16.59.



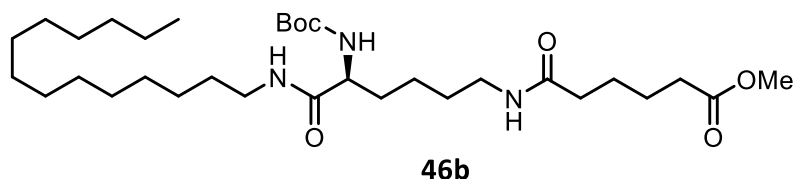
N1-((S)-5-amino-6-oxo-6-(tetradecylamino)hexyl)-N5-(((2R,5R)-5-(6-amino-9H-purin-9-yl)-3,4-dihydroxytetrahydrofuran-2-yl)methyl)glutaramide methanoic acid (45e). General procedure P was used to convert 45d to the title product in 29% yield. R_f = 0.23, 100% MeOH. ¹H NMR (800 MHz, DMSO-d₆) δ 8.35 (s, 1H), 8.33 – 8.27 (m, 2H), 8.18 (s, 1H), 8.11 (d, J = 11.4 Hz, 1H), 7.82 (t, J = 5.1 Hz, 1H), 7.36 (s, 1H), 7.14 (s, 1H), 5.85 (d, J = 6.4 Hz, 1H), 4.68 (t, J = 5.6 Hz, 1H), 4.04 (dd, J = 4.9, 3.1 Hz, 1H), 3.99 – 3.97 (m, 1H), 3.59 (s, 1H), 3.50 – 3.45 (m, 1H), 3.37 – 3.32 (m, 1H), 3.16 – 3.11 (m, 1H), 3.08 – 3.03 (m, 1H), 3.03 – 2.97 (m, 5H), 2.14 (t, J = 7.7 Hz, 1H), 2.07 (t, J = 7.2 Hz, 2H), 1.76 –

1.71 (m, 2H), 1.65 (s, 2H), 1.45 – 1.34 (m, 4H), 1.23 (s, 18H), 0.86 – 0.84 (m, 3H). ¹³C NMR (201 MHz, DMSO) δ 172.51, 172.06, 169.72, 156.64, 155.51, 152.88, 149.57, 141.02, 140.86, 140.09, 120.02, 88.57, 84.36, 72.96, 71.52, 39.08, 38.60, 35.27, 31.76, 29.52, 29.48, 29.31, 29.17, 29.12, 26.81, 22.56, 21.95, 14.36.



N2-(tert-butoxycarbonyl)-N6-(6-methoxy-6-oxohexanoyl)-L-lysine (46a).

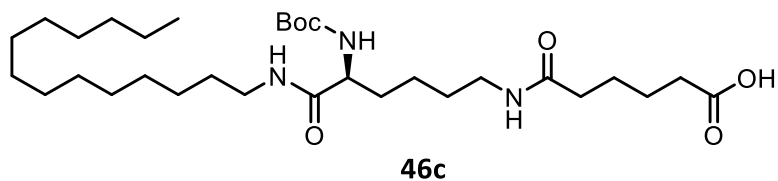
General procedure T was used to couple *N*²-[(1,1-dimethylethoxy)carbonyl]-L-Lysine and 5-(methoxycarbonyl)pentanoyl chloride to afford the title product.



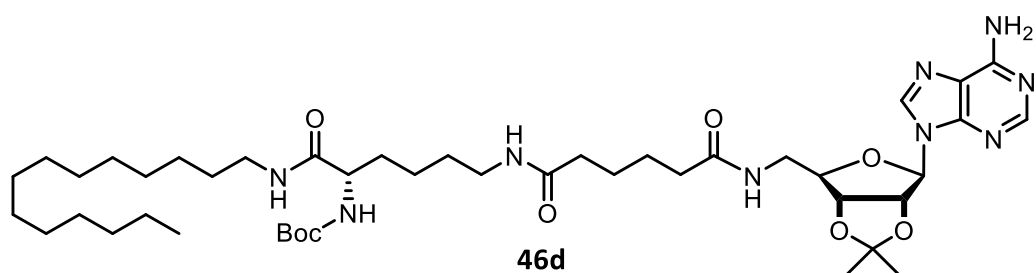
Methyl (S)-6-((5-((tert-butoxycarbonyl)amino)-6-oxo-6-

(tetradecylamino)hexyl)amino)-6-oxohexanoate (46b). General procedure R was used to couple tetradecylamine and 46a to afford the title product in 14% yield. *R*_f = 0.36, 5% MeOH/EtOAc. ¹H NMR (600 MHz, Chloroform-*d*) δ 6.87 (s, 1H), 6.54 (s, 1H), 5.57 (t, *J* = 7.2 Hz, 1H), 4.00 (d, *J* = 5.7 Hz, 1H), 3.40 (s, 3H), 3.22 – 3.12 (m, 5H), 2.29 (t, *J* = 6.6 Hz, 2H), 2.15 (t, *J* = 5.7 Hz, 2H), 1.78 – 1.69 (m, 2H), 1.65 – 1.55 (m, *J* = 5.4, 4.1 Hz, 2H), 1.49 – 1.43 (m, 4H), 1.38 (s, 9H), 1.34 – 1.29 (m, 4H), 1.26 – 1.19 (m, 18H), 0.83 (t, *J* = 7.0 Hz, 3H). ¹³C NMR (151 MHz, CDCl₃) δ 174.06, 173.09, 172.32, 155.90, 79.71, 54.34, 51.52,

50.25, 39.50, 38.80, 36.04, 33.61, 31.86, 29.64, 29.63, 29.61, 29.60, 29.57, 29.52, 29.41, 29.30, 29.28, 28.94, 28.28, 26.87, 25.10, 24.36, 22.71, 22.63, 14.07.

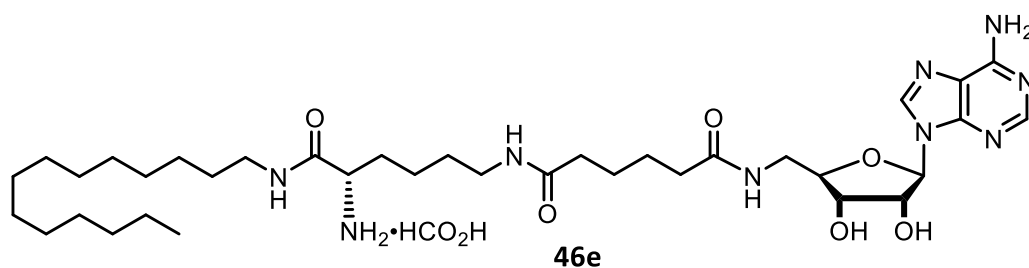


(S)-6-((5-((tert-butoxycarbonyl)amino)-6-oxo-6-(tetradecylamino)hexyl)amino)-6-oxohexanoic acid (46c). General procedure S was used to convert 46b to the title product in 82% yield. R_f = 0.51, 5% MeOH/EtOAc. ^1H NMR (600 MHz, Chloroform- d) δ 7.01 (s, 1H), 6.79 (s, 1H), 5.80 (s, 1H), 4.10 (s, 1H), 3.95 (s, 1H), 3.21 (s, 5H), 2.36 (s, 2H), 2.31 – 2.20 (m, 2H), 1.77 (s, 2H), 1.66 (s, 4H), 1.56 – 1.46 (m, 4H), 1.43 (s, 9H), 1.32 – 1.20 (m, 20H), 0.88 (t, J = 7.0 Hz, 3H). ^{13}C NMR (151 MHz, CDCl_3) δ 177.38, 176.18, 175.28, 158.59, 82.42, 56.99, 42.13, 41.50, 38.47, 36.17, 34.41, 32.19, 32.17, 32.16, 32.14, 32.12, 32.07, 31.85, 31.82, 31.35, 30.83, 29.39, 27.61, 26.81, 25.18, 23.45, 16.62.



Tert-butyl ((2S)-6-(6-((((4R,6R)-6-(6-amino-9H-purin-9-yl)-2,2-dimethyltetrahydrofuro[3,4-d][1,3]dioxol-4-yl)methyl)amino)-6-oxohexanamido)-1-oxo-1-(tetradecylamino)hexan-2-yl)carbamate (46d). General procedure R was used to couple 40b and 46c to afford the title product in 34% yield. R_f = 0.42, 20% MeOH/EtOAc.

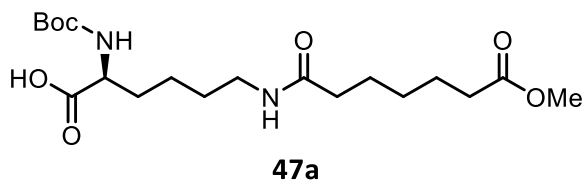
¹H NMR (600 MHz, Chloroform-d) δ 8.33 (s, 1H), 8.21 (s, 1H), 7.92 (s, 1H), 6.91 (s, 1H), 6.68 (s, 1H), 6.26 (s, 1H), 6.18 – 6.11 (m, 1H), 5.87 (d, J = 3.8 Hz, 1H), 5.28 (s, 1H), 4.86 – 4.82 (m, 1H), 4.49 (s, 1H), 4.11 (s, 1H), 3.48 (s, 1H), 3.31 (d, J = 14.3 Hz, 2H), 3.23 (s, 5H), 2.44 – 2.33 (m, 2H), 2.21 (t, J = 9.2 Hz, 2H), 1.72 (s, 2H), 1.62 (s, 3H), 1.55 – 1.47 (m, 4H), 1.43 (s, 9H), 1.35 (s, 2H), 1.25 (s, 24H), 0.88 (t, J = 6.8 Hz, 3H). ¹³C NMR (151 MHz, CDCl₃) δ 176.13, 175.36, 175.06, 158.64, 155.01, 151.31, 142.93, 123.43, 117.31, 94.76, 86.07, 85.04, 83.88, 82.22, 57.03, 53.01, 43.48, 42.07, 41.39, 38.67, 34.42, 32.20, 32.19, 32.16, 32.13, 32.08, 32.02, 31.87, 31.83, 30.89, 30.00, 29.43, 27.81, 25.20, 16.65.



N1-((S)-5-amino-6-oxo-6-(tetradecylamino)hexyl)-N6-(((2R,5R)-5-(6-amino-9H-purin-9-yl)-3,4-dihydroxytetrahydrofuran-2-yl)methyl)adipamide methanoic acid (46e).

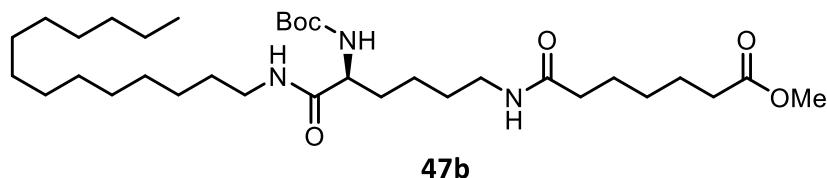
General procedure P was used to convert 46d to the title product in 22% yield. R_f = 0.24, 100% MeOH. ¹H NMR (800 MHz, DMSO-d₆) δ 8.34 (d, J = 15.1 Hz, 1H), 8.31 – 8.22 (m, 2H), 8.19 (d, J = 12.4 Hz, 1H), 8.11 (d, J = 11.4 Hz, 1H), 7.78 (d, J = 23.7 Hz, 1H), 7.35 (s, 1H), 7.12 (s, 1H), 5.85 (d, J = 6.3 Hz, 1H), 4.71 – 4.66 (m, 1H), 4.29 – 4.23 (m, 1H), 4.04 (s, 1H), 3.87 (s, 1H), 3.47 – 3.43 (m, 1H), 3.38 – 3.34 (m, 1H), 3.24 – 3.20 (m, 1H), 3.17 – 3.10 (m, 1H), 3.09 – 3.03 (m, 2H), 3.03 – 2.97 (m, 5H), 2.23 – 2.16 (m, 2H), 2.14 (d, J = 5.0

Hz, 2H), 2.10 – 2.01 (m, 4H), 1.64 (s, 2H), 1.53 – 1.43 (m, 2H), 1.43 – 1.34 (m, 4H), 1.23 (s, 20H), 0.88 – 0.83 (m, 3H).



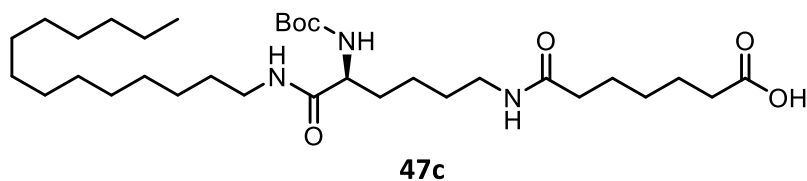
N2-(tert-butoxycarbonyl)-N6-(7-methoxy-7-oxoheptanoyl)-L-lysine (47a).

General procedure T was used to couple N^2 -[(1,1-dimethylethoxy)carbonyl]-L-Lysine and 6-(Methoxycarbonyl)hexanoyl chloride to afford the title product.

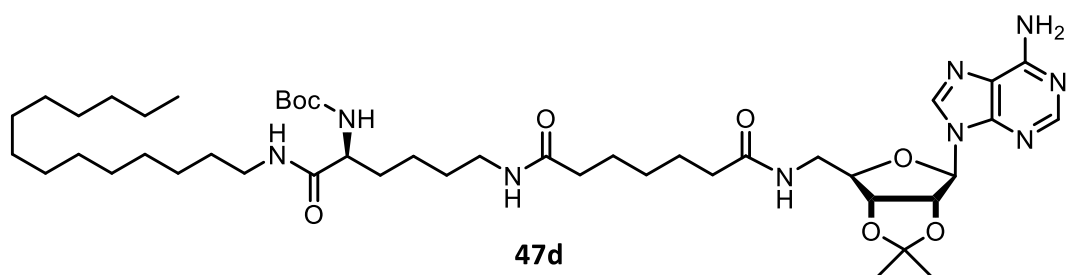


Methyl (S)-7-((5-((tert-butoxycarbonyl)amino)-6-oxo-6-

(tetradecylamino)hexyl)amino)-7-oxoheptanoate (47b). General procedure R was used to couple tetradecylamine and 47a to afford the title product in 30% yield. R_f = 0.69, 5% MeOH/EtOAc. ^1H NMR (600 MHz, Chloroform- d) δ 7.13 (s, 1H), 6.78 (s, 1H), 5.80 (s, 1H), 4.12 (s, 3H), 3.29 – 3.14 (m, 5H), 2.30 (t, J = 5.0 Hz, 2H), 2.19 (t, J = 7.4 Hz, 2H), 1.79 (s, 2H), 1.71 – 1.60 (m, 6H), 1.57 – 1.46 (m, 6H), 1.44 (s, 9H), 1.39 – 1.33 (m, 2H), 1.32 – 1.21 (m, 20H), 0.88 (t, J = 7.0 Hz, 3H). ^{13}C NMR (151 MHz, CDCl_3) δ 176.02, 175.69, 174.79, 158.30, 81.85, 62.59, 56.84, 41.90, 41.33, 38.65, 36.49, 34.70, 34.30, 32.08, 32.07, 32.06, 32.03, 31.99, 31.93, 31.76, 31.74, 31.58, 31.14, 30.75, 29.36, 27.85, 27.02, 25.28, 25.06, 16.62, 16.50.

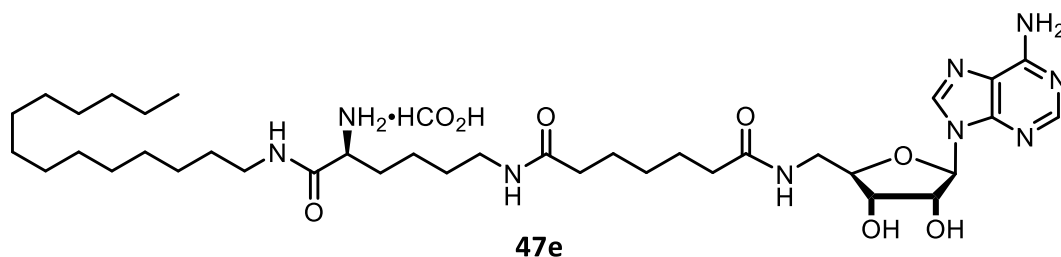


(S)-7-((5-((tert-butoxycarbonyl)amino)-6-oxo-6-(tetradecylamino)hexyl)amino)-7-oxoheptanoic acid (47c). General procedure S was used to convert 47b to the title product in 15% yield. R_f = 0.33, 5% MeOH/EtOAc. ^1H NMR (600 MHz, Chloroform- d) δ 6.93 (s, 1H), 6.33 (s, 1H), 5.70 (s, 1H), 4.12 (d, J = 7.0 Hz, 2H), 3.23 (s, 5H), 2.35 (s, 2H), 2.22 (s, 2H), 1.79 (s, 2H), 1.66 (s, 4H), 1.49 (s, 6H), 1.43 (s, 9H), 1.33 – 1.18 (m, 22H), 0.88 (t, J = 6.8 Hz, 3H). ^{13}C NMR (151 MHz, CDCl_3) δ 176.89, 174.85, 173.71, 172.69, 156.16, 80.14, 39.64, 38.93, 36.46, 33.90, 31.95, 29.70, 29.69, 29.66, 29.64, 29.59, 29.37, 29.33, 28.42, 28.31, 26.90, 22.69, 14.14.



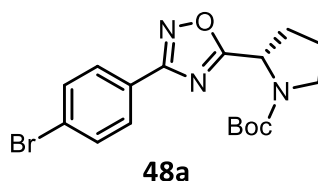
Tert-butyl ((2S)-6-(7-((((4R,6R)-6-(6-amino-9H-purin-9-yl)-2,2-dimethyltetrahydrofuro[3,4-d][1,3]dioxol-4-yl)methyl)amino)-7-oxoheptanamido)-1-oxo-1-(tetradecylamino)hexan-2-yl)carbamate (47d). General procedure R was used to couple **40b** and **47c** to afford the title product in 20% yield. R_f = 0.42, 20% MeOH/EtOAc. ^1H NMR (600 MHz, Methanol- d_4) δ 8.33 – 8.31 (m, 1H), 8.29 (s, 1H), 8.27 (s, 1H), 7.97 – 7.93 (m, 2H), 6.75 (d, J = 7.8 Hz, 1H), 6.16 (d, J = 3.0 Hz, 1H), 5.47 (dd, J = 6.3, 3.0 Hz, 1H),

5.00 (dd, $J = 6.3, 3.2$ Hz, 1H), 4.37 – 4.33 (m, 1H), 3.97 (d, $J = 6.1$ Hz, 1H), 3.59 (dd, $J = 14.0, 6.0$ Hz, 1H), 3.52 – 3.46 (m, 1H), 3.24 (dt, $J = 12.9, 6.4$ Hz, 1H), 3.17 (q, $J = 6.8$ Hz, 4H), 2.25 (t, $J = 7.6$ Hz, 2H), 2.18 (t, $J = 7.5$ Hz, 2H), 1.78 – 1.70 (m, 2H), 1.65 (dd, $J = 14.8, 7.2$ Hz, 4H), 1.62 (s, 3H), 1.52 (dq, $J = 13.0, 6.7$ Hz, 6H), 1.46 (s, 9H), 1.39 (s, 3H), 1.35 – 1.29 (m, 22H), 0.92 (t, $J = 6.9$ Hz, 3H). ^{13}C NMR (151 MHz, MeOD) δ 174.95, 174.65, 174.56, 173.70, 156.37, 156.09, 152.64, 152.51, 148.78, 140.73, 140.59, 119.46, 114.29, 90.80, 90.19, 84.73, 83.40, 82.11, 79.12, 38.96, 35.43, 31.70, 29.62, 29.41, 29.39, 29.35, 29.11, 28.68, 28.35, 27.45, 26.50, 25.17, 24.10, 22.37, 13.08.

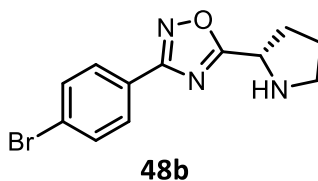


N1-((S)-5-amino-6-oxo-6-(tetradecylamino)hexyl)-N7-(((2R,5R)-5-(6-amino-9H-purin-9-yl)-3,4-dihydroxytetrahydrofuran-2-yl)methyl)heptanediamide methanoic acid (47e). General procedure P was used to convert **47d** to the title product in 40% yield. $R_f = 0.58$, 100% MeOH. ^1H NMR (600 MHz, DMSO- d_6) δ 8.35 (s, 1H), 8.28 – 8.23 (m, 1H), 8.17 (s, 1H), 8.12 (s, 1H), 7.78 (t, $J = 5.3$ Hz, 2H), 7.37 (s, 2H), 7.14 (s, 1H), 5.85 (d, $J = 6.3$ Hz, 1H), 4.72 – 4.66 (m, 1H), 4.07 – 4.03 (m, 1H), 3.97 (s, 1H), 3.51 – 3.42 (m, 1H), 3.36 (dt, $J = 13.9, 4.7$ Hz, 1H), 3.13 (dd, $J = 12.9, 6.3$ Hz, 1H), 3.09 – 2.95 (m, 5H), 2.13 (t, $J = 7.4$ Hz, 2H), 2.03 (t, $J = 7.1$ Hz, 2H), 1.68 – 1.54 (m, 4H), 1.49 (dq, $J = 15.6, 7.4$ Hz, 6H), 1.38 (dd, $J = 19.2, 12.2$ Hz, 6H), 1.30 – 1.19 (m, 18H), 0.86 (t, $J = 6.4$ Hz, 3H). ^{13}C NMR

(151 MHz, DMSO) δ 172.80, 172.40, 172.33, 156.65, 152.89, 152.80, 149.64, 140.86, 120.00, 88.29, 84.13, 73.04, 71.70, 41.35, 39.03, 38.62, 35.80, 35.74, 31.77, 29.54, 29.49, 29.38, 29.29, 29.19, 28.88, 28.74, 26.83, 25.62, 25.51, 22.58, 14.44.



Tert-butyl (S)-2-(3-(4-bromophenyl)-1,2,4-oxadiazol-5-yl)pyrrolidine-1-carboxylate (48a). 4-Bromobenzamidoxime (1.0 eq.), PyBOP (1.0 eq.), Boc-Proline (1.0 eq.), and DIEA (1.0 eq.) were dissolved in DMF (0.1 M) and the solution refluxed overnight. Then the solvent was evaporated; the residue was diluted in EtOAc and washed 3 times with 1 M HCl and once with brine; the organics dried over Na₂SO₄; and then purification by flash chromatography afforded the title product in 71% yield. R_f = 0.54, 20% EtOAc/Hex.



(S)-3-(4-bromophenyl)-5-(pyrrolidin-2-yl)-1,2,4-oxadiazole (48b). AcCl (5.0 eq.) was added to MeOH (0.5 M) and the solution stirred for ten minutes. **48a** (1.0 eq.) was added, transferred with additional MeOH, and the solution stirred at rt until complete by TLC analysis. The reaction was cooled to 0 degrees C and quenched with solid NaHCO₃, then filtered. The filtrate was concentrated and the residue taken up in EtOAc.

This was washed 3 times with 14 M NaOH and once with brine, and dried over Na₂SO₄.

The solvent was evaporated to afford the title product in 36% yield. R_f = 0.54, 50%

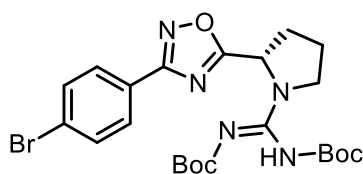
MeOH/EtOAc. ¹H NMR (598 MHz, cdcl₃) δ 7.97, 7.95, 7.95, 7.93, 7.62, 7.60, 5.19, 5.08,

5.06, 3.73, 3.71, 3.57, 3.56, 3.54, 3.53, 3.50, 2.42, 2.40, 2.40, 2.38, 2.16, 2.15, 2.07, 2.05,

2.05, 2.04, 2.03, 2.02, 1.99, 1.49, 1.47, 1.45, 1.39, 1.32, 1.31, 1.30, 1.29, 1.28, 1.27, 1.25,

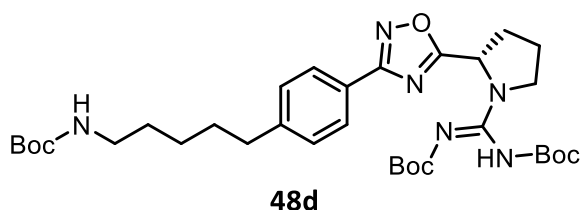
1.24, 1.23, 1.21. ¹³C NMR (150 MHz, cdcl₃) δ 167.61, 164.50, 132.18, 132.01, 128.91,

104.99, 80.48, 53.78, 46.33, 32.37.

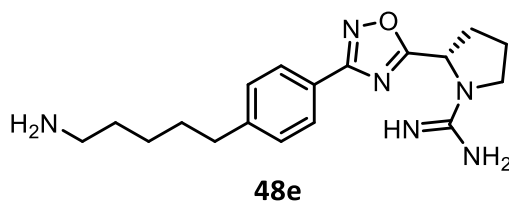


48c

Tert-butyl-((2-(3-(4-bromophenyl)-1,2,4-oxadiazol-5-yl)pyrrolidin-1-yl)((tert-butoxycarbonyl)amino)methylene)carbamate (48c). **48b** (1.0 eq.) and N,N'-Di-Boc-1H-pyrazole-1-carboxamidine (0.9 eq.) were dissolved in MeCN (0.2 M), then DIEA (3.0 eq.) was added and the solution stirred until complete by TLC (72 h). The reaction mixture was concentrated and immediately purified by flash chromatography to afford the title product in 80% yield. R_f = 0.54, 33% EtOAc/Hexanes. ¹H NMR (800 MHz, Methanol-d₄) δ 8.06 – 8.00 (m, 2H), 7.79 – 7.73 (m, 2H), 5.56 (s, 1H), 3.99 – 3.92 (m, 1H), 3.78 (s, 1H), 2.65 – 2.55 (m, 1H), 2.34 – 2.24 (m, 2H), 2.19 (dd, J = 12.8, 6.4 Hz, 2H), 1.55 (s, 18H). ¹³C NMR (201 MHz, MeOD) δ 182.71, 174.32, 170.26, 154.00, 134.75, 131.52, 128.46, 128.21, 57.74, 50.94, 33.88, 29.95, 26.54, 15.95.

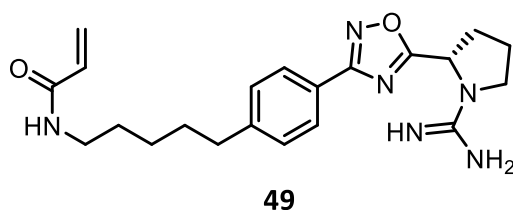


Tert-butyl-(((tert-butoxycarbonyl)amino)(2-(3-(4-(5-((tert-butoxycarbonyl)amino)pentyl)phenyl)-1,2,4-oxadiazol-5-yl)pyrrolidin-1-yl)methylene)carbamate (48d). General procedure C was used to couple **48c** and tert-butyl pent-4-enylcarbamate to afford the title product in 34% yield. $R_f = 0.33$, 75% EtOAc/Hexanes. ^1H NMR (800 MHz, Chloroform- d) δ 8.02 – 7.96 (m, 2H), 7.72 – 7.67 (m, 2H), 5.93 (s, 1H), 5.62 (s, 1H), 3.82 – 3.76 (m, 2H), 3.65 – 3.58 (m, 4H), 3.16 – 3.09 (m, 2H), 2.51 – 2.43 (m, 2H), 2.32 (s, 1H), 2.26 – 2.19 (m, 2H), 1.65 – 1.59 (m, 2H), 1.58 – 1.54 (m, 2H), 1.50 (s, 18H), 1.44 (s, 9H). ^{13}C NMR (201 MHz, CDCl_3) δ 179.56, 167.07, 162.45, 158.88, 156.53, 156.49, 131.63, 128.47, 125.28, 124.99, 78.48, 61.26, 53.70, 39.82, 31.45, 30.75, 29.00, 27.57, 27.44, 22.96, 22.41.



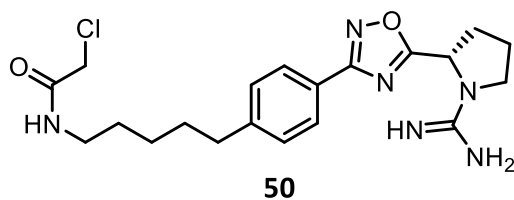
(S)-2-(3-(4-(5-aminopentyl)phenyl)-1,2,4-oxadiazol-5-yl)pyrrolidine-1-carboximidamide (48e). AcCl (10.0 eq.) was added to MeOH (0.25 M) and the solution stirred for ten minutes. **48d** (1.0 eq.) was added, transferred with additional MeOH, and the solution stirred at rt until complete by TLC analysis. The reaction was cooled to 0 degrees C and quenched with solid NaHCO_3 , then filtered. The filtrate was concentrated

and the residue taken up in DCM. This was washed 3 times with 3 M NaOH, once with water, and once with brine, and then dried over Na₂SO₄. The solvent was evaporated to afford the title product in 95% yield. ¹H NMR (598 MHz, Chloroform-d) δ 7.89 (s, 2H), 7.59 (s, 2H), 7.51 (d, J = 37.0 Hz, 2H), 5.33 (s, 2H), 5.16 (s, 3H), 3.65 (s, 2H), 3.54 (s, 1H), 2.37 (s, 2H), 2.15 (s, 2H), 1.25 (s, 6H), 0.94 – 0.79 (m, 2H). ¹³C NMR (150 MHz, cdcl₃) δ 179.59, 167.65, 132.14, 129.01, 127.72, 126.08, 125.28, 104.99, 54.40, 47.31, 33.69, 31.91, 31.20, 30.15, 29.69, 24.25, 22.67, 14.07.

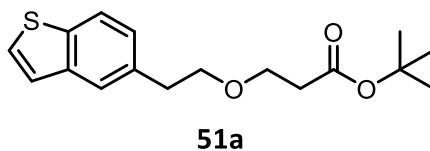


(S)-N-(5-(4-(5-(1-carbamimidoylpyrrolidin-2-yl)-1,2,4-oxadiazol-3-

yl)phenyl)pentyl)acrylamide (49). 48e (1.0 eq.) was dissolved in DCM (0.1 M), then DIEA (3.0 eq.) and acryloyl chloride (1.0 eq.) were added and the solution stirred at rt until complete by TLC. The reaction mixture was immediately purified by preparatory TLC to afford the title product 10% yield. R_f = 0.49, 100% EtOAc. ¹H NMR (800 MHz, DMSO-d₆) δ 9.53 (s, 3H), 8.05 – 7.97 (m, 2H), 7.86 (s, 2H), 7.65 (s, 1H), 6.06 – 5.85 (m, 2H), 5.48 (d, J = 45.8 Hz, 1H), 3.71 (s, 2H), 3.57 (s, 3H), 2.47 (s, 2H), 2.28 – 2.06 (m, 2H), 1.42 (d, J = 21.3 Hz, 2H), 1.32 (s, 4H), 0.93 (s, 2H).

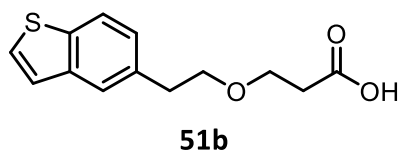


(S)-N-(5-(4-(5-(1-carbamimidoylpyrrolidin-2-yl)-1,2,4-oxadiazol-3-yl)phenyl)pentyl)-2-chloroacetamide (50). **48e** (1.0 eq.) was dissolved in DCM (0.1 M), then DIEA (3.0 eq.) and chloroacetyl chloride (1.0 eq.) were added and the solution stirred at rt until complete by TLC. The reaction mixture was immediately purified by preparatory TLC to afford the title product 24% yield. ¹H NMR (800 MHz, DMSO-*d*₆) δ 9.15 (s, 3H), 7.99 (d, *J* = 8.3 Hz, 2H), 7.86 – 7.84 (m, 2H), 5.47 (dd, *J* = 8.2, 3.6 Hz, 2H), 3.87 (d, *J* = 14.6 Hz, 1H), 3.79 (d, *J* = 13.6 Hz, 2H), 3.70 – 3.67 (m, 2H), 2.23 – 2.14 (m, 1H), 2.14 – 2.07 (m, 1H), 1.63 (s, 2H), 1.43 (s, 2H), 1.31 (s, 4H).

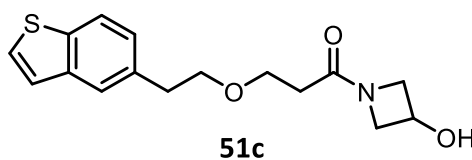


Tert-butyl 3-(2-(benzo[b]thiophen-5-yl)ethoxy)propanoate (51a). Benzo[b]thiophene-5-ethanol (1.0 eq.), *tert*-butyl acrylate (5.0 eq.), and Triton B (0.3 eq.) were dissolved in MeCN (0.2 M). The reaction stirred at rt until complete by TLC, then was immediately purified by preparatory TLC to afford the title product in 86% yield. *R*_f = 0.65, 20% EtOAc/Hexanes. ¹H NMR (598 MHz, Chloroform-*d*) δ 7.95 (d, *J* = 8.0 Hz, 1H), 7.86 (d, *J* = 7.9 Hz, 1H), 7.49 (td, *J* = 8.0, 7.6, 1.1 Hz, 1H), 7.46 – 7.43 (m, 1H), 7.18 (s, 1H), 3.96 (t, *J* = 6.7 Hz, 2H), 3.93 (t, *J* = 6.4 Hz, 2H), 3.35 (t, *J* = 6.6 Hz, 2H), 2.72 (t, *J* = 6.4 Hz,

2H), 1.64 (s, 9H). ¹³C NMR (150 MHz, cdcl₃) δ 170.88, 142.44, 140.02, 124.02, 123.50, 122.79, 122.03, 121.61, 70.99, 66.64, 36.30, 31.27, 28.08.

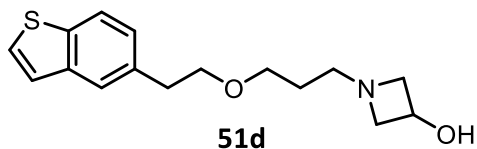


3-(2-(benzo[b]thiophen-5-yl)ethoxy)propanoic acid (51b). **51a** (1.0 eq.) was dissolved in DCM (0.2 M). TFA (3.0 eq.) was added and the mixture refluxed until complete by TLC. The reaction mixture was then directly purified by flash chromatography to afford the title product in quantitative yield. *R_f* = 0.47, 40% EtOAc/Hexanes. ¹H NMR (800 MHz, Methanol-*d*₄) δ 7.83 (d, *J* = 7.9 Hz, 1H), 7.75 (d, *J* = 7.9 Hz, 1H), 7.37 – 7.35 (m, 1H), 7.33 – 7.30 (m, 1H), 7.18 (d, *J* = 0.8 Hz, 1H), 3.83 (q, *J* = 6.2 Hz, 4H), 3.21 (t, *J* = 6.5 Hz, 2H), 2.64 (t, *J* = 6.8 Hz, 2H). ¹³C NMR (201 MHz, MeOD) δ 174.01, 142.41, 140.15, 139.60, 123.70, 123.21, 122.46, 121.40, 70.71, 66.18, 34.43, 30.66.



3-(2-(benzo[b]thiophen-5-yl)ethoxy)-1-(3-hydroxyazetidin-1-yl)propan-1-one (51c). General procedure B was used to couple **51b** and 4-hydroxyazetidine hydrochloride (1.5 eq.) to afford the title product in 88% yield. *R_f* = 0.33, 10% MeOH/EtOAc. ¹H NMR (800 MHz, Methanol-*d*₄) δ 7.83 (d, *J* = 8.0 Hz, 1H), 7.74 (d, *J* = 7.8 Hz, 1H), 7.35 (t, *J* = 7.5 Hz, 1H), 7.30 (t, *J* = 7.5 Hz, 1H), 7.13 (s, 1H), 5.03 (s, 1H), 4.36 –

4.30 (m, 2H), 4.14 (dd, $J = 10.5, 6.9$ Hz, 2H), 4.00 (dd, $J = 9.3, 4.2$ Hz, 1H), 3.79 (dd, $J = 10.6, 4.2$ Hz, 2H), 3.15 (t, $J = 6.2$ Hz, 2H), 2.44 – 2.29 (m, 4H). ^{13}C NMR (201 MHz, MeOD) δ 172.36, 142.77, 140.12, 123.77, 123.43, 122.62, 121.70, 121.60, 121.44, 117.31, 110.20, 70.62, 66.45, 59.96, 57.14, 31.92, 30.78.



1-(3-(2-(benzo[b]thiophen-5-yl)ethoxy)propyl)azetidin-3-ol (51d). Compound **51c** (1.0 eq.) was dissolved in THF (0.1 M), then lithium aluminum hydride (5.0 eq.) was added at 0 degrees C and the solution stirred 0.5 h. The mixture was cooled to 0 degrees C, then carefully quenched with 3 M NaOH. This solution was extracted 3 times with EtOAc. The combined organics were washed 3 times with water and once with brine, dried over Na_2SO_4 , and then purified by preparatory TLC to afford the title product in 59% yield. $R_f = 0.32$, 5% TEA / 15% MeOH / 80% EtOAc. ^1H NMR (800 MHz, Chloroform- d) δ 7.86 (d, $J = 7.9$ Hz, 1H), 7.77 (d, $J = 7.8$ Hz, 1H), 7.42 – 7.38 (m, 1H), 7.37 – 7.33 (m, 1H), 7.15 (s, 1H), 5.28 (s, 1H), 4.46 (p, $J = 5.7$ Hz, 1H), 3.80 (t, $J = 6.5$ Hz, 2H), 3.73 – 3.70 (m, 2H), 3.57 (t, $J = 6.2$ Hz, 2H), 3.18 – 3.12 (m, 2H), 2.71 – 2.65 (m, 2H), 1.76 (dt, $J = 13.2, 6.4$ Hz, 4H). ^{13}C NMR (201 MHz, CDCl_3) δ 142.67, 139.98, 139.57, 124.08, 123.68, 122.85, 122.13, 121.80, 121.65, 70.84, 68.56, 63.98, 62.10, 55.93, 31.39, 27.47.

6.4 References

1. FastStats - Deaths and mortality. *Centers Dis. Control Prev.* (2015). at <http://www.cdc.gov/nchs/fastats/deaths.htm>
2. Global cancer facts and figures 2nd edition. *Am. Cancer Soc.* (2011). at <http://www.cancer.org/acs/groups/content/@epidemiologysurveillance/documents/document/acspc-027766.pdf>
3. Cancer in developing countries. *Int. Netw. Cancer Treat. Res.* at <http://www.inctr.org/about-inctr/cancer-in-developing-countries/>
4. Siegel, R. *et al.* Cancer statistics, 2014. *CA. Cancer J. Clin.* **64**, 9–29 (2014).
5. Lo, B., Field, M. J. & Institute of Medicine (US) Committee on Conflict of Interest in Medical Research, Education and Practice. The pathway from idea to regulatory approval: examples for drug development. (2009). at <http://www.ncbi.nlm.nih.gov/books/NBK22930/>
6. Petrik, J. J. in *Ovarian Cancer* 371–376 (2013).
7. Sasaki, R. *et al.* Oncogenic transformation of human ovarian surface epithelial cells with defined cellular oncogenes. *Carcinogenesis* **30**, 423–431 (2009).
8. Learning about cancer surgery. *Am. Cancer Soc.* (2014). at <http://www.cancer.org/treatment/treatmentsandsideeffects/treatmenttypes/surgery/surgery-learning-about-cancer-surgery>
9. Sadeghi, M., Enferadi, M. & Shirazi, A. External and internal radiation therapy: past and future directions. *J. Cancer Res. Ther.* **6**, 239–248 (2010).
10. Lind, M. J. Principles of cytotoxic chemotherapy. *Medicine (Baltimore)* **36**, 19–23 (2008).
11. Chan, K.-S., Koh, C.-G. & Li, H.-Y. Mitosis-targeted anti-cancer therapies: where they stand. *Cell Death Dis.* **3**, e411 (2012).
12. UK, C. R. How chemotherapy works. (2015). at <http://www.cancerresearchuk.org/about-cancer/cancers-in-general/treatment/chemotherapy/about/how-chemotherapy-works>
13. Kayl, A. E. & Meyers, C. A. Side-effects of chemotherapy and quality of life in ovarian and breast cancer patients. *Curr. Opin. Obstet. Gynecol.* **18**, 24–28 (2006).
14. Sawyers, C. Targeted cancer therapy. *Nature* **432**, 294–297 (2004).
15. Hanahan, D. The hallmarks of cancer. *Cell* **100**, 57–70 (2000).
16. Hahn, W. C. & Weinberg, R. a. Modelling the molecular circuitry of cancer. *Nat. Rev. Cancer* **2**, 331–341 (2002).
17. Sharma, S. V & Settleman, J. Oncogene addiction: setting the stage for molecularly targeted cancer therapy. *Genes Dev.* **21**, 3214–3231 (2007).
18. Hanahan, D. & Weinberg, R. A. Hallmarks of cancer: the next generation. *Cell* **144**, 646–74 (2011).
19. Luo, J., Solimini, N. L. & Elledge, S. J. Principles of cancer therapy: oncogene and non-oncogene addiction. *Cell* **136**, 823–37 (2009).
20. Pray, L. a. Gleevec: the breakthrough in cancer treatment. *Nat. Educ.* **1**, 37 (2008).

21. Druker, B. J. *et al.* Efficacy and safety of a specific inhibitor of the BCR-ABL tyrosine kinase in chronic myeloid leukemia. *N. Engl. J. Med.* **344**, 1031–1037 (2001).
22. Capdeville, R., Buchdunger, E., Zimmermann, J. & Matter, A. Glivec (STI571, imatinib), a rationally developed, targeted anticancer drug. *Nat. Rev. Drug Discov.* **1**, 493–502 (2002).
23. What is CML. *Chronic Myelogenous Leuk. Soc. Canada* (2012). at <<http://cmlsociety.org/understanding-cml/>>
24. Cilloni, D. & Saglio, G. Molecular Pathways: BCR-ABL. *Clin. Cancer Res.* **18**, 930 (2012).
25. Druker, B. J. Translation of the Philadelphia chromosome into therapy for CML. *Blood* **112**, 4808–4817 (2008).
26. Masui, K. *et al.* A tale of two approaches: complementary mechanisms of cytotoxic and targeted therapy resistance may inform next-generation cancer treatments. *Carcinogenesis* **34**, 725–738 (2013).
27. Baudino, T. A. Targeted cancer therapy: the next generation of cancer treatment. *Curr. Drug Discov. Technol.* **12**, 3–20 (2015).
28. Berg, J. M., Tymoczko, J. L. & Stryer, L. in *Biochem. 5th Ed.* (2002).
29. Martindale, J. L. & Holbrook, N. J. Cellular response to oxidative stress: signaling for suicide and survival. *J. Cell. Physiol.* **192**, 1–15 (2002).
30. Lodish, H. *et al.* *Molecular Cell Biology. Perspective* **4**, (2008).
31. Bell, R. M., Exton, J. H. & Prescott, S. M. in *Handb. Lipid Res. Vol. 8 Lipid Second Messengers* (Snyder, F.) **1** (1996).
32. Spiegel, S., Foster, D. & Kolesnick, R. Signal transduction through lipid second messengers. *Curr. Opin. Cell Biol.* **8**, 159–167 (1996).
33. Carrasco, S. & Mérida, I. Diacylglycerol, when simplicity becomes complex. *Trends Biochem. Sci.* **32**, 27–36 (2007).
34. Newton, A. C. Protein kinase C: structure, function, and regulation. *J. Biol. Chem* **270**, 28495–28498 (1995).
35. Stoddard, N. C. & Chun, J. Promising pharmacological directions in the world of lysophosphatidic acid signaling. *Biomol. Ther.* **23**, 1–11 (2015).
36. Llona-Minguez, S., Ghassemian, A. & Helleday, T. Lysophosphatidic acid receptor (LPA) modulators: the current pharmacological toolbox. *Prog. Lipid Res.* **58**, 51–75 (2015).
37. Heise, C. E. *et al.* Activity of 2-substituted lysophosphatidic acid (LPA) analogs at LPA receptors: discovery of a LPA1/LPA3 receptor antagonist. *Mol. Pharmacol.* **60**, 1173–1180 (2001).
38. Hannun, Y. A. Functions of Ceramide in Coordinating Cellular Responses to Stress. *Science* **274**, 1855–1859 (1996).
39. Woodcock, J. Sphingosine and ceramide signalling in apoptosis. *IUBMB Life* **58**, 462–466 (2006).
40. Gulbins, E. & Li, P. L. Physiological and pathophysiological aspects of ceramide.

- Am. J. Physiol. - Regul. Integr. Comp. Physiol.* **290**, 11–26 (2006).
41. Hla, T. & Dannenberg, A. J. Sphingolipid signaling in metabolic disorders. *Cell Metab.* **16**, 420–34 (2012).
 42. Spiegel, S. *et al.* Sphingosine-1-phosphate in cell growth and cell death. *Ann. N. Y. Acad. Sci.* **845**, 11–18 (1998).
 43. Pyne, N. J. & Pyne, S. Sphingosine 1-phosphate and cancer. *Nat. Rev. Cancer* **10**, 489–503 (2010).
 44. Spiegel, S. & Milstien, S. Sphingosine-1-phosphate: an enigmatic signalling lipid. *Nat. Rev. Mol. Cell Biol.* **4**, 397–407 (2003).
 45. Blaho, V. a & Hla, T. An update on the biology of sphingosine 1-phosphate receptors. *J. Lipid Res.* **55**, 1596–1608 (2014).
 46. Hait, N. C., Milstien, S. & Spiegel, S. in *Lysophospholipid Recept. Signal. Biochem.* (Chun, J., Hla, T., Moolenaar, W. & Spiegel, S.) 71–83 (Wiley, 2013).
 47. Aarthi, J. J., Darendeliler, M. a & Pushparaj, P. N. Dissecting the role of the S1P/S1PR axis in health and disease. *J. Dent. Res.* **90**, 841–854 (2011).
 48. Ogretmen, B. & Hannun, Y. a. Biologically active sphingolipids in cancer pathogenesis and treatment. *Nat. Rev. Cancer* **4**, 604–616 (2004).
 49. Maceyka, M., Harikumar, K. B., Milstien, S. & Spiegel, S. Sphingosine-1-phosphate signaling and its role in disease. *Trends Cell Biol.* **22**, 50–60 (2012).
 50. Pyne, N., Ohotski, J., Bittman, R. & Pyne, S. The role of sphingosine 1-phosphate in inflammation and cancer. *Adv. Biol. Regul.* **54**, 121–129 (2014).
 51. Mendoza, A., Pitt, L. A. & Schwab, S. R. in *Lysophospholipid Recept. Signal. Biochem.* (Chun, J., Hla, T., Spiegel, S. & Moolenaar, W.) 475–488 (Wiley, 2013).
 52. Strader, C. R., Pearce, C. J. & Oberlies, N. H. Fingolimod (FTY720): A recently approved multiple sclerosis drug based on a fungal secondary metabolite. *J. Nat. Prod.* **74**, 900–907 (2011).
 53. Brinkmann, V. *et al.* Fingolimod (FTY720): discovery and development of an oral drug to treat multiple sclerosis. *Nat. Rev. Drug Discov.* **9**, 883–897 (2010).
 54. Brinkmann, V. *et al.* The immune modulator FTY720 targets sphingosine 1-phosphate receptors. *J. Biol. Chem.* **277**, 21453–21457 (2002).
 55. Kharel, Y. *et al.* Sphingosine kinase 2 is required for modulation of lymphocyte traffic by FTY720. *J. Biol. Chem.* **280**, 36865–36872 (2005).
 56. Brinkmann, V. FTY720 (fingolimod) in multiple sclerosis: therapeutic effects in the immune and the central nervous system. *Br. J. Pharmacol.* **158**, 1173–1182 (2009).
 57. Kohama, T. *et al.* Molecular cloning and functional characterization of murine sphingosine kinase. *J. Biol. Chem.* **273**, 23722 (1998).
 58. Liu, H. *et al.* Molecular cloning and functional characterization of a novel mammalian sphingosine kinase type 2 isoform. *J. Biol. Chem.* **275**, 19513–19520 (2000).
 59. Olivera, A. & Spiegel, S. Sphingosine kinase: a mediator of vital cellular functions. *Prostaglandins Other Lipid Mediat.* **64**, 123–134 (2001).

60. Johnson, K. R., Becker, K. P., Facchinetti, M. M., Hannun, Y. A. & Obeid, L. M. PKC-dependent activation of sphingosine kinase 1 and translocation to the plasma membrane: Extracellular release of sphingosine-1-phosphate induced by phorbol 12-myristate 13-acetate (PMA). *J. Biol. Chem.* **277**, 35257–35262 (2002).
61. Kee, T. H., Vit, P. & Melendez, A. J. Sphingosine kinase signalling in immune cells. *Clin. Exp. Pharmacol. Physiol.* **32**, 153–161 (2005).
62. Kharel, Y. *et al.* A rapid assay for assessment of sphingosine kinase inhibitors and substrates. *Anal. Biochem.* **411**, 230–235 (2011).
63. Igarashi, N. *et al.* Sphingosine kinase 2 is a nuclear protein and inhibits DNA synthesis. *J. Biol. Chem.* **278**, 46832–46839 (2003).
64. Neubauer, H. a & Pitson, S. M. Roles, regulation and inhibitors of sphingosine kinase 2. *FEBS J.* **280**, 5317–36 (2013).
65. Hait, N. C. *et al.* Regulation of histone acetylation in the nucleus by sphingosine-1-phosphate. *Science* **325**, 1254–1257 (2009).
66. Pitson, S. M. Regulation of sphingosine kinase and sphingolipid signaling. *Trends Biochem. Sci.* **36**, 97–107 (2011).
67. Mizugishi, K. *et al.* Essential role for sphingosine kinases in neural and vascular development. *Mol Cell Biol* **25**, 11113–21 (2005).
68. Pitman, M. R. & Pitson, S. M. Inhibitors of the sphingosine kinase pathway as potential therapeutics. *Curr. Cancer Drug Targets* **10**, 354–367 (2010).
69. Gandy, K. A. O. & Obeid, L. M. Targeting the sphingosine kinase/sphingosine 1-phosphate pathway in disease: review of sphingosine kinase inhibitors. *Biochim. Biophys. Acta* **1831**, 157–166 (2013).
70. Mathews, T. P. *et al.* Discovery, biological evaluation, and structure-activity relationship of amidine based sphingosine kinase inhibitors. *J. Med. Chem.* **53**, 2766–78 (2010).
71. Kennedy, A. J. *et al.* Development of amidine-based sphingosine kinase 1 nanomolar inhibitors and reduction of sphingosine 1-phosphate in human leukemia cells. *J. Med. Chem.* **54**, 3524–48 (2011).
72. Schnute, M. E. *et al.* Modulation of cellular S1P levels with a novel, potent and specific inhibitor of sphingosine kinase-1. *Biochem. J.* **444**, 79–88 (2012).
73. Kharel, Y. *et al.* Sphingosine kinase type 2 inhibition elevates circulating sphingosine 1-phosphate. *Biochem. J.* **447**, 149–157 (2012).
74. Wang, Z. *et al.* Molecular basis of sphingosine kinase 1 substrate recognition and catalysis. *Structure* **21**, 798–809 (2013).
75. Gustin, D. J. *et al.* Structure guided design of a series of sphingosine kinase (SphK) inhibitors. *Bioorganic Med. Chem. Lett.* **23**, 4608–4616 (2013).
76. Rex, K. *et al.* Sphingosine kinase activity is not required for tumor cell viability. *PLoS One* **8**, e68328 (2013).
77. Kharel, Y. *et al.* Sphingosine kinase type 1 inhibition reveals rapid turnover of circulating sphingosine 1-phosphate. *Biochem. J.* **440**, 345–353 (2011).
78. Loveridge, C. *et al.* The sphingosine kinase 1 inhibitor 2-(p-hydroxyanilino)-4-(p-

- chlorophenyl)thiazole induces proteasomal degradation of sphingosine kinase 1 in mammalian cells. *J. Biol. Chem.* **285**, 38841–38852 (2010).
79. Newton, J., Lima, S., Maceyka, M. & Spiegel, S. Revisiting the sphingolipid rheostat: evolving concepts in cancer therapy. *Exp. Cell Res.* **333**, 195–200 (2015).
 80. Patwardhan, N. N. *et al.* Structure–activity relationship studies and in vivo activity of guanidine-based sphingosine kinase inhibitors: discovery of SphK1- and SphK2-selective inhibitors. *J. Med. Chem.* **58**, 1879–1899 (2015).
 81. Santos, W. L. & Lynch, K. R. Drugging sphingosine kinases. *ACS Chem. Biol.* **10**, 225–233 (2015).
 82. Houck, J. D. *et al.* Structural requirements and docking analysis of amidine-based sphingosine kinase 1 inhibitors containing oxadiazoles. *ACS Med. Chem. Lett.* (2016). doi:10.1021/acsmmedchemlett.6b00002
 83. Blaho, V. a & Hla, T. An update on the biology of sphingosine 1-phosphate receptors. *J. Lipid Res.* **55**, 1596–1608 (2014).
 84. Hannun, Y. A. & Obeid, L. M. Principles of bioactive lipid signalling: lessons from sphingolipids. *Nat. Rev. Mol. Cell Biol.* **9**, 139–150 (2008).
 85. Lai, W.-Q., Wong, W. S. F. & Leung, B. P. Sphingosine kinase and sphingosine 1-phosphate in asthma. *Biosci. Rep.* **31**, 145–150 (2011).
 86. Long, D. A. & Price, K. L. Sphingosine kinase-1: a potential mediator of renal fibrosis. *Kidney Int.* **76**, 815–817 (2009).
 87. Zhang, Y. *et al.* Elevated sphingosine-1-phosphate promotes sickling and sickle cell disease progression. *J. Clin. Invest.* **124**, 2750–2761 (2014).
 88. Plano, D., Amin, S. & Sharma, A. K. Importance of sphingosine kinase (SphK) as a target in developing cancer therapeutics and recent developments in the synthesis of novel SphK inhibitors. *J. Med. Chem.* **57**, 5509–5524 (2014).
 89. Pitson, S. M. *et al.* Activation of sphingosine kinase 1 by ERK1/2-mediated phosphorylation. *EMBO J.* **22**, 5491–5500 (2003).
 90. Knott, K., Kharel, Y., Raje, M. R., Lynch, K. R. & Santos, W. L. Effect of alkyl chain length on sphingosine kinase 2 selectivity. *Bioorg. Med. Chem. Lett.* **22**, 6817–20 (2012).
 91. Kharel, Y. *et al.* Sphingosine type 2 inhibition and blood sphingosine 1-phosphate. *J. Pharmacol. Exp. Ther.* **355**, 23–31 (2015).
 92. Kharel, Y. *et al.* Sphingosine kinase type 2 inhibition elevates circulating sphingosine 1-phosphate. *Biochem. J.* **447**, 149–157 (2012).
 93. Warmus, J. S. *et al.* 2-Alkylamino- and alkoxy-substituted 2-amino-1,3,4-oxadiazoles-O-Alkyl benzohydroxamate esters replacements retain the desired inhibition and selectivity against MEK (MAP ERK kinase). *Bioorganic Med. Chem. Lett.* **18**, 6171–6174 (2008).
 94. McBriar, M. D. *et al.* Discovery of amide and heteroaryl isosteres as carbamate replacements in a series of orally active γ -secretase inhibitors. *Bioorganic Med. Chem. Lett.* **18**, 215–219 (2008).
 95. Boström, J., Hogner, A., Llinàs, A., Wellner, E. & Plowright, A. T. Oxadiazoles in

- medicinal chemistry. *J. Med. Chem.* **55**, 1817–1830 (2012).
96. Borg, S. *et al.* Synthesis of 1,2,4-oxadiazole-, 1,3,4-oxadiazole-, and 1,2,4-triazole-derived dipeptidomimetics. *J. Org. Chem.* **60**, 3112–3120 (1995).
 97. Garfinkle, J. *et al.* SI: Optimization of the central heterocycle of alpha-ketoheterocycle inhibitors of fatty acid amide hydrolase. *J. Med. Chem.* **51**, 4392–4403 (2008).
 98. Foss, F. W. *et al.* Synthesis and biological evaluation of sphingosine kinase substrates as sphingosine-1-phosphate receptor prodrugs. *Bioorganic Med. Chem.* **17**, 6123–6136 (2009).
 99. Gangloff, A. R. *et al.* Tetrabutylammonium fluoride as a mild and efficient catalyst. *Tetrahedron* **42**, 1441–1443 (2001).
 100. Schaefer, F. C. & Peters, G. a. Base-catalyzed reaction of nitriles with alcohols. A convenient route to imidates and amidine salts. *J. Org. Chem.* **26**, 412–418 (1961).
 101. Goldberg, K. *et al.* Oxadiazole isomers: all bioisosteres are not created equal. *Medchemcomm* **3**, 600 (2012).
 102. Jary, E. *et al.* Elimination of a hydroxyl group in FTY720 dramatically improves the phosphorylation rate. *Mol. Pharmacol.* **78**, 685–692 (2010).
 103. Deng, H. *et al.* Discovery of clinical candidate GSK1842799 As a selective S1P1 receptor agonist (prodrug) for multiple sclerosis. *ACS Med. Chem. Lett.* **4**, 942–947 (2013).
 104. Lim, K. G., Sun, C., Bittman, R., Pyne, N. J. & Pyne, S. (R)-FTY720 methyl ether is a specific sphingosine kinase 2 inhibitor: effect on sphingosine kinase 2 expression in HEK 293 cells and actin rearrangement and survival of MCF-7 breast cancer cells. *Cell Signal* **23**, 1590–1595 (2011).
 105. Parang, K. & Cole, P. A. Designing bisubstrate analog inhibitors for protein kinases. in *Pharmacol. Ther.* **93**, 145–157 (2002).
 106. Lavogina, D., Enkvist, E. & Uri, A. Bisubstrate inhibitors of protein kinases: from principle to practical applications. *ChemMedChem* **5**, 23–34 (2010).
 107. Kwarcinski, F. E., Fox, C. C., Steffey, M. E. & Soellner, M. B. Irreversible inhibitors of c-Src kinase that target a nonconserved cysteine. *ACS Chem. Biol.* **7**, 1910–1917 (2012).
 108. Gilbert, A. M. Recent advances in irreversible kinase inhibitors. *Pharm. Pat. Anal.* **3**, 375–386 (2014).
 109. Bauer, R. A. Covalent inhibitors in drug discovery: from accidental discoveries to avoided liabilities and designed therapies. *Drug Discov. Today* **20**, 1061–1073 (2015).
 110. Singh, J., Petter, R. C., Baillie, T. a & Whitty, A. The resurgence of covalent drugs. *Nat. Rev. Drug Discov.* **10**, 307–317 (2011).
 111. Evans, D. C., Watt, A. P., Nicoll-Griffith, D. A. & Baillie, T. A. Drug-protein adducts: an industry perspective on minimizing the potential for drug bioactivation in drug discovery and development. *Chem. Res. Toxicol.* **17**, 3–16 (2004).
 112. Lei, J., Zhou, Y., Xie, D. & Zhang, Y. Mechanistic insights into a classic wonder drug

- aspirin. *J. Am. Chem. Soc.* **137**, 70–73 (2015).
113. Mah, R., Thomas, J. R. & Shafer, C. M. Drug discovery considerations in the development of covalent inhibitors. *Bioorganic Med. Chem. Lett.* **24**, 33–39 (2014).
 114. Potashman, M. H. & Duggan, M. E. Covalent modifiers: an orthogonal approach to drug design. *J. Med. Chem.* **52**, 1231–1246 (2009).
 115. Tan, L. *et al.* Development of selective covalent Janus kinase 3 inhibitors. *J. Med. Chem.* **58**, 6589–6606 (2015).
 116. Zhou, W., Ercan, D., Jänne, P. A. & Gray, N. S. Discovery of selective irreversible inhibitors for EGFR-T790M. *Bioorganic Med. Chem. Lett.* **21**, 638–643 (2011).
 117. Lou, Y., Owens, T. D., Kuglstatter, A., Kondru, R. K. & Goldstein, D. M. Bruton's tyrosine kinase inhibitors: approaches to potent and selective inhibition, preclinical and clinical evaluation for inflammatory diseases and B cell malignancies. *J. Med. Chem.* **55**, 4539–4550 (2012).
 118. González-Bello, C. Designing irreversible inhibitors--worth the effort? *ChemMedChem* **11**, 22–30 (2016).
 119. Garuti, L., Roberti, M. & Bottegoni, G. Irreversible protein kinase inhibitors. *Curr. Med. Chem.* **18**, 2981–2994 (2011).
 120. Liu, Q. *et al.* Developing irreversible inhibitors of the protein kinase cysteinome. *Chem. Biol.* **20**, 146–159 (2013).
 121. Takamura, Y., Ono, K., Matsumoto, J., Yamada, M. & Nishijo, H. Effects of the neurotrophic agent T-817MA on oligomeric amyloid- β -induced deficits in long-term potentiation in the hippocampal CA1 subfield. *Neurobiol. Aging* **35**, 532–536 (2014).
 122. Topol, E. J. & Schork, N. J. Catapulting clopidogrel pharmacogenomics forward. *Nat. Med.* **17**, 40–41 (2011).
 123. Paugh, S. W. *et al.* A selective sphingosine kinase 1 inhibitor integrates multiple molecular therapeutic targets in human leukemia. *Blood* **112**, 1382–1391 (2008).
 124. Merrill, A. H. *et al.* Sphingolipidomics: a valuable tool for understanding the roles of sphingolipids in biology and disease. *J. Lipid Res.* **50 Suppl**, S97–S102 (2009).